

Pluripotent Stem Cell-based
Myocardial Tissue Engineering Using
Advanced Bioreactor Technology

Von der Naturwissenschaftlichen Fakultät
der Gottfried Wilhelm Leibniz Universität Hannover
zur Erlangung des Grades

DOKTOR DER NATURWISSENSCHAFTEN

Dr. rer. nat.

genehmigte Dissertation

von

Dipl.-Biol. George Kensah

geboren am 06.07.1976, in Düsseldorf

2012

Referent: Prof. Dr. rer. nat. Ulrich Martin
Medizinische Hochschule Hannover

Korreferent: Prof. Dr. rer. nat. Thomas Scheper
Gottfried Wilhelm Leibniz Universität Hannover

Tag der Promotion: 13.03.2012

Schlagwörter:

Myokardiales Tissue Engineering, Bioreaktor, induzierte pluripotente Stammzellen

Keywords:

Myocardial tissue engineering, bioreactor, induced pluripotent stem cells

For Mutti & Daddy and for the beauty of living things.

Mahalo.

Abstract

Myocardial tissue engineering (MTE) is a promising approach to generate functional cardiac tissue patches *in vitro* and might serve as an alternative for heart transplantation, which is to date, the only possible treatment for patients with end stage heart failure. The advent of reprogramming of somatic cells into induced pluripotent stem cells (iPSCs) raised hopes for the application of autologous pluripotent stem cell (PSC)-based regenerative strategies for heart failure patients. Therefore, cardiomyocytes (CMs) derived from iPSCs display a highly interesting cell source for MTE approaches. However, to date no data is available for iPSC-based cardiac tissue with relevant contractile forces.

In the presented PhD thesis current MTE methods were successfully adjusted and optimized to result in miniaturized bioartificial cardiac tissue (BCT), to compensate low CM numbers yielded from current PSC differentiation protocols. A novel advanced bioreactor system allowed for continuous stimulation, mechanical and microscopic assessment of BCTs over the complete cultivation period. Successful reproduction of reported data of current MTE approaches was possible with this system. Moreover, continuous β -adrenergic stimulation for 7 days, a novel conditioning method applied in this work, resulted in cardiac constructs with contraction forces more than twice as high as controls (2.88 ± 0.14 vs. 1.29 ± 0.06 mN). Quantitative RT-PCR analysis revealed hypertrophic responses in all treated groups. Next to active contraction forces, passive forces of BCTs and their modulation are of high interest, since they can influence CM maturation and interact with hemodynamic conditions present in the ventricle of the heart. To modulate these in a precise spatial manner, a novel highly controllable technique, i.e. two-photon induced collagen cross-linking, was employed. Under optimal conditions, this method resulted in successful tissue stiffening without impaired cell viability or contraction forces. Significant increase in passive forces of 40% was accompanied with a significantly increased Young's modulus of $\sim 15\%$ compared to controls (30.6 ± 0.9 vs. 26.5 ± 1.9 kPa). To apply iPSC-derived CMs to BCT culture, a genetic and a recently reported cytometric enrichment method were assessed. Optimization and simplification of differentiation and selection resulted in contractile cardiac bodies (CBs). In comparison to the cytometric approach, genetic selection resulted in higher CM purity (84.5 ± 1 vs. $99.8 \pm 0.07\%$) and higher cell numbers per inoculated iPSC (0.013 ± 0.005 vs. 1.68 ± 0.191) and was therefore applied to following MTE. This was done with a novel approach: Instead of single CMs, intact CBs were used together with fibroblasts, successfully resulting in contractile iPSC BCTs. Stimulation with ascorbic acid (AA) enhanced type I collagen deposition and CM activity and significantly improved contractile and passive forces. Application of a novel mechanic stimulus, i.e. growing incremental stretch, resulted in enhanced alignment of type I collagen fibers and in significantly increased anisotropic orientation of CMs with a significant elongation of sarcomeres. Contraction and passive forces were also significantly increased. Combination of both stimuli resulted in optimized iPSC BCTs with contractile forces of 1.42 ± 0.09 mN on day 21, which were almost twice as high as forces of controls (0.75 ± 0.06 mN). Passive forces were improved by the factor of three (3.78 ± 0.65 vs. 11.92 ± 1.49 mN). Electrophysiological assessment revealed field potential conduction velocities of 25 – 30 cm/s and responsiveness to cardiotropic drugs.

In conclusion, the advanced miniaturized bioreactor system presented in this study allowed for successful myocardial tissue engineering from primary cells, as well as from selected iPSC-derived cardiomyocytes. For both cell sources novel simulation strategies resulted in BCTs with contraction forces reported for the first time. Rapid progress in human PSC research, should lead to relevant CM-numbers to enable transfer of the herein described technology soon. Research concerning biocompatible matrices could also accelerate clinical application.

Zusammenfassung

Myokardiales Tissue Engineering (MTE) ist ein vielversprechender Ansatz um funktionales kardiales Gewebe *in vitro* herzustellen, welcher als mögliche Alternative zur Herztransplantation angesehen werden kann. Diese ist bis heute die einzige Behandlungsmöglichkeit für Patienten mit Herzversagen im Endstadium. Die Möglichkeit somatische Zellen in induzierte pluripotente Stammzellen (iPSCs) zu reprogrammieren hat Hoffnungen auf die Anwendung von autologen pluripotenten Stammzell (PSC)-Therapien für Patienten mit Herzversagen geweckt. Deshalb stellen Kardiomyozyten (CMs) aus iPSCs eine hochinteressante Zellquelle für MTE Ansätze dar, aber bis heute gibt es keine Daten über iPSC-basiertes kardiales Gewebe, welches relevante kontraktile Kräfte aufweist.

In der vorgelegten Dissertation wurden aktuelle MTE Methoden erfolgreich angepasst und für die Herstellung miniaturisierter bioartifizieller kardialer Gewebe (BCT) optimiert, um niedrige CM Zahlen, die aus derzeitigen PSC Differenzierungsprotokollen hervorgehen zu kompensieren. Ein neues fortschrittliches Bioreaktorsystem ermöglichte kontinuierliche Stimulation, mechanische und mikroskopische Überwachung von BCTs über den gesamten Verlauf der Kultivierung. Erfolgreiche Reproduktion berichteter Daten von derzeitigen MTE Ansätzen war mit diesem System möglich. Des Weiteren führte eine kontinuierliche β -adrenerge Stimulation, eine neue Konditionierungsmethode, die in dieser Arbeit angewandt wurde, zu kardialen Konstrukten mit doppelt so hohen Kontraktionskräften im Vergleich zu den Kontrollen (1.29 ± 0.06 vs 2.88 ± 0.14 mN). Quantitative RT-PCR Analyse zeigte hypertrophe Reaktionen in allen behandelten BCTs. Neben aktiven sind passive Kräfte von BCTs und deren Veränderung von hohem Interesse, da sie die Reifung von CMs beeinflussen und mit den haemodynamischen Bedingungen im Herzen interagieren. Um diese in einer räumlich präzisen Weise zu verändern wurde eine neue höchst kontrollierbare Technik, Zwei-Photonen induziertes Kollagen-Cross-Linking angewandt. Optimale Bedingungen führten zu einer erfolgreichen Gewebeversteifung ohne Beeinflussung von Zellvitalität, oder Kontraktionskräften. Die signifikante Erhöhung der passiven Kräfte um 40% wurde von einem signifikanten Anstieg im Young's Modulus um ~15% begleitet (30.6 ± 0.9 vs 26.5 ± 1.9 kPa). Für die Anwendung von iPSC abgeleiteten CMs in BCT Kultur wurde eine genetische, und eine kürzlich berichtete zytometrische Anreicherungsmethode beurteilt. Optimierung und Vereinfachung der Differenzierung und Selektion führte zu kontraktile kardialen Körperchen (CBs). Im Vergleich zum zytometrischen Ansatz führte die genetische Methode zu höherer CM-Reinheit (84.5 ± 1 vs $99.8 \pm 0.07\%$) und höheren Zellzahlen pro inokulierter iPSC (0.013 ± 0.005 vs 1.68 ± 0.19 Zellen/iPSC) und wurde deshalb für darauffolgendes MTE verwendet. Dies erfolgte durch einen neuen Ansatz: Anstelle von vereinzelt CMs wurden intakte CBs zusammen mit Fibroblasten verwendet, was erfolgreich zu kontraktile iPSC BCTs führte. Stimulation mit Ascorbat (AA) verstärkte die Typ I Kollagen Einlagerung und CM Aktivität und verbesserte die kontraktile und passiven Kräfte signifikant. Die Anwendung eines neuen mechanischen Stimulus, wachsende stufenweise Dehnung, führte zu verstärkter Ausrichtung von Typ I Kollagen Fasern und signifikant erhöhter anisotroper Orientierung von CMs zusammen mit einer signifikanten Verlängerung der Sarkomere. Passive und Kontraktionskräfte waren ebenfalls signifikant erhöht. Kombination beider Stimuli führte zu optimierten iPSC BCTs mit kontraktile Kräfte von 1.42 ± 0.09 mN an Tag 21, die fast doppelt so hoch waren wie die der Kontrollen (0.75 ± 0.06 mN). Passive Kräfte wurden um den Faktor drei erhöht (3.78 ± 0.64 vs 11.92 ± 1.49 mN). Elektrophysiologische Beurteilung zeigte FPs mit Weiterleitungsgeschwindigkeiten von 25 – 30 cm/s und ein Ansprechen auf kardiotope Substanzen.

Zusammenfassend erlaubte das fortschrittliche miniaturisierte Bioreaktorsystem, welches in dieser Studie vorgestellt wurde, das erfolgreiche myokardiale Tissue Engineering mit Primärzellen, als auch mit selektierten iPSC abgeleiteten Kardiomyozyten. Für beide Zellquellen resultierten neue Stimulierungsstrategien in BCTs mit Kontraktionskräften, von denen hier zum ersten mal berichtet wird. Der rasante Fortschritt in der humanen PSC-Forschung sollte bald zu relevanten CM-Mengen im humanen System führen um einen Transfer der hier beschriebenen Technologie zu ermöglichen. Die Forschung bezüglich biokompatibler Matrices könnte die klinische Anwendbarkeit ebenfalls beschleunigen.

Table of contents

1	Introduction	8
1.1	Cardiovascular diseases	8
1.2	Conventional treatment of cardiovascular diseases	8
1.2.1	Pharmacological therapies	9
1.2.2	Invasive treatments	9
1.2.3	Heart transplantation	10
1.3	Alternative treatment strategies for patients with end-stage heart conditions	11
1.3.1	Xenotransplantation	11
1.3.2	Mechanical assist devices	12
1.3.3	Induction of regenerative processes in the heart	13
1.3.4	Single cell-based cardiac regeneration strategies	15
1.3.5	Pluripotent stem cells (PSCs)	18
1.3.6	Direct reprogramming of somatic cells into cardiomyocytes	24
1.4	Enrichment methods for heart cells	24
1.5	Effects of single cardiomyocyte transplantation into infarcted hearts	26
1.6	Tissue engineering	27
1.6.1	Cardiac tissue engineering	28
1.6.2	Cell sources for cardiac tissue engineering	29
1.6.3	Matrices	30
1.6.4	Cardiac tissue engineering strategies	30
1.6.4.1	Cell seeding onto porous scaffolds	30
1.6.4.2	Repopulation of decellularized scaffolds	31
1.6.4.3	Cell (-aggregate) printing	32
1.6.4.4	Mixing of cells with liquid scaffolds	33
1.6.4.5	Scaffold-free approaches	35
1.7	Bioreactors in cardiac tissue engineering	36
2	Objectives	38
3	Manuscripts	40
3.1	A Novel Miniaturized Multimodal Bioreactor for Continuous <i>In Situ</i> Assessment of Bioartificial Cardiac Tissue during Stimulation and Maturation (Manuscript 1)	40
3.2	Two-photon induced collagen cross-linking in bioartificial cardiac tissue (Manuscript 2)	57
3.3	Direct Fusion of iPSC-derived Cardiac Bodies into Structurally and Functionally Homogenous Bioartificial Cardiac Tissue is Fibroblast-dependent and is supported by Ascorbic Acid and Mechanical Load (Manuscript 3)	70
4	Discussion	118
4.1	A Novel Miniaturized Multimodal Bioreactor for Continuous <i>In Situ</i> Assessment of Bioartificial Cardiac Tissue during Stimulation and Maturation (Manuscript 1)	119
4.1.1	Current demands on bioreactor design for stem cell-based myocardial tissue engineering	119
4.1.2	A novel bioreactor system	119
4.1.3	Reproduction of physiological properties reported for larger engineered myocardial tissue constructs	122
4.2	Two-photon induced collagen cross-linking in bioartificial cardiac tissue (Manuscript 2)	124
4.2.1	Passive forces in cardiac tissue	124
4.2.2	Modulation of mechanical properties of biological tissue	124
4.2.3	Photochemical stiffening of cardiomyocyte-free collagenous tissue	125
4.2.4	Effective laser induced collagen cross-linking is possible without affecting functional activity of BCTs	126
4.3	Fibroblast-dependent Fusion of iPSC-derived Cardiac Bodies results in structurally and functionally homogenous Bioartificial Cardiac Tissue and is supported by Ascorbic Acid and Mechanical Load (Manuscript 3)	128
4.3.1	Current challenges in pluripotent stem cell-based myocardial tissue engineering	128

4.3.2	Genetic selection of cardiomyocytes from iPSCs is superior to non-genetic selection in terms of yield and purity.....	130
4.3.3	Genetic selection results in artificial 3D aggregates with cardiomyocytes showing functional properties	131
4.3.4	Fibroblasts support cardiac tissue formation	132
4.3.5	Cardiac bodies can be used directly to generate homogeneous and functional bioartificial cardiac tissue	132
4.3.6	Morphology and contractility are positively affected by ascorbic acid-mediated changes in ECM organization of CB-based BCTs	133
4.3.7	CM orientation and maturation is mediated by increasing mechanical strain	134
4.3.8	Combination of novel stimuli results in optimized functionality of miPSC-derived BCTs	134
5	References	137
6	Appendix	155
	Table of figures	155
	List of abbreviations	156
	Curriculum vitae	160
	List of publications	163
	Danksagung	166
	Erklärung zur Dissertation.....	169

1 Introduction

1.1 Cardiovascular diseases

The general term “cardiovascular disease” (CVD) defines pathological alterations in the circulatory system, comprising hypertonic status, valvular defects, and ischemic heart conditions like coronary occlusions eventually resulting in myocardial infarction (MI). As reported by the World Health Organization, CVDs are still the number one killer in industrialized countries (WHO 2011). In 2010, roughly 15 million Europeans suffered from chronic myocardial insufficiency and 41% of fatalities in Germany were the result of CVDs with more than 350,000 cases. Almost 60,000 cases of death were caused by heart stroke, i.e. the ultimate stage of MI (Statistisches-Bundesamt-Deutschland 2011). There are several reasons known for the development of CVDs. Some rely on external factors such as stress, life style (Schwartz et al. 2003) and socioeconomic status (Kaplan 1993), whereas others are based on intrinsic factors such as congenital heart defects or genetics (Hoffman 1995; Arking & Chakravarti 2009), or as a result of a combination of both, such as the disposition to obesity (Poirier et al. 2006). Next to the dramatic impact on personal life in patients suffering from CVDs, the financial impact is remarkable. In 2003 alone, direct costs for CVD treatment accounted for 102 billion Euros in the European Union health care system. Additionally, 29 billion Euros were spent for informal care and 35 billion Euros were lost due to decreases in economic productivity. Taken together, this sums-up to 169 billion Euros in total for the European Union, with similar numbers for other industrialized regions (Tendera 2006).

1.2 Conventional treatment of cardiovascular diseases

Rhythmical heart disorders, such as atrial fibrillation, as risk factors for heart failure (HF), can be treated by electrical pacemakers or pharmacological interventions (Fuster et al. 2001). In cases of CVDs, especially in coronary artery diseases (CADs),

treatments vary from pharmacological, over minimal invasive, to open-heart surgery, depending on the severity of the condition.

1.2.1 Pharmacological therapies

To date, initial phases of CVDs can be addressed by application of certain drugs to treat symptoms, extent, and improve patient's quality of life. Symptomatic treatment of CVDs consists of blockade of endogenous neuro-humoral overstimulation by inhibition of i) β -adrenoreceptors, ii) the angiotensin-converting enzyme, and iii) the aldosterone-receptor. In cases of HF, mechanical relief of the myocardium is achieved by administration of diuretics, whereas for acute HF (AHF) contraction activity can be stimulated through application of cardiac glycosides (for a detailed review see Dickstein et al. 2008).

1.2.2 Invasive treatments

In severe cases of CAD, i.e. progressed stenoses or occlusions of coronary arteries, operative interventions have to be applied to prevent progression of ischemia eventually leading to HF.

Percutaneous transluminal coronary angioplasty (PTCA)

Coronary stents are applied via a catheter-based operation through the groin artery, a method termed "percutaneous transluminal coronary angioplasty" (PTCA). These prostheses are mostly made of metal, i.e. magnesium meshes, to provide stability and to allow for continuous opening and can be drug eluting to prevent re-occlusion. In cases of AHF, the extent to which this method is superior to optimal emergency pharmacological therapy, however, is a matter of discussion (Steg 2006). The same holds true for the beneficial effects of drug elution of these prostheses (C. W. Hwang et al. 2001; Serruys & Kutryk 2006).

Coronary artery bypass graft (CABG)

A surgical approach to treat occluded coronary arteries is the bypass operation. Here, appropriate autologous vessels from elsewhere in the body, normally veins from the

leg, are used to circumvent up to four coronary arteries. The medical term for this method is “coronary artery bypass graft” (CABG).

Comparison of these methods, i.e. PCTA and CABG, revealed, that both resulted in similar survival rates with more PCTA interventions resulting in necessary re-operations (Serruys et al. 2001; Rihal et al. 2003). Biryukova and colleagues concluded that the best outcome for the patient would be provided by multidisciplinary committee decisions on a case-to-case basis (Biryukova et al. 2010).

1.2.3 Heart transplantation

To date, due to the limited regeneration potential of the heart muscle after infarction, the only widely accepted treatment of end-stage heart failure is allogeneic heart transplantation from human donors. In the late sixties of the last century, Christiaan Barnard performed the first transplantation, with the patient’s death 18 days after transplantation due to a secondary infection (Barnard 1967). Intensive research on antisepsis, immunosuppression, and improvement in operation techniques, however, turned this approach into an accepted treatment in end-stage heart failure with a positive survival rate (Kobashigawa & Patel 2006). To date, almost 75% of patients survive the first five years after transplantation and more than 58% survive 15 years post operation (Roussel et al. 2008). Nevertheless, quality of life of transplant recipients is impaired largely by many risks that can occur after heart transplantation. Next to the thread of chronic rejection, implications based on necessary immunosuppressant medication include: infection, hypertension, diabetes mellitus, elevated cholesterol levels, renal disease and cancer (Hošková et al. 2008; Roussel et al. 2008; Doesch et al. 2010). Moreover, although several attempts have been made to raise readiness for organ donation in the public, the need for transplantable organs in an ageing society is high and rising, with more than 1700 patients on the waiting list in 2010 in Europe alone (Eurotransplant International Foundation 2011). These numbers almost doubled within the last ten years, as shown in figure 1.

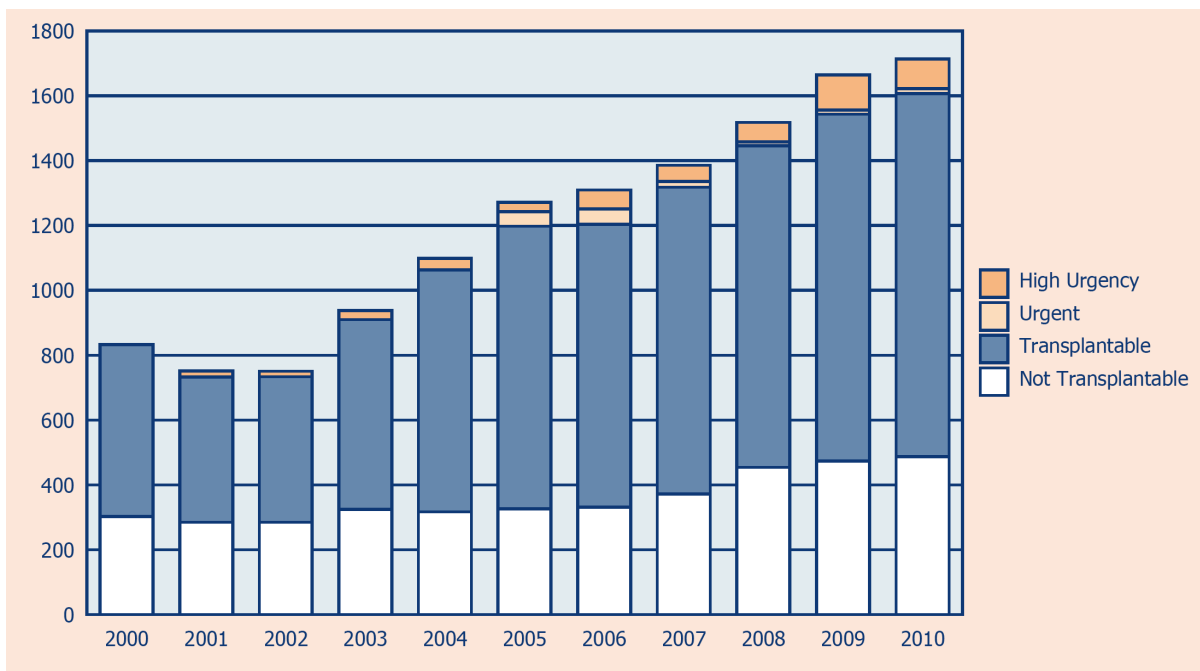


Figure 1: Heart waiting list of patients at year's end. From: Eurotransplant Annual Report 2011.

1.3 Alternative treatment strategies for patients with end-stage heart conditions

Due to the limitations and possible complications mentioned in previous sections, various alternatives to human cadaveric heart transplantation are subject of intensive research. All of these approaches have their benefits and drawbacks, but common to all is the desire to improve quality and extend patients' lives with the highest degree of safety.

1.3.1 Xenotransplantation

The feasibility to use cadaveric hearts from foreign species, to overcome the shortage of allogeneic heart transplants is by the approach to employ xenotransplantation strategies. Due to their high accessibility and comparable organ sizes, research is focusing on pigs as donor species, but the risk of rejection is even higher than in the allogeneic system (Dorling 2002; Sprangers et al. 2008). Rejection may be reduced by immunosuppression, as has been shown in a study of pig-to-baboon cardiac

transplantation, reporting less acute rejection in monkeys, that underwent constant antibody depletion (Lin et al. 1998). Transferring these results to human therapy implies the application of harsh and toxic immunosuppressive protocols. The issue of immunologic rejection can be addressed by the reduction of antigens in donor animals by generation of transgenic α 1-3 galactosyltransferase (α 1-3gal, a major xenoantigen in pig-to-primate transplantations) knockout pigs (Dai et al. 2002; Nottle et al. 2007). It has been reported, however, that even fetal-pig fibroblasts homozygous for the knockout of the α 1-3gal gene express low but detectable levels of the gal antigen (Sharma et al. 2003). Besides these challenges, there are concerns of xenozoonoses delivered by porcine endogenous retroviruses (PERV) (Blusch et al. 2002). PERV was shown to infect human endothelial cells *in vitro* productively, indicating another factor that renders this method not safe at the current state (U. Martin et al. 2000). Although the chance to exploit a source of inexhaustible supply of donor organs is intriguing, additional research has to be performed to define and improve safety of xenogeneic transplants, prior to their application to the clinic.

1.3.2 Mechanical assist devices

A bionic approach to improve insufficient ventricular function is the mechanical left ventricular assist device (LVAD), which works as a pump that is implanted into the apex of the defective ventricle (see fig. 2). Clinical trials have shown that the continuous flow device HeartMate II (HM II) was able to serve as a temporary bridging tool for patients with end-stage heart failure waiting for heart transplantation, and as a permanent, i.e. destination device (Lahpor et al. 2009). The major disadvantages of this system are the necessity to carry a power supply connected to the implant bearing the risk of infection, and the need for anticoagulation medication, which can lead to hemorrhage or stroke. Nevertheless, LVADs turned out to be valuable tools to extend lives of patients with end-stage heart failure and are to date the most reliable alternatives to organ transplantation with more than 2000 implants world-wide (Strüber et al. 2009). Further improvements in mechanics and less invasive power supply solutions could lead to an enhanced clinical acceptance and distribution of this approach.

Several researchers are focusing on alternative biological approaches to help patients with insufficient heart function that could circumvent drawbacks of mechanical devices mentioned above.

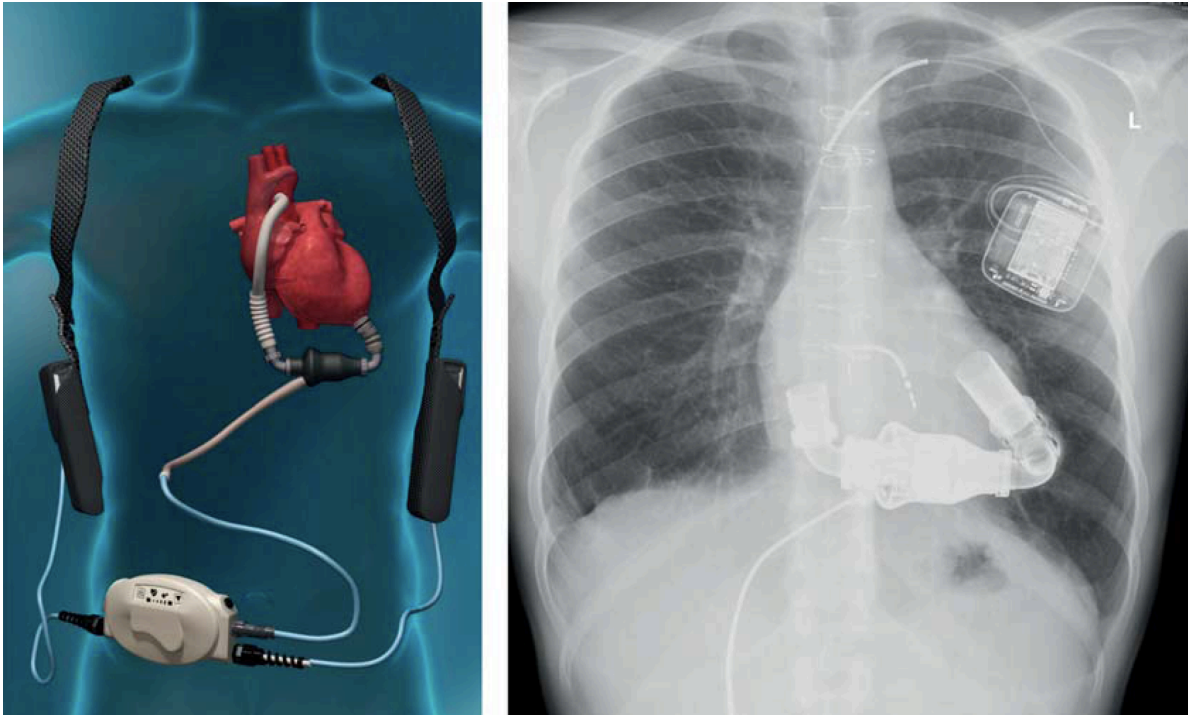


Figure 2: Mechanical assist device for myocardial defects. The left ventricular assist device HeartMate II serves as a continuous pump for end-stage heart failure. **Left:** Schematic representation of the assist device principle. **Right:** Chest X-ray showing the implanted device and the connection to the external power supply. From Strüber et al. 2009.

1.3.3 Induction of regenerative processes in the heart

It was thought for long time, that the post-natal mammalian heart does not have the potential to regenerate due to the extremely low cell-cycle activity in cardiomyocytes (Rumyantsev 1991). To study events of cell division, Soonpaa and colleagues employed transgenic mice, expressing β -galactosidase under a cardiomyocyte-specific promoter to histologically screen for nuclei, which have incorporated radiolabeled thymidine. In intact hearts, only 0.0006% of cardiomyocytes and 0.0083% of cardiomyocytes in infarcted hearts were found to be labeled, indicating

rare events of proliferation (Soonpaa & Field 1998). For the same reason, a different method to detect DNA-synthesis in human hearts was employed by Bergmann et al., which was based on the radiocarbon method (Bergmann et al. 2009). The worldwide pulse of the radioactive carbon isotope ^{14}C was increased dramatically during cold war due to atmospheric testing of nuclear weapons until 1963, when these tests were banned. This isotope was incorporated into plants and eventually entered the human food chain and, hence, human DNA. This occurrence was used to date the age of cells, by identifying, when the atmospheric ^{14}C levels matched those of the analyzed DNA. Isolated cardiomyocyte nuclei, sorted for the cardiac marker Troponin, revealed that there was DNA younger than the patient was, although these events were dramatically higher for non-myocyte nuclei. As human cardiomyocytes are known to be polyploid by the onset of puberty (Adler 1975) and that, in response to pathological workload, they commonly reinitiate DNA synthesis without nuclear division (Adler & Friedburg 1986), the authors analyzed the diploid DNA subset only. Mathematical modeling suggested that cardiomyocytes underwent age dependent renewal of ~1% at age 20, and 0.4% at age 75 per year. In human, next to the loss of 1 g (~ 2×10^7 cardiomyocytes) of myocardium per year due to ageing (Olivetti et al. 1991), pathological conditions, such as infarction of the left ventricle can lead to the loss of 25%, i.e. 2 – 4 billion cardiomyocytes within a few hours (Murry et al. 2006). Hence, unmodified intrinsic capacity of cardiomyocyte proliferation, which is indeed very low, does not suffice the emerging necessity for regeneration after infarction.

Recent findings, however, suggest that there is an inducible regenerative capacity in the post-natal mammalian heart. For rodents, Porrello et al. showed that a resection of the heart apex in neonatal mice leads to complete regeneration of the ventricle in size and function after three weeks (Porrello et al. 2011). On the other hand, this publication also reports that this phenomenon was not detectable in seven days old mice, hence, rendering this approach not applicable to regenerative therapies, which focus on the treatment of myocardial infarction in older patients. Nevertheless, these findings may contribute to the understanding of the potential to regenerate internal organs, which is a known process in amphibians and fish (Oberpriller 1974; Poss 2002). A recent study on zebrafish identified a population of GATA4⁺ cardiomyocytes

as the main contributor to myocardial restoration after severe injury (Kikuchi et al. 2010). Genetic approaches to induce cardiomyocytes to re-enter the cell cycle have been performed. In transgenic mice expressing the cell-cycle activator Cyclin D2 under control of a cardiomyocyte-restricted promoter, improved mechanical function after infarction and a reduced scar size was observed (Hassink et al. 2008). However, it has been reported, that manipulation of sensitive cell-cycle mechanisms can eventually lead to heart tumor formation (Field 1988). A recent report focuses on the improved survival of cells after infarction. Korf-Klingebiel and colleagues showed that cardiac-specific and tetracycline-controlled fibroblast growth factor 9 (FGF9) expression could reduce mortality in transgenic mice after myocardial infarction (Korf-Klingebiel et al. 2011). Moreover, FGF9 enhanced hypertrophy in non-infarcted myocardium, increased microvessel density and improved systolic function. The authors also found that FGF9 indirectly induces cardiomyocyte hypertrophy via paracrine release of bone morphogenetic protein 6 (BMP6) by endothelial cells. This was indicated by FGF9 transduced endothelial cell conditioned supernatant effects on cardiomyocytes *in vitro* and elevated BMP6 expression in the myocardium of transgenic mice *in vivo*. A non-genetic approach for myocardial regeneration is to induce cardiomyocyte proliferation by pharmacological means. This has been studied using signaling molecules, such as fibroblast growth factor 1 and periostin (Engel et al. 2006; Kühn et al. 2007). Recently, Bersell et al. showed that cardiomyocyte proliferation could be re-activated *in vitro* and *in vivo* through application of neuregulin 1 (NRG1) (Bersell et al. 2009). In infarcted mouse hearts, NRG1 injection led to reduced scar size and improved mechanical function. To date, these findings have not been confirmed independently, but in terms of future clinical therapies, pharmacological approaches would be more feasible and putatively safer than genetic manipulation, since a threat that is intrinsic to all stable genetic manipulation methods to date is the risk of insertional mutagenesis (Baum 2004).

1.3.4 Single cell-based cardiac regeneration strategies

Besides exploitation and enhancement of the intrinsic regenerative potential of the heart (limited by the lack of proliferative capacity of cardiomyocytes), another strategy

is the transplantation of (*in vitro* expanded) cells. These cells can be of autologous or allogeneic origin, and they vary in the degree of potency. The following chapter summarizes the current state of cell-based transplantation approaches.

Somatic stem and progenitor cells

Somatic stem cells represent the regenerative resource of many tissues like bone, skin, and gut. In their tissue of origin, they are located within a specialized environment referred to as the so-called „niche“. By asymmetrical cell division they self-renew and, at the same time give rise to committed progenitor cells, which in turn amplify and further differentiate into more specialized cell types. For cell therapy, adult stem and progenitor cells represent a valuable resource, because of their considerable proliferation and differentiation capacity as well as their potential for autologous application.

Whereas initial beliefs implied that only contractile cells have the potential to restore infarcted heart muscle tissue, currently many hints suggest that also other cell types lead to functional improvements after injection into the infarct region. This is most probably due to improved vascularization or mere paracrine effects, rather than transdifferentiation into cardiomyocytes (Murry et al. 2004).

Skeletal muscle-derived cells and skeletal myoblasts (SKMB)

The idea to utilize the high regenerative capacity of skeletal muscle led to the transplantation of autologous „satellite cell“-derived cells or so called skeletal myoblasts to repopulate scar tissue. Although these cells were shown to have high resistance against ischemia, to engraft and to improve left ventricular function after transplantation in rats, dogs and humans (K.-L. He et al. 2005), transplanted cells remained isolated and did not function in concert with host myocardium (Leobon et al. 2003; Dowell et al. 2003; K.-L. He et al. 2005; Formigli et al. 2010). In addition, they have been shown to promote the development of arrhythmia (Smits et al. 2003; Eisen 2008).

Bone marrow-derived cells (BMC)

BMCs represent a mixture of different cell types and have been reported to have versatile potential for myocardial repair (Orlic et al. 2001). Because bone marrow is relatively easy accessible by simple aspiration, high numbers of cells can be obtained without *in vitro/ex vivo* expansion. Hematopoietic stem cells (HSCs) and endothelial progenitor cells (EPCs) within the bone marrow are considered to have favorable potential to revascularize the infarct region (Orlic et al. 2001; Szmítko 2003). However, still controversy exists about transdifferentiation of HSCs and EPCs into cardiomyocytes (Nygren et al. 2004; Murry et al. 2004; Kolossov et al. 2006; Gruh et al. 2006). In addition, mesenchymal stromal cells (MSCs) within the BMC population might contribute to regeneration (see next paragraph). In worldwide clinical trials, BMCs have been used for the treatment of myocardial infarction, but conclusive data is still missing (Martin-Rendon et al. 2008).

Mesenchymal stromal cells (MSC)

MSCs are derived from easily accessible autologous sources like bone marrow, adipose tissue and cord blood, and were reported to share low immunogenic potential (Orlic et al. 2001). *In vitro*, they can be expanded and differentiated into cells with cartilage and bone phenotype. However, their ability to transdifferentiate into functional cardiomyocytes remains a matter of debate. A large body of studies claims transdifferentiation of MSCs into functional cardiomyocytes in coculture with neonatal cardiomyocytes with or without simultaneous overexpression of certain growth and transcription factors (Toma et al. 2002; Yoon et al. 2005; Roura et al. 2010; Z. He et al. 2011). But others question these findings (Rose, Jiang, et al. 2008a; Rose, Keating, et al. 2008b; Roura et al. 2010). Nevertheless, these cells are already used in clinical trials with reasonable success (Trounson et al. 2011). Some researches, however, point out that the described beneficial effects result from paracrine action and might also be exploited by less invasive application of proteins or small molecules (Mirotsov et al. 2007; Laflamme & Murry 2011).

Resident cardiac progenitor cells (CPCs)

In recent years, evidence was found for resident CPCs with regenerative potential. Different populations were characterized due to surface marker expression. Beltrami and colleagues described a population of cells with stem cell characteristics, i.e. expression of Lin⁻ c-kit⁺, which actively divided *in situ* and *in vitro* indicated by expression of the proliferation marker Ki67 and which gave rise to three different cell types (cardiomyocytes, smooth muscle cells and endothelial progenitor cells) by differentiation (Beltrami et al. 2003). Others report the identification of Isl1⁺ cardiac progenitors in mouse, rat and human, and claim their *in vitro* differentiation into cardiomyocytes (Laugwitz et al. 2005), however only in co-culture with neonatal cardiomyocytes. These findings were questioned soon by Tallini and colleagues, who did not find evidence for transdifferentiation *in vitro* (Tallini et al. 2009). Potential cardiac progenitors could also be isolated from murine, human and rhesus monkey heart biopsies by expansion of plastic-adherent tissue outgrowths (Messina 2004; Martens et al. 2011). These cells were shown to self-renew in culture. After growth factor administration *in vitro*, these cells assembled to aggregates, so called “cardiospheres”. After intramyocardial injection into mice, they led to functional improvements. However, reasons for that are discussed critically (Martens et al. 2011; Davis et al. 2010; Andersen et al. 2009).

1.3.5 Pluripotent stem cells (PSCs)

In contrast to controversially discussed multipotent adult stem cells as a cell source for regenerative strategies, there are a variety of other cell-types with known potential to serve as a source for cardiomyocytes *in vitro* and *in vivo*. Some, but not all, share properties of adult stem cells, being of autologous origin. Restrictions in terms of application to human therapy are mainly based on their tumorigenic potential, due to their extensive proliferative capacity and pluripotency (Hentze et al. 2009). The following section gives a brief overview to this rapidly growing field.

Embryonic stem cells (ESCs)

One intensively studied cell type for regenerative studies and strategies are embryonic stem cells. They are derived from the inner cell mass of pre-implantation embryos at the blastocyst stage and have the potential to self-renew *in vitro*, can be expanded indefinitely, and can differentiate into cells of all germ layers *in vitro* and *in vivo*, i.e. are pluripotent. The first murine embryonic stem cells were described in 1981 by two groups (G. Martin 1981; Evans & Kaufman 1981), with the first report on

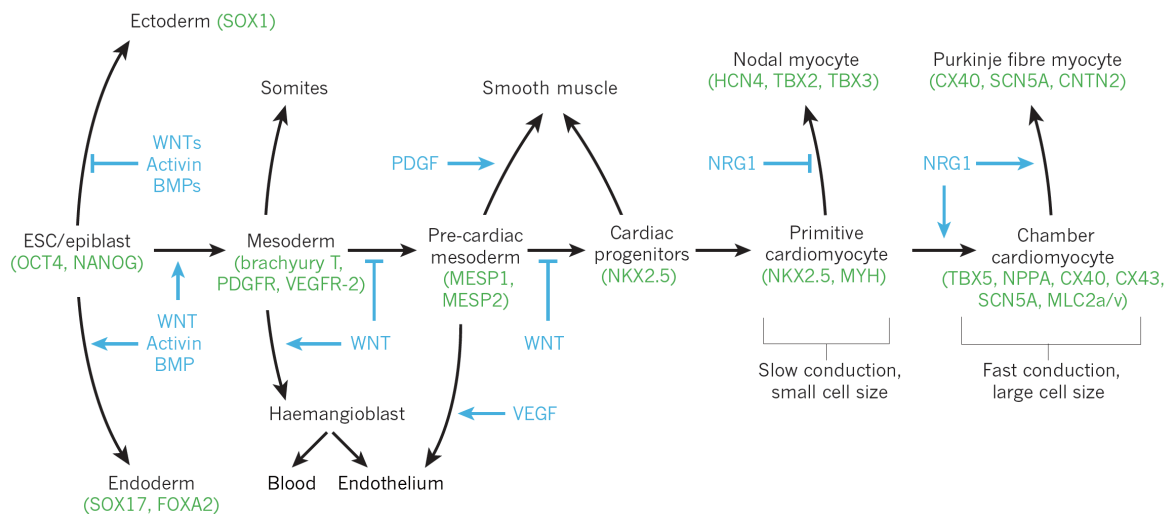


Figure 3: Cardiovascular lineages during mammalian embryonic development and ESC differentiation. Cardiac differentiation from ESCs closely mimics cardiac development in the embryo. In either case, the specification of the cardiovascular lineages involves a transition through a sequence of increasingly restricted progenitor cells, proceeding from a pluripotent state to mesoderm and then to cells committed to cardiovascular fates. Growth factors that regulate fate choices are listed at branch points (blue), and key transcription factors and surface markers for each cell state are listed under the cell types (green). The growth factors are useful for directing the differentiation of ESCs, whereas the markers are useful for purifying cells at defined developmental stages. Primitive cardiomyocytes in the embryonic heart tube and nodal or pacemaker cells show slow electrical propagation and a small cell size. By contrast, the eventual specification of working atrial and ventricular cardiomyocytes is accompanied by more rapid conduction, ion-channel remodeling and increased cell size. Although the field has made considerable progress towards determining the early events of cardiogenesis, a better understanding of how pacemaker and chamber-specific cardiac subtypes are formed is required for clinical applications. Abbreviations: BMPs, bone morphogenetic proteins; CNTN2, contactin-2; CX, connexin; FOXA2, forkhead box protein A2; HCN4, potassium/sodium hyperpolarization-activated cyclic nucleotide-gated channel 4; MESP, mesoderm posterior protein; MLC2a/v, myosin light chain 2a and/or 2v; MYH, myosin heavy chain; NPPA, natriuretic peptide precursor A; NRG1, neuregulin 1; PDGF, platelet-derived growth factor; PDGFR, PDGF receptor; SCN5A, sodium channel protein type 5 subunit α ; SOX, SRY-related high-mobility-group box; TBX, T-box transcription factor; VEGF, vascular endothelial growth factor; VEGFR-2, VEGF receptor-2. From: LaFlamme and Murry, 2011.

murine ESC-derived cardiomyocytes in 1985 (Doetschman et al. 1985). Primate ESC-lines were generated from rhesus monkey (Thomson & Kalishman 1995), human (Thomson et al. 1998) and cynomolgus monkey (Suemori et al. 2001) with robust cardiomyocyte differentiation capacity, as shown in independent studies (Kehat 2001; Schwanke et al. 2006; Nagata et al. 2003). Models for the general molecular pathways underlying cardiomyogenic differentiation of these cells recapitulate known mechanics of early mammalian embryonic heart development as shown in figure 3.

Next to the generation of cardiomyocytes from ESCs, *in vitro* differentiation of a cardiovascular progenitor population can be identified through its expression of the surface molecule kinase insert domain receptor (KDR, also known as fetal liver kinase 1 (Flk1), or vascular endothelial growth factor receptor 2 (VEGFR2)), that represents one of the earliest stages in mesoderm specification to the cardiovascular lineages (Kattman et al. 2006) (see fig. 3). Similar to the pharmacological approach (see section 1.3.3), the application of the signaling molecules activin A, bone morphogenic protein 4 (BMP4), vascular endothelial growth factor (VEGF) and dickkopf homolog 1 (DKK1) led to elevated numbers of a KDR⁺/cKit⁺ population. After transplantation, these cells gave rise to cardiac, endothelial and smooth muscle cells and further *in vitro* differentiation led to more than 50% of contracting cardiomyocytes (Yang et al. 2008). Moreover, the pluripotency marker octamer binding transcription factor 3/4 (Oct3/4) (see fig. 3) was not present in the resulting population. Therefore, the risk of pluripotent cell-mediated teratoma formation was reduced, but not excluded in this study. A recent publication also showed the generation of cardiovascular progenitors by induction of the transcription factor mesodermal posterior 1 (MesP1)-expression in murine ESCs, which resulted in overexpression of Brachyury, an early mesodermal marker (see fig. 3). Further differentiation of these cells resulted in an improvement of cardiac differentiation by 5-10 fold compared to unmodified ESCs (R. David et al. 2011b).

Although ESCs are a well-established source for cardiomyocytes with focus on pre-clinical testing of stem cell-derived cardiomyocytes, their therapeutic application in human is limited due to their allogeneic origin and their generation is matter of ethical

debate, due to their dependence on destroying human pre-implantation blastocysts. The German Stem Cell Act allowed research only on imported human embryonic stem cells generated before first of January 2001 (BMBF 2004). Just recently, this so called appointed date regulation was adjusted to the import of hESC generated outside Germany to the first of May 2007 (BMBF 2011). This strict regulation indicates the controversy concerning stem cell research in the public.

Alternative oocyte-dependent embryonic-like stem cells

Two alternative methods exist to derive stem cells from the blastocysts stage with pluripotent properties. For personalized autologous stem cells for regenerative strategies, somatic cell nuclear transfer (SCNT), also known as therapeutic cloning, has been studied intensively. The first studies on successful SCNT in the human system reported by the Hwang group (W. S. Hwang 2004; Koo et al. 2005), have been retracted by the “Science” journal in 2006 following the results of investigations on scientific misconduct in these publications (Kennedy 2006). Since then, no further studies have been published showing successful therapeutic cloning in the human system. Another method of deriving embryonic-like stem cells relies on the rare *in vivo* event of atypical activation of an oocyte to undergo cleavage, compaction and blastocyst formation without fertilization, known as parthenogenesis (Robertson & Evans 1983; Cibelli et al. 2002). This phenomenon can be induced chemically and can therefore be used to generate blastocysts, not designed for reproduction, and pluripotent stem cells can be derived from this method. However, both methods depend on oocytes, and the approach of therapeutic cloning limits public acceptance.

Spermatogonial stem cells

The presence of a pluripotent stem cell type in adult testis, which is responsible for maintaining spermatogenesis throughout life in the male, has long been suspected to provide an autologous stem cell source for male patients (Spradling et al. 2001). In 2006, Guan and colleagues found a way to produce spermatogonial stem cells (SSCs) from adult mouse testis (Guan et al. 2006). These cells are cultured similarly to mouse ESCs and differentiate into cells of all three germ layers *in vitro* and *in vivo*.

Detailed analysis revealed physiological properties of SSC-derived cardiomyocytes comparable to ESC-derived homologues, or early embryonic cardiomyocytes (Guan et al. 2007). In 2008, the production of pluripotent stem cells from adult human testis was reported (S. Conrad et al. 2008), but described methodology and results presented in this publication were soon questioned by the group of Hans Schöler (Ko et al. 2010), with similarities to the scandal surrounding the first patient-specific stem cells from therapeutic cloning (see previous section). The original article, however, is not yet retracted, but is matter of scientific debate.

Induced pluripotent stem cells (iPSCs)

Despite their robust cardiomyogenic potential, the method of production of ESC and their allogeneic origin, bearing the risk of immunological responses, are the major reasons for the search of other, autologous, and therefore patient specific alternatives to ESCs. To date, the most promising approach to robustly and stably derive pluripotent stem cells, yet oocyte-independent and of autologous origin, is a technique termed reprogramming.

In 2006, Takahashi and Yamanaka showed the first reversion of a differentiated somatic cell back to the state of pluripotency. It depends on the overexpression of the four transcription factors (TFs), i.e. octamer binding transcription factor 3/4 (Oct3/4, or Oct4), Sry-related high mobility group box transcription factor (Sox2), cellular myelocytomatosis oncogene (c-Myc), which can be combined in the abbreviation “OSKM” (Takahashi & Yamanaka 2006). Oct4, Sox2 and Klf4 together with their downstream target Nanog are key regulators of pluripotency (Schöler et al. 1990; Silva et al. 2009). The TF c-Myc was shown to negatively regulate differentiation and enhance proliferation (Adhikary & Eilers 2005). Moreover, c-Myc controls the chromosomal permissiveness for other factors, e.g. Oct4 and Sox2 by regulation of histone modifications (Takahashi & Yamanaka 2006) and in this context enhances efficiency of reprogramming. Later, others have developed different reprogramming strategies, but the detailed mechanisms are not yet completely uncovered (Na et al. 2010; L. David et al. 2011a). Just one year later, the generation of iPSCs from human somatic cells was independently reported by Yu et al., who exchanged the factors

Klf4 and the oncogene c-Myc, with Lin28 and Nanog (Yu et al. 2007), and Takahashi and colleagues with the original set of transcription factors (Takahashi et al. 2007). Phenotypic similarity to ESCs together with robust cardiomyogenic potential of these cells was soon described by several groups for mouse, rabbit and human iPSC clones, derived from different cell types, such as embryonic fibroblasts, adult fibroblasts and umbilical cord blood cells (Mauritz et al. 2008; Honda et al. 2010; Haase et al. 2009). Next to their incomplete characterization, one major concern preventing the application of these cells to the clinic is that the original iPSC technology was based on viral-mediated genomic integration of the necessary TFs. The latter bears the risk of insertional mutagenesis (Baum 2004). Recent publications, however, showed that reprogramming does not necessarily depend on viral vectors and/or stable integration of reprogramming factors (Jincho et al. 2010; Okita, Nakagawa, Hyenjong, Ichisaka & Yamanaka 2008b), thus clinical application of iPSCs can be envisioned in the near future. Another obstacle was the labor-intensive and costly generation of human iPSC-derived cardiomyocytes in relevant numbers for clinical application. Therefore, BurrIDGE and colleagues systematically analyzed more than 45 culture condition variables to raise the amount of cardiomyocytes from both, ESCs and iPSCs. This led to a dramatic increase of up to 90% of cardiomyocytes in the resulting populations for both, iPSCs and ESCs, indicating the high similarity of both cell types (BurrIDGE et al. 2011).

Similar to cardiovascular progenitors derived from ESCs, i.e. KDR⁺ cells (see ESC-section), iPSCs were shown to give rise to the same population, which could be FACS-sorted and also differentiated into cardiac cells after transplantation in infarcted mouse hearts and improved function (Mauritz et al. 2011). Since, in contrast to cardiomyocytes, these cells are still proliferative, this approach could also be helpful in generating large numbers of progenitor cells. Eventually, this could result in relevant numbers of cells from the cardiac lineage, i.e. endothelial and vascular smooth muscle cells, for future clinical applications.

1.3.6 Direct reprogramming of somatic cells into cardiomyocytes

To avoid the risk of tumor formation, an inherent property of pluripotent stem cells, a technique resembling the principles underlying the iPSC approach is examined. Reprogramming somatic cells with TFs to a state of elevated potency, but with a lower extent compared to iPSCs was reported in 2010 by Ieda and colleagues (Ieda et al. 2010). In this recent study, the aim of reprogramming was to convert specialized differentiated cells. Instead of using factors conferring pluripotency, as used for iPSC development, here overexpression of GATA4, Mef2c, Tbx5 known to play key roles in cardiac development has been shown to be able to reprogram murine embryonic, and postnatal cardiac, or skin fibroblasts to cardiomyocytes. Although, this approach has to be confirmed by independent research, it is a very interesting way to generate cardiomyocytes from adult cells circumventing the pluripotent state of reprogrammed cells. Ultimately, this could result in an *in vivo* application strategy of myocardial regeneration, comparable to the approach of induced CM cell-cycle re-entry described by Hassink, or Bersell (Hassink et al. 2008; Bersell et al. 2009) (see section 1.3.3).

1.4 Enrichment methods for heart cells

Since it has been shown that after transplantation into the heart, pluripotent stem cells can lead to the formation of teratoma, which contain cells of all three germ layers (Kolossov et al. 2006; Nussbaum et al. 2007), particular attention has to be paid on eliminating persistent pluripotent stem cells in cardiomyocyte preparations for regenerative approaches. There are several methods described to enrich primary and stem cell-derived cardiomyocytes. A genetic approach is the generation of transgenic cells with a construct allowing for selection provided by a cardiac-specific alpha myosin heavy chain (α MHC) promoter-driven antibiotic resistance (Klug et al. 1996). During *in vitro* cardiomyogenesis, this promoter turns on antibiotic resistance in cardiomyocytes only, and supplementation of culture medium with the selective antibiotic eliminates all non-resistant cells. Eventually, cardiomyocyte populations with >99% purity have been reported (Klug et al. 1996; Kolossov et al. 2006; Liau et al. 2011). As already described in the iPSC section, a main disadvantage of genetic

manipulation is the risk of insertional mutagenesis (Baum 2004). Therefore, non-genetic enrichment approaches are of high interest. An alternative method is to enrich cardiomyocytes using a discontinuous percoll gradient centrifugation, exploiting the specific cell density of cardiomyocytes, reported for cell preparation derived from neonatal rat heart (Wollert et al. 1996) and for embryonic stem cell-derived cardiomyocytes with more than 45% purity (Guo 2006). However, a large proportion of undefined cell types results from this method, and moreover in the latter study it was not assessed, whether persisting pluripotent stem cells could be excluded. Therefore, this enrichment method might not be feasible for transplantation aspects due to the risk of tumor formation. Two non-genetic approaches based on cytometry means have recently been reported. One strategy is to enrich CMs by antibody-based surface marker detection. Successful identification and exploitation of CM surface markers for enrichment has been reported for activated leukocyte cell-adhesion molecule (ALCAM) (Rust et al. 2009) and vascular adhesion molecule 1 (VCAM1) (Uosaki et al. 2011). Magnet-assisted cell separation (MACS) for CM enrichment and fluorescence-activated cell sorting (FACS) reanalysis revealed purities between 65 – 98%. To avoid time-consuming immunologic cell labeling procedures, Hattori and colleagues recently presented another cytometric approach (Hattori et al. 2009). Their study showed that the non-toxic mitochondrial dye tetramethylrodamin methyl ester (TMRM) is accumulated in cells proportionally to their metabolic activity. In differentiation cultures of pluripotent stem cells of human and murine origin, this phenomenon was exploited to purify TMRM^{bright} cells by FACS sorting. The resulting populations were highly enriched for CMs (>99%) and no signs of pluripotent stem cells were present. These CMs could be transplanted into mouse hearts and survived. However, besides the lack of data on beneficial effects in terms of functional improvements on infarcted hearts, it remains unclear whether this method is efficient enough to produce sufficient numbers of CMs needed for replacement therapies. Moreover, this method has yet to be reproduced independently by other researchers.

1.5 Effects of single cardiomyocyte transplantation into infarcted hearts

Direct application of selected pluripotent stem cell-derived cardiomyocytes in infarcted mouse hearts has been shown to lead to functional improvements (Klug et al. 1996; Kolossov et al. 2006), but electromechanical integration was lacking. Besides low survival rates of injected cells into the myocardium, i.e. less than 40%, the majority of cells were lost within the first few hours after injection (Qiao et al. 2009). The dramatic loss of injected cells, putatively based on anoikis, a phenomenon describing cell death following cell dissociation (Zvibel et al. 2002) can be hampered to a certain extent by the application of pro-survival factors prior to transplantation (Laflamme et al. 2007). However, a large proportion of cells does not stay at their desired area, but can be found in the lung, liver, kidneys, and spleen (Dow et al. 2005). Also, there have been reports of potential risks of inflammation evoked by injection of large numbers of single cells into the heart (Suzuki et al. 2004; Fukushima et al. 2007). Moreover, beneficial effects observed after cell transplantation might be explained by these responses only, instead of effects specifically mediated by cardiomyocytes, since a variety of cells and even cell free medium, i.e. phosphate buffered saline, injected into control infarcts had comparable effects (Mauritz et al. 2011; Laflamme & Murry 2011).

In conclusion, induced autologous heart regeneration, or limitation of pathological effects by chemical compounds, and the strategy to transplant cells of different phenotypes, were shown to improve heart function to a certain extent. Nevertheless, detailed analyses of mechanisms underlying these effects have to be performed, to exclude unwanted long term implications, like tumorigenesis, or inflammation. Due to the lack of spatial precision of these more globally administered techniques, clinical application might be difficult to achieve in the near future.

Another strategy for the regeneration of infarcted hearts is the application of preformed and well-characterized heart muscle tissue constructs, generated *in vitro*. This approach is termed tissue engineering.

1.6 Tissue engineering

Tissue engineering (TE) is defined by the combination of cells and matrices to fabricate functional tissue *in vitro* in order to regenerate, or remodel parts of damaged, or malfunctioning organs, or the whole organ itself. The general principle is depicted in figure 5, showing the critical factors, which allow for successful TE *in vitro*, when appropriately selected and applied (Moreno-Borchart 2004). Several tissue engineered constructs have been shown to be applicable in human regenerative therapy, e.g. tissue engineered bladders (Atala et al. 2006) or skin (Horch et al. 2005; Hunziker et al. 2006; Shevchenko et al. 2010). Hence, this approach might also be transferrable to the cardiac system.

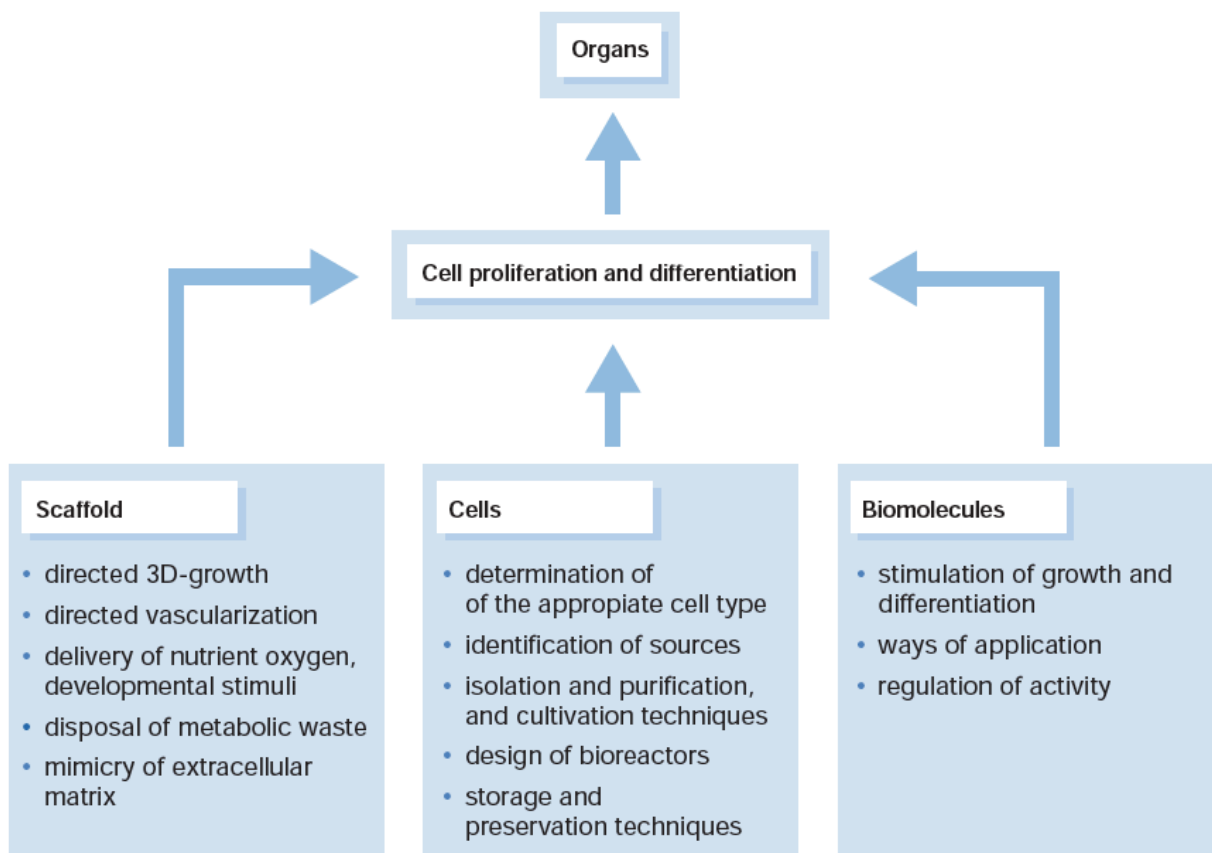


Figure 4: The three pillars of tissue engineering. From: Moreno-Borchart 2004.

1.6.1 Cardiac tissue engineering

The aim of cardiac tissue engineering is to produce solid tissue to replace large areas of defective myocardium, either as a result of myocardial infarction, or based on congenital defects (Kreutziger & Murry 2011; Eschenhagen 2011). This desired tissue construct has to be three-dimensional with enough passive strength to withstand the hemodynamic pressure in damaged areas of the ventricle. For myocardial tissue engineering (MTE) approaches aiming to replace damaged myocardium, it has to be flexible and strong enough to support heart function, but at the same time must not interfere with the recipient's frequency, to avoid fibrillation and arrhythmias. Due to the high metabolic activity of contracting cardiomyocytes, it has to connect to the host vasculature, to be provided with oxygen and nutrients and prevent hypoxia induced necrosis. Besides the desired combination of all properties mentioned above, it has also been shown that even non-contractile, cardiomyocyte-free engineered tissue patches can improve myocardial function to a certain extent, as has recently been reported for a chronic heart failure model (Lancaster et al. 2010).

Next to regenerative purposes, cardiac tissue engineering could be used to give insights into normal and pathological organogenesis, the development of cardiomyopathies *in vitro* and serve as a tool for human disease modeling. Recent advances in iPSC technology showed the possibility to generate pluripotent stem cells from patients with pathological heart conditions, e.g. long QT-syndrome, and to differentiate cardiomyocytes from these cells showing the pathological phenotype (Moretti et al. 2010; Itzhaki et al. 2011). Using these cells for cardiac tissue engineering could improve cardioactive drug screening for future therapies, as has been shown in 2D cultures of human ESC-derived cardiomyocytes (Caspi et al. 2009). Moreover, Hansen and colleagues showed that large scale *in vitro* analyses of pharmacologically interesting compounds in a 3D environment is a feasible method (Hansen et al. 2010).

1.6.2 Cell sources for cardiac tissue engineering

Primary cells

For establishment and improvement of cardiac tissue engineering strategies and for transplantation experiments, primary-derived cells, such as embryonic chick heart cells, neonatal mouse and rat heart cells are commonly used for proof-of-concept studies (Eschenhagen et al. 1997; Zimmermann et al. 2000; Fink et al. 2000).

Stem cells

As described in section 1.3.4, not all types of stem cells have the potential to generate sufficient numbers of cardiomyocytes, i.e. the essential cell type of contractile cardiac tissue patches. Therefore, due to their robust and well-characterized cardiomyogenic differentiation capacity, strong focus lies on ESC and iPSC derivatives for the application to cardiac tissue engineering. Interestingly, engineered cardiac constructs using cardiomyocytes derived from pluripotent stem cells do not behave comparable to constructs made with primary cardiomyocytes. Cell densities necessary to yield contractile tissue from stem cells are much higher compared to preparations with primary cells and exerted forces of most of these constructs are by far not as high as published data for neonatal rat cardiomyocyte-derived counterparts prepared and conditioned in a similar manner (Guo 2006; Shimko & W. C. Claycomb 2008; Tulloch et al. 2011). However, preparations of constructs with a combination of autologous primary (stem) cells, such as fibroblasts, or MSCs with *in vitro* generated cardiomyocytes were shown to produce better results than cardiomyocyte only approaches (Tulloch et al. 2011; Liao et al. 2011). This indicates, that the immature phenotype and highly artificial origin of these pluripotent stem cell-derived cardiomyocytes need novel MTE strategies to achieve heart muscle constructs that are comparable with state-of-the-art primary cardiomyocyte-based tissue engineered products.

1.6.3 Matrices

To allow cells to interact with each other and to provide stability, appropriate scaffold material is necessary in classical tissue engineering approaches. The materials used for cardiac tissue engineering vary from proteins present in the extracellular matrix of mammalian tissue such as collagens, fibrin, or carbohydrate polymers, to synthetic polymers, which are biocompatible, in part biodegradable and already in clinical use, such as polyurethane, poly-L-lactic acid and poly-glycolic-acid summarized in a review by Giraud (Giraud et al. 2007). Synthetic polymers have the advantage of low production costs and less quality variations, which are intrinsic to the processes of natural material production. Furthermore, biopolymers foreign to mammalian organisms, but biocompatible in medical terms are being used in cardiac tissue engineering, like Alginate from seaweed (Gerecht-Nir et al. 2004; Möller et al. 2011), or Chitosan derived from marine crustaceans (Blan & R. K. Birla 2008).

1.6.4 Cardiac tissue engineering strategies

Since there are various possibilities to combine cells with matrices to result in three-dimensional tissues, in cardiac tissue engineering several approaches have been studied with different success rates in terms of functionality. Some of these approaches have been shown to work and survive for a reasonable time *in vitro* and *in vivo*, and have characteristics similar to native heart muscle. Other strategies can be considered as proof-of-principle only, to show that cells seeded onto, or into matrices survive, and have cardiac properties to some extent. Nevertheless, all of the mentioned approaches might contribute to the improvement of already well-established tissue engineering approaches.

1.6.4.1 Cell seeding onto porous scaffolds

One classic tissue engineering strategy is to seed cardiac cells onto preformed porous scaffolds, and many studies have shown that this approach leads to three-dimensional contractile cardiac tissue constructs (Gerecht-Nir et al. 2004; Gerecht-Nir et al. 2006; Blan & R. K. Birla 2008; Barash et al. 2010; Möller et al. 2011). One

advantage of these scaffolds is, that they can be designed to harbor different compartments, e.g. for cells to attach in the desired manner, or force them into certain shapes, which can be used to perfuse the constructs with medium through pre-existing channels (Radisic et al. 2006; Radisic et al. 2007). As shown in these studies, the disadvantage is that the majority of seeded cells does not penetrate into these scaffolds to a large extent, but mainly populate the surface area of these scaffolds only. Moreover, these constructs do not exert relevant active forces, most probably due to the rigidity of the scaffolds against which the cardiomyocytes have to contract. This rigidity, however, might provide sufficient passive strength to support pump function of the remaining working myocardium needed in dilated areas of the infarcted ventricle.

1.6.4.2 Repopulation of decellularized scaffolds

Several studies have been performed to test whether it is possible to repopulate cadaveric tissue, which was decellularized before, i.e. by using detergents. A spectacular publication showed the effects of injecting primary cardiomyocyte populations into decellularized hearts of newborn rats (Ott et al. 2008). In this study, the given cell-free extracellular matrix structure of a former working heart served as a template to allow seeded cells to repopulate the tissue and regain function to some extent, i.e. leading to contractions of the whole construct when electrically stimulated. This seems to be an appealing strategy, since surgeons could personalize a cadaveric heart with cells matching the recipient's immune system and therefore reducing the risk of rejection. Besides the fact, that this method would still depend on organ donors it has not yet been shown to work after implantation, and appropriate function in terms of generated forces is questionable, since the presented morphology and distribution of reseeded cardiomyocytes was not mature and very heterogeneous. Furthermore, it remains unclear, whether the seeding efficiency would be higher in human hearts with even larger and thicker areas to be repopulated. Another reseeded approach is to take advantage of preserved vessel structures of decellularized porcine small intestine to surgically connect the implanted graft to the circulation of the recipient. The rationale behind this strategy is to prevent

hypoxic conditions within a large three-dimensional cardiac graft, which would eventually lead to necrosis of cardiomyocytes (Mertsching et al. 2005). Utilizing the present vasculature to provide vessel scaffolds for applied endothelial cells resulted in a patch with a network of partly repopulated vascular structures (Bar et al. 2010). Although the necessity to vascularize engineered cardiac tissue is of high concern in cardiac tissue engineering, no combination of this approach with cardiomyocytes has yet been reported and therefore, neither the benefit of this approach in terms of cardiomyocyte survival, nor contraction force data is available. In approaches of repopulating cell-free cadaveric structures the remaining risks of rejection, or inflammation due to incomplete decellularization, and interspecies antigens when xenogeneic material is used have to be analyzed (see section 1.3.1). Nevertheless, improvements in this field could eventually result in a combinational strategy for highly contractile tissue patches, with connections to the recipient's vasculature.

1.6.4.3 Cell (-aggregate) printing

The survival of cells seeded onto scaffolds by using a modified bubble-ink jet printer has been shown with different mammalian cell types (T. Xu et al. 2005), as well as laser directed printing of three-dimensional tissue (Ringeisen et al. 2004; Gruene et al. 2011). For cardiac tissue engineering Jakab et al. showed proof-of-concept that this method could be applied to cardiomyocyte / endothelial cell aggregates printed into pre-conditioned elastic collagen scaffolds, which led to contractile tissue with vessel-like structures within the constructs (Jakab et al. 2008). Next to the intriguing method of printing three-dimensional tissues, and eventually perhaps whole organs *de novo*, it has to be shown first, that resulting tissue patches are feasible for myocardial repair *in vivo*, since the presented morphology of cardiomyocytes did not show a mature phenotype and neither active nor passive force have been reported. Nevertheless, future improvements might result in precise spatial printing of cells into certain patterns and therefore enhancing tissue properties.

1.6.4.4 Mixing of cells with liquid scaffolds

A different principle is the use of liquid scaffolds, that exploit the self-assembly of certain extracellular matrix proteins by pH -, or temperature-sensitive properties, resulting in gel-like structures (Leikin et al. 1994; Kleinman et al. 1986). When cells are added to the mixture prior to consolidation, a homogeneous distribution of single cells throughout the tissue can be achieved. Depending on the cell types and conditions used, ongoing culture leads to formation of tissue with interconnected cells, which reorganize the provided extracellular matrix. Eschenhagen and colleagues, who used primary embryonic chick cardiomyocytes, introduced this principle to cardiac tissue engineering first (Eschenhagen et al. 1997). Ultimately, the generated tissue showed mature, anisotropic cardiomyocytes with aligned orientation and spontaneous contractions of the whole tissue with measurable forces. Since then, many studies based on this strategy confirmed and improved the robustness of this tissue engineering approach even with tremendous variations in tissue geometry and size (fig. 5 A – C). All of these approaches resulted in spontaneously contracting organoids with measurable active forces. The majority of these studies used primary cardiomyocytes (Fink et al. 2000; Yildirim et al. 2007; Hansen et al. 2010), but also stem cell-derived cardiomyocytes were utilized (Guo 2006; Shimko & W. C. Claycomb 2008; Tulloch et al. 2011; Schaaf et al. 2011).

Next to isotropic contraction measurements showing the Frank-Starling mechanism of the heart, detailed analysis of chronotropic and dromotropic responses to cardioactive drugs, or varying calcium levels was possible with tissue generated with this method. Even without structurally preformed vessels within these constructs, as described in previous sections, connection to the host's vasculature and functional improvement after transplantation onto defective myocardium was shown in rats (Zimmermann et al. 2006).

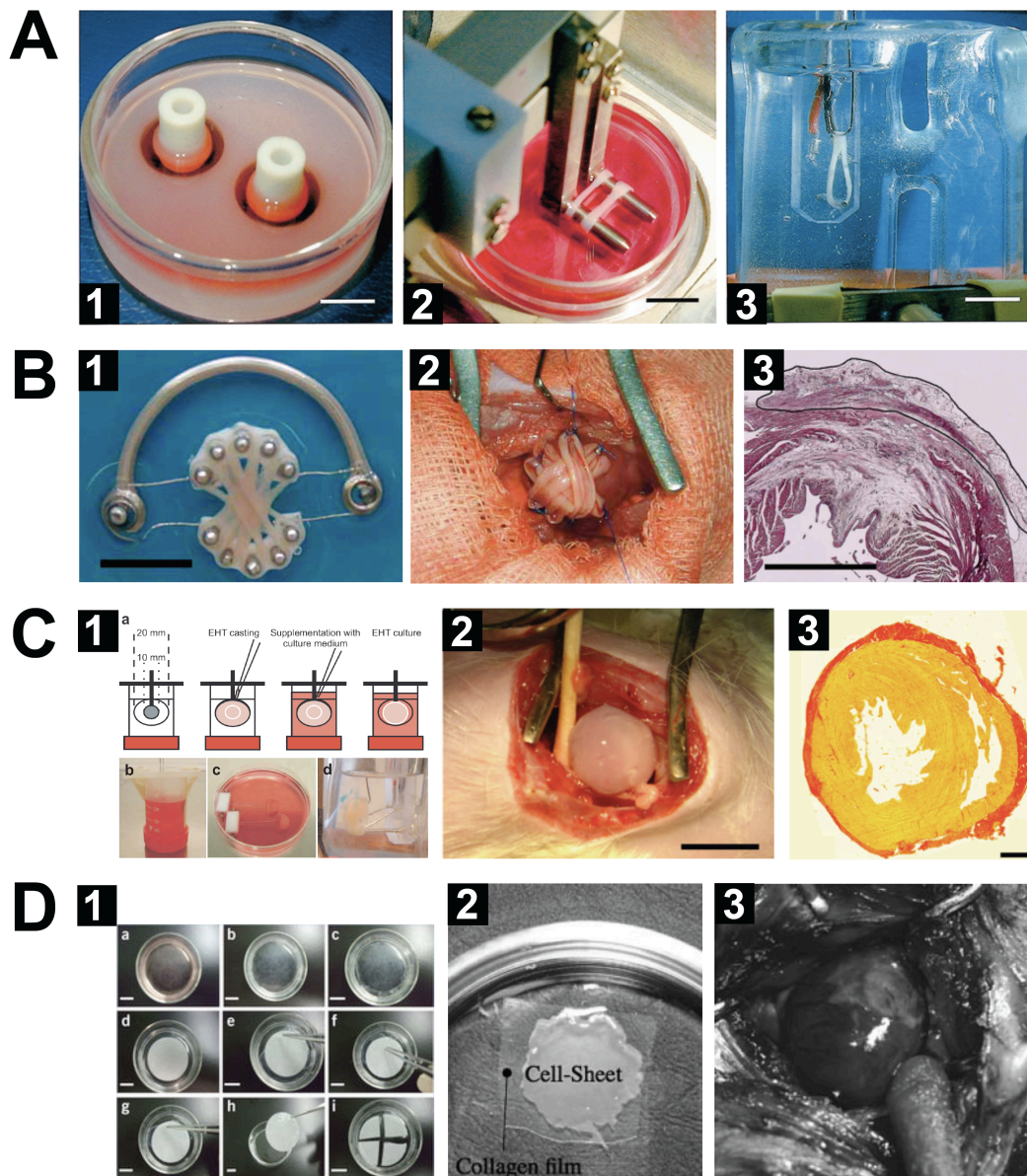


Figure 5: Cardiac tissue engineering strategies known to improve heart function, or electrically interconnect to the host myocardium *in vivo*. **A-C:** Contractile tissue produced by the combination with liquid matrix compounds and cells. **A:** Ring-shaped contractile tissue. 1: Self-assembled rings of tissue after casting on day four. 2: Mechanical conditioning in a stretch device. 3: Final force measurement in an organ bath on d14 (Zimmermann 2001). **B:** Multi-ring cardiac tissue construct. 1: Mechanical conditioning of an engineered tissue consisting of five stacked rings that contract synchronously. 2: Implantation onto infarcted area of a rat heart. 3: histological section of the left ventricular wall shows engraftment and survival after 28 days *in vivo* (Zimmermann et al. 2006). **C:** Pouch-like cardiac tissue. 1 Generation principle (a), cultivation (b), mechanical conditioning (c), and force measurement of pouch-like tissue (d). 2: Implantation around the heart of an adult rat. 3: Picosirius red stained section of an explant. Engineered tissue survived two weeks after implantation (Yildirim et al. 2007). **D:** Multilayered cardiac tissue generated with the cell sheet technology. 1: Production of cell sheet with temperature-dependent detachment of an intact layer of cardiomyocytes (a-c). Attachment onto a PVDF membrane (d-f), transfer onto a second previously detached layer of cells (g-f). 2: Multilayered cardiac cell sheet on collagen film for implantation. 3: Implantation onto the infarcted area of the heart of nude rat (Furuta et al. 2006).

1.6.4.5 Scaffold-free approaches

In contrast to the classical scaffold-based approach, it has been shown that it is not necessary to add additional scaffold compounds to the cells, but employ the matrix produced by the cells themselves. One approach is to utilize the ability of cells to aggregate in suspension culture, leading to tissue-like constructs using primary and human pluripotent stem cell-derived cardiomyocyte populations (Akins et al. 1999; Stevens et al. 2009). Both cell types led to spontaneously contracting tissue and, for the latter, passive forces similar to native myocardium and transplantation onto rat hearts was reported. Another approach to test whether additional extracellular matrices are dispensable was done by utilization of the compound poly(N-isopropylacrylamide) (PIPAAm), which changes from hydrophobic to hydrophilic properties in a temperature-dependent manner resulting in detachment of cell sheets in tissue culture (Okano et al. 1993). Primary cardiomyocyte populations were cultured on tissue culture plastic covered with PIPAAm and a decrease to temperatures below 21°C led to complete detachment of intact monolayers without enzymatic treatment, which then were able to be stacked to form three-dimensional tissue patches, as shown in figure 5 D (Shimizu et al. 2002; Shimizu et al. 2003; Furuta et al. 2006). It was reported that after transplantation onto infarcted hearts these constructs connect electrically to the host and have beneficial effects in terms of regaining heart function. However the interconnection between these stacked cell sheets seemed not to be very tight, if present at all, as has been reported in a recent study (Hata et al. 2010). For all matrix-free approaches, active force measurements have not been presented yet.

In contrast to direct application of cardiomyocytes to the infarcted heart, the main advantages of tissue engineering over these cell-based strategies are to efficiently define, characterize, and improve properties of three-dimensional engineered cardiac tissue *in vitro* prior to *in vivo* experiments (Eschenhagen 2011). Moreover, another benefit of tissue engineering is the precise spatial application of generated constructs to the damaged area, in contrast to the more or less random application via intra-coronary or ventricular injection and integration of single cells into the infarcted heart.

The superiority of the tissue engineering approach in terms of preciseness and persistence of applied cells was shown in a recent study, comparing these two approaches side by side (Sekine et al. 2011). Since myocardial tissue engineering is strongly depending on the provision of sufficient numbers of relevant cells, reports on improvements of differentiation strategies and up-scaling techniques are rapidly assessed and adopted in this emerging field.

1.7 Bioreactors in cardiac tissue engineering

It turned out that mechanical and electrical conditioning of engineered cardiac tissue leads to enhanced cell maturation and tissue formation in constructs based on primary cardiomyocytes (Fink et al. 2000; Radisic et al. 2004; Maidhof et al. 2011). For stem cell-derived cardiac tissue, mechanical stimulation was also shown to enhance forces (Guo 2006; Tulloch et al. 2011). Therefore, strategies in bioreactor design for cardiac tissue engineering try to combine these stimulation capacities (Fink et al. 2000; Akhyari et al. 2002; Zimmermann 2001; Zimmermann et al. 2006; R. K. Birla et al. 2007; Hansen et al. 2010; Barash et al. 2010). However, none of these bioreactor systems combines these features with detailed assessment functions, i.e. the possibility to evaluate forces, during mechanical load and electrical stimuli in a variable manner over the whole cultivation period in one single device. This would allow for repeated assessment of active and passive mechanical properties of tissue-engineered constructs over the whole cultivation period. One of the most critical time points during cardiac tissue engineering is the initial phase of tissue formation. As described by Tiburcy and colleagues in a primary cell-based cardiac tissue engineering approach, the majority of cell loss happens during the first three days of culture (Tiburcy et al. 2011). Therefore, an option for microscopic observation of changes in morphology during the initial phase of tissue culture would be of high interest. Improvement of cell survival could be addressed by changes in tissue preparation methods, and the application of factors that enhance survival described for stem cell-derived cardiomyocytes in a transplantation model (Laflamme et al. 2007), could be assessed *in vitro*. Suitability of alternative matrix components with respect to future clinical applications could also be observed during the critical initial

tissue formation. Moreover, fluorescent labeling of cells within the tissue either by marker expression or by fluorescent dyes could help to elucidate the function of specific cell types within the tissue, or the impact on tissue formation by different treatments over the entire cultivation time. Additionally, to simplify long-term culture, to allow for easy application of cardiotropic compounds and to reduce the risk of contamination, another desired function would be a perfusion system.

Advanced automated bioreactors that combine these properties would greatly enhance progress in stem cell-based myocardial tissue engineering by simplifying processes and analyses without the need to switch from stimulation to assessment systems. Especially the demand for new stimulation and cultivation approaches, indicated by the lack of comparable tissue formation and mechanical properties in stem cell-derived cardiac constructs, as mentioned above, increases the necessity for such versatile devices.

In summary, there are several strategies to engineer, modulate and stimulate myocardial tissue patches *in vitro*, with many of these approaches serving as proof-of-concept studies due to their focus on cardiomyocyte survival mostly resulting in contractile tissues. However, most of these organoids lack the proof of generating significant active forces, or fail to show that these tissues follow the Frank-Starling mechanism of the heart. These properties, resembling native and mature myocardium, are essential to consider myocardial tissue engineering for future clinical application as an alternative to heart transplantation. To date, the only approach that matches these properties and that has been reported independently by several research groups is the combination of cells with liquid, but rapidly consolidating matrix components, which also served as the basis for tissue-engineered constructs in the presented thesis.

2 Objectives

Since the heart has little regenerative capacities to restore larger defects after severe myocardial infarction, and donor organs for allogeneic heart transplantations are rare, research is focusing on alternatives.

In this study the feasibility of combining existing protocols for myocardial tissue engineering, based on primary cell populations, with a novel source for cardiomyocytes, i.e. murine induced pluripotent stem cells (miPSCs), was assessed.

To provide a reliable method for the assessment of prepared tissue constructs, a novel bioreactor system had to be designed. Next to the necessity of miniaturization, due to limited numbers of pluripotent stem cell (PSC)-derived cardiomyocytes generated by current protocols, the desired properties of this system were: i) the possibility to assess tissue constructs in wide-field fluorescence microscopic set ups over the whole cultivation period, ii) mechanical and electrical stimulation capacities, iii) non-invasive, continuous assessment of active and passive mechanical properties for repeated measurements, and iv) capacity to apply perfusion. Yet, this system should also allow for production of constructs with transplantable size for small animal models. To assess performance and robustness of this bioreactor system, primary cell population-based constructs were generated and stimulated mechanically and pharmacologically, to reproduce published data concerning mechanical and histological properties of state-of-the-art primary cell-based myocardial tissue engineered organoids (Zimmermann et al. 2006). The feasibility of extracellular matrix modulation in tissue constructs by a novel optical manipulation method, i.e. photosensitizer-dependent two-photon induced collagen cross-linking, was assessed. Here, cell viability in treated constructs and active and passive forces were analyzed in the bioreactor system.

Murine iPSCs were included into the novel bioreactor system. Since PSCs have the potential to generate teratomas after transplantation *in vivo*, a stringent purification system had to be established. To do this, a cytometric and a genetic approach were compared. For the genetic selection, a miPSC clone stably expressing an antibiotic

resistance gene under the control of a myocardial promoter (α myosin heavy chain, α MHC) had to be established and characterized. Furthermore, cardiogenic differentiation and selection protocols had to be adjusted to achieve optimal cardiomyocyte purities and numbers. To include iPSC-derived cardiomyocytes into myocardial tissue engineering, different approaches were analyzed for tissue generation, including different cell densities and application formats, i.e. single cells and cell aggregates, and the addition of other cell types to the cell/matrix composition. Furthermore, impact of ascorbic acid was evaluated and effects of a novel mechanical stimulus, i.e. growing stretch, was compared with conventional cyclic stretch stimulation. In terms of cardiomyocyte maturation and mechanical properties of resulting tissue, assessment was done in detail by gene expression analysis, mechanical testing and histology and by long-term microscopic observation.

3 Manuscripts

3.1 A Novel Miniaturized Multimodal Bioreactor for Continuous *In Situ* Assessment of Bioartificial Cardiac Tissue during Stimulation and Maturation (Manuscript 1)

Authors: George Kensah*, Ina Gruh*, Jörg Viering, Henning Schumann, Julia Dahlmann, Heiko Meyer, David Skvorc, Antonia Bär, Payam Akhyari, Alexander Heisterkamp, Axel Haverich, and Ulrich Martin

*authors contributed equally

Published in Tissue Engineering Part C: Methods, Volume 17, Issue 4, April 1, 2011, pp 463 – 473

Design, assembly and software control of the bioreactor system:

The design of bioreactor system with and selection of its components was done in cooperation with the Department of Medical Device Construction, Hannover Medical School, Hanover. Jörg Viering, Michael Breyvogel, Jörg Claus, Juri Huber, and Eric Mahnke did assembly of (electro-) mechanical components of the bioreactor system. LabView-based Software to control mechanics and sensor-systems of the bioreactor was done in collaboration with Henning Schumann.

Payam Akhyari (Clinic for Cardiovascular Surgery, Heinrich Heine University Düsseldorf, Düsseldorf, Germany) contributed to bioreactor design.

RNA-dependent gene analyses:

Ina Gruh and Julia Dahlmann did RNA isolation and quantitative real time PCR, as well as data analyses (Medical School Hannover, Hanover, Germany).

Optical projection tomography:

Heiko Meyer (Biomedical Optics Department, Laser Zentrum Hannover e.V.) analyzed DAPI-stained BCTs by means of optical projection tomography.

Preparation of the manuscript:

The manuscript was written in collaboration with Ina Gruh and Ulrich Martin.

A Novel Miniaturized Multimodal Bioreactor for Continuous *In Situ* Assessment of Bioartificial Cardiac Tissue During Stimulation and Maturation

George Kensah,^{1,2,*} Ina Gruh, Ph.D.,^{1,2,*} Jörg Viering,³ Henning Schumann, Ph.D.,³
Julia Dahlmann,^{1,2} Heiko Meyer, Ph.D.,^{2,4} David Skvorc,^{1,2} Antonia Bär, Ph.D.,^{1,†} Payam Akhyari, M.D.,^{1,‡}
Alexander Heisterkamp, Ph.D.,^{2,4,5} Axel Haverich, M.D.,^{1,2} and Ulrich Martin, Ph.D.^{1,2}

Stem cell-based cardiac tissue engineering is a promising approach for regenerative therapy of the injured heart. At present, the small number of stem cell-derived cardiomyocytes that can be obtained using current culture and enrichment techniques represents one of the key limitations for the development of functional bioartificial cardiac tissue (BCT). We have addressed this problem by construction of a novel bioreactor with functional features of larger systems that enables the generation and *in situ* monitoring of miniaturized BCTs. BCTs were generated from rat cardiomyocytes to demonstrate advantages and usefulness of the bioreactor. Tissues showed spontaneous, synchronized contractions with cell orientation along the axis of strain. Cyclic stretch induced cardiomyocyte hypertrophy, demonstrated by a shift of myosin heavy chain expression from the alpha to beta isoform, together with elevated levels of atrial natriuretic factor. Stretch led to a moderate increase in systolic force (1.42 ± 0.09 mN vs. 0.96 ± 0.09 mN in controls), with significantly higher forces observed after β -adrenergic stimulation with noradrenalin (2.54 ± 0.11 mN). Combined mechanical and β -adrenergic stimulation had no synergistic effect. This study demonstrates for the first time that mechanical stimulation and direct real-time contraction force measurement can be combined into a single multimodal bioreactor system, including electrical stimulation of excitable tissue, perfusion of the culture chamber, and the possibility of (fluorescence) microscopic assessment during continuous cultivation. Thus, this bioreactor represents a valuable tool for monitoring tissue development and, ultimately, the optimization of stem cell-based tissue replacement strategies in regenerative medicine.

Introduction

THE PREVALENCE OF CARDIOVASCULAR DISEASE has been increasing over the past years with symptoms ranging from mild impairments to severe conditions, ultimately requiring heart transplantation.¹ Tissue engineering strategies may provide new therapeutic options for the treatment of cardiovascular disease. Notably, especially in the case of congenital malformations, the transplantation of bioartificial cardiac tissue (BCT) generated *in vitro* may be superior to cell transplantation strategies in providing significantly greater functional support ameliorating cardiac performance.

In cardiac tissue engineering, scaffold materials have two major functions: providing a physiologic extracellular environment and stabilizing the constructs generated *in vitro*.^{2,3} One beneficial effect of artificial patch transplantation is the mechanical stabilization of injured tissue, thus preventing further dilation of ventricles and the risk of congestive heart failure.⁴

However, and in addition, the optimal tissue replacement construct should be able to exert contractile forces comparable to that of native cardiac tissue. With this in mind, the ideal cell source for cardiac tissue engineering would be patient-specific stem cell-derived cardiomyocytes. Cardiac

¹Leibniz Research Laboratories for Biotechnology and Artificial Organs, Department of Cardiac, Thoracic, Transplantation, and Vascular Surgery, Hannover Medical School, Hannover, Germany.

²REBIRTH-Cluster of Excellence, Hannover, Germany.

³Department of Medical Device Construction, Hannover Medical School, Hannover, Germany.

⁴Institute of Quantum Optics, Leibniz University Hannover, Hannover, Germany.

⁵Laser Zentrum Hannover e.V., Biomedical Optics Department, Hannover, Germany.

*These authors contributed equally to this work.

†Current affiliation: MediClin Heart Center Lahr/Baden, Lahr, Germany.

‡Current affiliation: Cardiac Surgical Research Group, Clinic for Cardiovascular Surgery, Heinrich Heine University Duesseldorf, Dues-seldorf, Germany.

differentiation has been demonstrated successfully for both embryonic stem cells^{5,6} and induced pluripotent stem cells^{7–10} from various species; however, these cells are currently not suitable for clinical application in patients due to the methods used in their generation. Despite recent promising results regarding scalable expansion^{11,12} and differentiation¹³ of embryonic and pluripotent stem cells, the available numbers of stem cell-derived cardiac cells have not been sufficient for the generation of BCT of appropriate sizes for therapeutic application so far. Therefore, the aim of this study was to generate a bioreactor for the development and testing of miniaturized bioartificial tissue, enabling small-scale stem cell-based cardiac tissue engineering.

It has been proposed that mechanical stretch can improve tissue formation and contractility of bioartificial cardiac grafts generated from primary chicken cardiomyocytes¹⁴ or cardiomyocytes of neonatal and fetal rodent origin.^{15,16} This has also been demonstrated for human heart cells seeded on gelatin scaffolds.¹⁷ Probable underlying mechanisms include a hypertrophic response of myocardium to a prolonged increase in cardiac workload (reviewed in ref.¹⁸). Analysis of the gene expression profile of neonatal ventricular rat cardiomyocyte cell cultures exposed to mechanical stretch *in vitro* showed increased expression of a number of genes, for example, heat shock protein 70, growth differentiation factor 15, and metallothionein-1.¹⁹ Interestingly, a robust change in expression levels of these genes was observed specifically after stretch-induced hypertrophy, whereas pharmacologically induced hypertrophy by treatment with phenylephrine yielded only moderate effects.¹⁹ Downstream targets of stretch-induced genes included several proteins of the cardiomyocyte contractile apparatus, as well as secreted proteins.^{20,21}

In the past, bioreactors were used to improve the mechanical properties of three-dimensional tissues generated *in vitro* from cardiomyocytes. However, it has been difficult to directly monitor the effects of mechanical stretch and other stimulants continuously during the course of tissue formation. Usually, measurements require transfer of the generated tissue from a cultivation vessel to a measurement device or organ bath chamber^{14,15,22}; therefore, force measurement has been predominantly used as an end-point analysis. With this approach, long-term data acquisition can only be managed with numerous replicate samples requiring a multiple of the cell numbers that would be needed in continuous analyses. Alternatively, indirect measurement of contraction forces via optical analysis has been proposed for noninvasive on-line monitoring during prolonged culture.²³

Herein we describe the design of a novel multimodal bioreactor for mechanical stimulation and real-time direct measurement of contraction forces under continuous sterile culture conditions. The bioreactor's transparent cultivation chamber allows for microscopic assessment of tissue development including fluorescence imaging. Additional functions include electric pacing of tissues, as well as the possibility to perfuse the central cultivation chamber, allowing for continuous medium exchange and/or controlled addition of pharmacologically active agents. In this study, our novel multimodal bioreactor was used to monitor the development of contractile properties during tissue maturation, investigating the effect of mechanical stretch in comparison to β -adrenergic stimulation with noradrenalin.

Material and Methods

Cell isolation

Neonatal rat cardiomyocytes were isolated from 1- to 3-day-old Sprague-Dawley rat pups as described previously²⁴ and enriched by discontinuous Percoll (GE Health Care) gradient centrifugation. During all experiments, the Principles of Laboratory Animal Care (NIH publication No. 86-23, revised 1985) as well as the Animal Welfare Law of Lower Saxony were followed.

Preparation of BCTs

A bipartite Teflon mold with a volume of 200 μ L was designed for BCT casting. Between the lower and the upper part, two titanium rods are held in position (distance 6 mm) and can be cast integrally with a liquid cell/matrix mixture. In brief, 10⁶ freshly isolated cardiomyocytes per construct were mixed with a liquid matrix based on rat tail collagen type I (R&D Systems) and Matrigel (BD Biosciences) as described by Zimmermann *et al.*¹⁵ BCTs were cast in the Teflon molds placed on agarose coated dishes; consequently, the bottomless molds allow for microscopic assessment of early tissue formation. After solidification, the tissue is suspended between the rods (Fig. 1A) and can be transferred to the cultivation chamber of the bioreactor. A detailed description of matrix and medium composition can be found in the online Supplementary Data (available online at www.liebertonline.com/tec).

Multimodal bioreactor system

A modular expandable bioreactor was designed to apply cyclic stretch to BCTs; each module connects a cultivation chamber to both a linear motor with integrated position measurement, and a force sensor (Fig. 1B, C). The bioreactor modules are placed in a standard cell culture incubator at 37°C, 5% CO₂, and 80% humidity (Fig. 1D). The cultivation chamber with a working volume of 1–8 mL was made of sterilizable polysulfone thermoplastic resin combined with a glass bottom for microscopic assessment. Two opposite mounting brackets hold the titanium rods and allow connection of the BCT to the linear motor on one side and the force sensor on the other via two opposing feedthroughs sealed with 0.2 mm silicon membranes to prevent medium leakage. Two lateral connections can be used for medium perfusion through the cultivation chamber; two fittings for electrodes integrated into the chamber lid allow for indirect electrical stimulation of the tissue embedded in conductive medium or Tyrode's solution (Fig. 1C). A stimulation current generator was developed for generating stimulation current pulses from 0 to 25 V with alternating polarity to prevent hydrolysis. Pulse width is software controlled ranging from 5 ms to 10 s. The linear motor consists of a PS01-235x80 stator and a PL01-12x130/80 slider and has a maximum stroke of 30 mm with a peak force of 44 N and a position repeatability of 0.01 mm, driven by an E400-AT servo controller (all from LinMot). The displacement is measured with an SM277 inductive displacement transducer (Schreiber Messtechnik). Forces are measured using a miniature bending beam load cell (Burster Praezisionsmesstechnik) with a measuring range of 0–1 N.

In this setting, the cultivation chambers can be easily detached from the bioreactor without leakage; therefore, they are

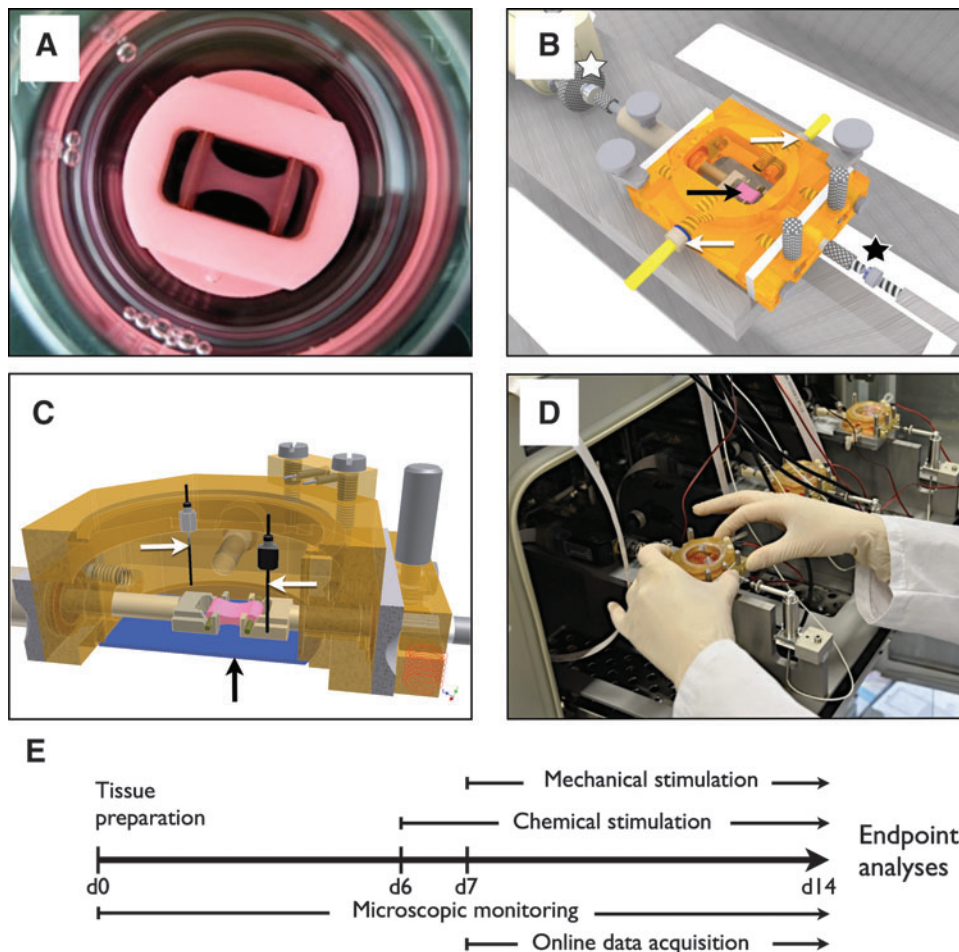


FIG. 1. Multimodal modular bioreactor system and experimental design. For bioartificial cardiac tissue (BCT) casting, a bipartite Teflon mold (A) was designed. Between the lower and the upper part, two titanium rods are held and can be cast integrally with a liquid cell–matrix mixture. After solidification, the tissue is suspended between the rods and can be transferred to the cultivation chamber of the bioreactor (depicted in B). Here, mounting brackets hold the rods (black arrow) and allow connection of the BCT to the linear motor (white asterisk) and the force sensor (black asterisk). Two lateral connections (white arrows) can be used for medium perfusion through the cultivation chamber. A glass bottom (black arrow) enables microscopic assessment; two fittings for electrodes (white arrows) integrated into the chamber lid allow for electric stimulation (C). The bioreactor modules are placed in a standard cell culture incubator (D). The experimental design is given in (E).

fully interchangeable between individual bioreactor stands and can be placed on a microscope stage for imaging. Alternatively, for continuous assessment within the bioreactor an integrated optical imaging system could be included.

Software control

Controllers are connected to a PC via USB; software (written in LabVIEW 8.6 for Windows XP) was developed for controlling motors and sensors of up to four bioreactor modules in parallel. Force sensors were calibrated with class F1 calibration weights (KERN & Sohn). Constant data acquisition and storage can be performed; all parameters of linear displacement (zero position, stroke, frequency, and wave shape) and electric stimulation (frequency, amplitude, and pulse width) can be adjusted while operations are running. Force and displacement data are displayed on-line in real-time diagrams and captured as CVS files (comma-separated values), which can be exported to common spreadsheet programs, e.g. MS Excel. For an improved signal-to-noise ratio of force data, an averager integrating multiple signals can be activated.

Experimental design

The experimental design consisted of cyclic strain stimulation experiments with BCTs and corresponding static control experiments under varying culture conditions (Fig. 1E). Each experiment started with the preparation of BCTs from freshly isolated neonatal rat cardiomyocytes cast in

Teflon molds. As noradrenalin (in ascorbic acid solution) has been described to support cardiomyocyte contractility in cell culture,²⁵ β -adrenergic stimulation was started on day 6 (d6) of culture by addition of 10 μ M noradrenalin and 30 μ M ascorbic acid (both from Sigma-Aldrich). After 7 days of cultivation, BCTs were transferred to the bioreactor. Mechanical stimulation was started on d7 of culture using 10% cyclic longitudinal strain (0.6 mm, sinus shaped) with a frequency of 1 Hz. Stretch stimulation was continuously applied for 7 days, force measurement was performed daily from d7 until d14. During mechanical stimulation, the connection of the BCT to the force sensor was fixed. The perfusion system was not active during these experiments; cell culture medium was exchanged manually every day.

Imaging

For assessment of cellular morphology during tissue formation, continuous live cell imaging of BCTs was performed with 25 nM tetramethylrhodamine methyl ester (TMRM; Invitrogen). TMRM is a nontoxic cationic, mitochondrial selective probe, which can be used to selectively stain cells with high metabolic activity such as cardiomyocytes.²⁶ Fluorescence images and time-lapse videos of BCTs were captured from d0 to d6 (in Teflon molds) and from d7 to d14 (in cultivation chambers detached from the bioreactor) using the AxioObserver Z1 fluorescence microscope with Axiovision software 4.70 (Zeiss). Three-dimensional analyses for volumetric cellular distribution were performed on d7, whereby

BCTs were fixed and used for whole-mount 4',6-diamidino-2-phenylindole (DAPI) staining of nuclei. Reconstructed images were generated from data acquired with a custom-made optical projection tomography setup. The resolution of the reconstructed data was calculated to be 5 μm . Fixed BCTs were kept in propylene glycol for index matching to decrease tissue scattering properties. DAPI was excited using a 355 nm microchip laser (Soliton). Fluorescence was captured using a 465 \pm 15 nm band pass filter (Semrock) with a CCD LUCA R (Andor).

Force measurement

Long-term spontaneous systolic contraction force was monitored daily for each tissue at 37°C, 5% CO₂ in an incubator, 30 min after medium exchange. Spontaneous active contraction forces were detected with no preload. On d14, maximum forces were captured upon electric stimulation of the tissues at different preloads. For these end-point analyses, all tissues were washed three times with Tyrode's solution (140 mM CaCl₂, 5.4 mM KCl, 1.8 mM CaCl₂, 10 mM Glucose, and 10 mM HEPES) and allowed to equilibrate in Tyrode's solution for 30 min before force measurement. With preload increasing by 0.1 mm increments, tissues were paced five times at each step (rectangular, 5 ms at 25 V).

Measured forces are given as absolute values in mN per BCT (mean \pm SEM for each group), thus representing forces normalized to equal starting quantities of cell number and matrix components.

Histological evaluation

For histological evaluation, BCTs were frozen, sectioned, and immunostained. Detailed procedures as well as specifications on the antibodies used can be found in the online Supplementary Data.

RNA isolation and quantitative real-time polymerase chain reaction

Total RNA was prepared from BCTs and used for cDNA synthesis. Real-time-polymerase chain reaction (PCR) was performed to assess expression levels of the cardiac myosin heavy chain isoforms alpha and beta (α -MHC, β -MHC), atrial natriuretic factor (ANF), connexin 43 (Cx43), as well as calsequestrin-2, all relative to the reference gene β -actin. Detailed procedures and specifications on the primers used can be found in the online Supplementary Data.

Statistical analysis

Statistical analysis was performed with GraphPad Prism software (version 5.03 for Windows; GraphPad Software). Values reported are means and standard errors of the mean. Unless stated otherwise, data were analyzed by one-way analysis of variance, with the Bonferroni multiple comparison test for comparison of any two groups, probability values <0.05 were considered significant.

Results

Generation of BCTs

After seeding neonatal rat cardiomyocytes with a liquid matrix mixture into Teflon molds, BCTs solidified within

30 min. Tissues formed by shrinkage and detachment from the mold resulted in a biconcave tissue band suspended between the two titanium rods (Fig. 2A). During the initial cultivation period, shrinkage led to a decrease of BCT cross-sectional area from 20 mm² at seeding to 1.26 \pm 0.04 mm² on d6 (data not shown). Further compaction of cells and matrix was observed for all BCT groups treated in our novel bioreactor. Compared to the untreated control, shrinkage was less pronounced in BCTs treated with stretch alone, whereas both β -adrenergic stimulation alone and combined mechanical and β -adrenergic stimulation led to a further reduction of the cross-sectional area to a minimum of 0.60 \pm 0.01 mm² on d14 (Fig. 2B).

Live cell fluorescence imaging after TMRM staining confirmed the presence of viable and metabolically active cardiomyocytes within the BCTs and demonstrated that tissue formation is associated with cardiomyocyte elongation and cellular alignment along the longitudinal axis of the constructs (Fig. 3A and Supplementary Video S1). Spontaneous contractions of single cardiomyocytes started from d2, and further cultivation led to synchronous beating of whole BCTs (Supplementary Fig. S1).

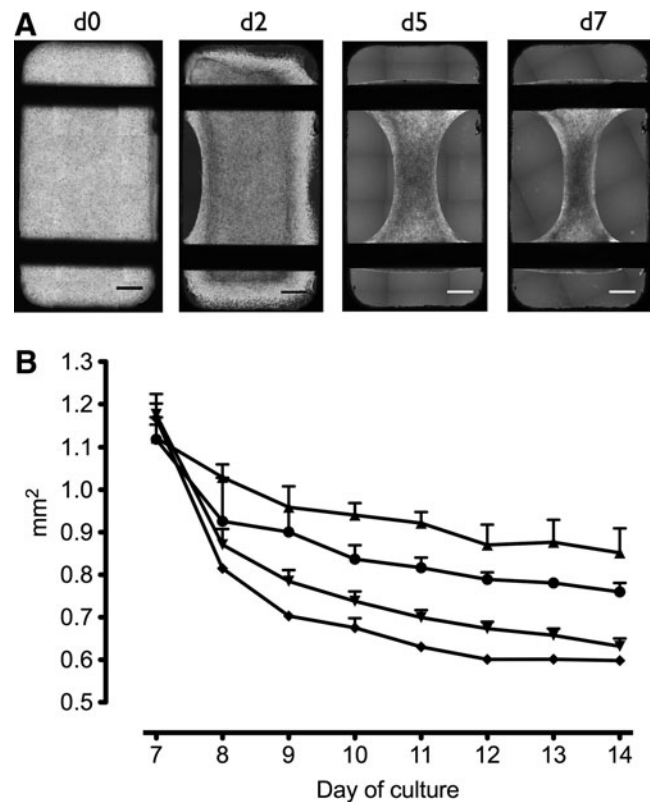


FIG. 2. Microscopic assessment of early tissue formation in BCTs on day 0 (d0), d2, d5, and d7 (from left to right) shows shrinkage and detachment from the Teflon mold resulting in a biconcave tissue band suspended between the titanium rods (A). Scale bar: 1 mm. To quantify shrinkage for individual groups treated with different stimuli: ●, none (negative control group); ▲, stretch; ▼, β -adrenergic stimulation; ◆, β -adrenergic stimulation + stretch; minimal diameters of the constructs were assessed daily from d6 to d14; the cross-sectional area was calculated based on the assumption of a circular shape (for all groups $n = 3$) (B).

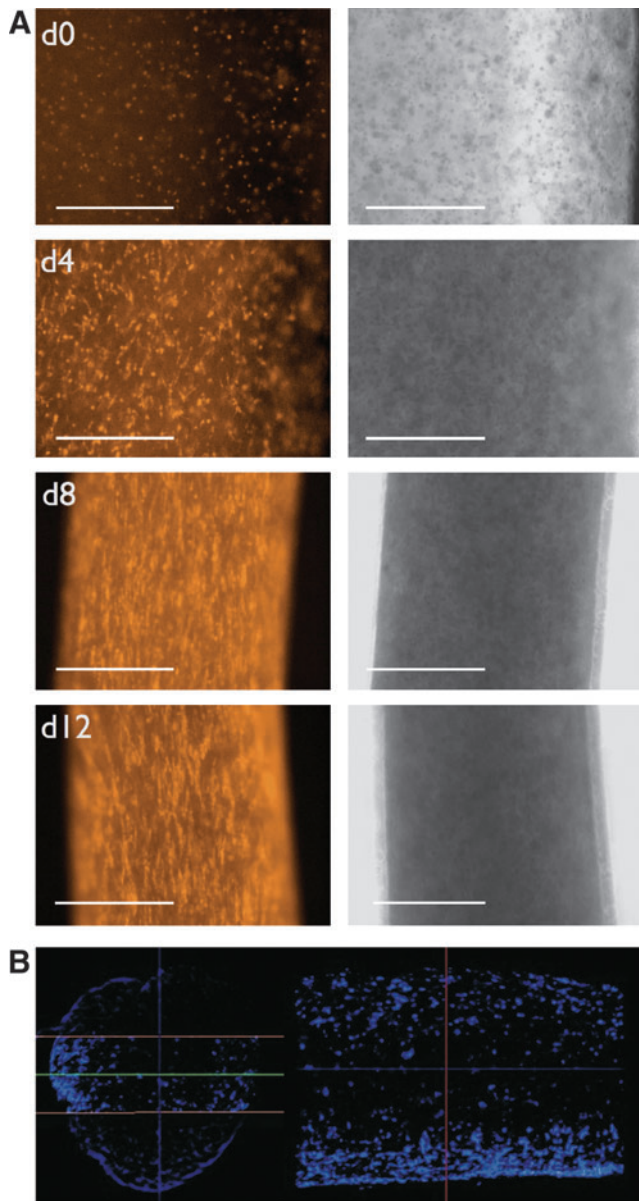


FIG. 3. Live cell fluorescence images of mitochondria-rich cardiomyocytes labeled selectively with tetramethylrhodamine methyl ester on d0, d4, d8, and d12 (top down) demonstrate cell elongation and alignment along the longitudinal axis of the BCTs during the course of tissue formation and maturation (A). Given are representative brightfield and fluorescence images of a control group BCT; scale bar: 500 μm . Three-dimensional optical projection tomography analysis of overall cellular distribution in BCTs was performed after whole-mount 4',6-diamidino-2-phenylindole staining of nuclei (B). A three-dimensional representation of the depicted virtual BCT slice can be found in Supplementary Video S2.

Three-dimensional analysis of whole-mount DAPI-stained BCTs using optical projection tomography showed cell distribution throughout the whole tissue on d7, although at lower numbers in the center of the tissue (Fig. 3B and Supplementary Video S2). BCTs could be maintained in culture for up to 6 weeks, with sustained spontaneous contraction activity (data not shown).

Cardiac-specific gene expression

To investigate whether mechanical stimulation or β -adrenergic stimulation of BCTs in our novel bioreactor could elicit a cellular response, differential gene expression of BCTs was analyzed by quantitative real-time PCR and compared to untreated controls (normalized to equal 1.00). We investigated several genes that have been associated with a hypertrophic response.^{20,27} Indeed, on d8 of cultivation (after 24 h of mechanical stimulation) the ratio of β -MHC to α -MHC expression was higher in all treated groups compared to the untreated controls (Fig. 4A). Similar ratios were detected for stretched (1.64 ± 0.04) and β -adrenergic-stimulated BCTs (1.51 ± 0.06); application of both β -adrenergic stimulation and stretch resulted in a further increase of β -MHC to α -MHC expression level ratio to 2.25 ± 0.13 (all $p < 0.05$ vs. control). Similarly, mechanical stimulation led to elevated ANF expression levels (2.34 ± 1.46 ; $p > 0.05$) (Fig. 4B). Compared to the untreated control group, significantly higher ANF expression levels were detected in the two groups treated with β -adrenergic stimulation, either without additional stretch (6.95 ± 1.14) or with stretch (6.17 ± 1.10 ; both $p < 0.05$); in this case, stretch did not lead to a further increase. Notably, on d14 (after 7 days of mechanical stimulation), treated BCTs showed indications of a sustained and intensified hypertrophic response. Here, BCTs stimulated both β -adrenergic with noradrenalin and with stretch showed the highest increase in β -MHC to α -MHC expression level ratio of 3.85 ± 1.44 (Fig. 4A; $p < 0.05$ vs. control) together with an increase in ANF expression level of 17.94 ± 7.59 (Fig. 4B; $p > 0.05$ vs. control).

Tissue morphology and composition

BCT morphology on d14 was assessed by costaining of tissue sections using cell type-specific antibodies. Viable cardiomyocytes were detected in all constructs and usually showed cellular alignment along the longitudinal axis of the tissue (Fig. 5, left panels). Cardiomyocytes were surrounded by nonmyocytes, with lower numbers of cardiomyocytes in the center of the tissue, as seen in the optical projection tomography analysis. Bundles of cardiomyocytes were notably thicker in the treatment groups and were occasionally found deeper in the tissue's center compared to the nontreated tissues. Cardiomyocytes showed well-developed sarcomeres in all groups and the presence of Cx43 indicated interconnections through gap junctions similar to neonatal rat heart (Fig. 5, middle and right panels). Interestingly, non-cardiomyocytes expressing Cx43 were found at the rim of the neonatal rat heart, as well as at the borders of BCTs. It has been suggested that overall cardiomyocyte content or efficiency of coupling via gap junctions in aligned cells might play a role in force development.^{28–30} Using quantitative real-time PCR, total expression levels of Cx43 on d14 of tissue formation were found to be slightly elevated in both groups treated with mechanical stimulation (either with or without β -adrenergic stimulation); however, the effect did not reach statistical significance (Supplementary Fig. S3A). Also, the cardiomyocyte content of BCTs assessed as calsequestrin-2 expression levels did not differ significantly among groups; here, a minor increase was observed after β -adrenergic stimulation (Supplementary Fig. S3B). The reduced shrinkage of BCTs treated with stretch only, resulting

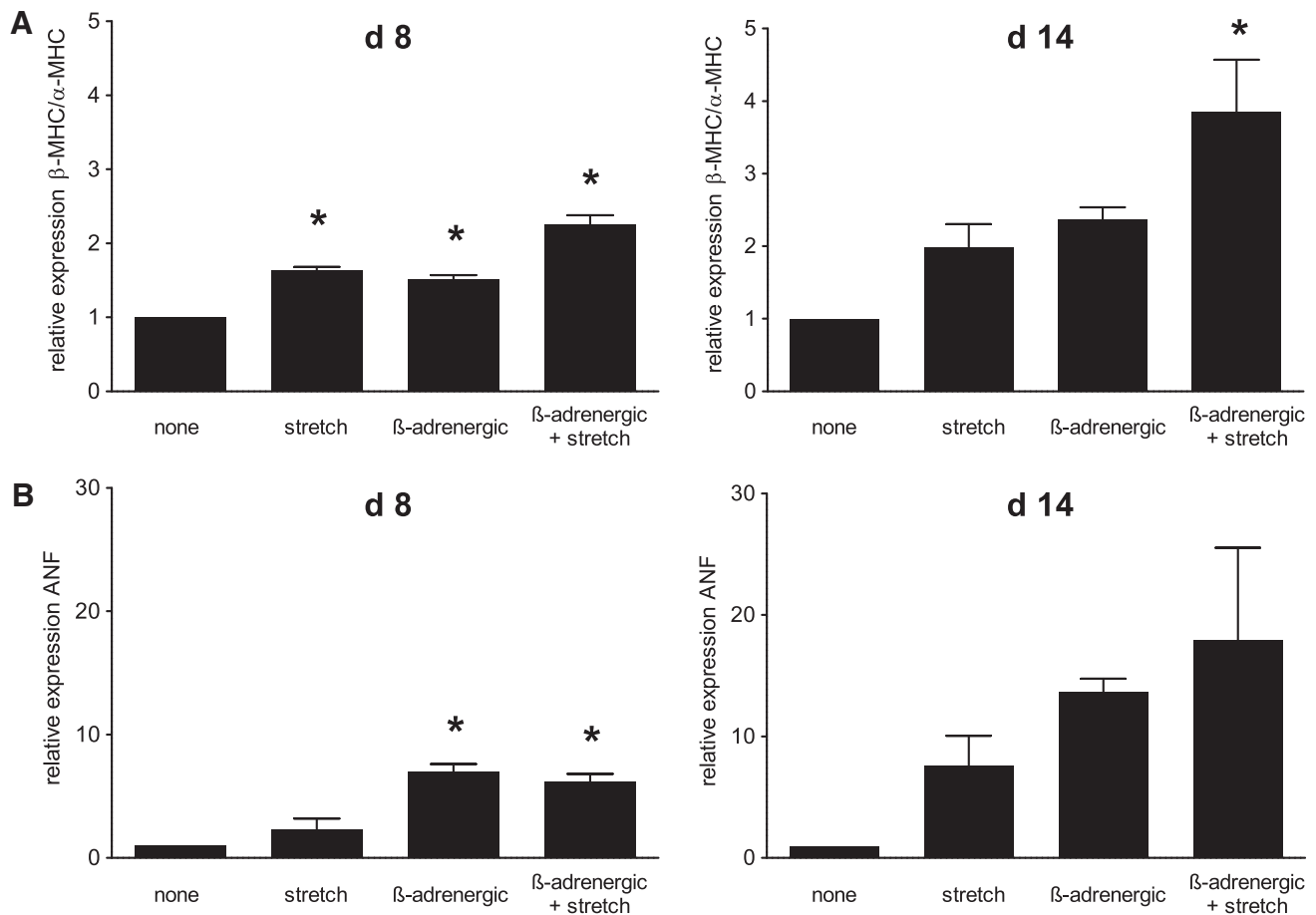


FIG. 4. Expression levels of cardiac marker genes were analyzed by quantitative real-time polymerase chain reaction on d8 and d14 of cultivation for individual groups treated with different stimuli: none (negative control), stretch, β -adrenergic stimulation, and β -adrenergic stimulation + stretch. Depicted is the ratio of β -MHC to α -MHC expression (A) and expression of atrial natriuretic factor (B). Expression levels were normalized to the reference gene β -actin using the $\Delta\Delta$ Ct-method, and compared to the untreated control group (normalized to equal 1.00). Data are presented as mean \pm SEM for two independent experiments, each with two polymerase chain reaction runs performed in triplicate; * $p < 0.05$ versus negative control group.

in the largest cross-sectional area on d14 (Fig. 2B), correlated with an increased protein-to-DNA ratio in this group (Supplementary Fig. S3C).

Mechanical properties

Long-term observation of spontaneous systolic forces with our bioreactor confirmed synchronous beating of BCTs. Recordings of contractions and a comparative analysis of beating frequencies over time are shown in the Supplementary Figure S1. While groups treated with β -adrenergic stimulation by noradrenalin initially showed an increased frequency of spontaneous contractions (d7 and d8), long-term exposure to noradrenalin resulted in beating frequencies similar to the other groups from d9 to d14. For tissues kept in the cell culture medium, systolic force was measured daily and found to increase over time for all groups (Fig. 6A). Compared to the untreated control group, significantly higher forces were observed for the two groups treated with β -adrenergic stimulation: without additional stretch already on d8, with stretch on d9 (two-way analysis of variance, $p < 0.05$). From d13 onward, BCTs treated with β -adrenergic

stimulation alone yielded significantly higher systolic forces than BCTs treated with β -adrenergic stimulation and stretch. Spontaneous systolic forces on d14 reached a maximum of 0.96 ± 0.09 mN for the untreated control group (Fig. 6B). While stretch alone resulted in a moderate increase to 1.42 ± 0.09 mN ($p > 0.05$), significantly higher contraction forces were measured on d14 after β -adrenergic stimulation (2.54 ± 0.11 mN) and β -adrenergic stimulation + stretch (2.09 ± 0.08 mN; both $p < 0.05$).

Most often, and in contrast to the long-term observation performed in our study, end-point analysis of contraction forces is performed applying a defined preload to the tissue. Thus, for a comparative analysis, measurements were repeated with preloads between 0.0 and 1.9 mm upon electrical pacing of the tissue in Tyrode's solution without supplements. As expected for functional myocardial fibers, forces increased with higher preload due to the Frank-Starling mechanism (example given in Fig. 6C). For each group, the optimal preload length L_{\max} resulting in maximum forces was determined and used for end-point comparison of the four groups. While absolute forces tended to be higher when measured under these conditions, with a maximum systolic

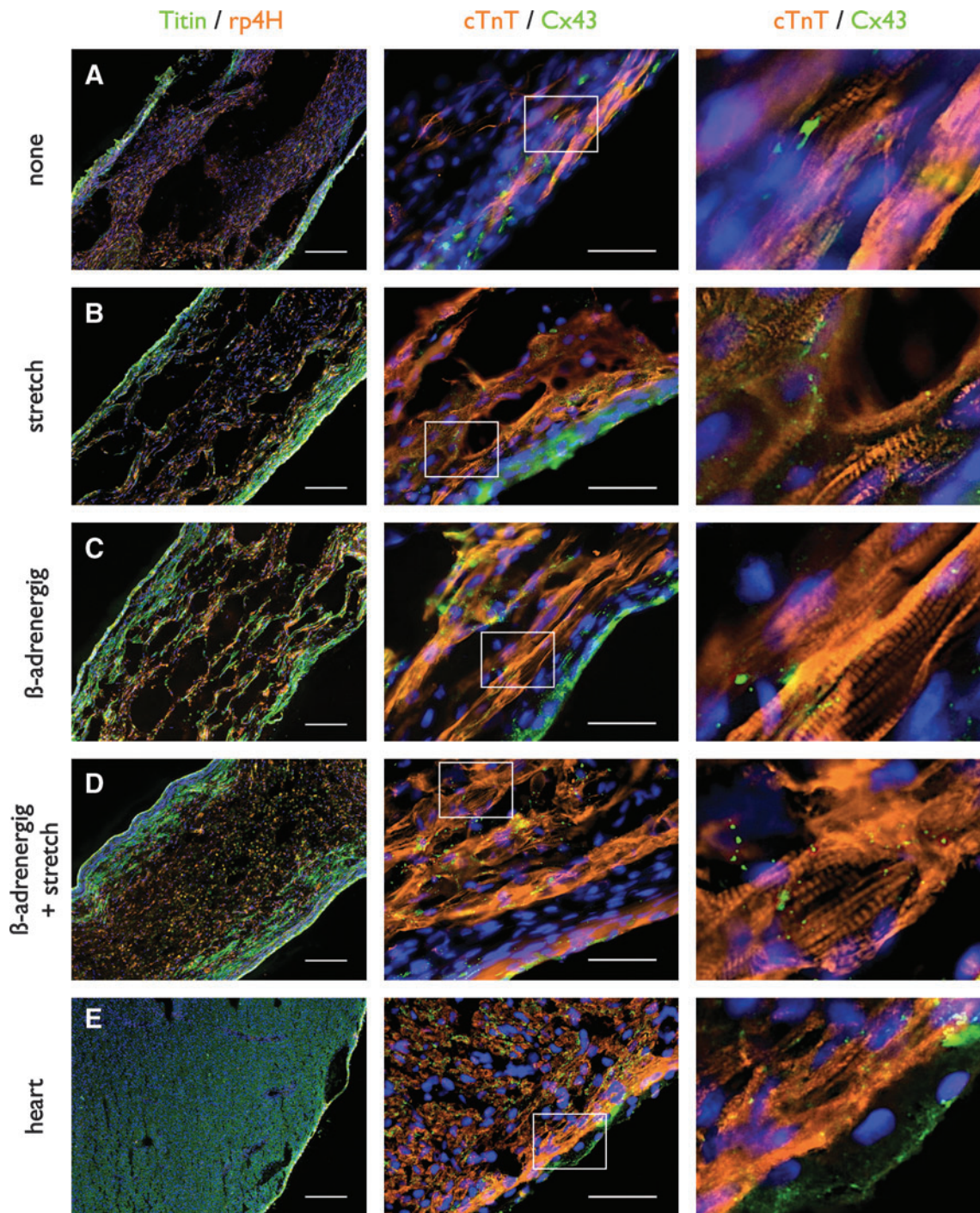


FIG. 5. Representative fluorescence microscopy images of immunostained tissue sections of different BCT groups: (A) none (negative control group); (B) stretch; (C) β -adrenergic stimulation; and (D) β -adrenergic stimulation + stretch. Cardiomyocyte distribution is demonstrated by costaining for titin (green) and prollyhydroxylase as a fibroblast marker (red) in the left panel. Scale bars = 200 μ m. The middle panel illustrates connexin 43 expression (green) in aligned cardiomyocytes (stained for cardiac troponin T, red) predominantly at the border of BCTs. High-magnification images are provided in the right panel. All nuclei were stained with 4',6-diamidino-2-phenylindole (blue). Also shown is native neonatal rat heart tissue (E). Scale bars = 50 μ m. Staining patterns of individual antibodies are shown in Supplementary Figure S2.

force of 2.88 ± 0.14 mN for the β -adrenergic stimulation group (Fig. 6D), differences between the analyzed groups were very similar to those observed for spontaneous contractions in the culture medium depicted in Figure 6B. With a BCT cross-sectional area of 0.63 ± 0.02 mm², as determined

by microscopic assessment, the strongest BCTs were those treated with β -adrenergic stimulation exerting a tensile strain of 4.57 ± 0.08 mN/mm². Notably, electrical pacing did not have a significant effect on systolic forces compared to spontaneous contractions under similar conditions (data not shown).

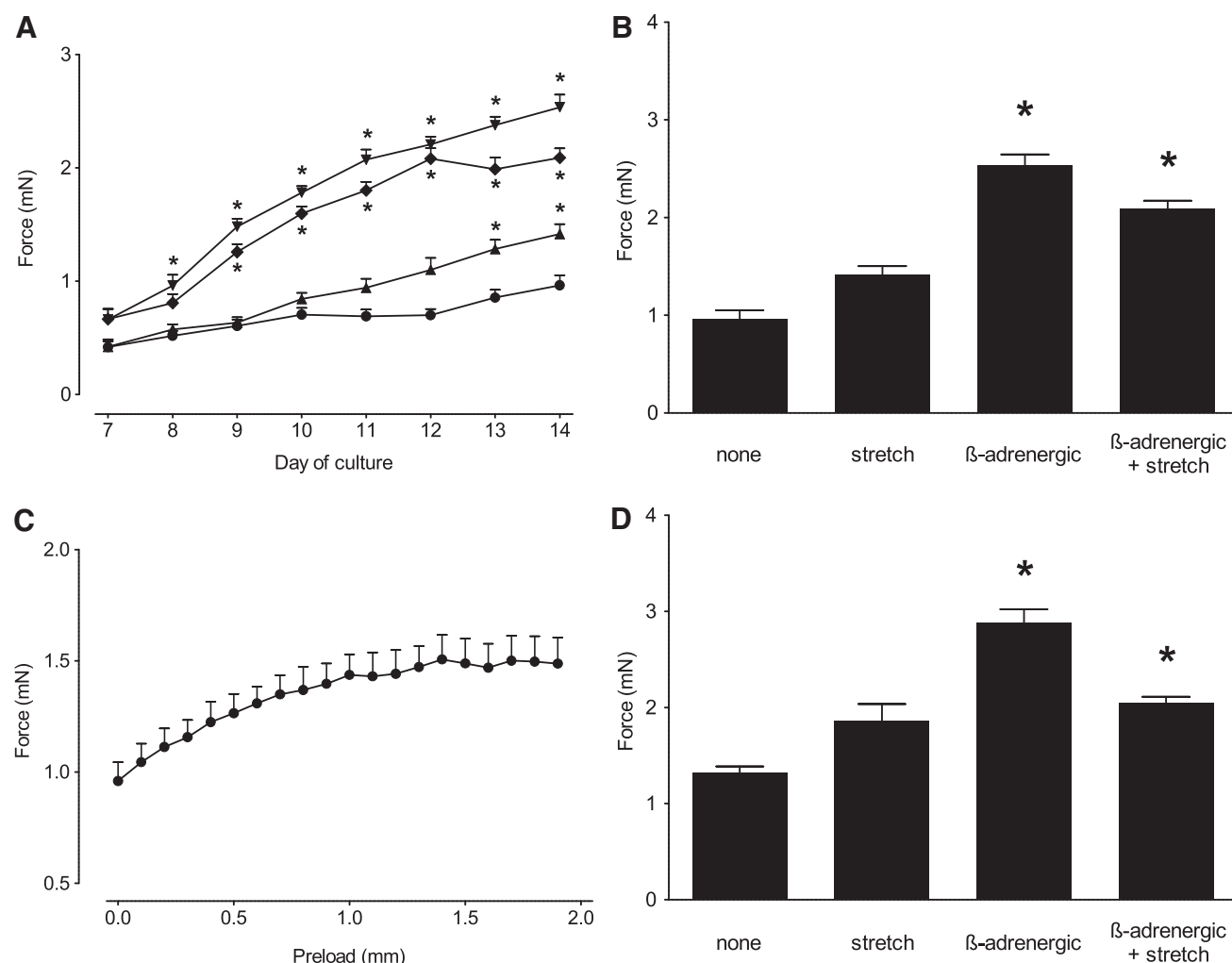


FIG. 6. Systolic contraction forces of BCTs were measured in the bioreactor during continuous cultivation. For individual groups treated with different stimuli: ●, none (negative control group; $n = 11$); ▲, stretch ($n = 6$); ▼, β -adrenergic stimulation ($n = 17$); ◆, β -adrenergic stimulation + stretch ($n = 13$); spontaneous systolic force development was assessed daily from d7 to d14 in the respective medium and analyzed using two-way analysis of variance (A). Systolic forces measured in medium on d14 are summarized in B. End-point analyses in Tyrode's solution were performed on d14; measurements at preload increasing by 0.1 mm increments were performed to determine the optimal preload L_{\max} corresponding to maximum systolic force (example for BCTs from the control group [$n = 10$] depicted in C). Maximum systolic forces measured at L_{\max} in Tyrode's solution for the respective groups (none, $n = 18$; stretch, $n = 8$; β -adrenergic stimulation, $n = 20$; β -adrenergic stimulation + stretch, $n = 8$) are given in (D). * $p < 0.05$ versus negative control group; all data are presented as mean \pm SEM.

In conclusion, long-term observation of spontaneous systolic forces in cell culture medium provides a good representation of maximum forces. Accordingly, for a valid comparison of systolic forces of different treatment groups, BCT transfer into a special organ bath is not required.

Discussion

Native heart tissue is characterized by a distinctive cycle of mechanical loading and unloading, which may be essential for successful cardiac tissue engineering.

The objective of this study was to investigate whether our novel multimodal bioreactor for mechanical stimulation, direct real-time force measurement, and imaging of small-scale tissue-engineered cardiac constructs could both influence and assess transient development of constructs over a 1-week

period in a sterile culture environment. To investigate the influence of mechanical load on engineered cardiac tissue, motorized stretching devices for the application of defined strain have been described.^{14,15,31} Traditional mechanical testing devices to measure mechanical properties of tissue-engineered constructs typically require discontinuation of the cultivation process and therefore provide only end-point measurements of the respective samples. On the other hand, sophisticated bioreactor systems have been developed allowing for long-term monitoring of contractile activity via software-based analysis of video-optically captured contractions.²³

This study demonstrates for the first time that these features can be combined into a single multimodal bioreactor system, including the possibility for electric stimulation of excitable tissue, perfusion of the culture chamber, and

microscopic assessment of tissue formation. The system was designed for small-scale cardiac tissue engineering, allowing the generation of tissue from small (stem) cell numbers, yet with a construct size large enough both to provide a true three-dimensional culture environment *in vitro*, and to be of an appropriate size for small animal transplantation models *in vivo*, without the immediate need for scale-up. If desired, scale-up can be easily achieved due to the flexibility of the modular bioreactor system. Current molds can be used for cell numbers ranging from 0.5 million to 4 million cells; other molds can be implemented for larger volumes and different geometries. A range of motors with different parameters (maximum stroke, peak force) are available as well as force sensors with a variety of measuring ranges. All components can be easily exchanged, which is a clear advantage over most existing systems.

Here, the novel system was used to provide a continuous monitoring of the developmental effects of mechanical stretch and β -adrenergic stimulation with noradrenalin on BCT. BCTs were generated using neonatal rat cardiomyocytes and displayed synchronized spontaneous contractions. Electrical stimulation in the bioreactor induced contractions of whole BCTs demonstrating the existence of a functional and excitable syncytium. However, it must be acknowledged that due to the spontaneous contractile activity, mechanical strain was present in all groups of BCTs to a certain degree. Thus, in our system, we were only able to investigate the effects of additional external mechanical loading.

Frank *et al.* demonstrated differential gene expression for cardiomyocytes stimulated by chemically induced contraction-related strain in comparison to mechanical stretch applied externally.¹⁹ In line with their results, known stretch-responsive genes were differentially up- or downregulated in response to mechanical stimulation in our system investigating three-dimensional tissue-engineered constructs. It should be noted that Frank *et al.* used phenylephrine, a selective agonist of α -adrenergic receptors, for pharmacologic induction of hypertrophy. In comparison, noradrenaline used in our study is a β -adrenergic stimulant of cardiomyocyte contractility; however, it has also been described to induce hypertrophy in cardiomyocytes via an α -adrenergic response.³² The expected hypertrophic response of cardiomyocytes to mechanical loading was confirmed by demonstrating a shift of cardiac MHC expression from the α -MHC isoform toward β -MHC. A reduction in α -MHC expression levels, reflecting changes in gene expression more toward a fetal phenotype,²⁰ was also described for three-dimensional cultures of murine embryonic stem cell-derived cardiomyocytes after application of 10% stretch at 1 Hz; however, higher frequencies led to the opposite effect.³¹ At the same time, we were able to detect upregulation of ANF expression both after mechanical and β -adrenergic stimulation, as was described before for stretched monolayer¹⁹ and three-dimensional cultures of rat cardiomyocytes,¹⁴ as well as ventricles of the hypertrophic rat heart.³³ From the quantitative real-time PCR data and the force measurements, we conclude that the mechanical stimulation applied in our bioreactor led to moderate hypertrophy in cardiomyocytes within the BCTs, which had a positive effect on systolic forces. However, it has to be considered that in an *in vivo* situation, hypertrophy can reflect either a compensatory or maladaptive response to loading.²⁷ Therefore, it will have to

be investigated whether longer periods of stimulation might have adverse effects on our BCTs.

While gene expression analysis clearly showed a hypertrophic response, we found that protein/DNA ratio was not a valid indicator of hypertrophy in our three-dimensional cultivation system, most likely due to the artificial cellular environment including substantial protein supplementation. Nevertheless, protein/DNA ratio showed good correlation with total BCT diameters.

Besides the direct effect of mechanical stretch on cell fate via stretch-responsive differential gene expression, stretch might also lead to enhanced perfusion of cell culture medium within the constructs. This could result in improved nutrition and oxygen supply together with enhanced removal of metabolic waste products and/or nonintegrated matrix components. As this bioreactor system allows for perfusion of the central culture vessel, it can be used for a comparative analysis of the effects of mechanical stimulation and continuous medium exchange at defined rates, or alternatively, to monitor pharmacological effects of soluble compounds on tissue contractility. Nutrition and oxygen supply are also major limiting factors for the generation of larger myocardial tissue constructs needed for future clinical application. To allow for perfusion, recent studies introduced blood vessels within bioengineered myocardial tissue, either by adding endothelial cells to generate prevascularized tissue *in vitro*³⁴ or by promoting neovascularization after transplantation *in vivo*.³⁵ These strategies might be used to generate larger tissue that more closely resembles native myocardium.

In line with previous reports, mechanical stimulation led to increased systolic forces compared to untreated control tissues in our experiments. After application of 5% unidirectional phasic stretch for 6 days, Fink *et al.* reported two- to fourfold higher force of contraction both under basal conditions and after stimulation with calcium or the β -adrenergic agonist isoprenaline.¹⁴ Zimmermann *et al.* demonstrated in a direct comparison of calcium response curves that engineered heart tissue benefited from mechanical load in addition to oxygen supplementation.³⁶ Using a similar system based on collagen and Matrigel, Clause *et al.* generated engineered early embryonic cardiac tissue using embryonic cardiac cells from chicken.³⁷ They reported a 1.6-fold increase in active stress at L_{max} following cyclic mechanical stretch stimulation for 48 h and concluded that contractile properties and cellular proliferative response to stretch mimic developing fetal myocardium.

A number of these studies used adrenoceptor agonists; however, mostly as an analytical tool.^{2,14,15,38} These studies demonstrated an increase in contractility in response to short-term application of isoprenaline, indicating functional adrenergic signaling in engineered heart tissue. Long-term application was described for instance by Claycomb *et al.* in a protocol designed for the maintenance of contractility in cultured cardiac HL-1 cells including continuous medium supplementation with noradrenalin.²⁵

Using our bioreactor system we were now able to demonstrate for the first time in a direct comparison that long-term chemical stimulation by addition of noradrenalin and ascorbic acid yielded significantly higher contraction forces in BCT, that is, increased by 2.5-fold, than mechanical stretch alone (1.4-fold). Notably, addition of noradrenalin was associated with an elevated contraction frequency in the first

2 days, but upon prolonged exposure, frequency returned to similar values as in the other groups. Moreover, interestingly, no additive or synergistic effect on systolic forces was observed for combined mechanical and β -adrenergic stimulation. Several studies investigated the influence of stretch on Cx43 expression in cultures of neonatal cardiomyocytes and described upregulation after mechanical stimulation.^{29,30} In our setting, no clear correlation was observed for either cardiomyocyte content or Cx43 expression levels with force development. However, Salameh *et al.* also demonstrated that application of stretch for 48 h resulted in lower Cx43 expression than stretch for 24 h.²⁹ This might explain why no significant upregulation of Cx43 was observed in our system after prolonged mechanical stimulation for 7 days.

For our strongest BCTs, we determined a maximum tensile strain of 4.57 ± 0.08 mN/mm², which is still well below the contraction force of ~ 50 mN/mm² exerted by the papillary muscle of native rat myocardial tissue.^{39,40} For engineered cardiac tissues, a direct comparison of absolute contractile forces among different studies is difficult due to variations of protocols and depends on a comparable assessment of tissue construct diameter. Frequently, authors chose to denote the forces measured per tissue construct. Although this does not consider changes in cell number over time through cell proliferation and death, we have back-calculated forces reported in individual studies to a starting amount of 10^6 cells used for tissue generation. Typically, studies using rat cardiomyocytes together with a collagen/Matrigel matrix reported forces between ~ 0.3 mN and ~ 1.5 mN/ 10^6 starting cells.^{14,15,22,23,36,38} Based on this calculation mode, the systolic forces of ~ 1 mN for untreated control BCTs were in the range of previous studies, indicating the functionality of BCTs generated with our bioreactor system. The maximum systolic forces of 2.88 ± 0.14 mN obtained after β -adrenergic stimulation were almost twofold higher than achieved so far.

In conclusion, first results with the novel bioreactor system substantiate the potential of mechanical stimulation to influence tissue-engineered cardiac construct development. At the same time, they provide an indication on the timing of structural and mechanical changes that occur during this process. In our experimental setup using primary cardiomyocytes, β -adrenergic stimulation had a stronger effect on systolic force development than mechanical stimulation. Nevertheless, it is conceivable that mechanical stimulation might provide important signals for cardiac differentiation of stem cells within three-dimensional tissues. While optimal mechanical properties for *in vivo* support of cardiac function have to be determined in future studies, the novel bioreactor described herein can be considered a valuable tool for *in vitro* analysis of BCT and thus for optimization of stem cell-based tissue replacement strategies in regenerative medicine.

Acknowledgments

The authors are grateful to Suzanne E. Dorfman for revising the article. We would like to thank Ingrid Schmidt-Richter and Anke Gawol for providing excellent technical assistance as well as Michael Breyvogel, Jörg Claus, Juri Huber, and Erik Mahnke for valuable contributing to the bioreactor setup. The monoclonal antibody 9D10 developed by M.L. Greaser was obtained from the Developmental

Studies Hybridoma Bank developed under the auspices of the NICHD and maintained by Department of Biology, The University of Iowa, Iowa City, IA. This work has been supported by the German Federal Ministry of Education and Research (01GN0520) as well as by the Cluster of Excellence REBIRTH.

Disclosure Statement

No competing financial interest exists.

References

1. WHO. Fact sheet, No. 317. Cardiovascular diseases. 2009.
2. Zimmermann, W.H., Melnychenko, I., and Eschenhagen, T. Engineered heart tissue for regeneration of diseased hearts. *Biomaterials* **25**, 1639, 2004.
3. Akhyari, P., Kamiya, H., Haverich, A., Karck, M., and Lichtenberg, A. Myocardial tissue engineering: the extracellular matrix. *Eur J Cardiothorac Surg* **34**, 229, 2008.
4. Dor, V., Sabatier, M., Montiglio, F., Civaia, F., and DiDonato, M. Endoventricular patch reconstruction of ischemic failing ventricle. a single center with 20 years experience. advantages of magnetic resonance imaging assessment. *Heart Fail Rev* **9**, 269, 2004.
5. Kehat, I., Kenyagin-Karsenti, D., Snir, M., Segev, H., Amit, M., Gepstein, A., *et al.* Human embryonic stem cells can differentiate into myocytes with structural and functional properties of cardiomyocytes. *J Clin Invest* **108**, 407, 2001.
6. Schwanke, K., Wunderlich, S., Reppel, M., Winkler, M.E., Matzkies, M., Groos, S., *et al.* Generation and characterization of functional cardiomyocytes from rhesus monkey embryonic stem cells. *Stem Cells* **24**, 1423, 2006.
7. Schenke-Layland, K., Rhodes, K.E., Angelis, E., Butylkova, Y., Heydarkhan-Hagvall, S., Gekas, C., *et al.* Reprogrammed mouse fibroblasts differentiate into cells of the cardiovascular and hematopoietic lineages. *Stem Cells* **26**, 1537, 2008.
8. Mauritz, C., Schwanke, K., Reppel, M., Neef, S., Katsirntaki, K., Maier, L.S., *et al.* Generation of functional murine cardiac myocytes from induced pluripotent stem cells. *Circulation* **118**, 507, 2008.
9. Zhang, J., Wilson, G.F., Soerens, A.G., Koonce, C.H., Yu, J., Palecek, S.P., *et al.* Functional cardiomyocytes derived from human induced pluripotent stem cells. *Circ Res* **104**, e30, 2009.
10. Haase, A., Olmer, R., Schwanke, K., Wunderlich, S., Merkert, S., Hess, C., *et al.* Generation of induced pluripotent stem cells from human cord blood. *Cell Stem Cell* **5**, 434, 2009.
11. Zweigerdt, R. Large scale production of stem cells and their derivatives. *Adv Biochem Eng Biotechnol* **114**, 201, 2009.
12. Olmer, R., Haase, A., Merkert, S., Cui, W., Palecek, J., Ran, C., *et al.* Long term expansion of undifferentiated human iPSC and ES cells in suspension culture using a defined medium. *Stem Cell Res* **5**, 51, 2010.
13. Xu, X.Q., Graichen, R., Soo, S.Y., Balakrishnan, T., Rahmat, S.N., Sieh, S., *et al.* Chemically defined medium supporting cardiomyocyte differentiation of human embryonic stem cells. *Differentiation* **76**, 958, 2008.
14. Fink, C., Ergun, S., Kralisch, D., Remmers, U., Weil, J., and Eschenhagen, T. Chronic stretch of engineered heart tissue induces hypertrophy and functional improvement. *FASEB J* **14**, 669, 2000.
15. Zimmermann, W.H., Schneiderbanger, K., Schubert, P., Didie, M., Munzel, F., Heubach, J.F., *et al.* Tissue engineering of a differentiated cardiac muscle construct. *Circ Res* **90**, 223, 2002.

16. Birla, R.K., Borschel, G.H., and Dennis, R.G. *In vivo* conditioning of tissue-engineered heart muscle improves contractile performance. *Artif Organs* **29**, 866, 2005.
17. Akhyari, P., Fedak, P.W., Weisel, R.D., Lee, T.Y., Verma, S., Mickle, D.A., *et al.* Mechanical stretch regimen enhances the formation of bioengineered autologous cardiac muscle grafts. *Circulation* **106**, I137, 2002.
18. Barki-Harrington, L., Perrino, C., and Rockman, H.A. Network integration of the adrenergic system in cardiac hypertrophy. *Cardiovasc Res* **63**, 391, 2004.
19. Frank, D., Kuhn, C., Brors, B., Hanselmann, C., Ludde, M., Katus, H.A., *et al.* Gene expression pattern in biomechanically stretched cardiomyocytes: evidence for a stretch-specific gene program. *Hypertension* **51**, 309, 2008.
20. Komuro, I., and Yazaki, Y. Control of cardiac gene expression by mechanical stress. *Annu Rev Physiol* **55**, 55, 1993.
21. Zhang, Y.H., Youm, J.B., and Earm, Y.E. Stretch-activated non-selective cation channel: a causal link between mechanical stretch and atrial natriuretic peptide secretion. *Prog Biophys Mol Biol* **98**, 1, 2008.
22. Naito, H., Melnychenko, I., Didie, M., Schneiderbanger, K., Schubert, P., Rosenkranz, S., *et al.* Optimizing engineered heart tissue for therapeutic applications as surrogate heart muscle. *Circulation* **114**, I72, 2006.
23. Hansen, A., Eder, A., Bonstrup, M., Flato, M., Mewe, M., Schaaf, S., *et al.* Development of a drug screening platform based on engineered heart tissue. *Circ Res* **107**, 35, 2010.
24. Wollert, K.C., Taga, T., Saito, M., Narazaki, M., Kishimoto, T., Glembofski, C.C., *et al.* Cardiotrophin-1 activates a distinct form of cardiac muscle cell hypertrophy. Assembly of sarcomeric units in series VIA gp130/leukemia inhibitory factor receptor-dependent pathways. *J Biol Chem* **271**, 9535, 1996.
25. Claycomb, W.C., Lanson, N.A., Jr., Stallworth, B.S., Egeland, D.B., Delcarpio, J.B., Bahinski, A., *et al.* HL-1 cells: a cardiac muscle cell line that contracts and retains phenotypic characteristics of the adult cardiomyocyte. *Proc Natl Acad Sci U S A* **95**, 2979, 1998.
26. Hattori, F., Chen, H., Yamashita, H., Tohyama, S., Satoh, Y.S., Yuasa, S., *et al.* Nongenetic method for purifying stem cell-derived cardiomyocytes. *Nat Methods* **7**, 61, 2010.
27. Frey, N., and Olson, E.N. Cardiac hypertrophy: the good, the bad, and the ugly. *Annu Rev Physiol* **65**, 45, 2003.
28. Black, L.D., 3rd, Meyers, J.D., Weinbaum, J.S., Shvelidze, Y.A., and Tranquillo, R.T. Cell-induced alignment augments twitch force in fibrin gel-based engineered myocardium via gap junction modification. *Tissue Eng Part A* **15**, 3099, 2009.
29. Salameh, A., Wustmann, A., Karl, S., Blanke, K., Apel, D., Rojas-Gomez, D., *et al.* Cyclic mechanical stretch induces cardiomyocyte orientation and polarization of the gap junction protein connexin 43. *Circ Res* **106**, 1592, 2010.
30. Salameh, A., Karl, S., Djilali, H., Dhein, S., Janousek, J., and Daehnert, I. Opposing and synergistic effects of cyclic mechanical stretch and alpha- or beta-adrenergic stimulation on the cardiac gap junction protein Cx43. *Pharmacol Res* **62**, 506, 2010.
31. Shimko, V.F., and Claycomb, W.C. Effect of mechanical loading on three-dimensional cultures of embryonic stem cell-derived cardiomyocytes. *Tissue Eng Part A* **14**, 49, 2008.
32. Simpson, P. Norepinephrine-stimulated hypertrophy of cultured rat myocardial cells is an alpha 1 adrenergic response. *J Clin Invest* **72**, 732, 1983.
33. Izumo, S., Nadal-Ginard, B., and Mahdavi, V. Proto-oncogene induction and reprogramming of cardiac gene expression produced by pressure overload. *Proc Natl Acad Sci U S A* **85**, 339, 1988.
34. Lesman, A., Habib, M., Caspi, O., Gepstein, A., Arbel, G., Levenberg, S., *et al.* Transplantation of a tissue-engineered human vascularized cardiac muscle. *Tissue Eng Part A* **16**, 115, 2010.
35. Martinez, E.C., Wang, J., Gan, S.U., Singh, R., Lee, C.N., and Kofidis, T. Ascorbic acid improves embryonic cardiomyoblast cell survival and promotes vascularization in potential myocardial grafts *in vivo*. *Tissue Eng Part A* **16**, 1349, 2010.
36. Zimmermann, W.H., Melnychenko, I., Wasmeier, G., Didie, M., Naito, H., Nixdorff, U., *et al.* Engineered heart tissue grafts improve systolic and diastolic function in infarcted rat hearts. *Nat Med* **12**, 452, 2006.
37. Clause, K.C., Tinney, J.P., Liu, L.J., Keller, B.B., and Tobita, K. Engineered early embryonic cardiac tissue increases cardiomyocyte proliferation by cyclic mechanical stretch via p38-MAP kinase phosphorylation. *Tissue Eng Part A* **15**, 1373, 2009.
38. Zimmermann, W.H., Fink, C., Kralisch, D., Remmers, U., Weil, J., and Eschenhagen, T. Three-dimensional engineered heart tissue from neonatal rat cardiac myocytes. *Biotechnol Bioeng* **68**, 106, 2000.
39. Brooks, W.W., and Conrad, C.H. Differences between mouse and rat myocardial contractile responsiveness to calcium. *Comp Biochem Physiol A Mol Integr Physiol* **124**, 139, 1999.
40. Han, Y.S., and Ogut, O. Regulation of fibre contraction in a rat model of myocardial ischemia. *PLoS One* **5**, e9528, 2010.

Address correspondence to:
Ina Gruh, Ph.D.

Leibniz Research Laboratories for Biotechnology
and Artificial Organs
Department of Cardiac, Thoracic, Transplantation,
and Vascular Surgery
Hannover Medical School
Carl-Neuberg-Str. 1
Hannover 30625
Germany

E-mail: gruh.ina@mh-hannover.de

Received: July 9, 2010

Accepted: December 6, 2010

Online Publication Date: January 11, 2011

Supplementary Data

Supplementary Material and Methods

Cell isolation

Neonatal rat cardiomyocytes were isolated from 1- to 3-day-old Sprague-Dawley rat pups as previously described.¹ In brief, a minced heart tissue suspension was sequentially digested with an enzyme mix of collagenase IV (Worthington, Biochemical Corporation) and pancreatin (Sigma-Aldrich). Single cells were collected in horse serum (Gibco), enriched for cardiomyocytes by discontinuous Percoll (GE Health Care) gradient centrifugation, and filtered through a 40 μ m filter. Cell number was determined using a CASY cell counter system (Roche Innovatis). During all experiments, the Principles of Laboratory Animal Care (NIH publication No. 86-23, revised 1985) as well as the Animal Welfare Law of Lower Saxony were followed.

Preparation of bioartificial cardiac tissues

To generate one bioartificial cardiac tissue (BCT), 10⁶ enriched cardiomyocytes were used together with 0.9 mg/mL rat tail collagen type I (neutralized with 0.1 N NaOH; R&D Systems), 10% (v/v) Matrigel (BD Biosciences), 12% horse serum (Gibco), 2% chicken embryo extract (US Biological), 2 mM L-glutamin (Gibco), 100 U/mL penicillin, and 100 μ g/mL streptomycin (both PAA Laboratories) in Dulbecco's modified Eagle's medium (Gibco). BCTs were cast in the Teflon molds placed on agarose-coated dishes, allowed to consolidate for 30 min, and covered with 5 mL of medium Dulbecco's modified Eagle's medium (high glucose) containing 12% horse serum (Gibco), 2% chicken embryo extract (US Biological), 2 mM L-glutamin (Gibco), 10 μ g/mL insulin (Sigma), and 100 U/mL penicillin and 100 μ g/mL streptomycin (PAA Laboratories). Tissues were cultured with daily medium exchange; medium without chicken embryo extract was used starting from day 8.

Long-term observation of tissue formation

Freshly prepared BCTs were covered with cultivation medium supplemented with 25 nM of the mitochondria-specific tetramethylrhodamine methyl ester (Invitrogen), placed in the incubation chamber of the inverted fluorescence microscope Axio Observer Z1 (Zeiss) with 80% humidity, 7% CO₂, and 37.5°C. Fluorescence and brightfield images were taken every 8 min for a period of 14 days. Fluorochrome-containing medium was exchanged daily. Imaging started at the border of the tissue until the central part of the tissue was thin enough to be captured entirely.

Histological evaluation

Tissues were embedded in Tissue-Tek (Sakura) and frozen at -80°C. Frozen tissues were sectioned using the HM 500 cryostat (Microm) and allowed to air-dry at room tempera-

ture over night. Sections were fixed by incubation with 2% paraformaldehyde for 10 min, blocked, and permeabilized with Tris-buffered saline containing 0.25% Triton-X 100 (Sigma) and the serum of the respective secondary antibody host species. Primary and secondary antibodies were diluted in phosphate-buffered saline with 5% bovine serum albumin. Following primary antibodies were used: Titin (The Developmental Studies Hybridoma Bank), cardiac Troponin T (Thermo Scientific), Cx43 (Sigma), and rP4H (Acris Antibodies). Appropriate secondary antibodies (DyLight 488, 549, 649; Jackson ImmunoResearch) were used. Nuclei were stained by 4',6-diamidino-2-phenylindole (Invitrogen). Sections were analyzed using the AxioObserver A1 fluorescence microscope using Axiovision software 4.70 (Zeiss).

RNA isolation and quantitative real-time polymerase chain reaction

Total RNA was prepared from BCTs using TriZol (Sigma-Aldrich). Contaminating DNA was digested by DNase I (Stratagene) for 15 min at 37°C followed by phenol/chloroform extraction. After ethanol precipitation, 500 ng RNA was used for random-primed cDNA synthesis with SuperScript™ II Reverse Transcriptase (Invitrogen). For quantitative real-time polymerase chain reaction (PCR) analysis, 1 μ L of cDNA was amplified with the Absolute™ QPCR SYBR® Green Mix (ABgene Ltd.) and 1 μ M of each primer in a 25 μ L reaction using a Mastercycler® ep realplex2 (Eppendorf, Hamburg, Germany). Sequences and specifications of primers can be found in the Supplementary Table S1. PCR conditions included an initial denaturation step at 95°C for 15 min, followed by 40 cycles of denaturation at 95°C for 1 min, annealing at T_A for 1 min, and polymerization at 72°C for 1 min. Uniform size of amplicons and absence of nonspecific products were controlled by melting curves. Relative expression levels compared to the reference gene β -Actin were calculated using the $\Delta\Delta$ Ct-method corrected for PCR efficiencies.² Data are presented as mean \pm SEM for two independent experiments, each with two PCR runs performed in triplicate.

DNA and protein isolation and quantitation

Genomic DNA was isolated from single frozen BCTs using the QIAamp DNA Micro Kit (Qiagen), and DNA concentration was determined with a Nanodrop1000 UV-Vis spectrophotometer (Thermo Fisher Scientific). For tissue protein measurement, snap-frozen BCTs were homogenized in impact resistant tubes containing 6N HCl and 1.4 mm ceramic spheres (Lysing Matrix D from MP Biosciences) in a FastPrep24 Homogenizer (MP Biosciences). After acid hydrolysis with 6N HCl at 110°C for 16 h, total protein content was assessed in the neutralized samples using a colorimetric bicinchoninic acid assay (BCA protein Assay Kit; Thermo

Fisher Scientific) followed by absorbance measurement at 562 nm using the Absorbance Detection Cartridge in a PARADIGM™ Detection Platform with Multimode Analysis Software (all Beckman Coulter) and comparison to standard curve data of bovine serum albumin dilution series.

References

1. Wollert, K.C., Taga, T., Saito, M., Narazaki, M., Kishimoto, T., Glembofski, C.C., *et al.* Cardiotrophin-1 activates a distinct form of cardiac muscle cell hypertrophy. Assembly of sarco-
2. Pfaffl, M.W. A new mathematical model for relative quantification in real-time RT-PCR. *Nucleic Acids Res* **29**, e45, 2001.
3. Frank, D., Kuhn, C., Brors, B., Hanselmann, C., Ludde, M., Katus, H.A., *et al.* Gene expression pattern in biomechanically stretched cardiomyocytes: evidence for a stretch-specific gene program. *Hypertension* **51**, 309, 2008.
4. Hansen, A., Eder, A., Bonstrup, M., Flato, M., Mewe, M., Schaaf, S., *et al.* Development of a drug screening platform based on engineered heart tissue. *Circ Res* **107**, 35, 2010.

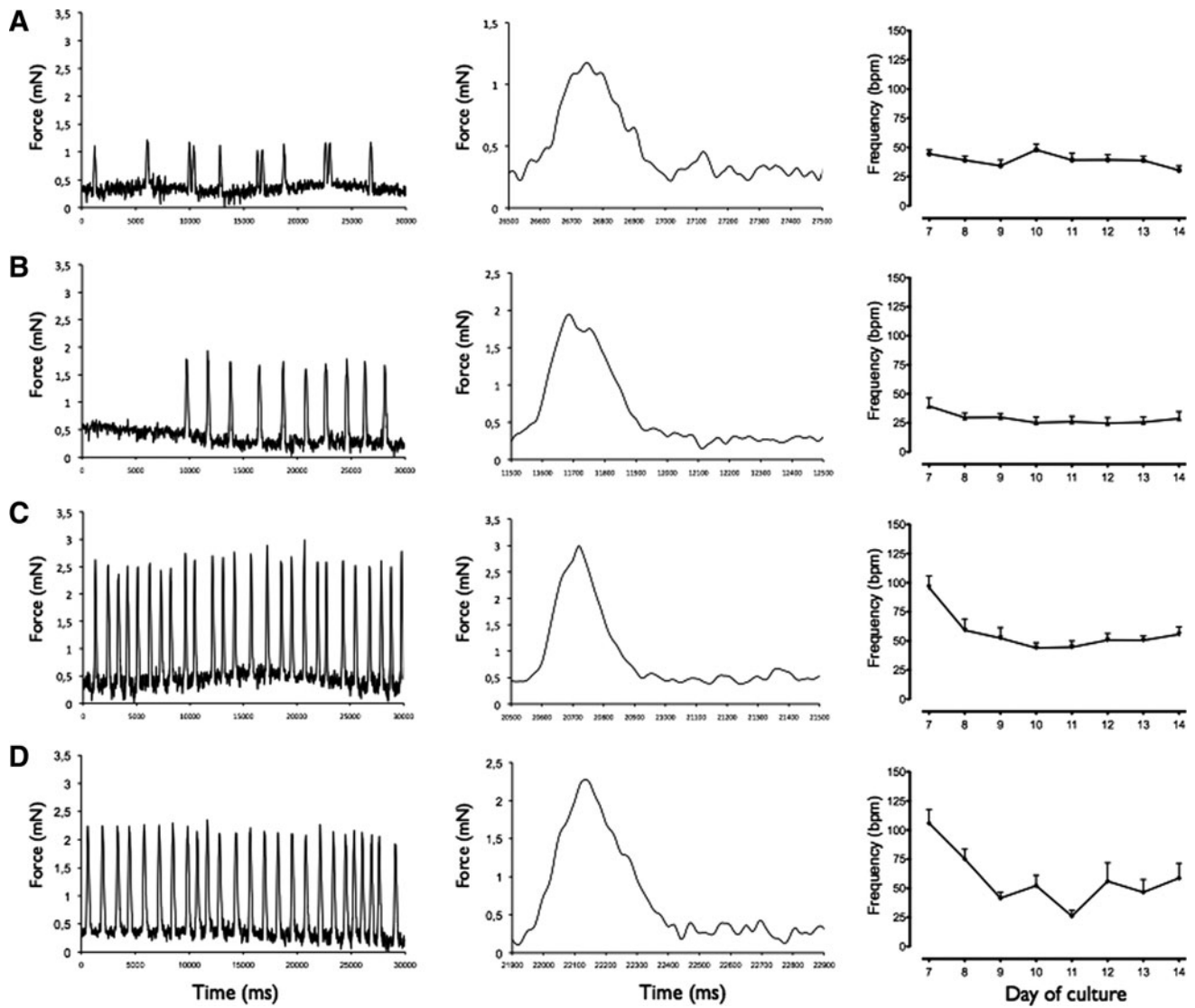
SUPPLEMENTARY TABLE S1. OLIGONUCLEOTIDES USED FOR QUANTITATIVE REAL-TIME POLYMERASE CHAIN REACTION

Name	Target	Position	T_A	Product (bp)	Sequence
β -Actin sense	GI 42475962	754	60	312	CAAGAGATGGCCACTGCC
β -Actin ras		1065			CTTGATCTTCATGGTGCTAGGA
α -MHC sense	GI186659509	44	60	276	GATGCCCAGATGGCTGACTT
α -MHC ras		319			GGTCAGCATGGCCATGTCCT
β -MHC sense	GI 8393806	5664	60	200	CGGAGGAACAGGCCAACACCA ^a
β -MHC ras		5863			GTCTCAGGGCTTCACAGGCATCC ^a
Atrial natriuretic factor sense	GI 202905	145	60	268	ATACAGTGCGGTGTCCAACA
Atrial natriuretic factor ras		412			AGCCCTCAGTTTGCTTTTCA
Connexin 43 sense	GI 33285446	553	60	195	CGGGGTCAACGTGGAGATGCAC
Connexin 43 ras		747			ACCGCGCTCAAGCTGAACCC
Calsequestrin-2 sense	GI 76563945	884	60	200	TCAAAGACCCACCCCTACGTC ^b
Calsequestrin-2 ras		1083			AGTCGTCTGGGTCAATCCAC ^b

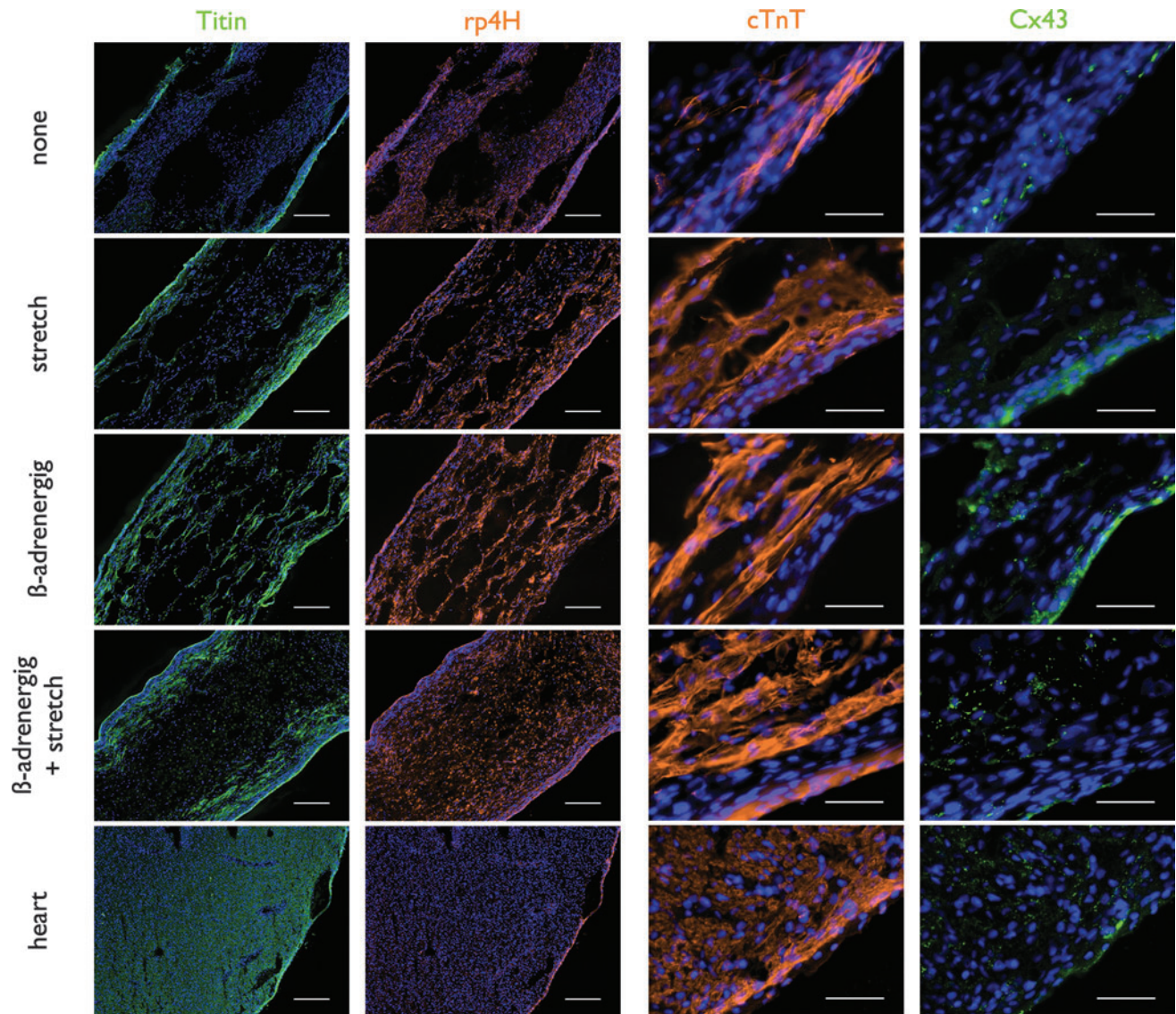
^aSequences taken from ref.³

^bSequence taken from ref.⁴

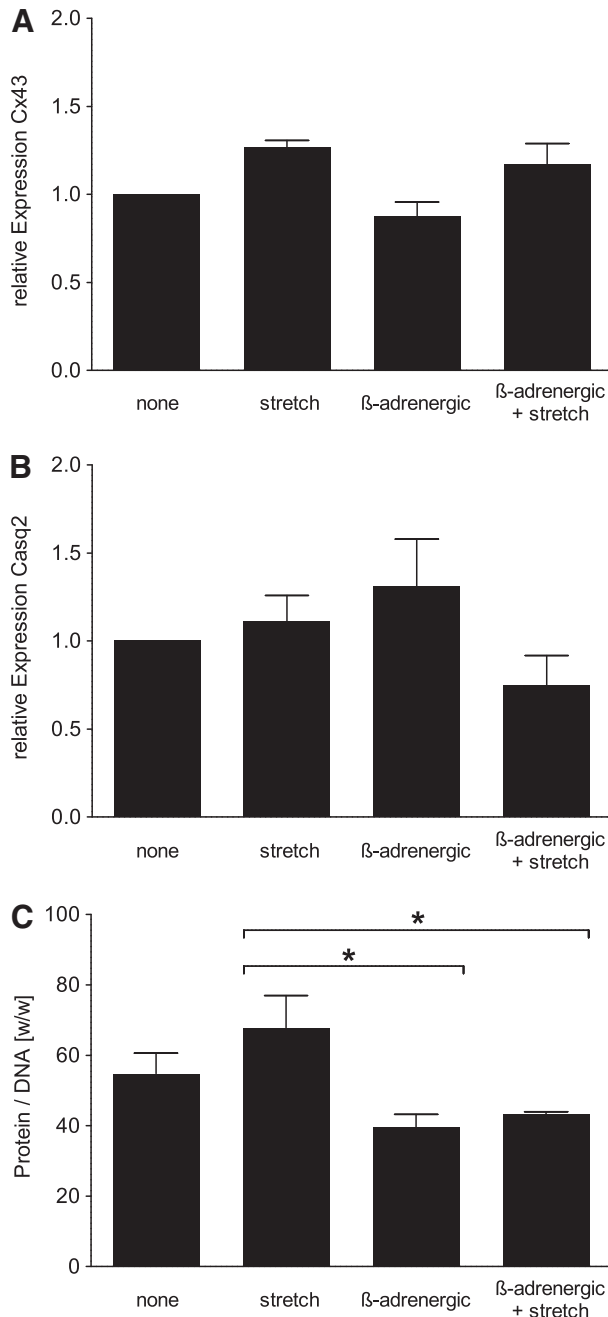
T_A , annealing temperature; MHC, myosin heavy chain.



SUPPLEMENTARY FIG. S1. Recordings of spontaneous active contraction forces measured with no preload were captured and displayed on-line in real-time diagrams. Representative images for groups treated with different stimuli: (A) none (negative control group); (B) stretch; (C) β -adrenergic stimulation; and (D) β -adrenergic stimulation + stretch, are shown in the left panel. Representative force peaks are displayed in the middle panel. Contraction frequencies were analyzed from d7 to d14 (right panel; $n \geq 10$).



SUPPLEMENTARY FIG. S2. Representative fluorescence microscopy images of immunostained tissue sections of different bioartificial cardiac tissue groups treated with different stimuli: none (negative control group); β -adrenergic stimulation; stretch; and β -adrenergic stimulation + stretch. Cardiomyocyte distribution is demonstrated by staining for titin (green) and prolylhydroxylase as a fibroblast marker (red) in the left panels. The right panels illustrate connexin 43 expression (green) in aligned cardiomyocytes (stained for cardiac troponin T, red) predominantly at the border of bioartificial cardiac tissues. All nuclei were stained with 4',6-diamidino-2-phenylindole (blue). Also shown is native neonatal rat heart tissue. Scale bars: 200 μm for left panels, and 50 μm for right panels.



SUPPLEMENTARY FIG. S3. (A, B) Expression levels were analyzed by quantitative real-time polymerase chain reaction on day 14 (d14) of cultivation for individual groups treated with different stimuli: none (negative control), stretch, β -adrenergic stimulation, and β -adrenergic stimulation + stretch. Depicted is the connexin 43 expression (A) and expression of calsequestrin-2 as a cardiomyocyte-specific gene (B). Expression levels were normalized to the reference gene β -actin using the $\Delta\Delta C_t$ -method, and compared to the untreated control group (normalized to equal 1.00). Data are presented as mean \pm SEM for two independent experiments, each with two polymerase chain reaction runs performed in triplicate; no significant differences were observed between all groups. (C) Protein/DNA ratio on d14 in response to different stimuli: none (negative control), stretch, β -adrenergic stimulation, and β -adrenergic stimulation + stretch. Data are presented as mean \pm SEM ($n \geq 3$; $*p < 0.05$).

SUPPLEMENTARY VIDEO S1. Time-lapse video of live cell fluorescence imaging of mitochondria-rich cardiomyocytes labeled selectively with tetramethylrhodamine methyl ester demonstrates cell elongation and alignment along the longitudinal axis of the bioartificial cardiac tissues (BCTs) in the course of tissue formation and maturation from d0 to d14. Given are fluorescence and brightfield videos of a control group BCT; scale bar: 500 μ m.

SUPPLEMENTARY VIDEO S2. Optical projection tomography analysis of overall cellular distribution in BCTs was performed after whole-mount 4',6-diamidino-2-phenylindole staining of nuclei (blue). A rotating three-dimensional representation of a virtual BCT slice shows overall cell distribution throughout the whole tissue on day 7, although lower cell numbers were detected in the center of the tissue.

3.2 Two-photon induced collagen cross-linking in bioartificial cardiac tissue (Manuscript 2)

Authors: Kai Kuetemeyer*, George Kensah*, Marko Heidrich, Heiko Meyer, Ulrich Martin, Ina Gruh, and Alexander Heisterkamp

*authors contributed equally

Published in Optics Express, Volume 19, Issue 17, August 15, pp 15996 – 16007

Experimental design:

Different groups for laser treatment were defined in collaboration with Kai Küttemeyer (Biomedical Optics Department, Laser Zentrum Hannover e.V., Hanover, Germany)

Laser treatment:

Kai Küttemeyer designed the optical setup for laser and performed the two-photon induced collagen cross-linking.

Optical projection tomography:

Marko Heidrich (Biomedical Optics Department, Laser Zentrum Hannover e.V., Hanover, Germany) did the optical projection tomography and data analyses after receiving DAPI-stained BCTs

Force data analyses:

Analyses of data derived from bioreactor experiments were done in cooperation with Kai Küttemeyer.

Fluorescence intensity analysis:

Kai Küttemeyer did analysis of captured fluorescence images.

Manuscript preparation:

The manuscript was written in collaboration with Kai Küttemeyer, Ina Gruh, Ulrich Martin (Hannover Medical School, Hanover, Germany) and Alexander Heisterkamp (Biomedical Optics Department, Laser Zentrum Hannover e.V., Hanover, Germany).

Two-photon induced collagen cross-linking in bioartificial cardiac tissue

Kai Kuetemeyer,^{1,4,*} George Kensah,^{2,4} Marko Heidrich,¹ Heiko Meyer,¹ Ulrich Martin,² Ina Gruh,^{2,3} and Alexander Heisterkamp^{1,3}

¹*Biomedical Optics Department, Laser Zentrum Hannover e.V., Hollerithallee 8, 30419 Hannover, Germany*

²*Department of Cardiac-, Thoracic-, Transplantation and Vascular Surgery, Leibniz Research Laboratories for Biotechnology and Artificial Organs (LEBAO), Carl-Neuberg-Str. 1, 30625 Hannover, Germany*

^{3,4}*Authors contributed equally to this work.*

[*k.kuetemeyer@lzh.de](mailto:k.kuetemeyer@lzh.de)

Abstract: Cardiac tissue engineering is a promising strategy for regenerative therapies to overcome the shortage of donor organs for transplantation. Besides contractile function, the stiffness of tissue engineered constructs is crucial to generate transplantable tissue surrogates with sufficient mechanical stability to withstand the high pressure present in the heart. Although several collagen cross-linking techniques have proven to be efficient in stabilizing biomaterials, they cannot be applied to cardiac tissue engineering, as cell death occurs in the treated area. Here, we present a novel method using femtosecond (fs) laser pulses to increase the stiffness of collagen-based tissue constructs without impairing cell viability. Raster scanning of the fs laser beam over riboflavin-treated tissue induced collagen cross-linking by two-photon photosensitized singlet oxygen production. One day post-irradiation, stress-strain measurements revealed increased tissue stiffness by around 40% being dependent on the fibroblast content in the tissue. At the same time, cells remained viable and fully functional as demonstrated by fluorescence imaging of cardiomyocyte mitochondrial activity and preservation of active contraction force. Our results indicate that two-photon induced collagen cross-linking has great potential for studying and improving artificially engineered tissue for regenerative therapies.

© 2011 Optical Society of America

OCIS codes: (190.4180) Multiphoton processes; (260.5130) Photochemistry; (170.1610) Clinical applications.

References and links

1. WHO (World Health Organization), "Cardiovascular Diseases," Fact Sheet Number 317, Geneva, Switzerland, January 2011.
2. W. H. Zimmermann, C. Fink, D. Kralisch, U. Remmers, J. Weil, and T. Eschenhagen, "Three-dimensional engineered heart tissue from neonatal rat cardiac myocytes," *Biotechnol. Bioeng.* **68**, 106–114 (2000).
3. W. H. Zimmermann, M. Tiburcy, and T. Eschenhagen, "Cardiac tissue engineering: a clinical perspective," *Future Cardiol.* **3**, 435–445 (2007).
4. K. L. Kreuziger and C. E. Murry, "Engineered human cardiac tissue," *Pediatr. Cardiol.* **32**, 334–341 (2011).
5. B. Bhana, R. K. Iyer, W. L. Chen, R. Zhao, K. L. Sider, M. Likhitanichkul, C. A. Simmons, and M. Radisic, "Influence of substrate stiffness on the phenotype of heart cells," *Biotechnol. Bioeng.* **105**, 1148–1160 (2010).

6. L. Moeller, A. Krause, J. Dahlmann, I. Gruh, A. Kirschning, and G. Draeger, "Preparation and evaluation of hydrogel-composites from methacrylated hyaluronic acid, alginate, and gelatin for tissue engineering," *Int. J. Artif. Organs* **34**, 93–102 (2011).
7. A. Marsano, R. Maidhof, L. Q. Wan, Y. Wang, J. Gao, N. Tandon, and G. Vunjak-Novakovic, "Scaffold stiffness affects the contractile function of three-dimensional engineered cardiac constructs," *Biotechnol. Prog.* **26**, 1382–1390 (2010).
8. C. Fink, S. Ergun, D. Kralisch, U. Remmers, J. Weil, and T. Eschenhagen, "Chronic stretch of engineered heart tissue induces hypertrophy and functional improvement," *FASEB J.* **14**, 669–679 (2000).
9. G. Kensah, I. Gruh, J. Viering, H. Schumann, J. Dahlmann, H. Meyer, D. Skvorc, A. Baer, P. Akhyari, A. Heisterkamp, A. Haverich, and U. Martin, "A novel miniaturized multimodal bioreactor for continuous *in situ* assessment of bioartificial cardiac tissue during stimulation and maturation," *Tissue Eng. Pt. C Methods* **17**, 463–473 (2011).
10. W. M. Elbjeirami, E. O. Yonter, B. C. Starcher, and J. L. West, "Enhancing mechanical properties of tissue-engineered constructs via lysyl oxidase crosslinking activity," *J. Biomed. Mater. Res.* **66**, 513–521 (2003).
11. T. S. Girton, T. R. Oegema, and R. T. Tranquillo, "Exploiting glycation to stiffen and strengthen tissue equivalents for tissue engineering," *J. Biomed. Mater. Res.* **46**, 87–92 (1999).
12. C. L. McIntosh, L. L. Michaelis, A. G. Morrow, S. B. Itscoitz, D. R. Redwood, and S. E. Epstein, "Atrioventricular valve replacement with the Hancock porcine xenograft: a five-year clinical experience," *Surgery* **78**, 768–775 (1975).
13. H. Dardik, I. M. Ibrahim, R. Baier, S. Sprayregen, M. Levy, and I. I. Dardik, "Human umbilical cord. A new source for vascular prosthesis," *JAMA, J. Am. Med. Assoc.* **236**, 2859–2862 (1976).
14. G. Wollensak, E. Spoerl, and T. Seiler, "Riboflavin/ultraviolet-A-induced collagen crosslinking for the treatment of keratoconus," *Am. J. Ophthalmol.* **135**, 620–627 (2003).
15. A. Jayakrishnan and S. R. Jameela, "Glutaraldehyde as a fixative in bioprostheses and drug delivery matrices," *Biomaterials* **17**, 471–484 (1996).
16. M. C. DeRosa and R. J. Crutchley, "Photosensitized singlet oxygen and its applications," *Coordin. Chem. Rev.* **233-234**, 351–371 (2002).
17. A. S. McCall, S. Kraft, H. F. Edelhauser, G. W. Kidder, R. R. Lundquist, H. E. Bradshaw, Z. Dedeic, M. J. C. Dionne, E. M. Clement, and G. W. Conrad, "Mechanisms of corneal tissue cross-linking in response to treatment with topical riboflavin and long-wavelength ultraviolet radiation (UVA)," *Invest. Ophthalmol. Visual Sci.* **51**, 129–138 (2010).
18. G. Wollensak, E. Spoerl, M. Wilsch, and T. Seiler, "Keratocyte apoptosis after corneal collagen cross-linking using riboflavin/UVA treatment," *Cornea* **23**, 43–49 (2004).
19. T. Tanabe, M. Oyamada, K. Fujita, P. Dai, H. Tanaka, and T. Takamatsu, "Multiphoton excitation-evoked chromophore assisted laser inactivation using green fluorescent protein," *Nat. Methods* **2**, 503–505 (2005).
20. K. Koenig, I. Riemann, P. Fischer, and K. H. Halbhauer, "Intracellular nanosurgery with near infrared femtosecond laser pulses," *Cell Mol. Biol. (Paris)* **45**, 195–201 (1999).
21. W. Denk, J. H. Strickler, and W. W. Webb, "Two-photon laser scanning fluorescence microscopy," *Science* **248**, 73–76 (1990).
22. D. Warther, S. Gug, A. Specht, F. Bolze, J. F. Nicoud, A. Mourrot, and M. Goeldner, "Two-photon uncaging: new prospects in neuroscience and cellular biology," *Bioorgan. Med. Chem.* **18**, 7753–7758 (2010).
23. K. Kuetemeyer, R. Rezgüi, H. Lubatschowski, and A. Heisterkamp, "Influence of laser parameters and staining on femtosecond laser-based intracellular nanosurgery," *Biomed. Opt. Express* **1**, 587–597 (2010).
24. P. K. Frederiksen, M. Jorgensen, and P. R. Ogilby, "Two-photon photosensitized production of singlet oxygen," *J. Am. Chem. Soc.* **123**, 1215–1221 (2001).
25. K. Koenig, "Multiphoton microscopy in life sciences," *J. Microsc.* **200**, 83–104 (2000).
26. A. Hopt and E. Neher, "Highly nonlinear photodamage in two-photon fluorescence microscopy," *Biophys. J.* **80**, 2029–2036 (2001).
27. S. Kalies, K. Kuetemeyer, and A. Heisterkamp, "Mechanisms of high-order photobleaching and its relationship to intracellular ablation," *Biomed. Opt. Express* **2**, 805–816 (2011).
28. A. Vogel, J. Noack, G. Huettman, and G. Paltauf, "Mechanisms of femtosecond laser nanosurgery of cells and tissues," *Appl. Phys. B* **81**, 1015–1047 (2005).
29. G. A. Blab, P. H. M. Lommerse, L. Cognet, G. S. Harms, and T. Schmidt, "Two-photon excitation action cross-sections of the autofluorescent proteins," *Chem. Phys. Lett.* **350**, 71–77 (2001).
30. W. R. Zipfel, R. M. Williams, R. Christie, A. Y. Nikitin, B. T. Hyman, and W. W. Webb, "Live tissue intrinsic emission microscopy using multiphoton-excited native fluorescence and second harmonic generation," *Proc. Natl. Acad. Sci. U.S.A.* **100**, 7075–7080 (2003).
31. R. A. Lorbeer, M. Heidrich, C. Lorbeer, D. F. Ramirez-Ojeda, G. Bicker, H. Meyer, and A. Heisterkamp, "Highly efficient 3D fluorescence microscopy with a scanning laser optical tomograph," *Opt. Express* **19**, 5419–5430 (2011).
32. M. H. Niemz, *Laser-Tissue Interactions: Fundamentals and Applications* (Springer, 2007).
33. B. A. Roeder, K. Kokini, J. E. Sturgis, J. P. Robinson, and S. L. Voytik-Harbin, "Tensile mechanical properties

- of three-dimensional type I collagen extracellular matrices with varied microstructure," J. Biomech. Eng. **124**, 214–222 (2002).
34. G. Wollensak, E. Spoerl, and T. Seiler, "Stress-strain measurements of human and porcine corneas after riboflavin-ultraviolet-A-induced cross-linking," J. Cataract Refractive Surg. **29**, 1780–1785 (2003).
 35. M. Eghbali and K. T. Weber, "Collagen and the myocardium: fibrillar structure, biosynthesis and degradation in relation to hypertrophy and its regression," Mol. Cell. Biochem. **96**, 1–14 (1990).
 36. C. Xu and W. W. Webb "Measurement of two-photon excitation cross sections of molecular fluorophores with data from 690 to 1050 nm," J. Opt. Soc. Am. B **13**, 481–491 (1996).
 37. B. P. Yu, "Cellular defenses against damage from reactive oxygen species," Physiol. Rev. **74**, 139–162 (1994).
 38. Z. H. Syedain, J. Bjork, L. Sando, and R. T. Tranquillo, "Controlled compaction with ruthenium-catalyzed photochemical cross-linking of fibrin-based engineered connective tissue," Biomaterials **30**, 6695–6701 (2009).
 39. A. Vogel and V. Venugopalan, "Mechanisms of pulsed laser ablation of biological tissues," Chem. Rev. **103**, 577–644 (2003).
 40. G. M. Fomovsky, J. R. Macadangang, G. Ailawadi, and J. W. Holmes, "Model-based design of mechanical therapies for myocardial infarction," J. Cardiovasc. Transl. Res. **4**, 82–91 (2011).
-

1. Introduction

Tissue engineering is a promising strategy for regenerative therapies to overcome the shortage of donor organs and tissues for transplantation purposes [1]. Three-dimensional tissue engineering aims at mimicking the characteristics of natural tissue in matrix composition and morphology, as well as cellular distribution and orientation. For cardiac tissue engineering, the following physiological properties are essential for the generation of functional transplantable tissue surrogates: i) spontaneous and synchronous contractility, ii) development of sufficient systolic (contraction) and diastolic (passive) forces to support the heart's pumping function and to withstand the hydrodynamic pressures in the heart, respectively. Several groups have shown the possibility to generate functional artificial cardiac tissue and its transplantation in animal models with beneficial effects to heart function after acute myocardial infarction [2–4].

Mechanical properties of the artificial tissue are mostly influenced by the initial seeding number and composition of cells, providing stabilization via their cytoskeleton and the production of extracellular matrix (ECM) proteins. By adjusting the initial addition of ECM components and/or composition of other biomaterials as scaffolds with different intrinsic mechanical properties, tissue mechanics can be defined in a wide range of requirements [5,6]. Vice versa, scaffold mechanical stiffness was found to have a significant influence on cardiomyocyte morphology and function, both when seeded as monolayer cultures [5] or in three-dimensional engineered cardiac constructs [7]. One way to modulate tissue properties *after* tissue generation is in vitro maturation and remodeling, e.g. by application of mechanical stretch stimulation in a bioreactor [8,9]. Another way is cross-linking of matrix components. In a transgenic approach, overexpression of lysyl oxidase was utilized to enzymatically cross-link ECM proteins, particularly collagen and elastin, to enhance the mechanical integrity of the ECM and thereby impart mechanical strength to the engineered tissue [10]. Alternatively, glycation, i.e. the non-enzymatic cross-linking of proteins by reducing sugars, was demonstrated to stiffen and strengthen tissue equivalents in a matter of a few weeks of incubation [11]. By contrast, chemical methods allow for fast and efficient cross-linking and might enable direct spatial control of tissue stiffness.

Chemical cross-linking has been established as an efficient method to stabilize collagen-based biomaterials, such as porcine heart valves [12] and blood vessels [13]. In ophthalmology, it is used to increase the human corneal stiffness to stop the progression of keratoconus [14]. Collagen cross-linking is generally induced by either aldehyde-reactions or UV-A irradiation with photosensitizers, such as riboflavin. Aldehyde cross-linking is presumed to result from covalent bond formation of aldehyde groups with amino groups or peptides. To avoid inflammatory reactions, cytotoxicity and calcification after implantation of cross-linked tissue into the patient, thorough removal or inactivation of excess aldehyde molecules is necessary [15].

UV-A irradiation of photosensitizers catalyzes carbonyl-based cross-linking reactions via one-photon photosensitized singlet oxygen production [16, 17]. However, the positive effect of both methods on the tissue stiffness is accompanied by cell apoptosis in the treated area. In cornea, this negative side effect is compensated by subsequent repopulation of treated areas with viable cells *in vivo* [18]. In case of cardiac tissue, repopulation is impaired by the non-proliferative phenotype of cardiomyocytes and most probably would result in the formation of a fibrous scar. Therefore, to apply cross-linking to cardiac tissue engineering, novel methods must be developed and evaluated which do not alter cell viability.

Compared to continuous UV-A illumination, the interaction of femtosecond (fs) laser pulses with biological tissue is based on nonlinear excitation. This enables higher penetration depths and impedes out-of-focus absorption and photodamage [25]. Therefore, fs laser in the near infrared (NIR) wavelength range are extensively used for therapeutic applications on a sub-cellular level, such as chromophore assisted laser inactivation of proteins [19], intracellular nanodissection [20] and laser uncaging [21]. All these applications have in common that biological samples are treated with a light-sensitive probe (e.g. fluorophore, caged compound) with a high multiphoton absorption cross-section prior to irradiation. These photosensitizers enhance the yield of chemical reactions with surrounding molecules leading to bond cleavage or rearrangements [22,23]. For example, Frederiksen et al. showed that singlet oxygen is largely produced by two-photon excitation of different photosensitizers [24]. Great care has to be taken in the photosensitizer selection, as two-photon absorption of intrinsic fluorophores induces severe photodamage including impaired cell division or apoptosis [25, 26]. At even higher laser intensities, higher-order effects become more important causing photobleaching of photosensitizers, oxidative stress and the formation of a low-density plasma [27, 28]. As the two-photon absorption cross-section scales super-linearly with the one-photon absorption cross-section, differences between extrinsic and intrinsic fluorophores are much more pronounced in the former case [29]. Consequently, nonlinear excitation with NIR wavelengths may be suitable for collagen cross-linking without compromising cell viability.

In this paper, we show the great potential of fs laser pulses for collagen cross-linking in bioartificial cardiac tissue. Collagen cross-linking was induced by raster-scanning the laser beam over riboflavin treated tissue. Subsequent stress-strain measurements were done to evaluate tissue stiffness and contractility while fluorescence microscopy was used to assess cell viability.

2. Materials and methods

2.1. Tissue preparation

Two cell sources were used for artificial tissue preparation: i) for proof-of-concept, murine embryonic fibroblasts (MEF) were used to generate a model system of collagen-rich artificial tissue, ii) neonatal rat cardiomyocytes (NRCM) were used to generate bioartificial cardiac tissue (BCT). Three-dimensional tissue was prepared as described earlier [9]. In brief, either $6 \cdot 10^5$ gamma-irradiated MEFs from CD1-ICR mice, or $1 \cdot 10^6$ freshly isolated cardiomyocytes (NRCMs) from Sprague-Dawley neonatal rats (enriched by discontinuous Percoll gradient centrifugation) were mixed with liquid extracellular matrix (consisting of 0.9 mg/ml collagen type I (R&D Systems), 10% Matrigel (BD Biosciences)) and poured into custom-made Teflon molds (220 μ l). The mixture was covered with 5 ml Dulbecco's modified Eagle's medium (DMEM) containing 12% horse serum, 2 mM L-glutamin (all Gibco), 2% chicken embryo extract (US Biological), 10 μ g/ml insulin (Sigma), 100 U/ml penicillin and 100 μ g/ml streptomycin (PAA Laboratories) and cultured in a standard incubator at 5% CO₂, 37°C and 80% humidity with daily medium exchange. Within the molds, the solidified tissue was suspended between two titanium rods and had an average cross-sectional area of 0.8 mm² on day 7 (see Fig. 1a).

All experiments were performed in accordance with the principles of Laboratory Animal

Care (NIH publication No. 86-23, revised 1985) as well as the Animal Welfare Law of Lower Saxony, Germany.

2.2. Optical Setup

The optical setup is shown in Fig. 1b. The laser source was a regeneratively amplified Ti:Sapphire laser system producing femtosecond pulses, either a Spectra Physics Spitfire Pro (120 fs, 800 nm, 5 kHz) or a Thales Bright (120 fs, 780 nm, 5 kHz). At the used wavelengths, riboflavin has a two-photon action cross-section of about 0.5 GM at 780 nm and 0.45 GM at 800 nm [30]. The laser beam was demagnified by a two-lens telescope to match the diameter of the following optics and attenuated by a variable neutral density (ND) filter. Two high-speed galvanometer mirrors (Litrack) were used to scan the laser beam in the x-y plane. Focusing into the tissue was achieved either by a 140-mm or 400-mm focal length lens. This resulted in a spot diameter of 130 and 380 μm as well as a rayleigh length of 17 and 145 mm, respectively, being much larger than the average tissue depth of 0.8 mm.

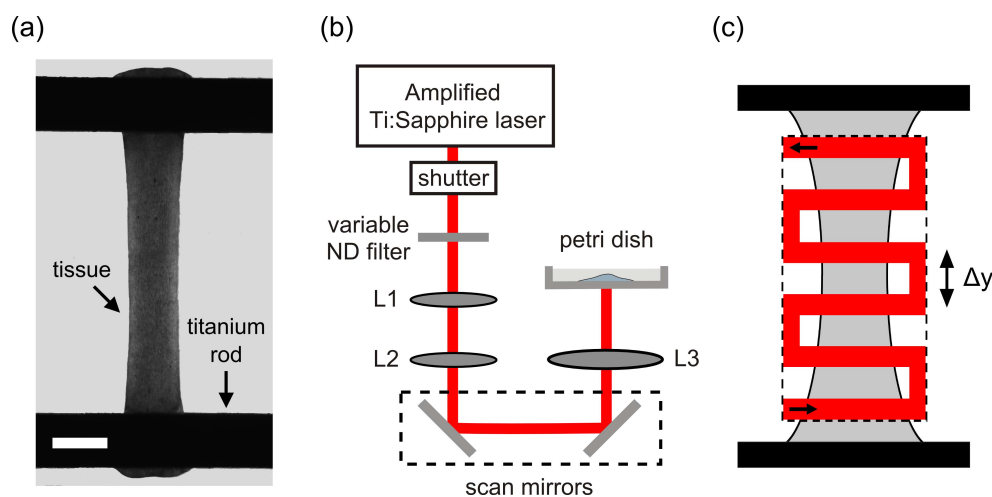


Fig. 1. (a) Phase contrast microscopy image of a MEF-based tissue suspended between titanium rods on day 7 prior to laser irradiation. Scale bar: 1 mm. (b) Schematic setup for two-photon induced collagen cross-linking. L1 / L2: $f_1=250$ and $f_2=-50$ mm plano-convex and plano-concave lenses; L3: focusing lens with $f=140$ mm or $f=400$ mm. (c) Tissue constructs were raster-scanned with a constant scanning speed and line separation Δy being equal to the focal spot radius.

2.3. Two-photon induced collagen cross-linking

After six days of cultivation, the photosensitizer riboflavin (RF, Sigma Aldrich) was added to one part of the tissue constructs at 0.01% (0.27 mM) concentration in the culture medium. This RF concentration is one order below that used for UV-A collagen cross-linking [14]. However, solutions with higher concentrations could not be made because of its limited solubility in the culture medium. On day seven, each tissue was transferred within the Teflon mold to a 35 mm glass bottom dish (ibidi GmbH) with a thickness of 170 μm . Collagen cross-linking was induced by raster scanning the laser beam over the tissue with a constant scanning speed and line separation (see Fig. 1c). The line separation Δy corresponded to the focal spot radius for both focusing lenses. Depending on the scanning parameters, the cross-linking procedure lasted approximately 30 seconds to 5 min. The experiments were done at room temperature and

normal atmosphere unless otherwise stated. Immediately after laser irradiation, each tissue was washed in culture medium without RF and further incubated for 24 hours at 37°C and 5% CO₂ humidified atmosphere.

2.4. Stress-strain measurements

Forces were measured in a bioreactor system that allows for continuous increase in strain and on-line force measurement in a standard incubator [9]. For MEF-based and bioartificial cardiac tissue (BCT), the increase in passive force as a function of increase in strain ($33.25 \pm 1.75 \mu\text{m/s}$) along the longitudinal axis of the tissue constructs was measured for each tissue in culture medium until the preload reached 20%. The engineering stress was calculated as force divided by the initial cross-sectional area. The slope of the linear region of the stress-strain curve ("Young's modulus") was determined by linear regression. To assess the active contractility of treated and untreated control groups of cardiac tissue, BCTs were electrically paced five times with no preload at 25 V with rectangular pulses (5 ms) prior to stress-strain measurements.

The statistical significance was tested using one-way analysis of variance (ANOVA) followed by multiple comparisons against the untreated control group using Dunnett's test. Differences were considered significant at $P < 0.05$.

2.5. Fluorescence microscopy

One day prior to cross-linking experiments, the tissue was incubated with 25 nM tetramethylrhodamine methyl ester (TMRM; Invitrogen). TMRM is a cationic fluorescent dye being rapidly and reversibly taken up by live cells and sequestered to active mitochondria, and therefore can be used to monitor the cellular metabolic activity. Re-staining with TMRM immediately after laser irradiation was performed to compensate for photobleaching. Images of the tissue cross-sectional area were obtained while sandwiched between two cover glasses. To analyze the volumetric cell density one day after cross-linking, tissues were fixed for 20 minutes in acetone and nuclei were stained with DAPI (Invitrogen). Fluorescence images were either captured with a commercial AxioObserver Z1 microscope (Carl Zeiss AG) or a custom made scanning laser optical tomograph (SLOT) described elsewhere [31]. In brief, SLOT is a highly efficient 3D fluorescence microscopy technique capable of imaging specimens with sizes up to several millimeters. For imaging, the specimen was mounted in a glass capillary filled with 100% glycerol for optical clearing.

3. Results

3.1. Collagen cross-linking in MEF-based tissue

The first set of experiments was done with the Spitfire Pro laser system. The focal spot radius and scanning speed were determined to 65 μm and 300 $\mu\text{m/s}$, respectively, corresponding to an irradiation time of approximately 5 minutes. In preliminary experiments, tissues were irradiated with different pulse energies to identify suitable parameters. The laser fluence was thereby defined as the pulse energy, divided by the focal area, times the number of pulses. Two laser fluences were chosen empirically for two-photon induced collagen cross-linking [28]: 160 and 320 J/cm^2 . For MEF-based tissue as our model system of collagen-rich artificial tissue, samples were divided into five groups: (1) untreated control, (2) RF treatment, (3) 160 J/cm^2 laser fluence with RF treatment and 320 J/cm^2 laser fluence (4) with and (5) without RF treatment.

All tissues exhibited similar stress-strain relationships 24 hours after irradiation. The stress-strain curves showed an initial nonlinear ("toe") region followed by a linear region from about 15% strain (see Fig. 2a). RF treatment alone did not influence the stress-strain relation. By

contrast, irradiation of RF treated tissues at 160 J/cm^2 resulted in an increased stiffness of 35% compared to untreated controls at 20% strain (see Fig. 2b). A similar rise was observed for the slope of the stress-strain relation in the linear region, the so-called Young's modulus (46.6 ± 0.3 vs. $34.8 \pm 2.3 \text{ kPa}$). When the laser fluence was doubled to 320 J/cm^2 , the positive effect on tissue stiffness was no longer observed, independent of RF treatment.

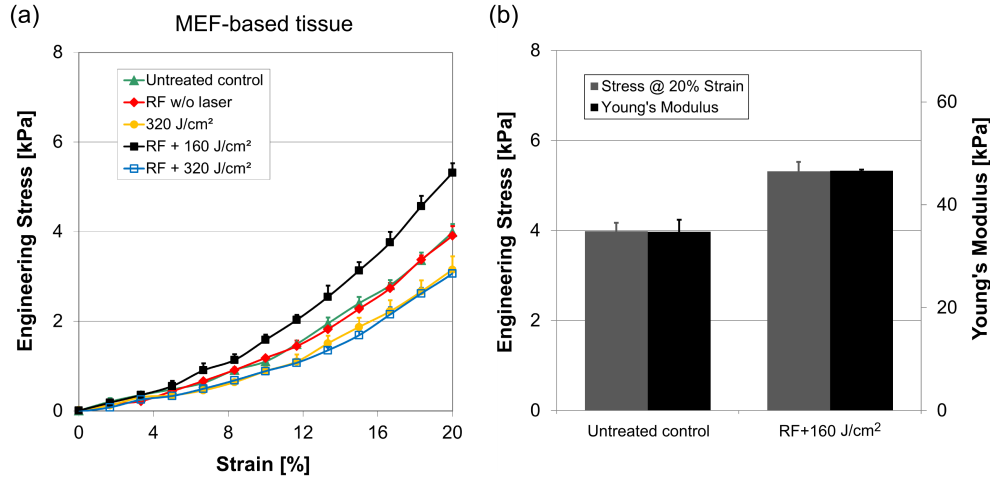


Fig. 2. (a) Stress-strain relation of MEF-based tissues after RF treatment and fs laser irradiation. RF or laser treatment alone did not have an effect on tissue stiffness. Increased stiffening occurred after RF treatment and irradiation at 160 J/cm^2 . At the higher fluence of 320 J/cm^2 , this positive effect was no longer observed. (b) Irradiation of RF treated tissues at 160 J/cm^2 resulted in an increase of engineering stress at 20% strain and Young's modulus by 35% compared to untreated controls. Each data point represents the mean \pm SEM of two experiments.

At the lower fluence, the TMRM and DAPI fluorescence intensities of irradiated and non-irradiated areas were comparable. Therefore, laser irradiation at these parameters had no detrimental effects on cell metabolic activity and density. By contrast, the metabolic activity was markedly reduced at the higher fluence (see Fig. 4a), independent of RF treatment. At the same time, no influence on cell density was found as indicated by unchanged DAPI fluorescence intensities (data not shown).

3.2. Collagen cross-linking in bioartificial cardiac tissue (BCT)

As a next step, collagen cross-linking in BCTs was evaluated under the same experimental conditions as in Sec. 3.1. BCTs were divided into four groups: (1) untreated control, 160 J/cm^2 laser fluence (2) with and (3) without RF treatment and (4) 320 J/cm^2 laser fluence with RF treatment.

As with MEF-based tissue, the tensile stress showed a nonlinear dependence on the strain amplitude, which changes into a linear dependence at 15% strain. However, the stiffness and Young's modulus of BCTs were about a factor three lower (data not shown). Irradiation of untreated BCTs at 160 J/cm^2 did not change the stress-strain relation. Using the same irradiation parameters for RF treated tissues resulted in an increased stiffness by 25% compared to untreated controls at 20% strain, while Young's modulus only increased by 6% (14.9 ± 1.7 vs. $14.1 \pm 1.4 \text{ kPa}$). At the higher fluence of 320 J/cm^2 , mechanical properties of tissues were no longer influenced. Because of the high variation of stiffness in all treatment groups, the measured differences were not statistically significant ($P > 0.25$).

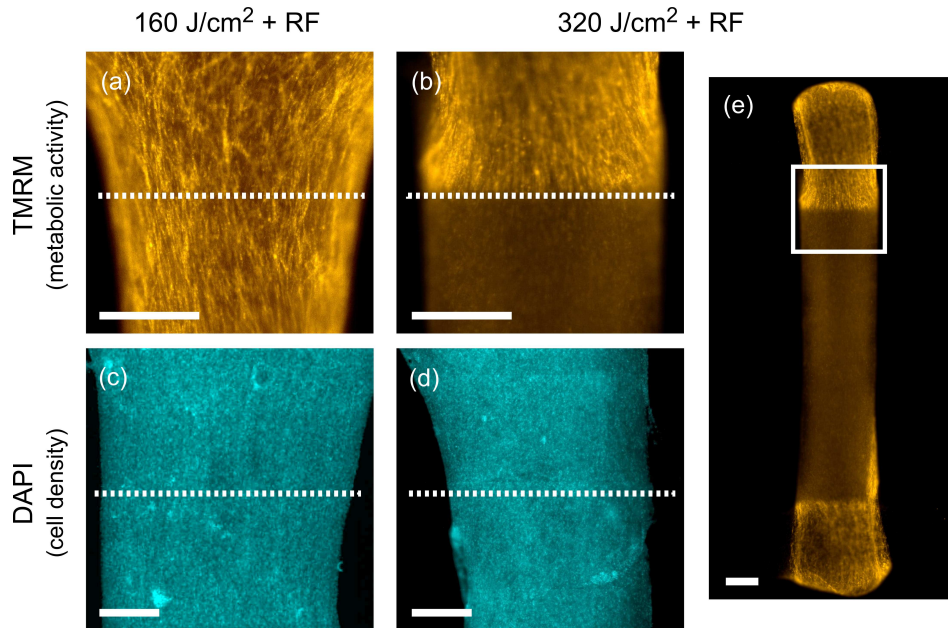


Fig. 3. Representative (a,b) TMRM and (c,d) DAPI fluorescence microscopy images of RF treated and laser irradiated BCTs: (a,c) 160 J/cm² laser fluence + RF; (b,d) 320 J/cm² laser fluence + RF. The white dotted lines separate the irradiated (bottom) and non-irradiated areas (top). A high magnification image of the boxed area in (e) is provided in (b). At the higher laser fluence, irradiation resulted in a marked decrease of TMRM fluorescence intensity, while DAPI fluorescence was still intense. Scale bar: 500 µm.

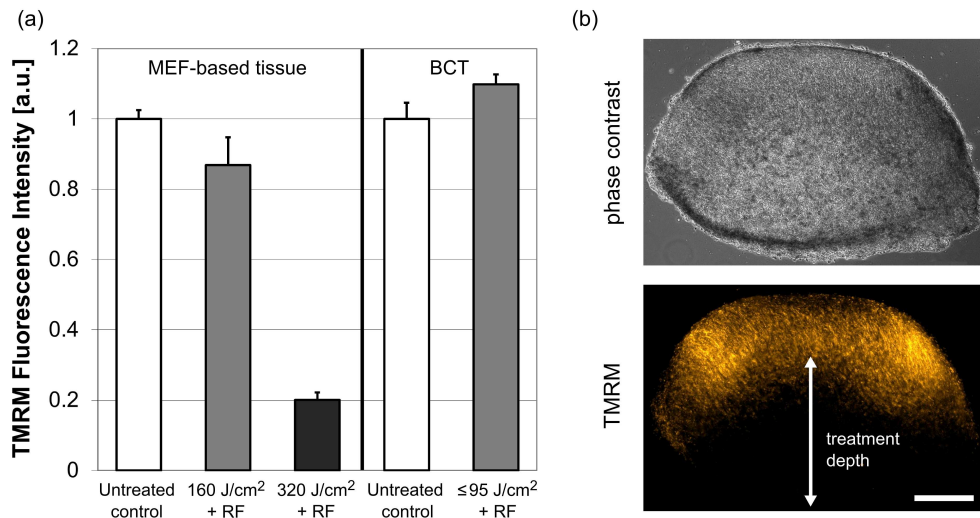


Fig. 4. (a) Average TMRM fluorescence intensity in untreated control and RF treated + laser irradiated MEF-based tissues and BCTs. Each bar represents the mean \pm SEM of two (MEF) and five (BCT) measurements. (b) Phase contrast and TMRM fluorescence images over the cross-sectional area of a BCT treated with RF and irradiated from below at 300 J/cm². The maximum depth of laser treatment was measured at an incident angle of 0° to about 520 µm. Scale bar: 200 µm.

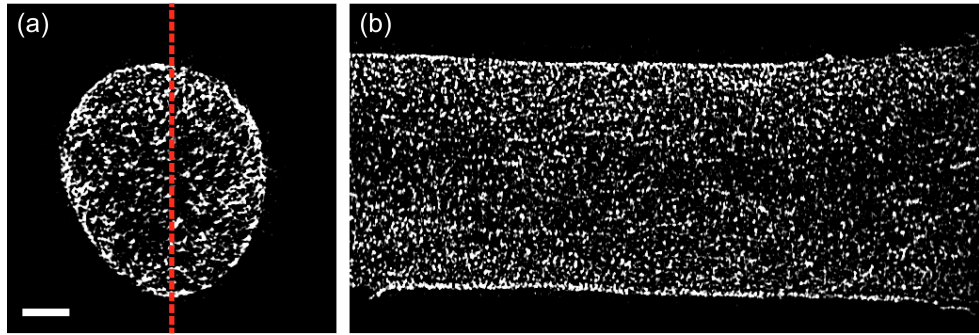


Fig. 5. Representative SLOM fluorescence images of cross-linked BCT after fixation and DAPI staining. The section plane of the right image is indicated by the red dashed line in the left image. No difference in the volumetric cell density was observed between irradiated and non-irradiated areas. Scale bar: 200 μm .

Similar to the previous section, irradiation at 160 J/cm^2 laser fluence had no influence on cell metabolic activity and density, as indicated by strong TMRM and DAPI fluorescence (see Fig. 3a and c). At the higher fluence, reduced metabolic activity was observed in irradiated areas, but without any change in volumetric cell density (see Figs. 3b and 5). TMRM fluorescence images of the BCT cross-sectional area in this parameter regime revealed that the depth of laser treatment decreased with increasing incident angle of the laser beam on the curved tissue surface (see Fig. 4b). The maximum depth of laser treatment was measured at an incident angle of 0° to about $520 \mu\text{m}$, being more than half the tissue depth.

In case of BCTs, tissue functionality can be directly assessed by measurement of contractile forces, which will be exerted by viable cardiomyocytes only. All BCT groups exhibited spontaneous active contraction with no preload both before and 24 hours after irradiation. Electrical stimulation in the bioreactor induced contraction forces up to 0.8 mN with no significant difference between the experimental groups ($P > 0.3$, data not shown).

3.3. Optimization of two-photon induced collagen cross-linking in BCTs

For the treatment of cardiac tissue, protocols were further optimized to reduce the stress applied to the cells and to improve the enhancement of mechanical properties. First, an infrared lamp was integrated into the setup and HEPES buffer was added to the culture medium to maintain optimal culture conditions outside the incubator (37°C and $5\% \text{ CO}_2$). Second, the focal spot diameter and scanning speed were increased from 130 to $380 \mu\text{m}$ and from 300 to $1300 \mu\text{m/s}$, respectively, to reduce the irradiation time to 30 s . Third, repetitive raster scanning of the tissue enabled the use of lower pulse energies for collagen cross-linking as multiphoton-induced photochemical effects accumulate over multiple pulses [23, 28]. However, to maintain a high sample throughput, the scanning pattern was only applied five times. Fourth, the experiments were done with the Thales Bright laser system at 780 nm at which the two-photon action cross-section of RF is about 10% higher [30].

Using optimized conditions, stress-strain measurements revealed a strong influence of the laser fluence on the mechanical properties (see Fig. 6). Significant tissue stiffening by 40% at 20% strain was only observed in a small window of laser fluences around 50 J/cm^2 ($P < 0.05$). The corresponding Young's modulus increased by about 15% (30.6 ± 0.9 vs. $26.5 \pm 1.9 \text{ kPa}$). Compared to Sec. 3.2, the enhancement of mechanical properties was improved by about a factor two. At the same time, no significant influence on active contraction force and cell metabolic activity was observed (see Fig. 4a), independent of the laser fluence up to 95 J/cm^2 ($P > 0.1$).

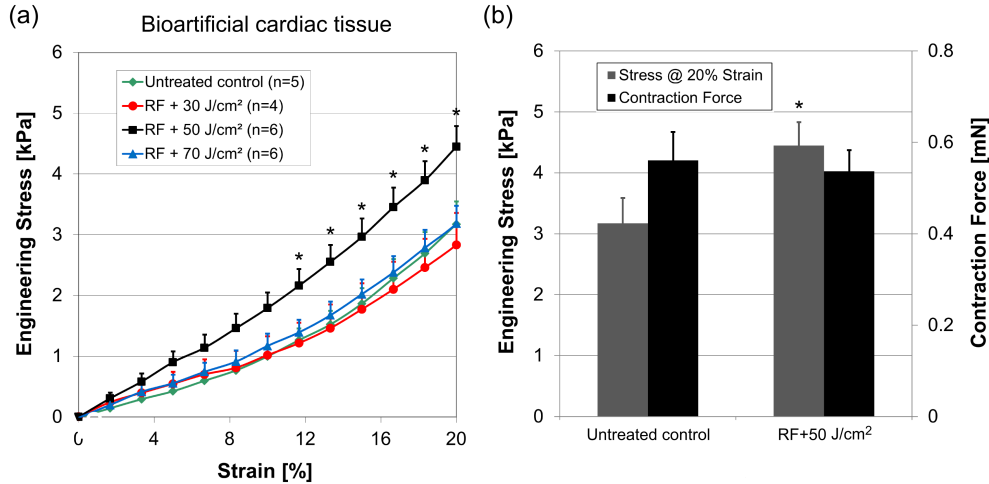


Fig. 6. (a) Stress-strain relation of bioartificial cardiac tissue (BCT) after optimization of the cross-linking procedure. Significant stiffening was observed in a small process window around 50 J/cm^2 . (b) Laser irradiation of RF treated BCTs at 50 J/cm^2 resulted in a significantly increased stiffness by 40% at 20% strain, while the active contraction force was comparable to untreated controls. Each data point represents the mean \pm SEM of at least four experiments. * $P < 0.05$ versus untreated control group.

4. Discussion and conclusion

The presented results indicate the great potential of femtosecond (fs) laser pulses for fast, efficient and non-toxic cross-linking of bioartificial collagenous tissue.

To induce collagen cross-linking, we irradiated riboflavin treated collagenous tissue with fs laser pulses in the NIR wavelength range at low pulse energies generally used for multiphoton-induced photochemistry [28]. The resulting maximum treatment depth was about $520 \mu\text{m}$, corresponding to 65% of the average tissue depth (see Fig. 4b). In contrast to existing methods, raster scanning of the laser beam enabled full spatial control of selective cross-linking in three-dimensional tissue [14, 15]. Owing to the surface curvature, the coupling efficiency of laser energy into tissue continuously decreased towards the edges of the tissue, as described by the Fresnel reflectivity equations and Snell's Law [32]. Consequently, only half the tissue volume was irradiated with about the same fluence. The achievable precision with our setup was in the order of $100 \mu\text{m}$, equivalent to the focal spot diameter. By applying tight focusing with high numerical aperture objectives, the focal spot diameter can be reduced to the sub-micrometer range [25]. In combination with a rotating stage for the tissue, homogeneous energy deposition and hence selective cross-linking within a sub-femtoliter volume is feasible in future experiments.

In our experiments, we used MEF-based and bioartificial cardiac tissue (BCT), containing fibroblasts and enriched primary cardiomyocytes with a lower proportion of fibroblasts, respectively, to examine the influence of different cell compositions. One-day post irradiation, the stress-strain relations of both tissue types exhibited a non-linear "toe" region followed by a linear region from about 15% strain, characteristic of collagenous tissue [33, 34]. At a fluence of 160 J/cm^2 , considerable tissue stiffening and increase in Young's modulus by 35% was observed in MEF-based tissues. Using the same parameters, the enhancement of mechanical properties was lower in BCTs (compare Figs. 2a and 6a). The higher increase in MEF-based tissues can be explained by the higher initial fibroblast content and hence a higher content

and/or turnover of extracellular matrix (ECM) molecules, such as collagen, over cultivation time [35].

As riboflavin is known to induce UV-A collagen cross-linking via one-photon photosensitized singlet oxygen production [16, 17], the observed increase in stiffness most likely resulted from similar processes upon two-photon excitation. This is underlined by two facts: i) riboflavin fluorescence was observed during fs laser beam raster scanning and ii) irradiation of untreated tissues did not influence the tissue stiffness. Although TMRM was present in the culture medium with a much higher two-photon action cross-section than riboflavin [36], it had no detectable influence on collagen cross-linking owing to the 10,000 times lower concentration and the selective accumulation in mitochondria.

Optimization of the experimental conditions and cross-linking protocol resulted in a significantly increased tissue stiffness by 40% at 20% strain in BCTs (see Fig. 6b). At the same time, Young's modulus increased by 15%. Compared to the first set of experiments, this was a two-fold improvement. In comparison, "biologic" cross-linking by over-expression of lysyl oxidase in smooth muscle cells seeded in collagen gels resulted in a doubling of Young's modulus for these constructs. However, this process was slow and required genetic modification [10]. Previous studies using UV-A irradiation for collagen cross-linking of riboflavin treated human corneas reported an even higher 4.5-fold enhancement of Young's modulus [34]. This can be mainly attributed to the much higher collagen content, much longer irradiation time of 30 minutes and 10-fold higher riboflavin concentration. As multiphoton-induced photochemical effects such as photosensitized singlet oxygen production accumulate over multiple pulses, we expect to further increase the tissue stiffening by using prolonged irradiation times [23].

UV-A cross-linking protocols for corneas are usually associated with cell death within the treated area followed by in-vivo repopulation [18]. In our approach, cell viability was maintained both in MEF-based tissue and BCT, as indicated by strong TMRM fluorescence in the irradiated area (see Figs. 3a and 4a). Furthermore, their volumetric density was not influenced and DAPI fluorescence was still intense (see Figs. 5 and 3c). As active contraction forces of irradiated BCTs were comparable to untreated controls (see Fig. 6b), we can conclude that cardiomyocytes remained fully functional after cross-linking. This could indicate that intracellular free radical scavengers like glutathione were able to neutralize the oxidative stress induced by fs laser irradiation [25, 37]. To the best of our knowledge, similar observations have only been made after one-photon induced cross-linking of fibrin-based engineered connective tissue [38]. Therefore, our experimental setup provides for the first time a fast and effective method to increase the stiffness of collagenous tissue without impairing cell viability. However, great care has to be taken in adjusting the laser fluence, as cellular metabolic activity markedly decreased and no positive effect on tissue stiffness was observed at very high fluences (see Fig. 3b and 2a). This is likely a result of excessive oxidative stress and/or progressive heat accumulation within the tissue during the scanning procedure [39]. Nevertheless, active contraction forces of those BCTs were comparable to untreated controls (see Fig. 6b)), providing evidence that cardiomyocytes were still functional.

Our results suggest a "window" of laser fluences, in which two-photon induced collagen cross-linking can be achieved while maintaining cell viability. To the best of our knowledge, this was not yet observed using one-photon absorption. To obtain a safe process window, the difference of the absorption cross-sections of riboflavin compared to intrinsic fluorophores, such as NAD(P)H, has to be sufficiently high [25]. Other groups have shown that the two-photon absorption cross-section scales super-linearly with the one-photon absorption cross-section [29]. Therefore, we assume that nonlinear excitation of riboflavin with NIR wavelengths is the only mechanism providing a large enough process window for minimally invasive collagen cross-linking. Future studies have to further optimize the laser fluence within the process window to

enhance the achievable increase in stiffness.

In conclusion, we demonstrated for the first time the fast and efficient cross-linking of riboflavin treated collagenous tissues with fs laser pulses in the NIR wavelength range. In contrast to existing methods, the laser-tissue interaction is based on nonlinear (two-photon) absorption. Our experimental data suggest that this provides a process window, in which collagen cross-linking is achieved while maintaining cell viability and functionality. The nonlinear laser-tissue interaction in combination with high spatial precision in the micrometer range offers the possibility for selective cross-linking of arbitrarily defined patterns in three-dimensional tissue engineered constructs.

Patterning of artificial cardiac tissue could be implemented to recapitulate the intrinsic anisotropy of native myocardial tissue. As tissue stiffness plays an important role in remodeling and regeneration after myocardial infarction, artificial tissue with precisely defined mechanical properties using two-photon induced cross-linking could provide new therapeutic strategies to mechanically support heart function. For instance, it was proposed that most of the benefit could be achieved by selectively stiffening the longitudinal direction without altering the circumferential direction [40]. Therefore, our fast, efficient and cell-compatible method for controlling the physical properties of the ECM is a valuable tool for studying and improving engineered cardiac tissue for regenerative therapies.

Acknowledgments

We would like to thank David Skvorc for excellent technical assistance. This work is supported by funding from the Deutsche Forschungsgemeinschaft (DFG, German Research Foundation) within the Cluster of Excellence "REBIRTH" (From Regenerative Biology to Reconstructive Therapy).

3.3 Direct Fusion of iPSC-derived Cardiac Bodies into Structurally and Functionally Homogenous Bioartificial Cardiac Tissue is Fibroblast-dependent and is supported by Ascorbic Acid and Mechanical Load (Manuscript 3)

Authors: George Kensah, Julia Dahlmann, Angelica Roa Lara, Azadeh Azizian, Jan Hegemann, David Skvorc, Anke Gawol, Robert Zweigerdt, Stefan Wagner, Matthias Ochs, Axel Haverich, Ina Gruh*, & Ulrich Martin*

*authors contributed equally

In preparation

Cytometric enrichment of cardiomyocytes:

Optimization of TMRM sorting of cardiomyocytes was done in collaboration with Julia Dahlmann. The Cell Sorting Facility of the Hannover Medical School, Hannover, performed FACS-based sorting of CMs under supervision of Matthias Ballmeier.

Gene expression analyses:

Ina Gruh, Julia Dahlmann and Anke Gawol did quantitative real time PCR analyses on cardiac bodies and miPSC-derived BCTs and data evaluation (Hannover Medical School, Hanover, Germany).

Electrophysiology:

Azadeh Azizian and Stefan Wagner (Department of Cardiology and Pneumology, Georg-August-University, Göttingen, Germany) did patch clamp analyses on genetically selected cardiomyocytes.

Angelica Roa-Lara did multi electrode array (MEA) analyses of genetically selected cardiomyocytes and iPSC-derived BCTs.

Electron microscopy:

Transmission electron microscopy was performed and analyzed by Dr. Jan Hegemann (Hannover Medical School).

Manuscript preparation:

The manuscript was written in collaboration with Julia Dahlmann, Ina Gruh and Ulrich Martin.

Direct Fusion of iPSC-derived Cardiac Bodies into Structurally and Functionally Homogenous Bioartificial Cardiac Tissue is Fibroblast-dependent and is supported by Ascorbic Acid and Mechanical Load

George Kensah¹, Julia Dahlmann¹, Angelica Roa Lara¹, Azadeh Azizian², Jan Hegermann³, David Skvorc¹, Anke Gawol¹, Robert Zweigerdt¹, Stefan Wagner², Matthias Ochs³, Axel Haverich¹, Ina Gruh^{*1}, & Ulrich Martin^{*1}

¹ Leibniz Research Laboratories for Biotechnology and Artificial Organs and Dept. of Cardiac, Thoracic, Transplantation and Vascular Surgery, Hannover Medical School, Cluster of Excellence REBIRTH, Hannover, Germany

² Department of Cardiology & Pneumology, Georg-August-Universitaet Goettingen, Goettingen, Germany

³ Institute of Functional and Applied Anatomy, Hannover Medical School, Hannover, Germany

*these authors contributed equally

Word count abstract: (max. 250)

Word count body: (max. 7000)

Figures & tables: (max. 8)

Keywords

Abstract

Aims - In a proof-of-concept-study we explored the potential use of purified murine induced pluripotent stem cell (iPSC)-derived cardiomyocytes to generate functional bioartificial cardiac tissue, investigating (BCT), and investigated the role of fibroblasts and external stimuli on tissue formation, maturation and functionality.

Methods and Results - Murine iPSC-derived pure (>99% troponin T⁺) 3D cardiomyocyte aggregates (Cardiac bodies) were generated by antibiotic selection of transgenic cells expressing a Zeocin resistance gene under control of the cardiac MYH6 promoter. Antibiotic selection yielded considerably more viable myocytes of higher purity than non-transgenic FACS sorting of iPSC-derived myocytes stained with the mitochondrial dye TMRM. Direct application of intact cardiac bodies for BCT generation was superior to single cell dissociation, which is associated with high levels of cardiomyocyte death. Notably, individual cardiac bodies fused over time resulting in a structurally and functionally homogenous syncytium. Continuous *in situ* characterization of BCTs for 21 days identified three critical factors for fusion of cardiac bodies and formation of a functional BCT: i) Fibroblasts in a defined ratio and ii) ascorbic acid supplementation support ECM re-modelling and CB fusion, while iii) incremental static stretch supports sarcomere alignment, structural and functional cardiomyocyte coupling. All factors together significantly improved contractile forces of BCTs.

Conclusion – Highly efficient enrichment of miPSC-derived cardiomyocytes in cardiac bodies constitutes a defined *in vitro* system, allowing novel insight into cardiac tissue formation and maturation, with potential impact on tissue engineering strategies for cardiac regeneration therapies.

Introduction

Current therapeutic strategies targeting cardiovascular diseases include the induction of endogenous regeneration ^{1,2}, the injection of single cells ^{3,4}, or the application of bioartificial tissue constructs ^{5,6}. In contrast to cell-based therapies, engineered myocardial tissue might enable replacement of scar tissue after infarction and reconstruction of congenital malformations. In animal models, functional tissue generated *in vitro* from primary cells supported the failing heart ⁵⁻⁷.

The identification of a suitable cell source is one of the most critical aspects of myocardial tissue engineering. Similar to embryonic stem cells (ESCs) ^{1,8}, induced pluripotent stem cells (iPSCs) ^{3,9} hold the capability to differentiate into cells of all three germ layers including cardiomyocytes (CM) ¹⁰⁻¹². Recent advance in reprogramming technology including generation of transgene-free iPSCs ^{4,13}, raised expectations on clinical application of iPSC in the foreseeable future.

So far, pluripotent stem cell-based engineered myocardial-like tissue has been generated almost exclusively using ESC-derivatives after cardiac differentiation in embryoid bodies (EBs), which usually contain non-cardiac cell types as well, including persisting pluripotent cells ¹⁴. However, to avoid the risk of teratocarcinoma formation after transplantation ¹⁵, rigorous purification of the desired cell type and removal of any residual pluripotent cells will be mandatory. Some studies used murine ESC-derived cardiomyocytes (mESC-CM) enriched by Percoll gradient centrifugation to generate contractile cardiac tissue ^{16,17}. Purified cardiomyocytes derived from transgenic cell lines expressing antibiotic resistance genes under transcriptional control of the cardiac α -myosin heavy chain (α -MHC) promoter were combined with matrices based on collagen ^{18,19} or fibrin ²⁰, or with the thermo-responsive cell sheet technology ²¹. Recently, Tulloch et al. provided proof-of-concept that TE protocols for human ESC-CM can also be applied to human iPSC-CM ²².

For survival of dissociated cardiomyocytes and formation of structurally homogenous and functional myocardial tissue, mixing with non-myocytes such as fibroblasts appear to be important ^{19,20,23}. Nevertheless, enzymatic dissociation of EBs and CM-enriched CBs typically yields low cardiomyocyte survival rates, thus leading to major loss of CMs ²⁴, and represents a critical limitation of this approach. Various additional factors were demonstrated to affect structure and cellular organization of bioartificial

cardiac tissue, including mechanical stimulation ^{5,17,18,25-27}, as well as matrix-associated ²⁸ and soluble factors ²⁹. So far, stem cell-based engineered cardiac tissue is certainly not comparable to native heart tissue, and few studies, only, have reported measurable contraction forces of engineered cardiac tissue derived from murine ^{16,20} or human stem cells ^{1,2}.

In this study, we demonstrate for the first time the potential of purified murine iPSC-derived cardiomyocytes (miPSC-CM) to generate functional bioartificial cardiac tissue (BCT). We directly compared cardiomyocyte purification using antibiotic-based selection from transgenic iPSC-derived EBs with a non-genetic approach ³⁰. We characterized the functional properties and subtypes of purified cardiomyocytes in resulting cardiac bodies (CBs) and implemented their direct application in myocardial tissue engineering without enzymatic dissociation. Supplementation with a defined proportion of fibroblast led to efficient CB fusion and functional coupling, resulting in structurally and functionally homogenous myocardial tissue. Finally, ascorbic acid as soluble factor and increasing static strain as novel mechanical stimulus were identified to significantly improve structure, stability and contractile forces of bioartificial cardiac tissue.

Materials and Methods

For detailed methodology, please see Supplementary material online.

Generation and selection of cardiomyocytes from murine iPSCs

Murine induced pluripotent stem cells (miPSC) were genetically modified to express a Zeocin™ resistance gene under control of the cardiac-specific α -myosin heavy chain (α -MHC) promoter. Cardiac differentiation was initiated by embryoid body (EB) formation in hanging drops followed by suspension culture. Antibiotic-mediated selection of cardiomyocytes (CM) from transgenic miPSC was initiated on d7 by medium supplementation with 400 μ g/ml Zeocin™ (Invitrogen), leading to cardiomyocyte-enriched aggregates termed cardiac bodies (CB). Cultures were monitored daily over a period of ten days, including dissociation and single cell seeding of samples for further assessment by RT-PCR. An alternative non-genetic selection method was employed, i.e. fluorescence-activated cell sorting (FACS) of mitochondria-rich CMs after staining with the non-toxic mitochondrial dye tetramethyl rhodamine methyl ester (TMRM)³⁰.

Functional characterisation of miPSC-derived cardiomyocytes

Selected cardiomyocytes were characterized using electrophysiological assessment. Action potentials were measured with the whole-cell patch clamp technique in a cell-attached configuration using a current clamp. Multi electrode arrays (MEAs) were used to record field potential changes of seeded cardiomyocytes.

Bioartificial cardiac tissue (BCT) preparation and culture

Two strategies for the preparation of BCTs were compared: i) use of dissociated cardiomyocytes on d14 – d16 of differentiation (d7 – d9 of selection; $1-1.5 \times 10^6$ CMs/BCT); ii) selected CBs were used directly for tissue preparation on d14, after one day of culture with Zeocin™ free medium to eliminate the selective agent. Matrix was prepared as described earlier²⁶. Different amounts of γ -irradiated murine fetal fibroblasts (Fb) were added. As controls, non-selected EBs were used for tissue

preparation. After solidification, tissues were covered with medium and cultured for seven days with daily medium exchange with or without L-ascorbic acid (30 μ M). Additional mechanical load was applied to CB/Fb-based tissues after transfer to a custom-made bioreactor using either uniaxial cyclic stretch (10%, 1 Hz) ²⁶, or incremental growing static stretch (G-stretch; 200 μ m = 3,33% elongation every second day) starting on day seven of tissue culture. Tissue formation was monitored microscopically; cells with high metabolism, i.e. CMs, were visualized by medium supplementation with 50 nM TMRM.

Force measurements

To determine active contraction (systolic) and passive (diastolic) force properties of BCTs, a custom-made bioreactor was used ²⁶. Measurements were performed by stretching the tissue in 100 μ m increments until 1.2 mm preload was reached. Initial tissue length (slack length) was 6 mm; due to incremental lengthening of tissues treated with G-stretch, overall length was 6.6 mm on d14 and 7.4 mm on d21 in this group. Tissues were paced electrically five times at each step (25 V, 5 ms) and contractions were recorded. Diastolic forces were determined as the difference between starting baseline and the baseline at each stretch step (Δ F). All measurements were done in BCT cultivation medium in a standard incubator at 37°C with 5% CO₂, and saturated humidity.

Gene expression analysis and assessment of tissue morphology

Gene expression of cells and BCTs was analysed using either semi-quantitative RT-PCR or quantitative real-time PCR after RNA isolation and reverse transcription. Protein expression was assessed using immuno-fluorescence imaging. Overall tissue structure and (sub-)cellular organization was analysed by transmission electron microscopy (TEM).

Statistical analysis

Statistical analysis was performed with GraphPad Prism software (version 5.03 for Windows; GraphPad Software). Values reported are means and standard errors of the mean. Unless stated otherwise, data were analyzed by one-way analysis of variance, with the Bonferroni multiple comparison test for comparison of any two groups, probability values <0.05 were considered significant.

Results

Genetic selection of CM is superior to TMRM-based selection with respect to cell purity and yield

We evaluated non-transgenic enrichment of iPSC-derived CMs from dissociated embryoid bodies using fluorescence-based cell sorting of TMRM^{bright} cardiomyocytes³⁰. After seeding and immunofluorescence staining, FACS-sorted cells showed successful enrichment of cardiomyocytes compared to unselected controls (Figure 1A&B).

In addition, miPSCs were genetically modified to allow for antibiotic selection of cardiomyocytes based on integration of a Zeocin[™] resistance gene under control of the cardiac α -MHC promoter (Suppl. Fig. 1A&B). Zeocin[™] was found to efficiently enrich cardiomyocytes within differentiated EBs, resulting in TMRM^{bright} contracting cardiac bodies (CB) within 10 days of selection (Figure 1C and Suppl. Fig. 1C), while Oct4-GFP⁺ pluripotent cells persisted in unselected control EBs (Figure 1D and Suppl. Fig. 1C). After CB dissociation and seeding, $99.8 \pm 0.07\%$ of the viable cells were staining positive for cardiac troponin T and Nkx2.5 (vs. $84.5 \pm 1\%$ for TMRM-based selection, Figure 1E&1F). Moreover, Zeocin[™] selection of transgenic miPSCs yielded a much higher cell mass of 1.68 ± 0.191 viable cells/ iPSC initially inoculated for differentiation than TMRM-based selection (0.013 ± 0.005 cell per iPSC) (Figure 1G). Consequently, to obtain sufficient cell numbers for cardiac tissue engineering, we used the antibiotic selection approach for all following experiments.

α -MHC promoter-based Zeocin[™]-selected cardiac bodies contain functional cardiomyocytes of ventricular, atrial, pacemaker and purkinje-like phenotype

Selected CBs represent a three-dimensional culture of almost pure cardiomyocytes (Fig. 2A). Quantitative PCR showed increasing expression levels of cardiac connexins (Cx40, Cx43 and Cx45), as well as myosin heavy chain (α -MHC and β -MHC) over time (Figure 2B). However, levels of Cx40 and Cx45 were significantly higher in CBs than in the heart, while Cx43 was reduced, therefore miPSC-derived CBs can be considered a highly artificial cardiac cell culture system. In line with this fact, CBs expressed significantly lower levels of collagen types I and III than heart

tissue, which contains other collagen-synthesizing cell types including fibroblasts (Figure 2B).

Nevertheless, functional characteristics of CMs from Zeocin™ selected CB were demonstrated by electrophysiological characterization. Using the whole-cell patch clamp technique, spontaneous action potentials (AP) were detected in miPSC-CM from CBs (Figure 2C), with a majority of ventricular-like and pacemaker-like cells (both 28 %; with 6% atrial-like and 6% Purkinje-like cells; see Supplementary table 4), similar to cardiomyocytes derived from other pluripotent stem cells ³¹. In multi electrode array measurements, Zeocin™-selected CMs displayed cardiomyocyte characteristic field potential waveform (Figure 2D), and responded to cardiotropic substances (isoproterenol, lidocaine, quinidine, Figure 2 E-G) comparable to early, embryonic-like CMs ¹⁰.

Generation of functionally and structurally homogenous myocardial tissue from iPSC-derived cardiac bodies is fibroblast-dependent

As previous reports demonstrated the importance of fibroblasts for cardiomyocyte survival, coupling and generation of functional well structured myocardial tissue ^{6,19,20}, iPSC-derived cardiomyocytes, enzymatically dissociated into single cells from Zeocin™-selected CBs, were mixed with different amounts (0 – 25%) of mitotically inactivated murine fetal (d13) fibroblasts and matrix. Indeed, the addition of fibroblasts was essential for solid tissue formation and CM survival (Figure 3A&B). However, even with the optimal amount of 30% fibroblasts, the use of single cell miPSC-derived CMs sparsely resulted in spontaneously and simultaneously contracting tissues, with maximal forces between 150 and 500 μ N (n=30; data not shown).

In a novel approach, we directly used whole cardiac bodies for the preparation of bioartificial cardiac tissue to prevent the disruption of pre-formed functional cell-cell-contacts. CBs without fibroblast supplementation resulted in the formation of contractile BCTs with CBs fused to some extent, however with incomplete ECM remodelling (Figure 3C and supplementary video XY) and lack of stability preventing force measurements. All fibroblast-supplemented experimental settings, with a

Fibroblast (Fb) -content between 8 and 30%, resulted in spontaneously and simultaneously contracting well organized tissue with high density of viable TMRM^{bright} cardiomyocytes up to 21 days of cultivation (Figure 3D). BCTs with a fibroblast content of 10 % of the total cell number generated the highest systolic forces of 0.754 ± 0.167 mN measured on d21 (Figure 3E). In contrast, the use of unselected EBs together with fibroblasts resulted in the formation of disorganized tissue with persistent pluripotent cells (shown by Oct4-GFP expression), large cystic outgrowths and impaired contractility (Suppl. Fig. 3).

Ascorbic acid affects miPSC-derived bioartificial cardiac tissue morphology and contractility via changes in ECM organization

BCT preparation experiments with fibroblast titration as described above and constant medium supplementation with ascorbic acid (AA) from day zero led to elevated forces on d21 compared to AA-free BCTs (Figure 3F), with highest values upon addition of 10% fibroblasts, which was therefore used for all further experiments.

AA-treated BCTs showed enhanced sarcomeric organization (Figure 4A), more CM-CM contacts (intercalated discs)(Figure 4B), elevated collagen deposition (Figure 4C & 4D) with significantly increased collagen I fibre width (21.08 ± 0.8696 μ m vs. 10.97 ± 0.4033 μ m, Figure 5A) and enhanced fibre alignment compared to the controls on d21 (Figure 5B). Also, TMRM intensities, measured on d21 were slightly higher in the treated group, indicating higher metabolic activity (Figure 5C), as well as Titin intensities of stained CMs in longitudinal sections of BCTs (Figure 5D). Contraction forces at Lmax were significantly higher compared to the controls (0.966 ± 0.081 mN vs. 0.623 ± 0.033 mN on d14 and 1.146 ± 0.109 mN vs. 0.754 ± 0.059 mN on d21) (Figure 6A), with a clear Frank-Starling mechanism visible the stress-strain relationship and a significant impact of AA already visible at preload ≥ 0.3 mm (Figure 6D).

Typically, electrical pacing with simultaneous contractions of all cardiomyocytes yielded higher forces than spontaneous contractions with incomplete synchronization of cells within the tissue (see Suppl. fig. 2D). Therefore, we propose the ratio of force

amplitudes (spontaneous vs. paced) as an index of functional coupling of cells; it increased during culture and a higher ratio/improved synchronization was found in the AA-treated group than in the AA-free group (Fig 6B). In terms of passive forces (stiffness), BCTs treated with AA showed significantly higher values on d14 (7.363 ± 1.345 mN vs. 2.938 ± 0.513 mN) and d21 (9.529 ± 1.347 mN vs. 3.775 ± 0.649 mN) compared to untreated controls, both when determined at L_{max} (Fig. 6C) and in stress/strain measurements (Fig. 6E). Similarly, strain-dependent passive force increase was observed in AA-treated tissue constructs prepared from fibroblasts only (Fig. 6E).

Increasing stretch affects miPSC-derived bioartificial cardiac tissue morphology and contractility via cellular maturation including sarcomere length changes

Common protocols for mechanical stimulation of artificial cardiac tissue use cyclic uniaxial stretch (5 - 10%, 1 – 2 Hz) ^{6,18,22,25,26,32}. Applied to our CB-based tissue constructs together with AA, cyclic stretch (10%; 1 Hz) neither increased measured active forces (0.767 ± 0.066 mN on d14 and 0.795 ± 0.068 mN on d21, $n= 5$), nor improved tissue morphology and contraction (data not shown).

We considered the possibility that cyclic stretch might interfere with spontaneous contractions of miPS-derived cardiomyocytes because of their organization in the pre-formed micro-tissue environment of cardiac bodies. It has been demonstrated that a constant change of mechanical loading conditions can induce re-alignment of cells and matrix molecules in collagen-based scaffolds ³³. Therefore, we hypothesized that the application of growing static strain could influence structure and functionality of CB-derived myocardial tissue and may result in higher force development.

For this reason, we applied incrementally growing static strain, i.e. stepwise increase of static preload from d7 – d21 with 200 μ m increments every second day. Compared to controls with constant basic preload, this led to the improved formation of elongated tissue from individual CBs, with more uniform distribution of viable cardiomyocytes and better alignment along the longitudinal axis of the BCT (Figure 7A) together with improved sarcomeric organization within CMs on d21 (Figure 7B). Growing strain led to preferential deposition of the ECM protein laminin at the lateral

cell membrane (Figure 7C), at the same time, collagen I fibres were thicker in treated constructs (Figure 7D), but to a lesser extent as in the AA-treated group (Figure 5A). An increase in collagen I fibre alignment was also detected, although not significant (Figure 5B). TMRM and Titin intensities measured on d21 were significantly higher compared to the controls (Figure 5C&D), indicating higher CM activity and higher sarcomeric protein content in CMs. Moreover, and in contrast to AA, treatment with growing strain resulted in significantly increased sarcomere length within BCTs (Figure 5E).

Treatment with increasing strain had no effect on coupling of CMs within the BCTs when comparing paced with spontaneous contraction forces (Figure 6B). Nevertheless, application of incremental static stretch improved maximum systolic force development on d14 and d21, however, less than in the AA-treated group (Figure 6A&F). In contrast, diastolic forces of stretched BCTs were higher compared to the controls and AA-treated BCTs (Figure 6C&G). Again, responses to strain in stretched CB-based constructs were recapitulated in stretched CM-free constructs (Figure 6G). Notably, higher forces observed after mechanical stimulation with incremental static stretch did not result in gene expression level changes usually associated with a hypertrophic response (assessed for cardiac genes β -MHC, ANF, BNP and Act1a; Suppl. Fig. 5A-D).

Combined ascorbic acid treatment and increasing stretch lead to optimized miPSC-derived bioartificial cardiac tissue functionality

Combination of both stimuli reflected morphological changes in constructs treated with one stimulus only. Broad, well-organized and longitudinal aligned CM bundles with Cx43 gap junctions were abundant, comparable with the stretched BCT group (Suppl. Fig 6 B). Collagen I fibres were of comparable thickness as observed in the group treated with AA, only (Figure 5A); increased collagen I alignment was observed, although not significant (Figure 5B). Metabolic activity visualized by TMRM, Titin intensities and sarcomere length were comparable to the BCT group treated with growing strain, only (Figure 5C&D).

Active contraction forces measured on d14 and d21 showed that the combined treatment with ascorbic acid and incremental preload during cultivation had an additional effect on cardiac mechanical properties, compared to the untreated and single stimulant groups, and resulted in forces of 1.216 ± 0.132 mN on d14 and 1.422 ± 0.094 mN on d21 (Figure 6A), again with a physiological stress-strain relationship (Figure 6H). In conclusion, compared to untreated controls on d21 maximum active forces almost doubled and passive forces were about three times higher when measured at L_{max} (Figure 6C&I). Combined treatment led to highest values of passive forces also in fibroblast-only constructs (Figure 6I).

Optimized miPSC-derived BCTs after combined ascorbic acid treatment and increasing stretch demonstrated expression levels of α -MHC, Cx40 and Cx45, as well as collagen type I, comparable to those of the neonatal mouse heart (Figure 8A). In contrast, levels of β -MHC and collagen type III were significantly lower than in neonatal heart, as well as Cx43, which was about tenfold less. Despite this finding, efficient cardiomyocyte coupling could be demonstrated using MEA measurement of whole-mounted BCTs (Figure 8B). We detected characteristic FP recordings with propagation delay over the whole array (Figure 8C,D) and a conduction velocity of 25-30 cm/s; moreover miPSC-derived bioartificial cardiac tissue responded to cardiotropic drugs isoproterenol, lidocaine and quinidine (Figure 8E-H).

Discussion

In this study we demonstrate rigorous purification of pluripotent stem cell-derived cardiomyocytes. Antibiotic selection of transgenic cells as described for ESC-derived cardiomyocytes^{18,20} was significantly more efficient with respect to purity and yield than non-transgenic enrichment using TMRM-based FACS sorting described by Hattori et al.³⁰. Here, the low yield of viable CMs, might be explained by increased CM sensitivity to dissociation due to their tight cell/cell and cell/ECM attachment³⁴ and/or sensitivity to shear stress in flow cytometry because of the high degree of CM anisotropy. Nevertheless, in our study we found TMRM-labelling extremely valuable to selectively monitor CM viability. Similarly, in our hands, the use of single selected CMs sparsely led to contracting tissue with reduced cell viability and forces comparable to engineered cardiac tissue based on non-selected pluripotent stem cell-derived CMs from either mouse or man^{16,22}.

In this study we describe for the first time that pure CMs in autonomously contracting highly defined units, i.e. cardiac bodies (CBs), can be used directly, i.e. without disruption of pre-formed functional cell-cell-contacts, for the generation of three-dimensional functional bioartificial cardiac tissue (BCT). Notably, this was possible only because the EB-based selection procedure was optimized to eliminate any residual Oct4-GFP^{positive} pluripotent stem cells in CBs and BCTs, thus reducing the risk of tumor formation after transplantation. Our miPSC-derived CBs have to be considered a highly artificial cell culture system of 3D-monocultures of pure cardiomyocytes at an early developmental stage, as demonstrated by gene expression and electrophysiological analysis. We hypothesized that these cells may still display a high degree of structural and functional plasticity (and migratory capacity) to enable fusion of entire non-dissociated CBs and substantial remodelling towards structural and functional homogenous cardiac tissue with high cardiomyocyte viability. Indeed, the generation of miPSC cardiac body-based BCTs resulted in a functional syncytium with forces of the same magnitude achieved by state of the art cardiac tissue engineered constructs based on primary cells using similar numbers of CMs per volume^{1,2}.

In situ characterization of CB-based miPSC-BCTs in a bioreactor for 21 days allowed us to identify critical effectors of tissue formation and functionality and their

mechanisms of action: Fibroblast supplementation in a defined ratio led to enhanced cardiomyocyte survival and the generation of stable BCTs with higher forces, mainly supporting tissue formation via ECM remodelling. This is in line with reports on improved contractile force generation in engineered heart tissue of primary rat heart populations containing a higher fraction of fibroblasts ⁶. The process window of an appropriate fibroblast ratio for optimized force generation in miPSC-derived BCTs was surprisingly narrow. Liao et al. determined an optimal ratio of 3% cardiac fibroblast in mESC-derived engineered cardiac tissue based on a fibrin-matrix ²⁰; Miragoli et al. observed maximum impulse conduction velocity in cultured strands of rat cardiomyocytes using ~7% cardiac fibroblasts ³⁵. Differences might be explained by the facts i) that we used the novel approach of tissue formation from cardiac bodies instead of single cells, and ii) that we chose irradiated mouse fetal fibroblasts (embryonic d13) to avoid any potential cardiomyocyte contamination (which we could frequently observe even after several passages of cardiac fibroblast cultures). Interestingly, our optimized fibroblast ratio of 10% reflects the *in vivo* content of mouse heart on postnatal day 1, while a significantly higher number of 26% fibroblasts is present in the adult heart ³⁶.

We found that ascorbic acid supported fibroblast-dependent matrix re-organization, leading to improved force transduction. Besides its radical scavenger properties ³⁷, AA has been shown to exert a regulatory effect both on pro-collagen expression ³⁸ and collagen post-transcriptional modification ³⁹, and can also act as a pro-oxidant in differentiating mouse ESC ⁴⁰. AA has been described to enhance differentiation of ESC into CM ⁴¹ and improve embryonic cardiomyoblast cell survival ⁴². In our study we mainly observed a positive effect of AA on ECM and cellular organization within BCTs. This was demonstrated by increased collagen fibre width and alignment, adding to the passive forces, and improved coupling and metabolic activity of cardiomyocytes, altogether resulting in higher active contraction forces as well as modulation of contraction frequency.

Another critical factor for tissue functionality identified in this study is mechanical stimulation. While incremental static stretch has been shown to induce rabbit skeletal muscle growth *in vivo* ⁴³, it has not been applied in cardiac tissue engineering before. Common protocols for mechanical stimulation of artificial cardiac tissue use cyclic uniaxial stretch (5 - 10%, 1 -2 Hz), which is usually accompanied by a hypertrophic

response^{6,18,26,32}. In our study, mechanical stimulation with incremental static stretch led to significantly higher forces as compared to cyclic stretch and consequently was used in all further experiments. While uni-axial cyclic stretch might interfere with spontaneous isotropic contractions of early cardiomyocytes within cardiac bodies, growing stretch could be beneficial to recapitulate the physiological conditions of the growing embryonic myocardium with its increasing systolic and diastolic pressure and continuously increasing contractile force⁴⁴. Constant static stretch had already been demonstrated to induce re-alignment of cells and matrix molecules in collagen-based scaffolds³³, therefore we considered it as a possible mechanical clue to re-organize CBs towards an anisotropic cardiac tissue.

In our study, growing stretch had a significant impact on cardiomyocyte alignment and function as demonstrated by increased TMRM fluorescence, it induced highly organized laminin deposition within stretched BCTs and led to improved sarcomere alignment as well as increased sarcomere length. Similarly, an increase in myofibre density and developmental improvement in the alignment of myocytes was described as additional underlying mechanisms of an increase in contraction forces during embryonic heart development, which cannot be contributed to the accumulation of contractile proteins (MHC), only⁴⁵. In development, regional myofibre alignment is observed preferentially at sites of regional orthotropic epicardial wall strain⁴⁶ and higher forces from aligned tissue generated *in vitro* have been demonstrated⁴⁷.

Interestingly, we did not observe evidence for hypertrophy in BCT groups treated with growing stretch. However, it is currently unclear whether this is due to the mode of stretching or, alternatively, might be attributed to an immature phenotype of the miPSC-derived cardiomyocytes, as *in vivo* the occurrence of a “developmental hypertrophy” in the growing mouse heart was reported only after postnatal day 5⁴⁸.

These positive effects of fibroblast addition, ascorbic acid supplementation and growing mechanical stretch described above, were successfully combined for optimized miPSC-derived bioartificial cardiac tissue with improved functionality. So far, no data has been available on the contraction forces of miPSC-derived bioartificial cardiac tissue. However, systolic forces obtained with our novel cardiac body-based protocols are 17,5-23 fold higher than reported recently for human iPSC-derived tissue generated from enriched cardiomyocytes and cardiac fibroblasts^{14,22}

and in the same range as observed for murine ESC-derived cardiac tissue from selected cardiomyocytes and ventricular fibroblasts ²⁰.

We conclude that highly efficient enrichment of miPSC-derived cardiomyocytes in cardiac bodies allowed novel insight into cardiac tissue formation and maturation, with potential impact on tissue engineering strategies for cardiac regeneration therapies. Moreover, it might soon be possible to address the problem of insufficient vascularization of *in vitro* generated working myocardium through the application of MSCs, as proposed by Tulloch, et al. ²², or more likely, cardiovascular progenitor cell types selectable from iPSCs as shown by Mauritz, et al. ¹². In any case, cardiac tissue patches with improved functionality should also be valuable for high throughput pharmacological testing and iPSC-based cardiac disease modelling ^{49,50}. They provide reproducible three-dimensional cell culture models, and in combination with suitable read-out systems such as our bioreactor, they could enable the investigation of certain mechanistic aspects of disease and regeneration already *in vitro*, as demonstrated in this study.

Acknowledgements

We thank Matthias Ballmeier for excellent assistance in TMRM-based flow-cytometric cell enrichment of cardiomyocytes and Virginija Jazbutyte for contributing neonatal mouse heart RNA samples. We are thankful to Hans Schöler and Holm Zaehres for providing the batch culture of OG2-iPS cells, and to Kristin Schwanke and Monica Jara Avaca for the derivation and identification of a clonal line with outstanding cardiac differentiation potential, thereof. This work was funded by the Cluster of Excellence REBIRTH (DFG EXC 62/1) and by the German Ministry for Education and Science (BMBF, 01GN0520).

References

1. Schwanke K, Wunderlich S, Reppel M, et al. Generation and Characterization of Functional Cardiomyocytes from Rhesus Monkey Embryonic Stem Cells. *Stem Cells*. 2006;24(6):1423–1432.
2. Porrello ER, Mahmoud AI, Simpson E, et al. Transient Regenerative Potential of the Neonatal Mouse Heart. *Science*. 2011;331(6020):1078–1080.
3. Nakagawa M, Koyanagi M, Tanabe K, et al. Generation of induced pluripotent stem cells without Myc from mouse and human fibroblasts. *Nature Biotechnology*. 2007;26(1):101–106.
4. Jincho Y, Araki R, Hoki Y, et al. Generation of Genome Integration-free Induced Pluripotent Stem Cells from Fibroblasts of C57BL/6 Mice without c-Myc Transduction. *Journal of Biological Chemistry*. 2010;285(34):26384–26389.
5. Zimmermann W-H, Didié M, Wasmeier GH, et al. Cardiac grafting of engineered heart tissue in syngenic rats. *Circulation*. 2002;106(12 Suppl 1):I151–7.
6. Naito H, Melnychenko I, Didié M, et al. Optimizing engineered heart tissue for therapeutic applications as surrogate heart muscle. *Circulation*. 2006;114(1 Suppl):I72–8.
7. Sekine H, Shimizu T, Dobashi I, et al. Cardiac Cell Sheet Transplantation Improves Damaged Heart Function via Superior Cell Survival in Comparison with Dissociated Cell Injection. *Tissue Eng Part A*. 2011;17(23-24):2973–2980.
8. Kehat I, Kenyagin-Karsenti D, Snir M, et al. Human embryonic stem cells can differentiate into myocytes with structural and functional properties of cardiomyocytes. *J. Clin. Invest*. 2001;108(3):407–414.
9. Takahashi K, Yamanaka S. Induction of Pluripotent Stem Cells from Mouse Embryonic and Adult Fibroblast Cultures by Defined Factors. *Cell*. 2006;126(4):663–676.
10. Mauritz C, Schwanke K, Reppel M, et al. Generation of functional murine cardiac myocytes from induced pluripotent stem cells. *Circulation*. 2008;118(5):507–517.
11. Haase A, Olmer R, Schwanke K, et al. Generation of induced pluripotent stem cells from human cord blood. *Cell Stem Cell*. 2009;5(4):434–441.
12. Mauritz C, Martens A, Rojas SV, et al. Induced pluripotent stem cell (iPSC)-derived Flk-1 progenitor cells engraft, differentiate, and improve heart function in a mouse model of acute myocardial infarction. *Eur Heart J*. 2011.
13. Okita K, Nakagawa M, Hyenjong H, Ichisaka T, Yamanaka S. Generation of Mouse Induced Pluripotent Stem Cells Without Viral Vectors. *Science*. 2008;322(5903):949–953.

14. Schaaf S, Shibamiya A, Mewe M, et al. Human Engineered Heart Tissue as a Versatile Tool in Basic Research and Preclinical Toxicology de Windt LJ, ed. *PLoS ONE*. 2011;6(10):e26397.
15. Hentze H, Soong PL, Wang ST, et al. Teratoma formation by human embryonic stem cells: Evaluation of essential parameters for future safety studies. *Stem Cell Research*. 2009;2(3):198–210.
16. Guo XM. Creation of Engineered Cardiac Tissue In Vitro From Mouse Embryonic Stem Cells. *Circulation*. 2006;113(18):2229–2237.
17. Wang X, Wei G, Yu W, et al. Scalable Producing Embryoid Bodies by Rotary Cell Culture System and Constructing Engineered Cardiac Tissue with ES-Derived Cardiomyocytes in Vitro. *Biotechnol Prog*. 2006;22(3):811–818.
18. Shimko VF, Claycomb WC. Effect of Mechanical Loading on Three-Dimensional Cultures of Embryonic Stem Cell-Derived Cardiomyocytes. *Tissue Eng*. 2007.
19. Pfannkuche K, Neuss S, Pillekamp F, et al. Fibroblasts facilitate the engraftment of embryonic stem cell-derived cardiomyocytes on three-dimensional collagen matrices and aggregation in hanging drops. *Stem Cells Dev*. 2010;19(10):1589–1599.
20. Liao B, Christoforou N, Leong KW, Bursac N. Pluripotent stem cell-derived cardiac tissue patch with advanced structure and function. *Biomaterials*. 2011:1–8.
21. Matsuura K, Masuda S, Haraguchi Y, et al. Creation of mouse embryonic stem cell-derived cardiac cell sheets. *Biomaterials*. 2011;32(30):7355–7362.
22. Tulloch NL, Muskheli V, Razumova MV, et al. Growth of Engineered Human Myocardium With Mechanical Loading and Vascular Coculture. *Circ Res*. 2011;109(1):47–59.
23. Xi J, Khalil M, Spitkovsky D, et al. Fibroblasts support functional integration of purified embryonic stem cell-derived cardiomyocytes into avital myocardial tissue. *Stem Cells Dev*. 2011;20(5):821–830.
24. Huang C-C, Liao C-K, Yang M-J, et al. A strategy for fabrication of a three-dimensional tissue construct containing uniformly distributed embryoid body-derived cells as a cardiac patch. *Biomaterials*. 2010;31(24):6218–6227.
25. Fink C, Ergün S, Kralisch D, et al. Chronic stretch of engineered heart tissue induces hypertrophy and functional improvement. *FASEB J*. 2000;14(5):669–679.
26. Kensah G, Gruh I, Viering J, et al. A Novel Miniaturized Multimodal Bioreactor for Continuous In Situ Assessment of Bioartificial Cardiac Tissue During Stimulation and Maturation. *Tissue Eng Part C Methods*. 2011;17(4):463–473.
27. Gwak S-J, Bhang SH, Kim I-K, et al. The effect of cyclic strain on embryonic stem cell-derived cardiomyocytes. *Biomaterials*. 2008;29(7):844–856.
28. Baharvand H, Azarnia M, Parivar K, Ashtiani SK. The effect of extracellular matrix on embryonic stem cell-derived cardiomyocytes. *J Mol Cell Cardiol*. 2005;38(3):495–

503.

29. Pedrotty DM, Klinger RY, Kirkton RD, Bursac N. Cardiac fibroblast paracrine factors alter impulse conduction and ion channel expression of neonatal rat cardiomyocytes. *Cardiovasc Res*. 2009;83(4):688–697.
30. Hattori F, Chen H, Yamashita H, et al. Nongenetic method for purifying stem cell–derived cardiomyocytes. *Nat Meth*. 2009;7(1):61–66.
31. Guan K, Nayernia K, Maier LS, et al. Pluripotency of spermatogonial stem cells from adult mouse testis. *Nature*. 2006;440(7088):1199–1203.
32. Guo Y, Zhang X-Z, Wei Y, et al. Culturing of ventricle cells at high density and construction of engineered cardiac cell sheets without scaffold. *International heart journal*. 2009;50(5):653–662.
33. Lee EJ, Holmes JW, Costa KD. Remodeling of Engineered Tissue Anisotropy in Response to Altered Loading Conditions. *Annals of biomedical engineering*. 2008;36(8):1322–1334.
34. Li RK, Mickle DA, Weisel RD, et al. Human pediatric and adult ventricular cardiomyocytes in culture: assessment of phenotypic changes with passaging. *Cardiovasc Res*. 1996;32(2):362–373.
35. Miragoli M, Gaudesius G, Rohr S. Electrotonic modulation of cardiac impulse conduction by myofibroblasts. *Circ Res*. 2006;98(6):801–810.
36. Banerjee I, Fuseler JW, Price RL, Borg TK, Baudino TA. Determination of cell types and numbers during cardiac development in the neonatal and adult rat and mouse. *Am. J. Physiol. Heart Circ. Physiol*. 2007;293(3):H1883–91.
37. Englard S, Seifter S. The biochemical functions of ascorbic acid. *Annu. Rev. Nutr*. 1986;6:365–406.
38. Clark AG, Rohrbaugh AL, Otterness I, Kraus VB. The effects of ascorbic acid on cartilage metabolism in guinea pig articular cartilage explants. *Matrix Biol*. 2002;21(2):175–184.
39. Peterkofsky B. Ascorbate requirement for hydroxylation and secretion of procollagen: relationship to inhibition of collagen synthesis in scurvy. *Am. J. Clin. Nutr*. 1991;54(6 Suppl):1135S–1140S.
40. Crespo FL, Sobrado VR, Gomez L, Cervera AM, McCreath KJ. Mitochondrial reactive oxygen species mediate cardiomyocyte formation from embryonic stem cells in high glucose. *Stem Cells*. 2010;28(7):1132–1142.
41. Takahashi T. Ascorbic Acid Enhances Differentiation of Embryonic Stem Cells Into Cardiac Myocytes. *Circulation*. 2003;107(14):1912–1916.
42. Martinez EC, Wang J, Gan SU, et al. Ascorbic acid improves embryonic cardiomyoblast cell survival and promotes vascularization in potential myocardial grafts in vivo. *Tissue Eng Part A*. 2010;16(4):1349–1361.

43. Cox VM, Williams PE, Wright H, et al. Growth induced by incremental static stretch in adult rabbit latissimus dorsi muscle. *Exp. Physiol.* 2000;85(2):193–202.
44. Ishiwata T. Developmental Changes in Ventricular Diastolic Function Correlate With Changes in Ventricular Myoarchitecture in Normal Mouse Embryos. *Circ Res.* 2003;93(9):857–865.
45. Siedner S, Kruger M, Schroeter M, et al. Developmental changes in contractility and sarcomeric proteins from the early embryonic to the adult stage in the mouse heart. *The Journal of Physiology.* 2003;548(2):493–505.
46. Alford PW, Taber LA. Regional epicardial strain in the embryonic chick heart during the early looping stages. *J Biomech.* 2003;36(8):1135–1141.
47. Black L, Meyers J, Weinbaum J, Shvelidze Y, Tranquillo R. Cell-induced alignment augments twitch force in fibrin gel-based engineered myocardium via gap junction modification. *Tissue Eng Part A.* 2009.
48. Leu M, Ehler E, Perriard JC. Characterisation of postnatal growth of the murine heart. *Anat. Embryol.* 2001;204(3):217–224.
49. Moretti A, Bellin M, Welling A, et al. Patient-specific induced pluripotent stem-cell models for long-QT syndrome. *N. Engl. J. Med.* 2010;363(15):1397–1409.
50. Itzhaki I, Maizels L, Huber I, et al. Modelling the long QT syndrome with induced pluripotent stem cells. *Nature.* 2011;471(7337):225–229.

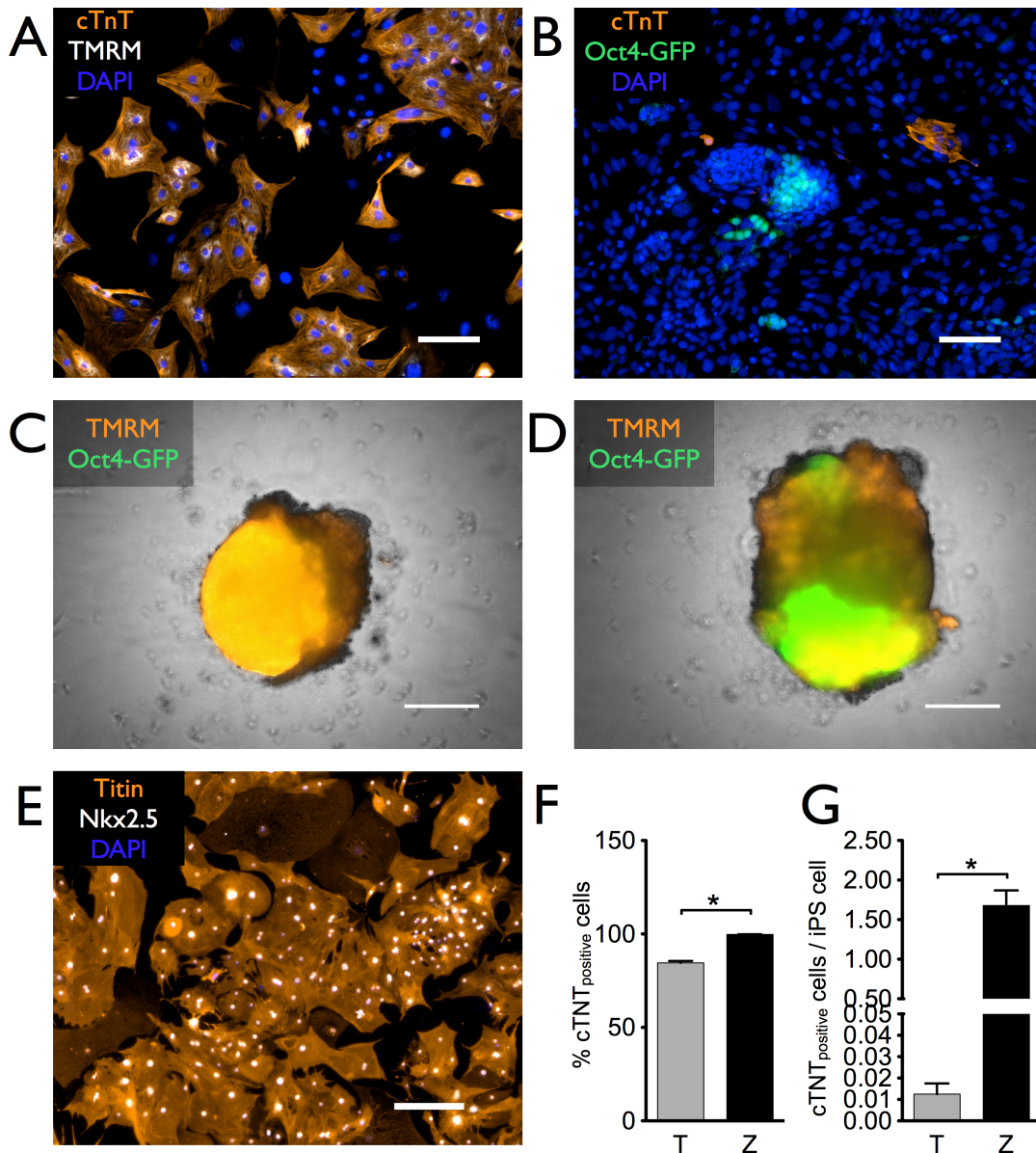


Figure 1: Genetic selection of miPSC-derived cardiomyocytes is superior to TMRM-based selection with respect to cell purity and yield

(A) TMRM sorting led to enrichment of cTnT positive cells (red, double staining with TMRM-fluorescence (white), compared to the non-selected control (B). (C) α MHC Zeo^R selection of CMs in floating EBs resulted in TMRM^{bright} cardiac bodies on day 14, while unselected EB showed persistent Oct4 promoter-driven GFP fluorescence (green, D). (E) Optimized α MHC Zeo^R purified CM population stained positive for Titin (red), Nkx2.5 (white), and nuclei (DAPI, blue). α MHC Zeo^R selection resulted in higher cardiomyocyte yield (F) and purity (G) compared to non-genetic TMRM-based sorting. All scale bars 200 μ m.

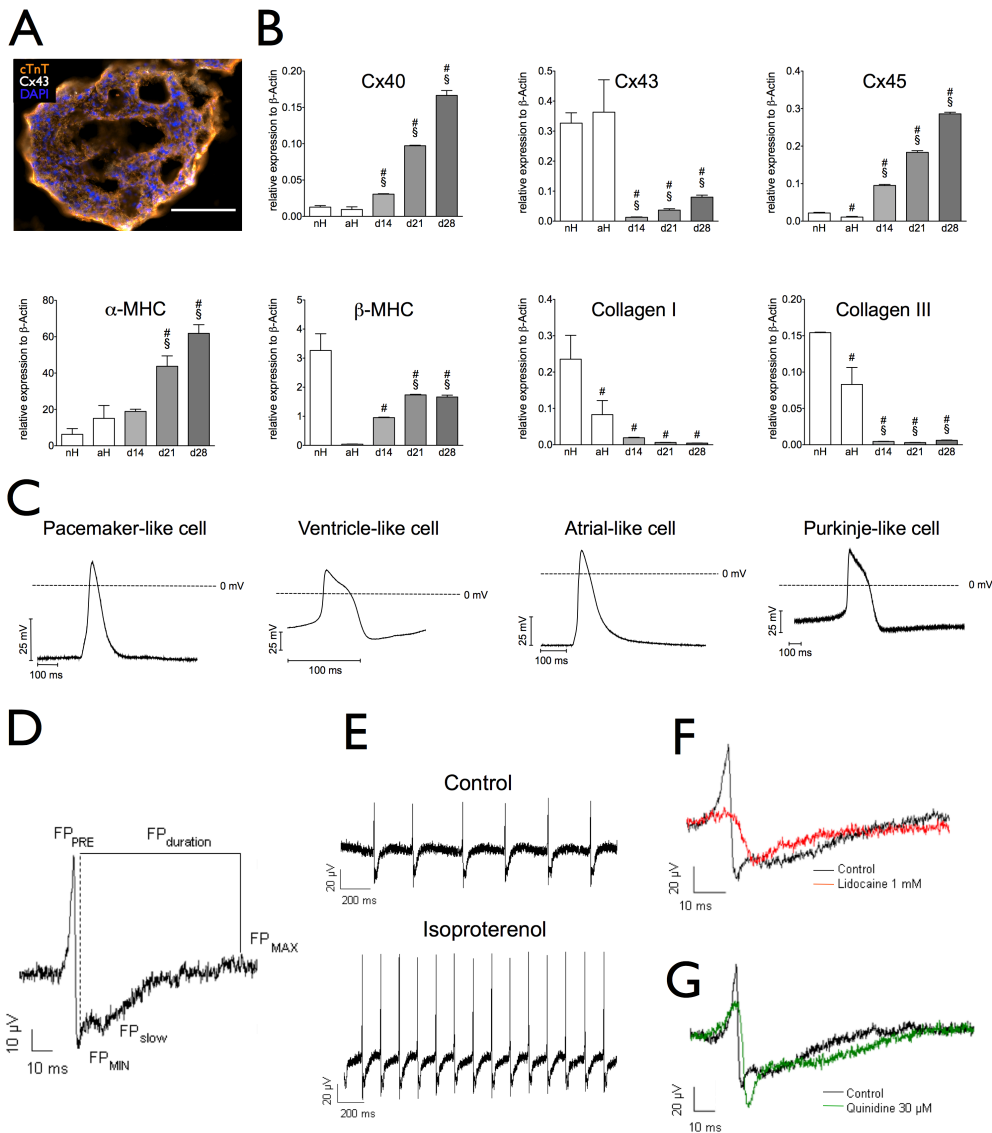


Figure 2: Selected cardiac bodies represent artificial 3D-cultures of pure and functional miPSC-derived cardiomyocytes

(A) Cardiac bodies after α MHC Zeo^R selection consist of cardiomyocytes, only, staining positive for cTnT (red), Cx43 (white), and nuclei (DAPI, blue); scale bar 100 μ m. (B) For CBs on d14, d21 and d28 of differentiation, quantitative real time PCR detected gene expression levels distinct from mouse neonatal (d1-3; nH) and adult heart tissue (aH), including a highly artificial cardiac connexin expression pattern. Data are presented as mean \pm SD for three experiments, with PCR runs performed in triplicate (#, $p \leq 0.05$ to nH; §, $p \leq 0.05$ to aH). (C) Electrophysiological analysis using patch clamp technique demonstrated action potentials (APs) from miPSC-derived cardiomyocytes after selection with distinct AP morphologies representing pacemaker-, ventricle-, atrial-, and purkinje-like cardiomyocytes. (D) Multi electrode array analysis of plated miPSC-derived cardiomyocytes showed representative field potential waveform. (E) β -adrenergic stimulation with isoproterenol led to an increase in contraction frequency, (F) the INa blocker lidocaine to slowing of the fast FP component (FPMIN) corresponding to the Na⁺ peak, and the HERG (IKr) blocker quinidine to prolongation of the FP duration (G).

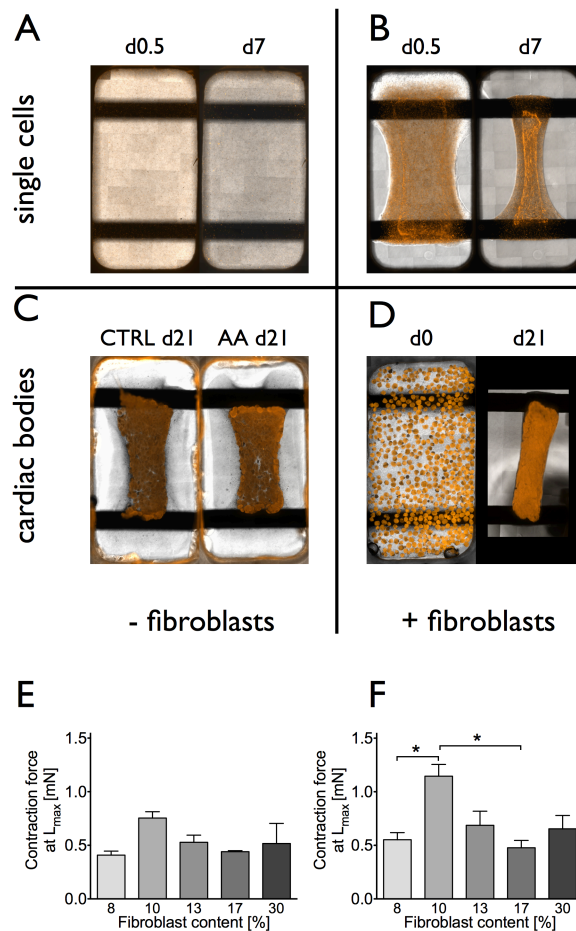


Figure 3: Fibroblasts are essential for bioartificial cardiac tissue formation from miPS-derived cardiomyocytes

(A) BCTs containing single cell dissociated cardiomyocytes only, did not consolidate and TMRM fluorescence as indicator of cardiomyocyte viability decreased. (B) Addition of 30% mitotically inactivated fetal fibroblasts led to rapid remodeling of the matrix and improved cardiomyocyte survival. (C) Selected CBs (400) without fibroblasts resulted in the formation of BCTs with CBs fused to some extent, with incomplete ECM remodeling and lack of stability. (D) Selected cardiac bodies with fibroblast addition led to efficient BCT formation and long-term survival of actively contracting cardiomyocytes without re-emergence of Oct4/GFP^{positive} cells, and measurable systolic forces on day 14 (E). (F) Systolic force measurements (d14) showed highest values for supplementation with 10% fibroblasts (of total cell number) and ascorbic acid.

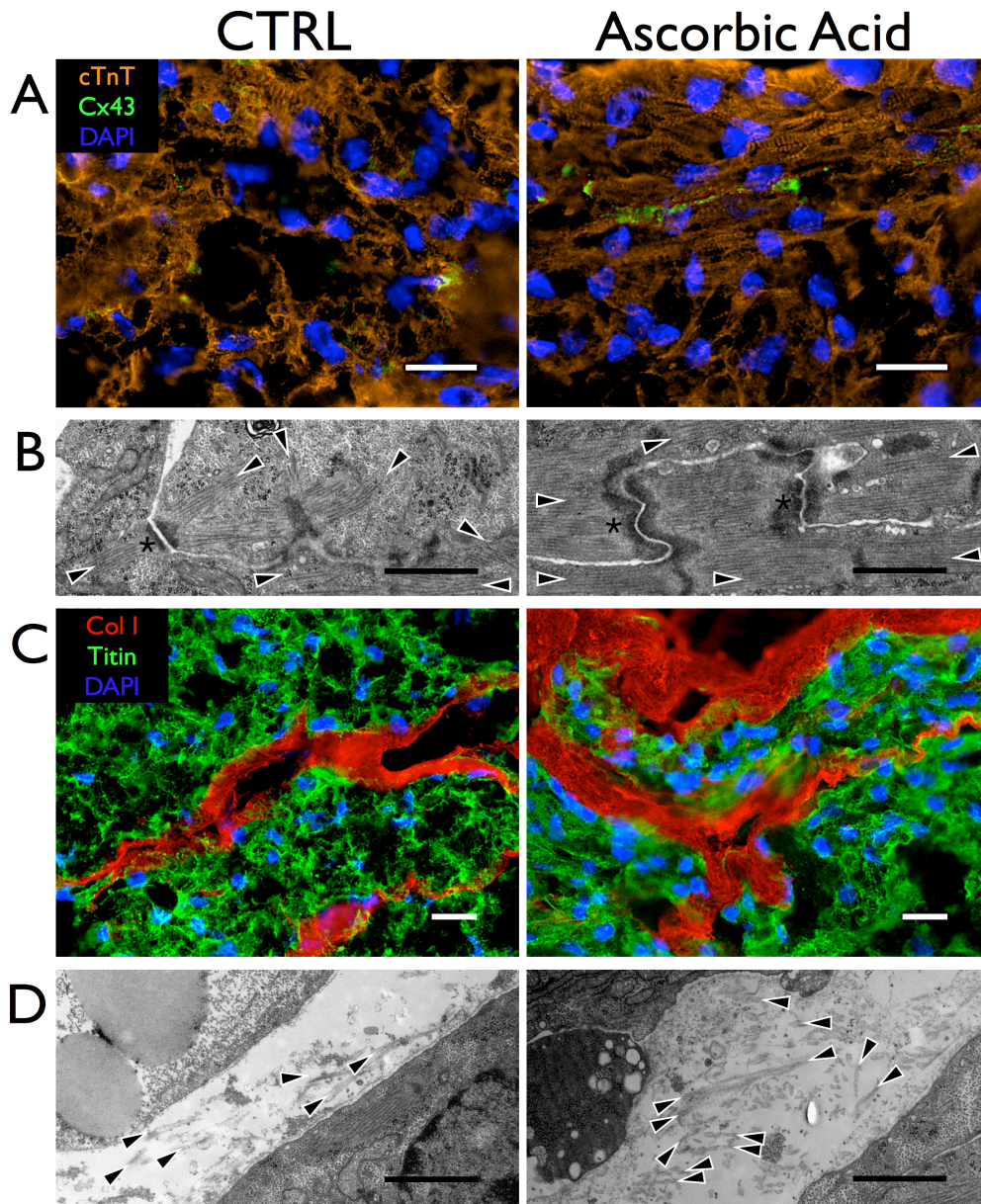


Figure 4: Ascorbic acid critically affects miPSC-derived bioartificial cardiac tissue morphology and ECM organization

(A) Immunofluorescence staining against cardiac troponin T (red)/connexin 43 (green) in sections of CB-based iPS-BCTs cultivated under control conditions (left) or with ascorbic acid (AA, right), AA-treated BCTs showed longitudinally arranged (anisotropic) cardiomyocytes with distinct cross-striation. (B) Transmission electron microscopy (TEM) showed more prominent cell-cell contacts between cardiomyocytes (intercalated discs, asterisks) in tissues treated with AA; arrowheads indicate the orientation of sarcomeres, showing more random orientation in the control. (C) Immunofluorescence staining against collagen type I (red)/titin (green) showed more prominent collagen fiber bundles in the AA-treated group. (D) TEM showed accumulation of collagen in the intracellular space next to cardiomyocytes and elevated occurrence of collagen fibrils in the tissues treated with AA (both right). (A), (C): Nuclei stained with DAPI (blue); Scale bars 20 μm . (B), (D) Scale bars 1 μm .

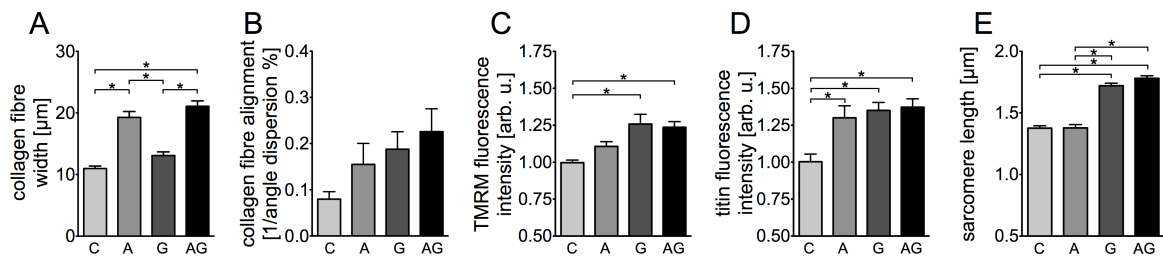


Figure 5: Comprehensive overview on morphological parameters of miPSC-derived bioartificial cardiac

Immunofluorescence images were analyzed for miPSC-derived BCTs from different treatment groups: C, control; A, ascorbic acid; G, growing stretch; AG, ascorbic acid and growing stretch, combined. (A) Immunostaining against collagen type I was analyzed for collagen fibre width and collagen fibre alignment (B, given as [1/angle dispersion %]). Fluorescence intensities of TMRM in viable BCTs (C) and titin staining of fixed cryosections (D) are given in arbitrary units. (E) Sarcomere length in BCTs was determined from high magnification images of cross-striated CMs after immunostaining against cardiac troponin T. All columns are means \pm SEM.

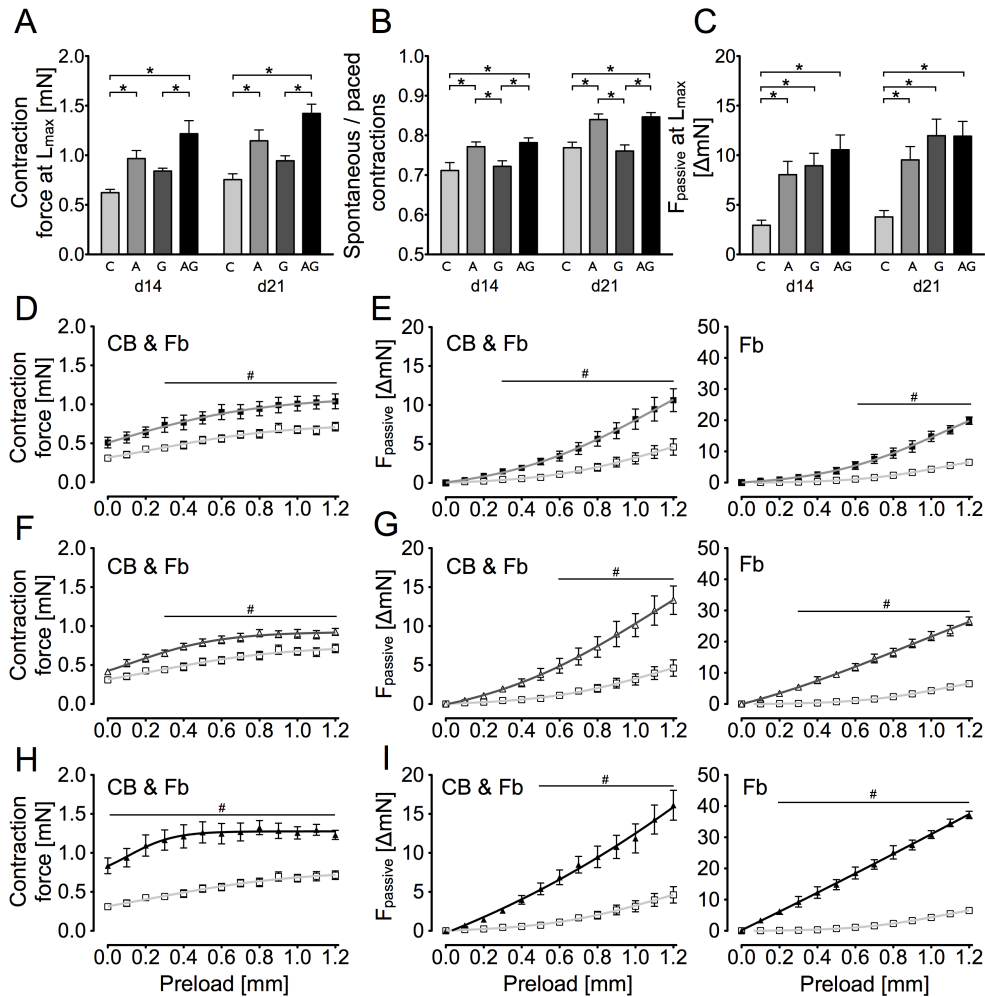


Figure 6: Comprehensive overview on functional parameters of miPSC-derived bioartificial cardiac tissue

(A) Maximum force over time of BCTs from different treatment groups: C, control; A, ascorbic acid; G, growing stretch; AG, ascorbic acid and growing stretch, combined; were measured after electrical pacing (25 V, 10 ms) at optimal length (L_{max}). Means \pm SEM, $n = 8-9$ per group. (B) Ratio of spontaneous/paced twitch force as an index of electrical coupling of CBs within BCTs. Means \pm SEM, $n = 8-9$ per group. (C) Diastolic force increase over time in CB-based iPS-BCTs. (D), (F), (H) End-point measurements on d21 in CB-based iPS-BCTs, treated with ascorbic acid (D), growing stretch (F), or ascorbic acid and growing stretch (H), compared to untreated controls (open squares). Stretch increase with 0.1 mm increments was performed to determine the optimal preload L_{max} corresponding to maximum systolic force. (E), (G), (I) Diastolic force / strain-relationship in CB-based iPS-BCTs, treated with ascorbic acid (E), growing stretch (G), or ascorbic acid and growing stretch (I), compared to untreated controls (open squares). Symbols represent mean baseline force \pm SEM ($n=8-9$ per group). MEF-only constructs treated under same conditions showed same tendencies in passive force difference (right panels, $n = 4$ per group).

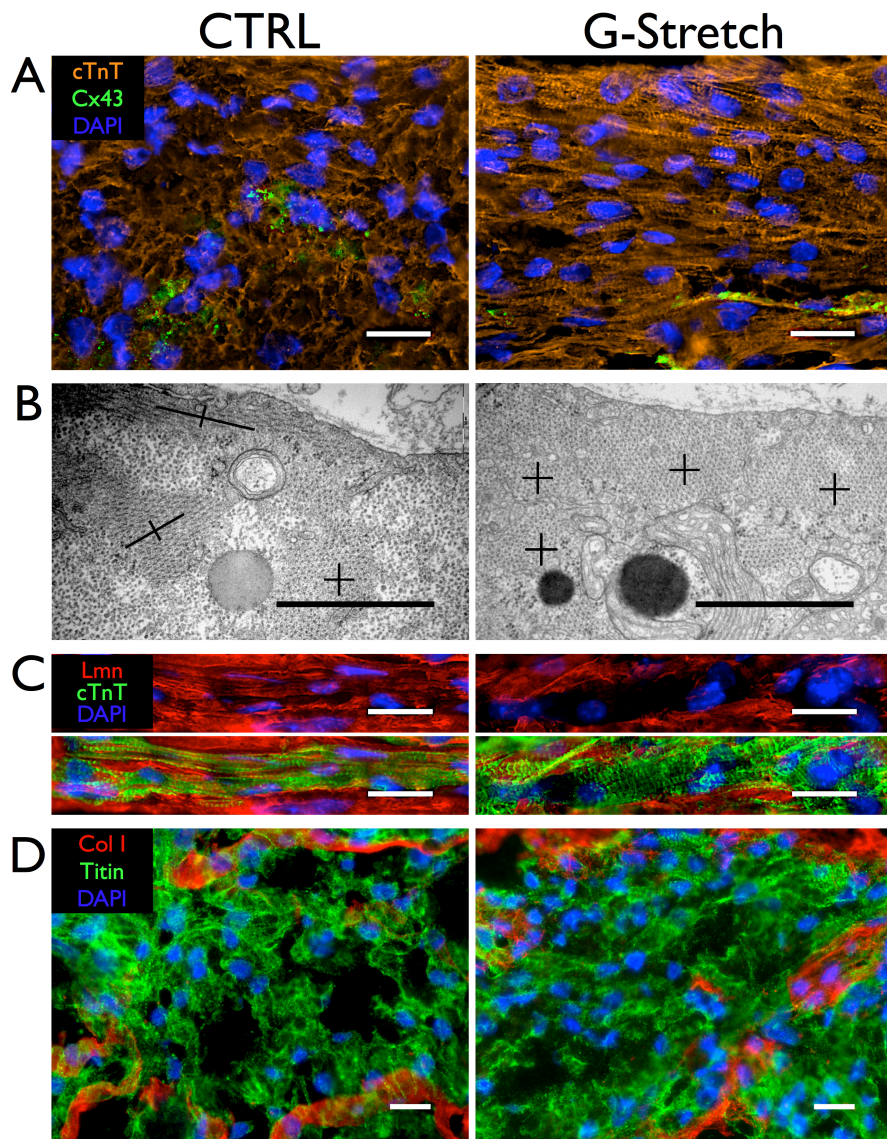


Figure 7: Increasing stretch critically affects miPSC-derived bioartificial cardiac tissue morphology and sub-cellular organization

(A) Immunofluorescence staining against cardiac troponin T (red)/connexin 43 (green) in sections of CB-based iPS-BCTs cultivated under control conditions (left) or with growing stretch (G-Stretch, right), G-treated BCTs showed more uniform distribution of viable cardiomyocytes and better alignment along the longitudinal axis of the BCT. (B) Transmission electron microscopy (TEM) showed improved sarcomeric organization within CMs on d21 (symbols indicate sarcomere orientation) in cross-sections of stretched BCTs. (C) Immunofluorescence staining against laminin (red) / cardiac troponin T (green) preferential deposition of laminin at the lateral cell membrane of stretched BCTs. (D) Immunofluorescence staining against collagen type I (red) / titin (green) showed no significant difference of stretched BCTs and controls. (A), (C), (D): Nuclei stained with DAPI (blue); Scale bars 20 μm . (B) Scale bars 1 μm .

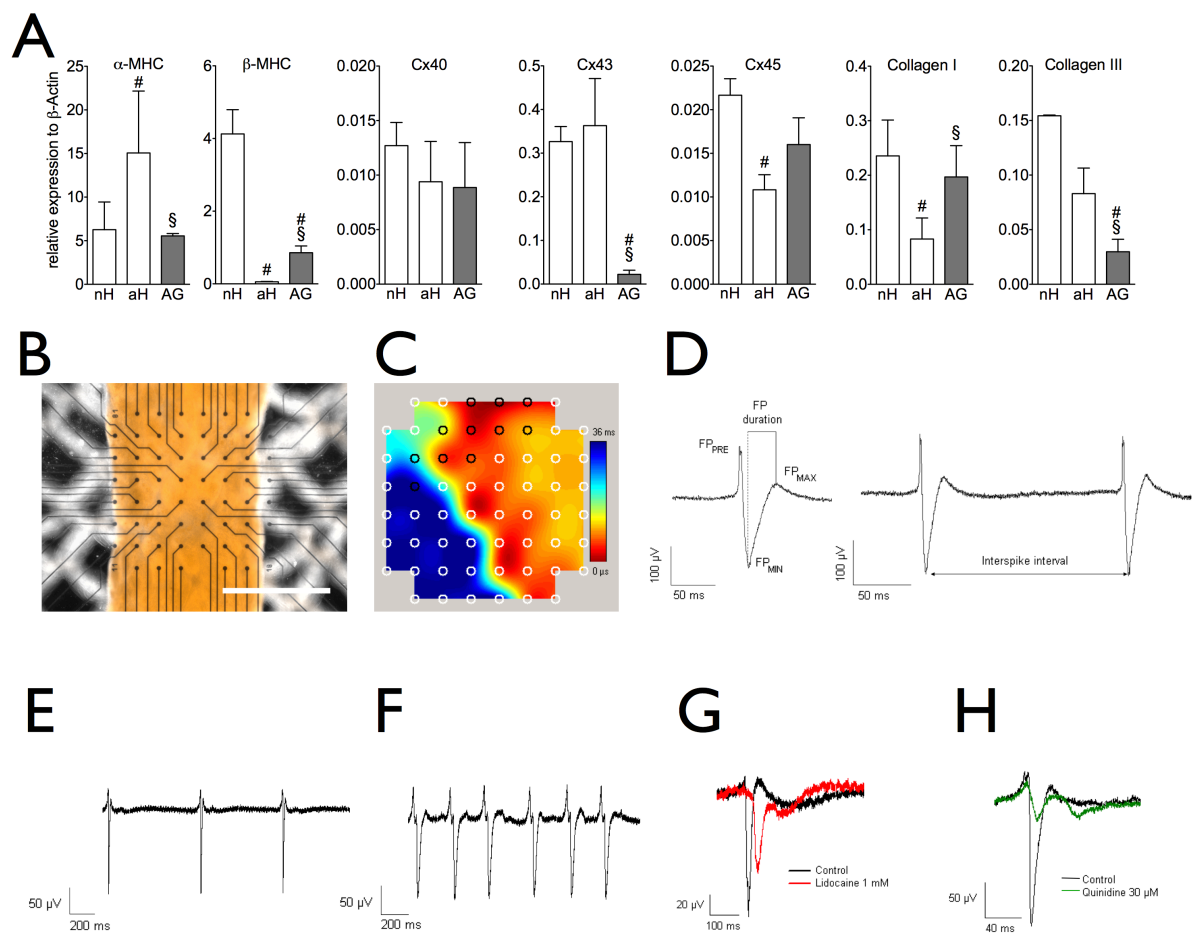


Figure 8: Combined ascorbic acid treatment and increasing stretch lead to optimized miPSC-derived bioartificial cardiac tissue functionality

(A) Quantitative real time PCR analysis of miPSC-derived BCTs on d21 after combined ascorbic acid treatment and growing stretch (AG) demonstrated expression levels of α -MHC, Cx40 and Cx45, as well as collagen type I, comparable to those of the neonatal mouse heart (nH). In contrast, levels of Cx43, β -MHC and collagen type III were significantly lower than in neonatal heart. Values for adult mouse heart (aH) are given for comparison; Data are presented as mean \pm SD ($n=4-6$ with PCR runs performed in triplicate; #, $p \leq 0.05$ to nH; §, $p \leq 0.05$ to aH). (B) A miPSC-BCT (d21) was labeled with TMRM and plated on a multielectrode array (MEA). Scale bar 1 mm. (C) Spatio-temporal color-mapping of FP spreading in one BCT showed the delay of excitation spreading within the tissue under static-ascorbic acid treated conditions. Representative FP recordings (D) before and after administration of 10 μ M isoproterenol (E,F), 1mM lidocaine (G) and 30 μ M quinidine (H) demonstrated physiological drug responsiveness in miPSC-CM derived BCTs.

Supplementary Materials and Methods

Murine iPSC culture

Undifferentiated murine iPSCs, expressing eGFP under control of the Oct3/4 promoter {Mauritz:2011ij}, were cultured on mitotically inactivated feeder layer of γ -irradiated murine embryonic fibroblasts (MEFs) (5×10^4 cells/cm²). Culture medium was composed of Dulbecco's modified Eagle medium (DMEM; Invitrogen) supplemented with 15% fetal bovine serum (Thermo Fisher) 0.2 mM L-glutamine 0.1 mM β -mercaptoethanol 0.1mM non-essential amino acids (all Invitrogen), and 0.1% human leukemia factor (LIF)- conditioned medium, produced by human embryonic kidney 293 cells transiently transfected with a human LIF expression plasmid. iPSC colonies were detached every 3 to 4 days with 0.2% collagenase IV (Invitrogen), dissociated into single cells with 0.025% trypsin (Sigma-Aldrich) and 0.1% chicken serum (Invitrogen) in PBS, and seeded onto a fresh feeder layer.

Establishment of a transgenic miPSC clone for antibiotic selection

Oct4-eGFP transgenic iPSCs were derived from embryonic fibroblasts of OG2 mice by Oct4, Sox2, c-Myc, and Klf4 overexpression. These iPSCs were transfected by microporation with a vector conferring ZeocinTM resistance under control of the cardiac specific alpha myosin heavy chain (α MHC) promoter and a constitutively expressed hygromycin resistance using the chicken β -actin promoter CBA (Supplemental Figure 1A). Hygromycin-resistant cells were clonally expanded and checked for unaltered cardiac differentiation potential as well as expression of the reporter genes (data not shown). Semi-quantitative RT-PCR confirmed resistance gene (Zeo^R) expression in the transfected clone on d10 of cardiac differentiation (Supplemental Figure 1B).

Cardiac differentiation of miPSC

To induce cardiac differentiation, the hanging drop (HD) method was employed using 1×10^3 cells / droplet in 33 μ l miPSC differentiation medium (IMDM+Glutamaxx, 0.1 mM non-essential amino acids, L-Gln, 0.1 mM 2-mercaptoethanol (all Invitrogen),

15% FCS (Thermo Scientific)). On day 3, embryoid bodies (EBs) were either transferred i) individually to 96 well plates to avoid clotting of EBs (1 EB in 130 μ l differentiation medium on 1% agarose), or iia) to 150 mm petri dishes (1600 EBs in 20 ml (12.5 μ l / EB) for static suspension differentiation, or iib) to 150 mm petri dishes with agitation on an orbital shaker at 70 rpm for dynamic suspension culture. All approaches were supplemented with 100 μ M L-ascorbic acid-2-phosphate (Sigma) from d3 until d7 for enhanced cardiac differentiation.

Cardiomyocyte TMRM sorting and enrichment quantification

TMRM FACS sorting was done by dissociating unselected EBs on d13-14 followed by incubation with 25 – 50 nM TMRM in PBS. Cells were FACS-sorted with a FACSAria (BD), or MoFlo (Fa XY) for TMRM^{bright} cells as described by Hattori et al. (REF), with TMRM^{dim} and Oct4-eGFP^{bright} cells being excluded. To evaluate CM enrichment efficiency of TMRM FACS sorting, 1×10^5 cells were seeded onto fibronectin coated dishes and were grown for additional three days. Mosaic micrographs of the whole wells (n = 2) were taken for TMRM staining before and for cardiac Troponin T (Firma XY) after fixation. An overlay of both micrographs revealed cells double positive for TMRM and cTnT and purity quantification was done by counting of cTnT^{pos} and cTnT^{neg} cells, identified by DAPI nuclei counter staining.

Antibiotic cardiomyocyte selection and time course evaluation

To evaluate the fate of CMs, differentiation and Zeocin (Invivogen) containing selection medium (400 μ g Zeocin / ml differentiation medium) was constantly supplemented with TMRM. Stable expression of eGFP under control of the Oct3/4-promotor enabled real time monitoring of persisting undifferentiated miPSCs. Aggregates were either selected in static, or dynamic (70 rpm on an orbital shaker) conditions starting on day 7 of differentiation and cross sectional areas from individual aggregates were determined from day seven until day 17. Gene expression analysis was performed on day 7, 10, 14 and 17 for both selection strategies by RT-PCR. To determine cell viability and selection efficiency, aggregates were dissociated every other day by a 1:1 mixture of collagenase IV (0.2%,

Invitrogen) and Accutase (PAA) starting on day 8. Single cells were counted with a CASY system (Roche) and 10^5 cells were seeded onto 24 wells (Nunc) coated with 5 $\mu\text{g/ml}$ fibronectin (Sigma) and grown for additional three without selective agent. To quantify CMs and growth of unselected non-CMs and to assess cell recovery after dissociation, subsequent immunofluorescence staining was done for Titin and Nkx2.5 using the appropriate secondary antibodies.

Dynamic suspension cultures yielded improved and faster enrichment of CMs with depletion of persistent undifferentiated miPSCs, as visualized by complete loss of reduced Oct4-eGFP^{pos} cells promoter-driven GFP expression and confirmed through highly sensitive RT-PCR (Supplemental Figure 1 C-E). Selection was terminated between differentiation day 13 and 14 when the number of living cells after selection and dissociation ($1.6 \pm 0.3 \times 10^6$ on dd13 and $1.579 \pm 0.46 \times 10^6$ on dd14) was stable and the highest percentage of recovered cells after dissociation and seeding was obtained ($88 \pm 1.8\%$ for dd13 and $68 \pm 2.6\%$ for dd14, Supplemental Figure 1F).

Functional characterization of miPSC derived CMs

To observe cell distribution and morphology within resulting CBs, cryosections of aggregates were immuno-stained for cardiac Troponin T (cTnT, Fa XY) and Connexin 43 (Cx43, Fa XY). Gene expression analysis was performed by quantitative RT-PCR on samples from d14, d21 and d28 of differentiation, with antibiotic selection from d7 to d14. Electrophysiology was assessed on single cells derived from selected CBs using either the whole-cell patch clamp technique, or the MEA-system (Multi-Channel-Systems). Cells were seeded onto fibronectin-coated substrates and measurements were performed on day 16 for MEA measurements, or between days 17 to 21 (patch clamp).

Whole-patch clamp recordings

The membrane potential (E_m) of single cardiomyocytes was measured at room temperature using ruptured-patch whole cell current clamp as described previously (Guan et al Nature 2006). Microelectrodes (5-10 M Ω) were filled with (mM): 120 K-aspartate, 10 HEPES, 8 KCl, 7 NaCl, 5 Mg-ATP, 1 MgCl₂, adjusted to pH 7.2 with

KOH. The bath solution contained 135 mM NaCl, 10 mM HEPES, 10 mM glucose, 5.4 mM KCl, 1 mM MgCl₂, 1 mM CaCl₂, adjusted to pH 7.4 with NaOH. Myocytes were mounted on the stage of microscope (Nikon Eclipse TE2000-U). Fast capacitance, generated largely by the pipette itself, was compensated in a cell-attached configuration. Liquid junction potentials were usually between 3-6 mV. Spontaneous action potentials (APs) were recorded 2 min after patch rupture and followed for about 2 min. Signals were filtered with 2.9 and 10 kHz Bessel filters, and recorded with an EPC10 amplifier (HEKA Elektronik, Lambrecht/Pfalz, Germany) using the Patchmaster software. Action potentials analysis was done using MS Excel[®] to determine the maximum rate of rise of the AP upstroke (dV/dt_{max}), AP amplitude (APA), AP duration at 80% of repolarisation (APD 80), and the maximum diastolic potential (MDP). Results were displayed using GraphPad Prism[™]. Pacemaker-like APs are characterized by prominence of phase 4 depolarization, slow dV/dt_{max} , less negative MDP, and a smaller APA. The ventricle-like APs can be distinguished by high dV/dt_{max} and APA, and the presence of a significant plateau phase of the AP resulting in a long AP duration. The atrial-like APs show a triangular shape with a high dV/dt_{max} and APA but a short duration. The Purkinje-like APs are characterized by a high dV/dt_{max} and APA, the presence of a notch and a prominent plateau-phase.

Multi electrode array measurement

Multi electrode arrays (MEAs) were used to record field potential changes. Single cardiomyocytes were plated on fibronectin coated (25µg/ml) MEAs (Multichannel Systems) and exposed to 10 µM isoproterenol, 1 mM lidocaine or 30 µM quinidine (all Sigma). For the analysis of three-dimensional bioartificial cardiac tissue, constructs were placed on MEAs and allowed to attach over night before recording of field potentials.

Microscopic assessment of cardiac bodies and tissues

To visualize cells with high metabolism, i.e. CMs, culture medium was constantly supplemented with 50 nM TMRM (Hattori et al. 2009). Brightfield and TMRM-

fluorescence micrographs of dissociated cells, EBs and whole tissues were taken using the AxioObserver Z1 (Zeiss) microscope together with a motorized stage. To acquire multiple images the AxioVision software modules Mosaix and Time lapse (Zeiss) were used. Experiments were conducted in a cultivation chamber at 37°C with saturated humidity and 10% CO₂. Mosaix images were taken every 15 min and compiled for a time lapse movie.

Gene expression analysis by PCR

Gene expression of cells and BCTs was analysed using either semi-quantitative RT-PCR or quantitative real-time PCR after RNA isolation and reverse transcription. Total RNA was prepared from cultured cells using TriZol Reagent (Invitrogen). Contaminating DNA was digested by DNase I (Fermentas, St. Leon-Rot, Germany) for 30 min at 37°C followed by phenol/chloroform-extraction. After ethanol precipitation, 50-100 ng RNA was used for random-primed cDNA synthesis with the RevertAid™ H Minus First Strand cDNA Synthesis Kit (Fermentas). cDNA (1 µl) was amplified with PCR using 1.25 U GoTaq DNA Polymerase (Promega, Madison, USA) in GoTaq reaction buffer 5x reaction buffer, using 0.4 µM of each primer (Eurofins MWG Operon, Ebersberg, Germany) and 0.4 µM dNTPs (GE Healthcare, Munich, Germany) in a 25 µl reaction using a Mastercycler® ep Gradient S (Eppendorf, Hamburg, Germany). PCR conditions included an initial denaturation step at 94°C for 1 min; PCR cycles included denaturation at 94°C for 30 sec, annealing at T_A for 1 min, and polymerization at 72°C for 1 min; a final extension step of 10 min at 72°C was added. Sequences and specifications of primers and details on respective PCR conditions can be found in table S1. Reactions without reverse transcriptase were performed in parallel to control for any remaining contaminations of genomic DNA (+/- RT).

For quantitative real-time PCR analysis, 1 µl of cDNA was amplified with the ABsolute™ QPCR SYBR® Green Mix (ABgene Ltd, Epsom, UK) and 1 µM of each primer in a 25 µl reaction using a Mastercycler® ep realplex2 (Eppendorf, Hamburg, Germany). Sequences of primers can be found in table S2. PCR conditions included an initial denaturation step at 95°C for 15 min, followed by 40 cycles of denaturation at 95°C for 1 min, annealing at T_A for 1 min, and polymerization at 72°C for 1 min.

Uniform size of amplicons and absence of nonspecific products were controlled by melting curves. Relative expression levels compared to the reference gene β -Actin were calculated using the $\Delta\Delta C_t$ -method (GENEX 5 software from MultiD analysis AB, Goeteborg, Sweden). Unless indicated otherwise, data are presented as mean \pm SD for two independent experiments, each with two PCR runs performed in triplicate.

Gene expression analysis by immuno-fluorescence imaging

Cells were fixed with 2% paraformaldehyde and stained by indirect immunostaining. For histological analysis tissues were frozen in TissueTek (Sakura) at -80°C , sectioned (thickness: 12 μm) using the HM 500 cryostat (Microm), fitted to object slides and air dried overnight. Samples were fixed with 2% paraformaldehyde before staining with appropriate primary and secondary antibodies using standard protocols. Corresponding isotype antibodies were used for negative control staining. For a detailed description of antibodies see Supplementary Table S2 Nuclei were stained with DAPI. Images were captured using a fluorescence microscope (Zeiss AxioOserver Z1) and Axiovision software 4.71 (Zeiss).

Bioartificial Cardiac Tissue (BCT) preparation with iPSC-derived CMs

For single cell-based BCT production, between 1 and 1.5×10^6 selected CMs (day 14 of differentiation) were used to prepare BCTs either with, or without between 15 and 35% γ -irradiated murine fetal fibroblasts (FBs). Together with collagen type I (Cultrex) and Matrigel (BD Biosciences), the resulting mixture (220 μL) was poured into custom made silicone molds. For CB-based BCT preparation, between 400 and 5400 day 14 CBs containing $1.6 \pm XY$ selected CMs were used either with, or without FBs (between 8 and 33%) resulting in the same volume when mixed with liquid matrix components as described above. After solidification of the cell/matrix mixture (30 min at 37°C in a standard incubator) in custom made silicone molds, the constructs were covered with 5 ml medium BCT medium with chick embryo extract for seven days and without for additional 14 days.

Force measurements

Force measurements were performed as described previously (Kensah et al). In brief, constructs were placed into a custom made bioreactor and stretched by 100 μm increments to 1.2 mm. BCTs were electrically paced at each step 5 times at 25 V, after the baseline reached a steady state. To determine passive forces (Δ mN) differences between baseline at original length and baseline at each preload step were determined (see supplemental figure 2). All measurements were performed in BCT culture medium without AA.

Sarcomere length measurements

Since high fluorescence background was observed in BCTs stained for cardiomyocyte Z-discs by alpha actinin, an indirect sarcomere length measurement method was employed, i.e. measurement of distances between two adjacent cardiac Troponin T signals representing the space between two M-bands in cardiomyocytes. Accuracy of this method was tested by comparison of distances between alpha actinin^{pos} Z-discs (n=88) and the distances between two cTnT signals (n=70) in similar areas of sections from the same adult mouse heart. BCTs were washed in phosphate buffered saline without Ca²⁺ and Mg⁺ and slowly frozen in TissueTek (XY) on dry ice to prevent freezing of contracting CMs. On different sections of each tissue (n = 4 – 7 for each group) only sarcomeres of anisotropic cardiomyocytes oriented in parallel to the contraction direction of the tissue (n = 77 – 184 for each group, mostly found at the lateral border of BCTs), were assessed (see Supplementary figure S4).

Collagen fibre analysis in BCTs

To compare collagen fibre width and alignment in the BCT groups, two immunostained slices of two biological replicas per group were analyzed. Due to the presence of cell-free collagen fibres especially at both apical ends of the tissues based on the self assembly properties of matrigel (REF Matrigel), only fibres associated with cells between the titanium rod suspensions were chosen for width and orientation measurements. Orientation of collagen fibres was assessed by angle measurement in relation to the tissue's contraction direction (n = 75 – 90 per group)

and dispersion was expressed as percent ($90^\circ \pm 100\% \pm 1$). Reciprocal values of relative angle dispersion were defined as alignment score of collagen fibres (Hansen et al. 2010).

Fluorescence intensity quantification

Intensity of TMRM and Titin fluorescence was quantified by comparing treated groups normalized to the control. Micrographs were captured with equal exposure times. Only samples stained in parallel under equal conditions were compared. For TMRM fluorescence assessment, three biological replicates were measured per group and five areas were compared per replicate. For Titin fluorescence quantification, four tissue sections of each group and five prominent cardiomyocyte containing areas per section were assessed after immunofluorescence staining.

Electron microscopy

Tissues were fixed in 1.5 % formaldehyde and 1.5 % glutaraldehyde at room temperature for 30 min and then at 4 °C over night. After dehydration in acetone the samples were embedded in EPON. 40 nm sections were mounted onto formvar coated copper grids, stained with 4 % uranyl acetate and lead citrate (Reynolds, 1963) and observed in a Morgagni TEM (FEI), operated in the bright field mode at 80 kV. Images were taken with a 2K side mounted Veleta CCD camera.

Reynolds, E. S. (1963). The use of lead citrate at high pH as an electron-opaque stain in electron microscopy. *J. Cell Biol.* **17**, 208-213

Supplementary Tables

Table S1: Primers and conditions used for PCR

Name	Target	Position	T _A	Product	Sequence
α-MHC sense	GI 255918224	209	60 °C	276 bp	GATGCCAGATGGCTGACTT
α-MHC ras		484			GGTCAGCATGGCCATGTCCT
Acta1 sense	GI 142378163	170	60 °C	268 bp	ATACAGTGCGGTGTCCAACA
Acta1 ras		437			AGCCCTCAGTTTGCTTTTCA
ANF sense	GI 145966868	752	60 °C	312 bp	CAAGAGATGGCCACTGCC
ANF ras		1063			CTTGATCTTCATGGTGCTAGGA
β-Actin sense	GI 118131045	27	60 °C	151 bp	TTGCTACCCTCAGGTGGCTCCGAG
β-Actin ras		177			TGCAGCCCCAAATGCAGCCATC
BNP sense	GI 46575906	175	60 °C	112 bp	CTGGCTCACTGTCTGTTC
BNP ras		286			GCAACCAGGCTGAATGGTAT
Connexin40 sense	GI 166091435	264	60 °C	131 bp	TGGACAAGGTCCAAGCCTAC
Connexin40 ras		394			ACAGCGAAAGGCAGACTGTT
Connexin43 sense	GI 226874806	737	60 °C	112 bp	AAGAGCAGAGCCAACCAAAA
Connexin43 ras		848			CCCACCTCAAACACAGTCCT
Connexin45 sense	GI 118131144	3876	60 °C	142 bp	GAGCGGAGAGTACTGGATCG
Connexin45 ras		4017			GTTCCGGGCTGATGTACCAGT
Collagen1 sense	GI 226423932	2970	60 °C	110 bp	ACCAAAAGGTGATGCTGGAC
Collagen1 ras		3079			GACCTCGTGCTCCAGTTAGC
Collagen3 sense	GI 126012538	524	50 °C	354 bp	GGCCAAGGTCATCCATGA
Collagen3 ras		877			TCAGTGTAGCCCAGGATG
GAPDH sense	GI 125490391	41	55 °C	173 bp	CTCGGGGTGCCACCTTC
GAPDH ras		213			TCTGAGCCTGGTCCGATTCCA
Oct3/4 sense			55 °C	250 bp	ACGACGTGACCCTGTTTCATC
Oct3/4 ras					GTCGGTCACTCTGCTCCT
Zeocin sense					
Zeocin ras					

Table S2: Antibodies used for immuno-fluorescence staining**A: Primary Antibodies used for immuno-fluorescence staining**

Species	Class	Name	Label	Vendor	Dilution
Mouse	IgM	Anti-Titin	-	Hybridoma Banks, University of Iowa	1:30
Mouse	IgM	Isotype control antibody	-	DakoCytomation, Glostrup, Denmark	1:85
Rabbit	IgG	Anti-Nkx2.5	-	Santa Cruz Biotechnology, Heidelberg, Germany	1:50
Rabbit	IgG	Isotype control antibody	-	Santa Cruz Biotechnology, Heidelberg, Germany	1:100
Mouse	IgG1	Anti-Collagen I	-	Sigma-Aldrich, Hamburg, Germany	1:2000
Mouse	IgG1	Isotype control antibody	-	DakoCytomation, Glostrup, Denmark	1:29
Mouse	IgG1	Anti-Cardiac troponin T	-	Thermo Scientific, Dreieich, Germany	1:100
Mouse	IgG1	Isotype control antibody	-	DakoCytomation, Glostrup, Denmark	1:50
Mouse	IgM	Anti-Connexin 43	-	Sigma-Aldrich, Hamburg, Germany	1:1000
Mouse	IgM	Isotype control antibody	-	DakoCytomation, Glostrup, Denmark	1:99

B: Secondary Antibodies used for immuno-fluorescence staining

Species	Class	Name	Label	Vendor	Dilution
Goat	-	Anti-mouse IgM	DyLight 549	Dianova, Hamburg, Germany	1:300
Donkey	-	Anti-mouse IgM	DyLight 549	Dianova, Hamburg, Germany	1:300
Donkey	-	Anti-rabbit IgG	DyLight 649	Dianova, Hamburg, Germany	1:300
Goat	-	Anti-mouse IgG	DyLight 488	Dianova, Hamburg, Germany	1:300
Goat	-	Anti-mouse IgG	DyLight 549	Dianova, Hamburg, Germany	1:300
Goat	-	Anti-mouse IgM	DyLight 649	Dianova, Hamburg, Germany	1:300

Table S3:**Selected miPSC-cardiomyocyte action potential characteristics**

	Pacemaker-like n=9	Ventricle-like n=9	Atrial-like n=2	Purkinje-like n=2
C_M (pF) [n]	31.4±7.1 [11]	35.2±14.8 [12]	11.6±11.5 [6]	60.4±40.5 [3]
AP Amplitude (mV)	34.3±6.0	70.5±5.7	61.8±8.7	77.6±7.3
APD 80 (ms)	114.9±10.3	184.9±27.2	95.6±5.4	221.2±55.6
Max. dV/dt (Vs ⁻¹)	3.1±0.67	11.0±3.5	20.3±10.1	9.7±4.9
MDP (mV)	-30.3±4.8	-45.5±4.4	-42.4±7.7	-47.3±3.4
SAF (Hz)	0.60±0.11	0.59±0.11	0.77±0.10	0.22±0.04

Data are mean±SEM. n indicates the cell number; APA, AP amplitude; APD80, AP duration measured at 80% repolarization; Max. dV/dt, maximum rate of rise of AP; MDP, maximum diastolic potential; and SAF, spontaneous AP frequency.

Supplementary Figures

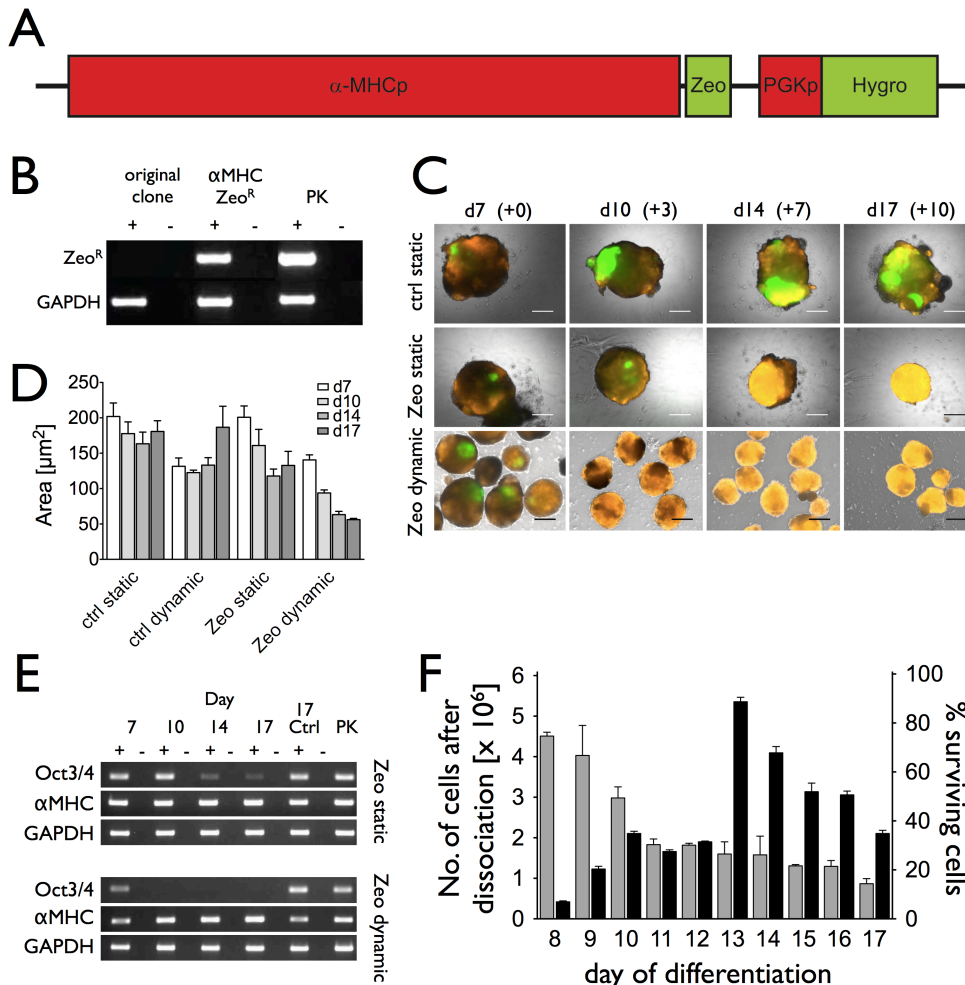


Figure S1: Dynamic suspension culture leads to optimized antibiotic selection of miPSC-derived cardiomyocytes

(A) Murine iPSCs were transfected by microporation with a vector conferring Zeocin™ resistance under control of the cardiac specific alpha myosin heavy chain (α MHC) promoter and a constitutively expressed hygromycin resistance using the phosphoglycerate kinase promoter (PGK). (B) Semi-quantitative RT-PCR confirmed resistance gene (Zeo^R) expression in the transfected clone on d10 of cardiac differentiation. (C) Upper row: non-selected control EBs during differentiation from d7-d17. Middle row: Zeocin selection from d7 on showed slow extinction of Oct4-driven GFP^{positive} cells in static suspension (still present on day 10), whereas dynamic selection led to rapid loss of GFP and homogeneous appearance of TMRM^{bright} cardiac bodies. (D) Consequently, dynamic suspension selection resulted in a more rapid decline of EB sizes, given as cross-sectional projection area (μm^2), and of Oct4 expression levels detected by RT-PCR (E). (F) The optimal selection duration of 13 to 14 days was chosen based on an optimal combination of total cell numbers after dissociation (counted with CASY cell counter) and highest values for cell recovery of viable cardiomyocytes determined after seeding.

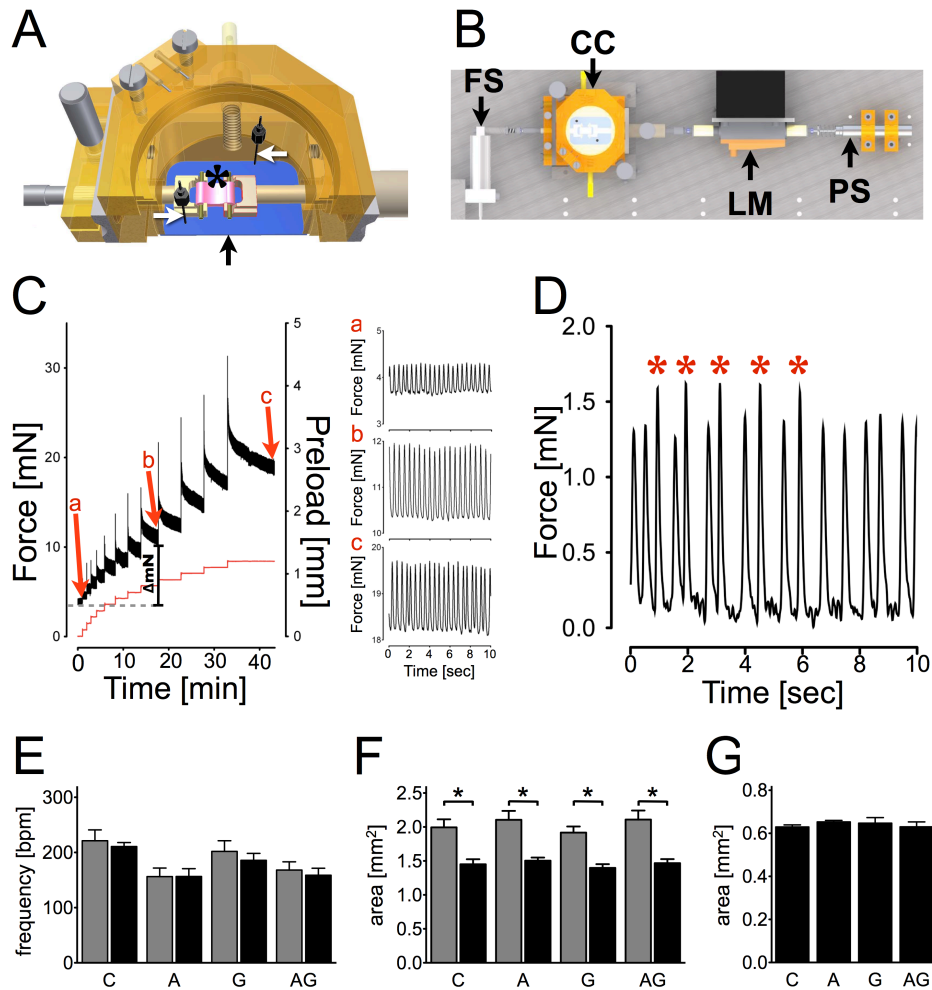


Figure S2: Bioreactor for defined preload and force measurements

(A) Constructs (see asterisk) were placed into a custom made bioreactor cultivation chamber (CC) which allows for electrical stimulation (electrodes denoted by white arrows). (B) Constructs were stretched using a linear motor (LM), for force measurements with the force sensor (FS), 100 μm increments were used up to a final preload of 1.2 mm (controlled by a path sensor, PS). BCTs were electrically paced at each step 5 times at 25 V, after the baseline reached a steady state. (C) To determine passive forces (delta mN) differences between baseline at original length and baseline at each preload step were determined. (D) Original twitch force recording of one BCT (treated with ascorbic acid and growing stretch, combined) on day 21. Asterisks indicate synchronized twitches induced by electrical pacing. Spontaneous twitches showed smaller amplitudes. (E) Frequencies of spontaneous contractions of BCTs from different treatment groups: C, control; A, ascorbic acid; G, growing stretch; AG, ascorbic acid and growing stretch, combined; were measured on day 14 (light grey) and day 21 (dark grey). AA-treated CB-based miPS-BCTs displayed lower contractions frequencies, G-stretch did not influence frequencies compared to the untreated control; in all groups frequencies did not change significantly over time. (F) Cross-sectional areas of CB-based miPS-BCTs determined microscopically and analyzed using ImageJ software. They showed no significant differences between treatment groups, however clear compaction over time was observed from d14 (light grey) to d21 (dark grey). (G) Similarly, tissue cross-sectional area of fibroblast-only tissue did not vary between treatment groups.

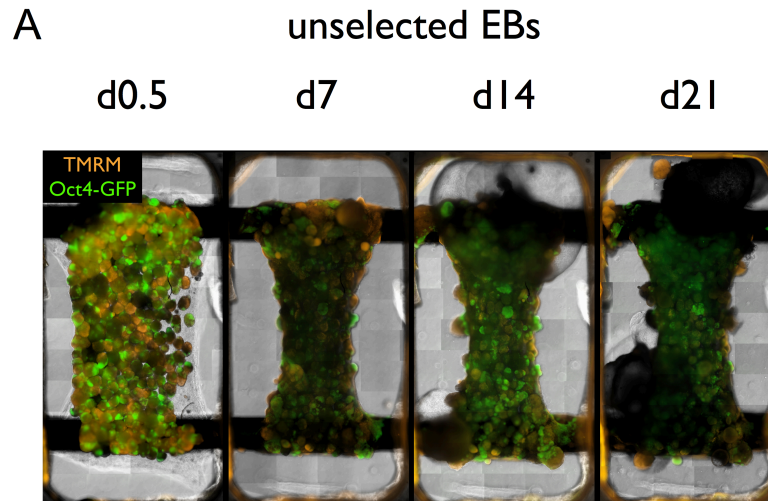


Figure S3: BCT formation using non-selected embryoid bodies

(A) Non-selected embryoid bodies (d14) formed tissue without fibroblast addition, but GFP-fluorescence showed persistent pluripotent cells, proliferating and forming cystic structures; TMRM fluorescence decreased substantially. Contractions of isolated EBs within these BCTs discontinued over cultivation time and were no longer observed on d21.

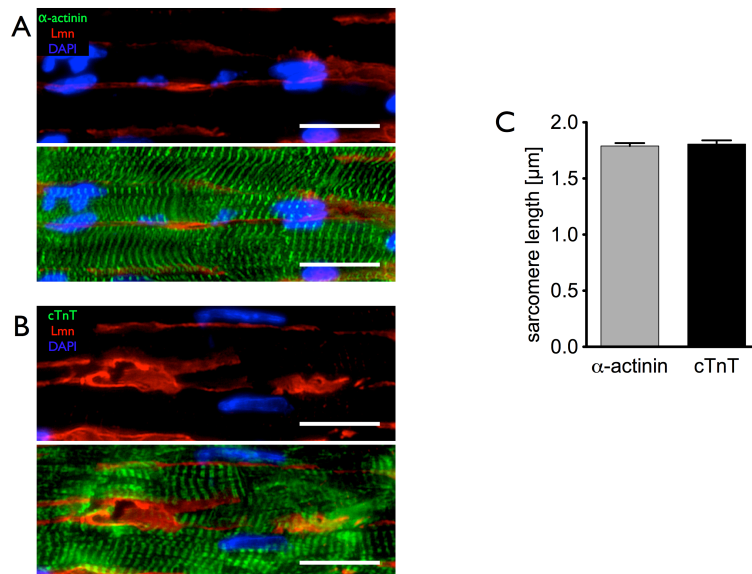


Figure S4: Sarcomere length measurements

Measurement of distances between two adjacent cardiac Troponin T signals representing the space between two M-bands in cardiomyocytes was used, because high fluorescence background was observed in BCTs stained for cardiomyocyte Z-discs by alpha actinin. Accuracy of this method was tested by comparison of (A) distances between alpha actinin^{pos} Z-discs (n=88) and (B) the distances between two cTnT signals (n=70) in similar areas of sections from the same adult mouse heart. (C) Quantitative analysis of sarcomere length showed no difference between both methods.

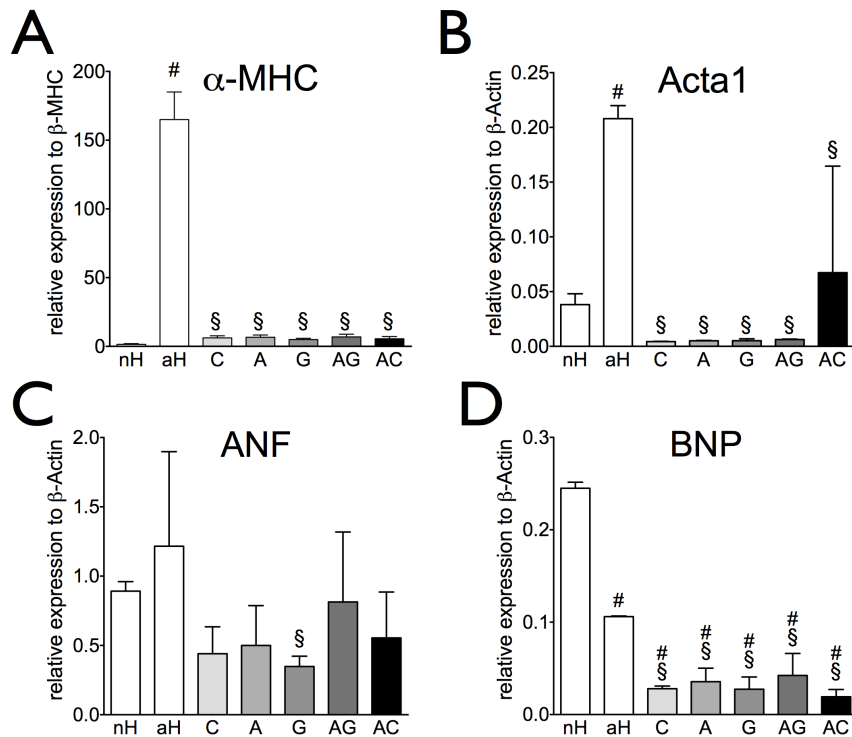


Figure S5: Hypertrophy-related gene expression levels in miPS-BCTs treated with ascorbic acid and/or stretch

Cardiac hypertrophy associated gene expression levels of α -MHC, β -MHC, Acta1, ANF and BNP were assessed by quantitative real time PCR in comparison to neonatal mouse heart and adult mouse heart tissue. On day 21 of cultivation, the expression levels did not differ significantly between the groups. Only a moderate increase of ANF expression was observed after combined treatment with ascorbic acid and incremental preload, however not above expression levels in the native heart. Data are presented as mean \pm SD for three experiments, with PCR runs performed in triplicate.

Ascorbid acid & G-stretch

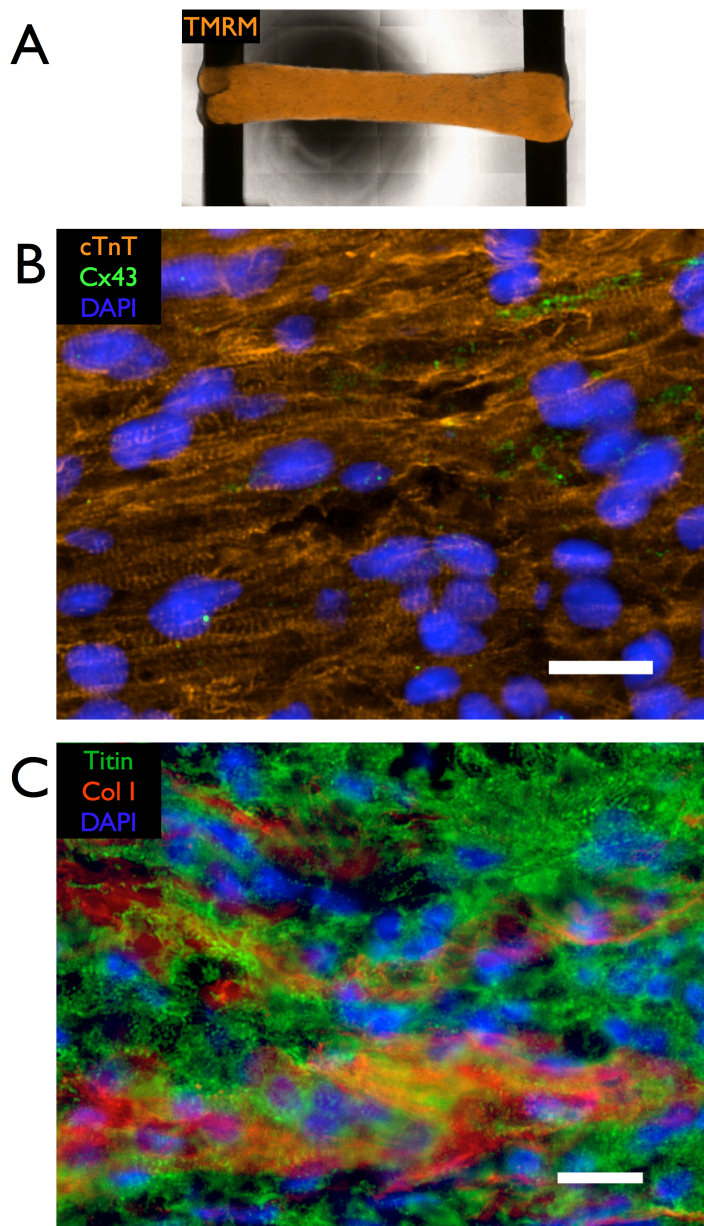


Figure S6: Combined ascorbic acid treatment and increasing stretch led to optimized miPSC-derived bioartificial cardiac tissue functionality

(A) CB based-BCT on day 21 after seven 200 μm increments of G-stretch showed high vitality by bright and regular distributed TMRM fluorescence intensity. Cardiac bodies were fused to a simultaneously contracting tissue with a total length of 7.4 mm. Cardiomyocyte distribution is demonstrated in a longitudinal section of the respective tissue by co-immunostaining for (B) cardiac troponin T (red) and Cx43 (green); or (C) titin (red) and collagen I (green) as extracellular matrix marker. Nuclei stained with DAPI (blue); Scale bars 20 μm .

Supplementary Videos

(in preparation)

4 Discussion

In contrast to the restricted differentiation potential of adult stem cells, two types of pluripotent stem cells (PSCs) have been independently reported to robustly give rise to cell types of all three germ layers: embryonic stem cells (ESCs) and the very recently developed induced pluripotent stem cells (iPSCs) (Takahashi & Yamanaka 2006). The latter cell type especially raises hopes for future clinical applications, because it can be efficiently generated from easily accessible adult somatic cells. Its autologous origin thus makes it highly attractive and should be preventing immunological responses after therapeutic administration. Recent findings, however, indicate that in some iPSC-derivates abnormal expression of antigens, not expressed during normal development, or ESC differentiation, lead to T-cell-dependent immune response (Zhao et al. 2011). The threat of insertional mutagenesis, due to viral integration during the process of reprogramming is addressed by alternative, non-integrating reprogramming strategies (Jincho et al. 2010; Okita, Nakagawa, Hyenjong, Ichisaka & Yamanaka 2008a). Concerning the yield in iPSC-derived cardiomyocytes, over the last years, attempts have been made to improve efficiency of cardiomyogenic *in vitro* differentiation with substantial success (BurrIDGE et al. 2011). Furthermore, it was shown that cardiovascular progenitor cells with an intermediate differentiation state, which can give rise to all cell types present in the working heart can be generated and enriched from iPSCs differentiations (Mauritz et al. 2011). At present, research is focusing on reducing the risk of teratoma formation by persistent PSCs in applied populations. One strategy aims at modifying iPSC technology to circumvent the generation of a pluripotent state and to directly generate cardiomyocytes from adult somatic cells (Ieda et al. 2010). Another strategy is to enrich stem cell-derived cardiomyocytes and thereby to eliminate persisting undifferentiated pluripotent cells (Klug et al. 1996; Hattori et al. 2009).

Rapid progress in this challenging field over the last few years indicates that future application of iPSC-derivatives in regenerative medicine including the generation of iPSC-derived patient-specific bioartificial cardiac tissue for reconstructive therapies is conceivable.

Therefore, in the presented thesis, several myocardial tissue engineering aspects concerning effectiveness of miniaturization of engineered constructs, improvement of stimulation and monitoring procedures, as well as applicability of iPSC-derived cardiomyocytes to cardiac tissue engineering were assessed.

4.1 A Novel Miniaturized Multimodal Bioreactor for Continuous *In Situ* Assessment of Bioartificial Cardiac Tissue during Stimulation and Maturation (Manuscript 1)

4.1.1 Current demands on bioreactor design for stem cell-based myocardial tissue engineering

Myocardial tissue engineering (MTE) is a promising approach to overcome shortage of transplantable hearts. In order to produce functional myocardial tissue surrogates, it is essential to define, characterize and improve functionality of engineered tissue *in vitro* prior to *in vivo* studies. To this aim, specialized bioreactor systems are desirable that provide tissue stimulation functionalities and allow the assessment of a large number of parameters using small sample numbers and sizes, to efficiently handle resources, i.e. matrix compounds and cells. Due to the limited yield in cardiomyocytes (CMs) using current differentiation protocols, miniaturization is necessary to optimize pluripotent stem cell-derived tissue constructs. However, the possibility of surgical manipulation of the tissue should not be compromised. A modular bioreactor design will give the chance to adapt conditions rapidly to changing needs for experimental design, e.g. changes in the range of actors, and sensors, or changes in tissue dimensions. Moreover, insights especially into initial phases of tissue formation are essential, to observe effects of variations in cell composition and matrix compounds, eventually enabling improvement of desired properties of engineered constructs.

4.1.2 A novel bioreactor system

In this work, the following provisions led to successful combination of all desired features into one modular bioreactor system. With a volume of 220 μl (10 x 4 x 5 mm), bipartite and bottom-less Teflon molds allowed for convenient release of tissue

constructs and microscopic observation, respectively. Molds were sealed prior to each experiment with non-adhesive agarose in standard multi-well plastic culture dishes to prevent leakage. Due to cost effectiveness, simplicity in production accompanied by enhanced adjustability, original Teflon molds used in this study were recently replaced by silicone molds with same dimensions (unpublished data). After consolidation of the liquid cell/matrix mixture resulting in a premature bioartificial cardiac tissue (BCT), bottom transparency enabled for observation of cell-cell and cell-matrix interactions by means of fluorescence microscopic time-lapse analysis supported by the non-toxic dye TMRM. This cationic fluorescent dye is rapidly and reversibly taken up by live cells and sequestered to active mitochondria. Hattori and colleagues exploited this effect to cytometrically identify cells with the highest metabolic activity in cell populations derived from PSCs, i.e. cardiomyocytes (Hattori et al. 2009). This was adapted for microscopic observations in this study and revealed cell elongation and tissue shrinkage over time with the most drastic effects during initial phases of culture, i.e. day zero - day seven. For mechanical, chemical and electrical stimulation purposes, and to assess physiological properties, after initial tissue formation (from day 3 on), BCTs could be transferred to a central cultivation chamber. In these vessels sealing was conferred by a system of thin flexible silicon membranes that, at the same time, allowed for external mechanical manipulation and force measurements by cantilevers spanning the membranes without impairing sterility. BCTs were held in place at original length by brackets attached to the cantilevers and tight positional control was given by a computer-assisted and position sensor-controlled linear motor, which, in this study, was used for cyclic stretch of BCTs. Connections to the motor, as well as to the force sensor, positioned oppositely to the mechanical actor, was conferred by magnets, allowing for effortless attachment and detachment of the central cultivation vessel. To prevent uncontrolled changes in tissue length, cantilevers were fixed to actual positions prior to detachment from the bioreactor. In experiments performed in the presented study, permanent microscopic assessment of the BCT in the cultivation vessel over the whole cultivation period was limited only by continuous application of mechanical manipulation. This restriction was recently solved by modifications of the original bioreactor system described in the

manuscript. Now one bioreactor unit, i.e. the central cultivation chamber connected to sensor and actors, can be placed in the incubation chamber of the fluorescence microscope, allowing for continuous mechanical conditioning concomitant with optical assessment (unpublished data). Electrical stimulation, in this study limited to pacing of BCTs during endpoint maximum force measurements, was conferred by a computer-controlled current generator connected to platinum wires submerged in medium allowing for current pulses of 0 to 25 V with alternating polarity to prevent hydrolysis. Perfusion was possible via connections attached to the cultivation chamber, but has not been used in the presented study, where medium exchange was done manually every other day, or when necessary.

To date, the bioreactor presented in this study is the only one that combines the possibility of continuous microscopic and mechanical assessment of generated constructs in parallel with the application of mechanical and electrical stimuli mimicking conditions in the heart, i.e. mechanical load in various forms and the defined electrical stimulation of excitable cells, respectively (Fink et al. 2000; Zimmermann 2001; Hansen et al. 2010; R. Birla & Borsches 2005; Brown et al. 2008; Shimko & W. C. Claycomb 2008) The ability to repeatedly assess active and passive forces and contraction frequencies, i.e. the essential parameters to define functionality of engineered cardiac muscle, on the same tissue construct, without interrupting cultivation, provides a valuable means for the improvement of MTE. This especially holds true in MTE approaches using PSC-derived CMs, which are of immature state and differ from CMs derived from primary, natural cell sources, e.g. neonatal animals, to a large extent due to their artificial background (Hansen et al. 2010; Schaaf et al. 2011). Hence, this indicates the necessity for novel stimulation and conditioning strategies for PSC-based MTE to match properties of state-of-the-art engineered constructs using primary CMs, eventually resulting in applicable alternatives to heart transplantation. Since all components of this device except the central cultivation chamber are commercially available, independent reproduction of results should be possible, which is not the case for studies using custom-made sensors.

4.1.3 Reproduction of physiological properties reported for larger engineered myocardial tissue constructs

To outline the characteristics of the newly developed bioreactor system and the hereby-produced tissue engineered constructs, studies were performed to emphasize comparability of miniaturized tissue construct properties to those reported by other researchers. Therefore, BCTs were prepared with similar cell densities as reported previously for larger systems and exposed to different stimuli. Cyclic mechanical load (day 7 – day 14), reported to regulate the phenotype and physiology of CMs in 2D and in 3D culture (Frank et al. 2007; Fink et al. 2000; R. Birla & Borschel 2005) and β -adrenergic stimulation (day 6 – day 14) were applied either alone, or in combination. In MTE, β -adrenergic stimulation is used conventionally as an analytical tool during force or frequency measurements (Fink et al. 2000; Zimmermann et al. 2004). To assess feasibility of noradrenalin-mediated β -adrenergic stimulation as a novel conditioning strategy, it was used as a long-term supplementation, as described for higher concentrations by Claycomb and colleagues for 2D cultivation of cardiac HL1 cells to maintain contractility (W. Claycomb & Lanson 1998). Mechanical load and β -adrenergic stimulation confirmed the previously reported effects on hypertrophic responses of CMs (Komuro & Yazaki 1993). In stimulated BCTs, a shift in myosin heavy chain (MHC) isoform expression from α MHC to β MHC, also known as an indicator for transformation of CMs into a more immature phenotype, was observed. Furthermore, up-regulation of atrial natriuretic factor (ANF) expression was detected in all treated constructs, which is an additional marker for hypertrophy as shown in 2D (Frank et al. 2007) and 3D (Fink et al. 2000) cultures of CMs and in ventricles of the hypertrophied heart (Izumo et al. 1988). Changes in Connexin 43 (Cx43) expression was not depending on treatment, in contrast to previous reports (Salameh, Wustmann, et al. 2010b; Salameh, Karl, et al. 2010a), which may be due to differences in stimulation durations analyzed. Common to all tested conditions was the observation of elevated CM densities at the lateral borders with a gradient decrease to the centre of the constructs. Differences, however, were obvious by the elevated occurrence of aligned, anisotropic CMs, being more prominent in treated groups. In terms of contractility, expected elevation in frequency occurred only during

the first days of β -adrenergic stimulation. This was followed by a return to lower frequencies similar to those measured for mechanically stimulated, or non-stimulated BCTs. Repeated daily spontaneous force measurements at slack length from day 7 to day 14 revealed that β -adrenergic stimulated BCTs, alone, or in combination with mechanical stimulation were stronger than BCTs treated with mechanical load only and untreated controls. Interestingly, no additional effect was observed in double stimulated BCTs. Comparison between daily spontaneous and endpoint paced maximum force developments excluded an acute effect of noradrenalin on contraction force, since paced measurements were performed in noradrenalin-free Tyrode's solution after excessive washing steps of BCTs. Moreover, qualitative differences between groups in spontaneous force measurements resembled those detected in maximum force determination measurements. The latter also clearly showed, that BCTs followed the Frank-Starling mechanism of the heart, i.e. preload-dependent increase in contraction forces, which is a major parameter to determine functionality of engineered myocardial constructs.

These results prove the comparability of BCTs generated in the presented integrated miniaturized bioreactor system with established larger systems since contraction forces generated by miniaturized BCTs matched those reported by others, i.e. between ~ 0.3 to 1.5 mN per 10^6 starting cells (Fink et al. 2000; Zimmermann et al. 2000; Zimmermann et al. 2002; Zimmermann et al. 2006; Naito 2006; Hansen et al. 2010). Moreover, absolute contractile forces of 2.88 ± 0.14 mN, generated by the novel β -adrenergic-based conditioning approach described in this study, were almost twofold higher than what has been achieved so far. Nevertheless, compared to the native adult myocardium with a maximum tensile contraction force of ~ 50 mN/mm² (Brooks & C. H. Conrad 1999; Han & Ogut 2010) there still is room for improvement, since miniaturized BCTs generated contractile tensions ~ 10 times lower (4.57 ± 0.08 mN/mm²).

4.2 Two-photon induced collagen cross-linking in bioartificial cardiac tissue (Manuscript 2).

4.2.1 Passive forces in cardiac tissue

For rat heart preparations, passive forces of 6.8 ± 2.8 kPa for neonatal and 25.6 ± 15.9 kPa for adult tissue were reported (Bhana et al. 2010). The same study verified effects of substrates with different passive forces on primary heart cells and it was shown that phenotypes were more mature in terms of force development and morphology of cardiomyocytes on substrates with ~ 50 kPa. In an earlier report, passive forces of 10 kPa were found to significantly improve rat cardiomyocyte survival, morphology and force development in 2D cultures (Jacot et al. 2008). For 3D constructs, similar effects were reported, however, with optimal matrix stiffness of 2.35 ± 0.03 kPa (Marsano et al. 2010). Besides high variations in these studies for the most beneficial substrate stiffness values, probably due to different measurement techniques, these data indicate the high importance of ECM properties on cardiomyocyte function. This might be true especially for immature PSC-derived cardiomyocytes. Therefore, tight control over properties of ECM stiffness, in case of BCTs mainly composed of type I collagen, may be a key factor to improve properties of engineered cardiac tissue in terms of *in vitro* maturation and *in vivo* function in future recipient's heart.

4.2.2 Modulation of mechanical properties of biological tissue

Biological mechanisms to enhance stiffness of engineered tissue constructs were reported using different approaches. It was described by growth factor application-mediated increase in matrix production, as shown for transforming growth factor β (TGF- β) administration (Mann & Schmedlen 2001), by mechanical induction of ECM production by cyclic stretch (Kim & Mooney 2000) and by genetically induced over expression of ECM cross-linking enzymes, as described for the enzyme lysyl oxidase (LO) (Elbjeirami et al. 2003). Cross-linking of ECM components is also possible by chemical processes. Because these are generally based on aldehyde-reactions, excess aldehyde molecules have to be thoroughly removed or inactivated, to avoid

inflammatory reactions, cytotoxicity and calcification, when therapeutically applied (Jayakrishnan & Jameela 1996). An alternative way to influence tissue's stiffness is the employment of photochemical processes based on the transformation of light into other forms of energy. In this case, these mechanisms can be used to induce collagen cross-linking resulting in altered passive forces of tissues.

Photosensitizer-mediated ultraviolet A (UV-A) collagen cross-linking is commonly used in ophthalmologic interventions to stop progression of keratoconus (Wollensak, Spoerl & Seiler 2003a). The application of UV light, however, leads to cell death, which is dispensable in case of epithelial corrections, due to repopulation of the damaged areas by residing proliferative cells *in vivo* (Wollensak et al. 2004). For cardiac tissue engineering, it is not applicable, due to the postmitotic state of the main cell type used, i.e. cardiomyocytes. Therefore, in this study an alternative optical method was employed and assessed for its feasibility in cardiac tissue engineering, i.e. two-photon laser induced cross-linking.

Two-photon laser induced collagen cross-linking is mediated by a photosensitizer, such as riboflavin (RF, also known as vitamin B₂), which enhances the production of reactive singlet oxygen, resulting in cross-linking (Crutchley 2002; McCall et al. 2010)(for a detailed review: see (Vogel et al. 2005)).

4.2.3 Photochemical stiffening of cardiomyocyte-free collagenous tissue

In this study, an optical setup was used that employed femtosecond (fs) laser pulses at near infrared (NIR) wavelengths. These laser systems are already in use for therapeutic applications, such as chromophore assisted laser inactivation of proteins (Tanabe et al. 2005), intracellular nano dissection (König et al. 1999) and laser uncaging (Denk et al. 1990). Due to their nonlinear interaction mechanisms, they result in high penetration depths and reduce the risk of photo-damage, which eventually would lead to apoptosis or impaired cell division (König 2000). To gain full spatial control during tissue treatment, this setup allowed for raster scanning of samples during irradiation. In contrast to existing methods, this tight focusing enables cross-linking in a more precise manner, than exposing the tissue with a broad

irradiation focus commonly used in UV-A mediated collagen cross-linking treatments (Wollensak, Spoerl & Seiler 2003a; Jayakrishnan & Jameela 1996). In this setting, RF served as biocompatible photosensitizer and was added one day prior to laser treatment.

To discriminate between intrinsic biological and two-photon induced collagen cross-linking, immature tissue constructs (i.e. day six after casting) with low passive forces were used in all experiments. To determine a process window for non-destructive laser treatment, γ -irradiated fibroblast-based tissue constructs were used. Passive force measurements were performed one day later by constantly increasing the preload to 20% of the original length using the bioreactor setup described in manuscript 1. Stretch-dependent force curves showed a nonlinear toe region followed by a linear region, which is a characteristic response of collagenous tissue to increasing mechanical strain (Roeder et al. 2002; Wollensak, Spoerl & Seiler 2003b). A laser fluence of 160 J/cm² was determined empirically to be optimal for induction of collagen cross-linking in fibroblast-based tissue. This laser fluence stiffened the tissue by 20% and the Young's modulus, as a determinant of stiffness in elastic material, was increased by the same percentage compared to the controls.

4.2.4 Effective laser induced collagen cross-linking is possible without affecting functional activity of BCTs

In initial experiments cardiomyocyte containing constructs were treated in the same way as fibroblast-based tissue and showed similar, but less pronounced responses to laser treatment (about a factor of three less compared to fibroblast constructs, data not shown). Metabolic activity was not affected by irradiation with 160 J/cm², but at higher laser power (320 J/cm²), it was markedly reduced in treated areas, as indicated by the mitochondrial dye TMRM. Laser-induced photo bleaching was excluded by overnight incubation of constructs with the dye. High laser fluence, however, did not result in obvious reduction of cell density in the treated areas, determined by visualization of DAPI-stained nuclei by a custom made scanning laser optical tomography (SLOT), a technique allowing for 3D fluorescence microscopy of three-

dimensional samples with sizes of up to several millimeters (Lorbeer et al. 2011). Lower stiffness-values in these constructs were putatively based on the reduced fibroblast content and therefore a reduced collagen production, and/or turnover values over cultivation time (Eghbali & Weber 1990). To improve collagen cross-linking in these constructs without impairing cardiomyocyte functionality, adjustments in laser treatment were done. The optical setup was exchanged with a system of higher two-photon action. The focal spot diameter and scanning speed were increased to reduce irradiation time of constructs. These measures allowed for repetitive raster scanning with lower laser pulse energies for collagen cross-linking, exploiting the accumulation of multiphoton-induced photochemical effects over multiple pulses (Kuetemeyer et al. 2010; Vogel et al. 2005). Furthermore, culture conditions were adjusted to reduce the risk of artifacts based on sub-optimal conditions for the constructs outside the incubator during laser treatment. In the course of irradiation the medium was buffered with HEPES to reduce pH-dependent stress on cells and temperature was kept constantly at 37°C using an infrared lamp. In this modified setup, three laser fluences, i.e. 30, 50 and 70 J/cm², were analyzed. Passive force determination showed that significant tissue stiffening (40% at 20% strain) was present in the group with medium laser fluence (50 J/cm²) and the corresponding Young's modulus was increased by about 15% (30.6 ± 0.9 vs. 26.5 ± 1.9 kPa). There were no significant differences in this group compared to the control in terms of active contraction forces. At the same time, no implications on TMRM fluorescence intensity were observed, indicating no negative effect of this treatment in terms of CM viability. Similar to previous results from fibroblast constructs (see section 4.2.3), neither laser treatment alone, nor constructs treated with riboflavin only showed increased tissue stiffening. These data support the assumption of two-photon induced collagen cross-linking as the underlying mechanism for altered mechanic properties. To date, a similar rapid effect has only been described by UV-A-induced collagen cross-linking via one-photon photosensitized singlet oxygen production, bearing the threat of impairing cell function and viability and limited control over spatial precision (Crutchley 2002; McCall et al. 2010). In contrast, the method described in this study shows for the first time, that two-photon induced collagen

cross-linking can be applied to highly sensitive *in vitro* engineered cardiac tissue, without impairing functionality and viability of cells. Although observed effects in this study were lower than reported for UV-A-based cross-linking of human corneas with Young's modulus enhancements of up to 4.5 fold (Wollensak, Spoerl & Seiler 2003b), accumulation of photosensitized singlet oxygen production might be exploited to further optimize this novel method by prolonged irradiation time or repeated application during tissue culture. Biologic cross-linking in tissue engineering based on over-expression of LO in cells seeded on collagen gels was reported to result in a two-fold change in Young's modulus (Elbjeirami et al. 2003). The process described herein did not reach this alteration in terms of stiffening. However, it is much faster and more controllable in terms of spatial precision.

In conclusion, the presented method allows for rapid, efficient and cell-compatible manipulation of mechanical properties of BCTs, ultimately leading to functional improvement of engineered tissue constructs. For example, enhanced spatial control of two-photon induced collagen cross-linking could allow for precise stiffness patterning of BCT to recapitulate the intrinsic anisotropy of native myocardium. In myocardial infarction it was proposed, that most of the benefit could be achieved by selectively stiffening the longitudinal direction without altering the circumferential direction (Fomovsky et al. 2011). To assess these and other attempts on engineered cardiac tissue *in vitro*, the minimal-invasive method of *in situ* collagen manipulation presented in this study could be a valuable tool.

4.3 Fibroblast-dependent Fusion of iPSC-derived Cardiac Bodies results in structurally and functionally homogenous Bioartificial Cardiac Tissue and is supported by Ascorbic Acid and Mechanical Load (Manuscript 3)

4.3.1 Current challenges in pluripotent stem cell-based myocardial tissue engineering

There are several reports on cardiac tissue engineering based on pluripotent stem cell-derived cardiomyocytes (Shimko & W. C. Claycomb 2008; Stevens et al. 2009).

However, only a few of these publications showed data on spontaneous contractile forces. Two studies used non-enriched ESC-derived CMs with a purity of ~50% and reached forces of ~0.5 mN for mouse constructs with a starting cell number of 2.77×10^6 in 230 μl (Guo 2006) and of ~0.08 mN for human constructs with 4×10^6 cells in 100 μl (Tulloch et al. 2011). The latter study also reported proof-of-principle for the generation of human iPSC-derived cardiac constructs, however, no force development was presented for these. In a study reporting the generation of murine ESC-based cardiac constructs derived from genetically purified cardiomyocyte populations with 2×10^6 cells in 1 ml, no force or other contractile data were available (Shimko & W. C. Claycomb 2008). A possible reason for this was recently explained in a study by Liao and colleagues, where a contractile analysis failed, due to the lack of contractility in engineered patches made of genetically purified murine ESC-derived CM-populations (7.83×10^5 cells in 120 μl) (Liao et al. 2011). Assessment of these constructs revealed, that CMs survived, but did not remodel the matrix, to interconnect and therefore lacked the ability to actuate the whole tissue in concert. However, after addition of 3% rat ventricular fibroblasts to the initial cell mixture, tissue formation was achieved with forces of up to ~1.9 mN, comparable to reports of constructs based on primary heart cells (see manuscript 1). However, the window of optimal fibroblast content was very narrow, as was shown by significantly lower forces yielded with suboptimal fibroblast contents. Although being the first report on cardiac tissue engineering resulting in constructs with relevant forces, it remains unclear, whether the added ventricular fibroblasts were CM-free. Our own studies revealed that the use of the same cell population of cardiac fibroblasts, even after repeated passaging to reduce the CM content, resulted in contractile BCTs, indicating contamination with persistent and contractile CMs (unpublished data). Therefore, this might not be the appropriate cell type to reliably assess contributions of fibroblasts to forces developed by PSC-derived tissue constructs.

Of additional interest is, that all studies providing contractile force data are based on the principle of the combination of cells with liquid, self-assembling biological ECM components as described by Eschenhagen et al. (Eschenhagen et al. 1997). The same approach which was favored in our studies.

4.3.2 Genetic selection of cardiomyocytes from iPSCs is superior to non-genetic selection in terms of yield and purity

Populations derived from PSC differentiations contain cardiomyocytes to a certain extent only, depending on the differentiation protocol used (Kehat 2001; Laflamme et al. 2007; X. Q. Xu et al. 2008; Kattman et al. 2011; BurrIDGE et al. 2011), and persisting undifferentiated cells bear the risk of tumor formation when transplanted (Hentze et al. 2009). Therefore, stringent selection is necessary prior to transplantation of PSC-derived engineered cardiac tissue. Two strategies were employed to enrich cardiomyocytes from differentiation cultures of murine iPSC. The first was a genetic approach based on the stable transfection of miPSC with a construct conferring antibiotic resistance under the control of the CM-specific promoter α -MHC and an ubiquitarily expressed hygromycin resistance, to select for successfully transfected cells (Klug et al. 1996; Kolossov et al. 2006). One main disadvantage intrinsic to stable genetic manipulation is based on random integration bearing the risk of insertional mutagenesis (Baum 2004). Therefore, the second approach was non-genetic, based on the higher accumulation of the mitochondrial and non-toxic dye tetramethylrhodamine ester (TMRM) in metabolically active CMs. Hattori and colleagues exploited this phenomenon in PSC differentiations to select for CMs by cytometrically means, i.e. FACSsorting of TMRM^{bright} cells, which they reported to consist of CMs only, with no persisting undifferentiated cells (Hattori et al. 2009). Genetic selection was performed on differentiation cultures of iPSCs from day 7 to day 17 and resulted in contractile cardiac bodies (CBs). TMRM FACSsorting was done with unselected cells on day 14 of differentiation. To compare efficiencies of selection methods, cells from both approaches were counted and grown in differentiation medium to observe growth of non-CMs. Quantification showed, that the genetic approach was ~130 times more efficient compared to the non-genetic method in terms of viable cells per inoculated iPSC assessed directly after each enrichment method (1.68 ± 0.191 vs. 0.013 ± 0.005 cell / iPSC). Reasons for that might be that the dissociation of tightly interconnected cardiomyocytes prior to sorting leads to cell loss (Li et al. 1996), or sorting itself is harmful for CMs due to shear stress. Moreover, the purity was higher in the genetic approach ($99.8 \pm 0.07\%$) than in the cytometric

enrichment method ($84.5 \pm 1\%$). Hence, the latter is technically not mature enough concerning efficiency and stringency, but would have to be improved. Both methods, however, resulted in pluripotent cell-free populations.

In conclusion, the non-genetic approach resulted in enriched cardiomyocyte populations, but is, in our hands, not yet capable to produce sufficient cardiomyocytes for BCT production. Nevertheless, non-genetic methods are highly desirable for clinical application, and since there have been improvements for the generation of iPSC (avoiding genetic manipulation) and progress in direct reprogramming of somatic cells into cardiomyocytes, it might be envisioned to expect genetically non-modified cardiomyocytes for regenerative purposes, soon. However, because of the cell numbers needed for tissue engineering strategies described in this study, only genetically selected cardiomyocytes were used.

4.3.3 Genetic selection results in artificial 3D aggregates with cardiomyocytes showing functional properties

Detailed analysis of selected CBs showed sponge-like structures of the aggregates, and revealed an artificial connexin (Cx) expression pattern with significantly higher Cx40 and Cx45 expression than in the neonatal or adult mouse heart. However, the most prominent connexin isoform in the heart, i.e. Cx43 (van Kempen et al. 1991; Velde et al. 1995) was expressed significantly lower than in neonatal and adult heart. Common to all Cx isoform expressions was their increase over the assessed time course (day 14 - day 21). In addition, myosin heavy chain (MHC) expression was increasing over time, with the adult isoform, i.e. α MHC (Lyons et al. 1990), being significantly higher expressed compared to the heart controls from day 21 on. Expression of the more immature isoform β -MHC was in between expression levels of neonatal and adult mouse heart. Significantly lower expression levels for type I and III collagens can be explained by the lack of fibroblasts in CBs, since these cells are the main contributors to extracellular matrix expression in the heart (Carver et al. 1991). Electrophysiological assessment of selected CMs revealed the presence of pacemaker-, ventricle-, atrial-, and purkinje-like action potentials (APs) and

responsiveness to cardioactive drugs as it was reported for other PSC-derived early CM populations (Guan et al. 2007; Mauritz et al. 2008).

In conclusion, although selected CMs do not fully resemble expression patterns of the native heart, they are functional in terms of contractility and excitability.

4.3.4 Fibroblasts support cardiac tissue formation

In line with previous reports, using pure single CM populations to generate cardiac tissue constructs (Shimko & W. C. Claycomb 2008; Liau et al. 2011) we were not able to generate functional actively contracting tissue, since the cells did not interconnect to form a functional syncytium. Instead, the cells kept a rounded shape and cellular activity was fading over time as indicated by TMRM fluorescence decrease (tested until day 7). However, when supplemented with γ -irradiated murine fetal fibroblasts (Fbs), tissue formed similarly to BCTs derived from neonatal rat cardiomyocytes (NRCMs) within the first days of culture (see manuscript 1). CM within these constructs remained viable and connected to some extent, but most of these approaches failed to generate forces comparable with BCTs generated with NRCM, which is in line with most of the data from reports using single cell CMs (Guo 2006; Tulloch et al. 2011). In contrast to the study of Liau and colleagues, supplementing their cardiac tissue constructs with rat ventricular fibroblasts, which might contain contaminating CMs contributing to force development (Liau et al. 2011), the fibroblast source used in the presented study did not lead to contractile tissue, when exclusively used for tissue preparation.

4.3.5 Cardiac bodies can be used directly to generate homogeneous and functional bioartificial cardiac tissue

To address the inadequate force generation of engineered constructs using single cell-based protocols, a novel strategy was assessed, i.e. direct application of undissociated CBs into BCT preparations. Similar to the single cell approach, the addition of γ -irradiated fetal murine Fb greatly enhanced tissue formation, however, survival and formation of a functional syncytium to some extent was also possible

with CBs only. All tested CB and Fb concentrations, i.e. 400 - 800 CB/BCT and 8 - 30% Fbs, resulted in contractile tissue formation. Since a concentration of 650 CBs / BCT supplemented with 10% fibroblasts in 220 μ l matrix was found to be optimal in terms of contractile force development (0.75 ± 0.17 mN) and exhibited rising force-length relationships reminiscent with the Frank-Starling mechanism of the heart, it was used for further experiments.

4.3.6 Morphology and contractility are positively affected by ascorbic acid-mediated changes in ECM organization of CB-based BCTs

To further enhance forces of CB-based tissue, ascorbic acid (AA) was added to BCT culture, since a positive effect of this supplement in terms of enhanced passive and active forces was detected in a previous study using NRCM BCTs (unpublished data). In the CB/Fb system, addition of AA resulted in significant broadening and increased alignment of type I collagen fibers within the tissue on day 21. This might be explained by its effects on collagen synthesis in terms of pro-collagen expression (Clark et al. 2002) and collagen post-transcriptional modification (Peterkofsky 1991). The effect of higher metabolic activity, indicated by a moderate, but not significant increase in TMRM fluorescence and the significantly higher titin fluorescence compared to the controls could be mediated by the radical scavenger effect of AA (Englard & Seiffter 1986). In addition, sarcomeric organization was enhanced and cell-cell contacts between cardiomyocytes were more prominent as determined by transmission electron microscopy (TEM). Contraction forces were significantly higher in AA treated groups compared to the controls when measured on day 14 and day 21. Differences between paced and spontaneous contraction forces, were significantly lower in tissues treated with AA, indication a more synchronized state of CB contractions within the BCTs. Enhanced mechanical interconnections between individual CBs might explain this observation, since passive forces were significantly higher in AA treated BCTs. These elevated forces are most probably conferred by the increased type I collagen deposition. In tissue constructs containing only Fbs as the main contributors to type I collagen deposition, similar strain dependent passive forces were observed, supporting this assumption.

4.3.7 CM orientation and maturation is mediated by increasing mechanical strain

Since application of the classical mechanic stimulus in cardiac tissue engineering, i.e. cyclic uniaxial stretch (Fink et al. 2000; Naito 2006; Guo 2006; Shimko & W. C. Claycomb 2008; Tulloch et al. 2011), did not lead to improvement in terms of morphology and contraction forces, another mechanical stimulus was applied to BCTs. We assumed the possibility to force CBs (and CMs within) from a rounded shape into an elongated shape, eventually resulting in improved and anisotropic CM orientation and organized contractility within BCTs. To this goal, we applied incremental growing stretch to BCTs from day 7 until day 21. Indeed, this novel stimulus resulted in elevated alignment of type I collagen fibers, significantly increased TMRM and titin fluorescence, similar to the effects observed for AA treated BCTs. Moreover, sarcomeres were significantly longer, which was not the case for AA stimulated BCTs, and laminin deposition was preferentially located at lateral CM membranes. However, in contrast to the chemical stimulus, mechanical conditioning neither increased type I collagen fiber width significantly, nor decreased the difference between paced and spontaneous contractions. Nevertheless, active contraction forces were elevated compared to controls, but less pronounced as in AA treated BCTs, whereas passive forces were higher when determined at L_{max} . Fb-only constructs treated in the same way showed similar stress/strain curves, yet to a higher extent. This indicates that the increase in collagen fiber alignment determined for mechanically stimulated BCTs is sufficient to greatly enhance passive forces in these constructs and largely depends on fibroblasts.

4.3.8 Combination of novel stimuli results in optimized functionality of miPSC-derived BCTs

After identifying effects of single treatments, a combination of both stimuli was applied. This revealed beneficial effects observed for each stimulus alone, but additional outcomes were also observed. These were: Increased collagen fiber width (chemical treatment) and alignment (chemical and mechanical treatment), TMRM and titin fluorescence intensities (chemical and mechanical treatment) and sarcomere

length (mechanical treatment), as well as for synchronized contractions (chemical treatment) and active and passive forces measured at L_{max} (chemical and mechanical stimulus). Compared to untreated controls, passive forces on day 21 were about three times higher (3.78 ± 0.65 vs. 11.92 ± 1.49 mN). In terms of contractile function, the additional effect of combined treatment was clearly detectable with the highest forces measured in this study (1.22 ± 0.13 on d14 and 1.42 ± 0.09 mN on day 21). Compared to untreated controls on day 21 (0.75 ± 0.06 mN) active forces almost doubled. Combined treatment also resulted in the highest passive forces in Fb-only constructs.

In contrast to expression levels assessed for CBs, optimized iPSC BCTs showed expression levels for α -MHC, Cx40, Cx43, and type I collagen on day 21 comparable to those of neonatal mouse heart. Interestingly, without hypertrophic responses to mechanical load, which was detected for engineered cardiac tissue in own studies (see manuscript 1) and by others for uni-axial stretch (Naito 2006; Guo 2006; Shimko & W. C. Claycomb 2008). It is not clear whether this due to difference in the mode of stretch. Alternatively, this might be attributed to an immature phenotype of the miPSC-derived cardiomyocytes, since *in vivo* the occurrence of a developmental hypertrophy was reported only after postnatal day 5 (Leu et al. 2001). Similar differences in expression levels to neonatal heart as detected for CB were observed for β -MHC, type III collagen and Cx43, which was about tenfold less. Despite these differences in Cx43 expression, electrophysiological measurements of whole-mounted iPSC BCTs revealed, that coupling of CMs was not impaired and maybe compensated by other gap junctional proteins, e.g. Cx40 and Cx45. This was indicated by characteristic FP recordings over the whole array and a conduction velocity of 25 - 30 cm/s. Furthermore, responsiveness to the cardiotropic drugs isoproterenol, lidocaine and quinidine was detectable.

In conclusion, the following findings were described for the first time for PSC-derived myocardial tissue engineered constructs: 1. Successful cardiac tissue formation can be achieved from highly defined, autonomously contracting units, i.e. cardiac bodies (CBs) without disruption of pre-formed functional cell-cell contacts, in a Fb-dependent

manner. 2. Ascorbic acid greatly enhances tissue morphology and improves contractile function of cardiomyocytes. 3. Application of a novel mechanical stimulus, i.e. growing stretch, improves CM orientation and maturation dramatically.

Systolic forces of optimized murine iPSC-derived BCTs were about 17.5 - 23 times higher than described for human ESC-derived cardiac constructs using non-enriched CM populations (Tulloch et al. 2011; Schaaf et al. 2011). For selected murine ESC-derived CM-based constructs using ventricular Fbs as supplemental cell source, reported forces were in the same range (Liau et al. 2011). Although being an artificial system, presented miPSC BCTs might allow novel insights into cardiac tissue formation and maturation with potential impact on tissue engineering strategies. To address the issue of vascularization *in vitro*, effects of different cell types that showed beneficial effects could be tested in detail (Tulloch et al. 2011) (Mauritz et al. 2011). Furthermore, in terms of *in vitro* testing, this system might be a valuable tool for three-dimensional iPSC-based cardiac disease modeling, which has recently been shown in conventional cell culture (Moretti et al. 2010; Itzhaki et al. 2011).

Rapid progress in human PSC research, should lead to relevant CM-numbers to enable transfer of the herein described technology soon. Research concerning biocompatible matrices could also accelerate clinical application.

5 References

- Adhikary, S. & Eilers, M., 2005. Transcriptional regulation and transformation by Myc proteins. *Nature Reviews Molecular Cell Biology*, 6(8), pp.635–645.
- Adler, C.P., 1975. Relationship between deoxyribonucleic acid content and nucleoli in human heart muscle cells and estimation of cell number during cardiac growth and hyperfunction. *Recent advances in studies on cardiac structure and metabolism*, 8, pp.373–386.
- Adler, C.P. & Friedburg, H., 1986. Myocardial DNA content, ploidy level and cell number in geriatric hearts: post-mortem examinations of human myocardium in old age. *Journal of molecular and cellular cardiology*, 18(1), pp.39–53.
- Akhyari, P. et al., 2002. Mechanical stretch regimen enhances the formation of bioengineered autologous cardiac muscle grafts. *Circulation*, 106(12 Suppl 1), pp.1137–42.
- Akins, R.E. et al., 1999. Cardiac Organogenesis in Vitro: Reestablishment of Three-Dimensional Tissue Architecture by Dissociated Neonatal Rat Ventricular Cells. *Tissue Engineering*, 5(2), pp.103–118.
- Andersen, D., Andersen, P. & Schneider, M., 2009. Murine “Cardiospheres” Are Not a Source of Stem Cells with Cardiomyogenic Potential - Andersen - 2009 - STEM CELLS - Wiley Online Library. *Stem*
- Arking, D.E. & Chakravarti, A., 2009. Understanding cardiovascular disease through the lens of genome-wide association studies. *Trends in Genetics*, 25(9), pp.387–394.
- Atala, A. et al., 2006. Tissue-engineered autologous bladders for patients needing cystoplasty. *Lancet*, 367(9518), pp.1241–1246.
- Bar, A. et al., 2010. The pro-angiogenic factor CCN1 enhances the re-endothelialization of biological vascularized matrices in vitro. *Cardiovascular Research*, 85(4), pp.806–813.
- Barash, Y. et al., 2010. Electric Field Stimulation Integrated into Perfusion Bioreactor for Cardiac Tissue Engineering. *Tissue Engineering Part C: Methods*, 16(6), pp.1417–1426.
- Barnard, C.N., 1967. The operation. A human cardiac transplant: an interim report of a successful operation performed at Groote Schuur Hospital, Cape Town. *South African medical journal = Suid-Afrikaanse tydskrif vir geneeskunde*, 41(48), pp.1271–1274.
- Baum, C., 2004. Chance or necessity? Insertional Mutagenesis in Gene Therapy and Its Consequences. *Molecular Therapy*, 9(1), pp.5–13.

- Beltrami, A.P. et al., 2003. Adult cardiac stem cells are multipotent and support myocardial regeneration. *Cell*, 114(6), pp.763–776.
- Bergmann, O. et al., 2009. Evidence for Cardiomyocyte Renewal in Humans. *Science*, 324(5923), pp.98–102.
- Bersell, K. et al., 2009. Neuregulin1/ErbB4 Signaling Induces Cardiomyocyte Proliferation and Repair of Heart Injury--multipart-boundary Content-Type: application/pdf Range: bytes 1915208-1921073/1929004. *Cell*, 138(2), pp.257–270.
- Bhana, B. et al., 2010. Influence of substrate stiffness on the phenotype of heart cells. *Biotechnology and Bioengineering*, 105(6), pp.1148–1160.
- Birla, R. & Borschel, G., 2005. In Vivo Conditioning of Tissue-engineered Heart Muscle Improves Contractile Performance - Birla - 2005 - Artificial Organs - Wiley Online Library. *Artificial organs*.
- Birla, R.K., Huang, Y.C. & Dennis, R.G., 2007. Development of a Novel Bioreactor for the Mechanical Loading of Tissue-Engineered Heart Muscle. *Tissue Engineering*, 13(9), pp.2239–2248.
- Biryukova, E. et al., 2010. Comparison of mid-term outcome in patients with three-vessel and/or left main disease undergoing percutaneous coronary intervention and coronary artery bypass graft surgery. *European journal of cardio-thoracic surgery : official journal of the European Association for Cardio-thoracic Surgery*, 37(4), pp.905–911.
- Blan, N.R. & Birla, R.K., 2008. Design and fabrication of heart muscle using scaffold-based tissue engineering. *Journal of Biomedical Materials Research Part A*, 86A(1), pp.195–208.
- Blusch, J.H., Patience, C. & Martin, U., 2002. Pig endogenous retroviruses and xenotransplantation. *Xenotransplantation*, 9(4), pp.242–251.
- BMBF, 2011. BMBF › Forschung › Das Stammzellgesetz. pp.1–2. Available at: [Accessed October 16, 2011].
- BMBF, 2004. Gesetz zur Sicherstellung des Embryonenschutzes im Zusammenhang mit Einfuhr und Verwendung menschlicher embryonaler Stammzelle. pp.1–3.
- Brooks, W.W. & Conrad, C.H., 1999. Differences between mouse and rat myocardial contractile responsiveness to calcium. *Comparative biochemistry and physiology. Part A, Molecular & integrative physiology*, 124(2), pp.139–147.
- Brown, M.A., Iyer, R.K. & Radisic, M., 2008. Pulsatile perfusion bioreactor for cardiac tissue engineering. *Biotechnology progress*, 24(4), pp.907–920.

- Burridge, P.W. et al., 2011. A universal system for highly efficient cardiac differentiation of human induced pluripotent stem cells that eliminates interline variability. *PLoS ONE*, 6(4), p.e18293.
- Carver, W. et al., 1991. Collagen expression in mechanically stimulated cardiac fibroblasts. *Circulation research*, 69(1), pp.116–122.
- Caspi, O. et al., 2009. In vitro electrophysiological drug testing using human embryonic stem cell derived cardiomyocytes. *Stem Cells and Development*, 18(1), pp.161–172.
- Cibelli, J.B. et al., 2002. Parthenogenetic stem cells in nonhuman primates. *Science*, 295(5556), p.819.
- Clark, A.G. et al., 2002. The effects of ascorbic acid on cartilage metabolism in guinea pig articular cartilage explants. *Matrix biology*, 21(2), pp.175–184.
- Claycomb, W. & Lanson, N., 1998. HL-1 cells: A cardiac muscle cell line that contracts and retains phenotypic characteristics of the adult cardiomyocyte. In *Proceedings of the Proceedings of the*
- Conrad, S. et al., 2008. Generation of pluripotent stem cells from adult human testis. *Nature*, 456(7220), pp.344–349.
- Crutchley, R., 2002. ScienceDirect - Coordination Chemistry Reviews : Photosensitized singlet oxygen and its applications. *Coordination Chemistry Reviews*.
- Dai, Y. et al., 2002. Targeted disruption of the alpha1, 3-galactosyltransferase gene in cloned pigs. *Nature*.
- David, L. et al., 2011a. Looking into the Black Box: Insights into the Mechanisms of Somatic Cell Reprogramming. *Genes*, 2(1), pp.81–106.
- David, R. et al., 2011b. Induction of MesP1 by Brachyury(T) generates the common multipotent cardiovascular stem cell. *Cardiovascular Research*.
- Davis, D.R., Ruckdeschel Smith, R. & Marbán, E., 2010. Human cardiospheres are a source of stem cells with cardiomyogenic potential. *Stem Cells*, 28(5), pp.903–904.
- Denk, W., Strickler, J. & Webb, W., 1990. Two-photon laser scanning fluorescence microscopy. *Science*, 248(4951), pp.73–76.
- Dickstein, K. et al., 2008. ESC Guidelines for the diagnosis and treatment of acute and chronic heart failure 2008: The Task Force for the Diagnosis and Treatment of Acute and Chronic Heart Failure 2008 of the European Society of Cardiology. Developed in collaboration with the Heart Failure Association of the ESC (HFA)

- and endorsed by the European Society of Intensive Care Medicine (ESICM). *European Heart Journal*, 29(19), pp.2388–2442.
- Doesch, A.O. et al., 2010. Malignancies After Heart Transplantation: Incidence, Risk Factors, and Effects of Calcineurin Inhibitor Withdrawal. *TPS*, 42(9), pp.3694–3699.
- Doetschman, T.C. et al., 1985. The in vitro development of blastocyst-derived embryonic stem cell lines: formation of visceral yolk sac, blood islands and myocardium. *Journal of embryology and experimental morphology*, 87, pp.27–45.
- Dorling, A., 2002. Clinical Xenotransplantation: Pigs Might Fly? - Dorling - 2002 - American Journal of Transplantation - Wiley Online Library. *American Journal of Transplantation*.
- Dow, J. et al., 2005. Washout of transplanted cells from the heart: a potential new hurdle for cell transplantation therapy. *Cardiovascular Research*, 67(2), pp.301–307.
- Dowell, J.D. et al., 2003. Myocyte and myogenic stem cell transplantation in the heart. *Cardiovascular Research*, 58(2), pp.336–350.
- Eghbali, M. & Weber, K.T., 1990. Collagen and the myocardium: fibrillar structure, biosynthesis and degradation in relation to hypertrophy and its regression. *Molecular and cellular biochemistry*, 96(1), pp.1–14.
- Eisen, H.J., 2008. Skeletal myoblast transplantation: no MAGIC bullet for ischemic cardiomyopathy. *Nature clinical practice. Cardiovascular medicine*, 5(9), pp.520–521.
- Elbjeirami, W.M. et al., 2003. Enhancing mechanical properties of tissue-engineered constructs via lysyl oxidase crosslinking activity. *Journal of Biomedical Materials Research Part A*, 66(3), pp.513–521.
- Engel, F.B. et al., 2006. FGF1/p38 MAP kinase inhibitor therapy induces cardiomyocyte mitosis, reduces scarring, and rescues function after myocardial infarction. *Proceedings of the National Academy of Sciences of the United States of America*, 103(42), pp.15546–15551.
- Englard, S. & Seifter, S., 1986. The biochemical functions of ascorbic acid. *Annual review of nutrition*, 6(1), pp.365–406.
- Eschenhagen, T., 2011. The beat goes on: human heart muscle from pluripotent stem cells. *Circulation research*, 109(1), pp.2–4.
- Eschenhagen, T. et al., 1997. Three-dimensional reconstitution of embryonic cardiomyocytes in a collagen matrix: a new heart muscle model system. *The*

- FASEB journal : official publication of the Federation of American Societies for Experimental Biology*, 11(8), pp.683–694.
- Eurotransplant International Foundation, 2011. *Annual Report 2010*,
- Evans, M.J. & Kaufman, M.H., 1981. Establishment in culture of pluripotential cells from mouse embryos. *Nature*, 292(5819), pp.154–156.
- Field, L.J., 1988. Atrial natriuretic factor-SV40 T antigen transgenes produce tumors and cardiac arrhythmias in mice. *Science*, 239(4843), pp.1029–1033.
- Fink, C. et al., 2000. Chronic stretch of engineered heart tissue induces hypertrophy and functional improvement. *The FASEB journal : official publication of the Federation of American Societies for Experimental Biology*, 14(5), pp.669–679.
- Fomovsky, G.M. et al., 2011. Model-based design of mechanical therapies for myocardial infarction. *Journal of cardiovascular translational research*, 4(1), pp.82–91.
- Formigli, L. et al., 2010. Skeletal myoblasts for heart regeneration and repair: state of the art and perspectives on the mechanisms for functional cardiac benefits. *Current pharmaceutical design*, 16(8), pp.915–928.
- Frank, D. et al., 2007. Gene Expression Pattern in Biomechanically Stretched Cardiomyocytes.
- Fukushima, S., Varela-Carver, A. & Coppen, S., 2007. Direct intramyocardial but not intracoronary injection of bone marrow cells induces ventricular arrhythmias in a rat chronic ischemic heart failure model. *Circulation*.
- Furuta, A. et al., 2006. Pulsatile cardiac tissue grafts using a novel three-dimensional cell sheet manipulation technique functionally integrates with the host heart, in vivo. *Circulation research*, 98(5), pp.705–712.
- Fuster, V. et al., 2001. ACC/AHA/ESC Guidelines for the Management of Patients With Atrial Fibrillation: Executive Summary A Report of the American College of Cardiology/American Heart Association Task Force on Practice Guidelines and the European Society of Cardiology Committee for Practice Guidelines and Policy Conferences (Committee to Develop Guidelines for the Management of Patients With Atrial Fibrillation) Developed in Collaboration With the North American Society of Pacing and Electrophysiology. *Circulation*, 104(17), pp.2118–2150.
- Gerecht-Nir, S. et al., 2006. Biophysical regulation during cardiac development and application to tissue engineering. *The International Journal of Developmental Biology*, 50(2-3), pp.233–243.
- Gerecht-Nir, S. et al., 2004. Three-dimensional porous alginate scaffolds provide a

- conductive environment for generation of well-vascularized embryoid bodies from human embryonic stem cells. *Biotechnology and Bioengineering*, 88(3), pp.313–320.
- Giraud, M.-N. et al., 2007. Current State of the Art in Myocardial Tissue Engineering. *Tissue Engineering*, 13(8), pp.1825–1836.
- Gruene, M. et al., 2011. Laser printing of three-dimensional multicellular arrays for studies of cell-cell and cell-environment interactions. *Tissue Engineering Part C: Methods*, 17(10), pp.973–982.
- Gruh, I. et al., 2006. No evidence of transdifferentiation of human endothelial progenitor cells into cardiomyocytes after coculture with neonatal rat cardiomyocytes. *Circulation*, 113(10), pp.1326–1334.
- Guan, K. et al., 2007. Generation of functional cardiomyocytes from adult mouse spermatogonial stem cells. *Circulation research*, 100(11), pp.1615–1625.
- Guan, K. et al., 2006. Pluripotency of spermatogonial stem cells from adult mouse testis. *Nature Cell Biology*, 440(7088), pp.1199–1203.
- Guo, X.M., 2006. Creation of Engineered Cardiac Tissue In Vitro From Mouse Embryonic Stem Cells. *Circulation*, 113(18), pp.2229–2237.
- Haase, A. et al., 2009. Generation of Induced Pluripotent Stem Cells from Human Cord Blood. *Stem Cell*, 5(4), pp.434–441.
- Han, Y.S. & Ogut, O., 2010. Regulation of fibre contraction in a rat model of myocardial ischemia. *PLoS ONE*, 5(3), p.e9528.
- Hansen, A. et al., 2010. Development of a drug screening platform based on engineered heart tissue. *Circulation research*, 107(1), pp.35–44.
- Hassink, R.J. et al., 2008. Cardiomyocyte cell cycle activation improves cardiac function after myocardial infarction. *Cardiovascular Research*, 78(1), pp.18–25.
- Hata, H. et al., 2010. Engineering a novel three-dimensional contractile myocardial patch with cell sheets and decellularised matrix. *European journal of cardio-thoracic surgery : official journal of the European Association for Cardio-thoracic Surgery*, pp.1–6.
- Hattori, F. et al., 2009. Nongenetic method for purifying stem cell-derived cardiomyocytes. *Nature Methods*, 7(1), pp.61–66.
- He, K.-L. et al., 2005. Autologous skeletal myoblast transplantation improved hemodynamics and left ventricular function in chronic heart failure dogs. *The Journal of heart and lung transplantation : the official publication of the International Society for Heart Transplantation*, 24(11), pp.1940–1949.

- He, Z. et al., 2011. Transduction of Wnt11 promotes mesenchymal stem cell transdifferentiation into cardiac phenotypes. *Stem Cells and Development*, 20(10), pp.1771–1778.
- Hentze, H. et al., 2009. Teratoma formation by human embryonic stem cells: Evaluation of essential parameters for future safety studies. *Stem Cell Research*, 2(3), pp.198–210.
- Hoffman, J.I.E., 1995. Incidence of congenital heart disease: I. Postnatal incidence. *Pediatric Cardiology*, 16(3), pp.103–113.
- Honda, A. et al., 2010. Generation of induced pluripotent stem cells in rabbits: potential experimental models for human regenerative medicine. *Journal of Biological Chemistry*, 285(41), pp.31362–31369.
- Horch, R.E. et al., 2005. Tissue engineering of cultured skin substitutes. *Journal of Cellular and Molecular Medicine*, 9(3), pp.592–608.
- Hořková, L. et al., 2008. Ischaemic heart disease is a risk factor for renal failure after heart transplantation. *International Journal of Cardiology*, 123(3), pp.358–360.
- Hunziker, E. et al., 2006. Translation from research to applications. *Tissue*
- Hwang, C.W., Wu, D. & Edelman, E.R., 2001. Physiological transport forces govern drug distribution for stent-based delivery. *Circulation*, 104(5), pp.600–605.
- Hwang, W.S., 2004. Evidence of a Pluripotent Human Embryonic Stem Cell Line Derived from a Cloned Blastocyst. *Science*, 303(5664), pp.1669–1674.
- Ieda, M. et al., 2010. Direct reprogramming of fibroblasts into functional cardiomyocytes by defined factors. *Cell*, 142(3), pp.375–386.
- Itzhaki, I. et al., 2011. Modelling the long QT syndrome with induced pluripotent stem cells. *Nature*, 471(7337), pp.225–229.
- Izumo, S., Nadal-Ginard, B. & Mahdavi, V., 1988. Protooncogene induction and reprogramming of cardiac gene expression produced by pressure overload. *Proceedings of the National Academy of Sciences of the United States of America*, 85(2), pp.339–343.
- Jacot, J.G., McCulloch, A.D. & Omens, J.H., 2008. Substrate stiffness affects the functional maturation of neonatal rat ventricular myocytes. *Biophysical journal*, 95(7), pp.3479–3487.
- Jakab, K. et al., 2008. Tissue Engineering by Self-Assembly of Cells Printed into Topologically Defined Structures. *Tissue Engineering Part A*, 14(3), pp.413–421.
- Jayakrishnan, A. & Jameela, S.R., 1996. Glutaraldehyde as a fixative in

- bioprostheses and drug delivery matrices. *Biomaterials*, 17(5), pp.471–484.
- Jincho, Y. et al., 2010. Generation of genome integration-free induced pluripotent stem cells from fibroblasts of C57BL/6 mice without c-Myc transduction. *Journal of Biological Chemistry*, 285(34), pp.26384–26389.
- Kaplan, G., 1993. Socioeconomic factors and cardiovascular disease: a review of the literature. *Circulation*.
- Kattman, S.J. et al., 2011. Stage-specific optimization of activin/nodal and BMP signaling promotes cardiac differentiation of mouse and human pluripotent stem cell lines. *Cell Stem Cell*, 8(2), pp.228–240.
- Kattman, S.J., Huber, T.L. & Keller, G.M., 2006. Multipotent flk-1+ cardiovascular progenitor cells give rise to the cardiomyocyte, endothelial, and vascular smooth muscle lineages. *Developmental Cell*, 11(5), pp.723–732.
- Kehat, I., 2001. Human embryonic stem cells can differentiate into myocytes with structural and functional properties of cardiomyocytes. *Journal of Clinical Investigation*, 108(3), pp.407–414.
- Kennedy, D., 2006. Editorial Retraction. *Science*, 311(5759), pp.335b–335b.
- Kikuchi, K. et al., 2010. Primary contribution to zebrafish heart regeneration by gata4+ cardiomyocytes. *Nature*, 464(7288), pp.601–605.
- Kim, B.S. & Mooney, D.J., 2000. Scaffolds for engineering smooth muscle under cyclic mechanical strain conditions. *Journal of biomechanical engineering*, 122(3), pp.210–215.
- Kleinman, H.K. et al., 1986. Basement membrane complexes with biological activity. *Biochemistry*, 25(2), pp.312–318.
- Klug, M.G. et al., 1996. Genetically selected cardiomyocytes from differentiating embryonic stem cells form stable intracardiac grafts. *Journal of Clinical Investigation*, 98(1), pp.216–224.
- Ko, K. et al., 2010. Human adult germline stem cells in question. *Nature*, 465(7301), pp.E1; discussion E3.
- Kobashigawa, J.A. & Patel, J.K., 2006. Immunosuppression for heart transplantation: where are we now? *Nature clinical practice. Cardiovascular medicine*, 3(4), pp.203–212.
- Kolossov, E. et al., 2006. Engraftment of engineered ES cell-derived cardiomyocytes but not BM cells restores contractile function to the infarcted myocardium. *Journal of Experimental Medicine*, 203(10), pp.2315–2327.

- Komuro, I. & Yazaki, Y., 1993. Control of Cardiac Gene Expression by Mechanical Stress. *Annual Review of Physiology*, 55(1), pp.55–75.
- Koo, J. et al., 2005. Patient-Specific Embryonic Stem Cells Derived from Human SCNT Blastocysts. *Science*.
- Korf-Klingebiel, M. et al., 2011. Conditional transgenic expression of fibroblast growth factor 9 in the adult mouse heart reduces heart failure mortality after myocardial infarction. *Circulation*, 123(5), pp.504–514.
- König, K., 2000. Multiphoton microscopy in life sciences. *Journal of microscopy*, 200(2), pp.83–104.
- König, K. et al., 1999. Intracellular nanosurgery with near infrared femtosecond laser pulses. *Cellular and molecular biology (Noisy-le-Grand, France)*, 45(2), pp.195–201.
- Kreutziger, K.L. & Murry, C.E., 2011. Engineered Human Cardiac Tissue. *Pediatric Cardiology*, 32(3), pp.334–341.
- Kuetemeyer, K. et al., 2010. Influence of laser parameters and staining on femtosecond laser-based intracellular nanosurgery. *Biomedical optics express*, 1(2), pp.587–597.
- Kühn, B. et al., 2007. Periostin induces proliferation of differentiated cardiomyocytes and promotes cardiac repair. *Nature Medicine*, 13(8), pp.962–969.
- Laflamme, M.A. & Murry, C.E., 2011. Heart regeneration. *Nature*, 473(7347), pp.326–335.
- Laflamme, M.A. et al., 2007. Cardiomyocytes derived from human embryonic stem cells in pro-survival factors enhance function of infarcted rat hearts. *Nature Biotechnology*, 25(9), pp.1015–1024.
- Lahpor, J. et al., 2009. European results with a continuous-flow ventricular assist device for advanced heart-failure patients☆. *European Journal of Cardio-Thoracic Surgery*.
- Lancaster, J. et al., 2010. Viable fibroblast matrix patch induces angiogenesis and increases myocardial blood flow in heart failure after myocardial infarction. *Tissue Engineering Part A*, 16(10), pp.3065–3073.
- Laugwitz, K.-L. et al., 2005. Postnatal isl1+ cardioblasts enter fully differentiated cardiomyocyte lineages. *Nature*, 433(7026), pp.647–653.
- Leikin, S., Rau, D.C. & Parsegian, V.A., 1994. Direct measurement of forces between self-assembled proteins: temperature-dependent exponential forces between collagen triple helices. *Proceedings of the National Academy of Sciences of the*

- United States of America*, 91(1), pp.276–280.
- Leobon, B. et al., 2003. Myoblasts transplanted into rat infarcted myocardium are functionally isolated from their host. *Proceedings of the National Academy of Sciences of the United States of America*, 100(13), pp.7808–7811.
- Leu, M., Ehler, E. & Perriard, J.C., 2001. Characterisation of postnatal growth of the murine heart. *Anatomy and embryology*, 204(3), pp.217–224.
- Li, R., Mickle, D. & Weisel, R., 1996. Human pediatric and adult ventricular cardiomyocytes in culture: assessment of phenotypic changes with passaging. *Cardiovascular*
- Liau, B. et al., 2011. Pluripotent stem cell-derived cardiac tissue patch with advanced structure and function. *Biomaterials*, pp.1–8.
- Lin, S.S. et al., 1998. The role of antibodies in acute vascular rejection of pig-to-baboon cardiac transplants. *Journal of Clinical Investigation*, 101(8), pp.1745–1756.
- Lorbeer, R.-A. et al., 2011. Highly efficient 3D fluorescence microscopy with a scanning laser optical tomograph. *Optics express*, 19(6), pp.5419–5430.
- Lyons, G.E. et al., 1990. Developmental regulation of myosin gene expression in mouse cardiac muscle. *The Journal of Cell Biology*, 111(6), p.2427.
- Maidhof, R. et al., 2011. Biomimetic perfusion and electrical stimulation applied in concert improved the assembly of engineered cardiac tissue. *Journal of Tissue Engineering and Regenerative Medicine*.
- Mann, B. & Schmedlen, R., 2001. Tethered-TGF- β increases extracellular matrix production of vascular smooth muscle cells. *Biomaterials*.
- Marsano, A. et al., 2010. Scaffold stiffness affects the contractile function of three-dimensional engineered cardiac constructs. *Biotechnology progress*, 26(5), pp.1382–1390.
- Martens, A. et al., 2011. Rhesus monkey cardiosphere-derived cells for myocardial restoration. *Cytotherapy*, 13(7), pp.864–872.
- Martin, G., 1981. Isolation of a pluripotent cell line from early mouse embryos cultured in medium conditioned by teratocarcinoma stem cells. In *Proceedings of the National Academy of* Proceedings of the National Academy of
- Martin, U. et al., 2000. Productive infection of primary human endothelial cells by pig endogenous retrovirus (PERV). *Xenotransplantation*, 7(2), pp.138–142.
- Martin-Rendon, E. et al., 2008. Autologous bone marrow stem cells to treat acute

- myocardial infarction: a systematic review. *European Heart Journal*, 29(15), pp.1807–1818.
- Mauritz, C. et al., 2008. Generation of Functional Murine Cardiac Myocytes From Induced Pluripotent Stem Cells. *Circulation*, 118(5), pp.507–517.
- Mauritz, C. et al., 2011. Induced pluripotent stem cell (iPSC)-derived Flk-1 progenitor cells engraft, differentiate, and improve heart function in a mouse model of acute myocardial infarction. *European Heart Journal*.
- McCall, A.S. et al., 2010. Mechanisms of corneal tissue cross-linking in response to treatment with topical riboflavin and long-wavelength ultraviolet radiation (UVA). *Investigative ophthalmology & visual science*, 51(1), pp.129–138.
- Mertsching, H. et al., 2005. Engineering of a vascularized scaffold for artificial tissue and organ generation. *Biomaterials*, 26(33), pp.6610–6617.
- Messina, E., 2004. Isolation and Expansion of Adult Cardiac Stem Cells From Human and Murine Heart. *Circulation research*, 95(9), pp.911–921.
- Mirotsov, M. et al., 2007. Secreted frizzled related protein 2 (Sfrp2) is the key Akt-mesenchymal stem cell-released paracrine factor mediating myocardial survival and repair. *Proceedings of the National Academy of Sciences*, 104(5), pp.1643–1648.
- Moreno-Borchart, A., 2004. Building organs piece by piece. Accomplishments and future perspectives in tissue engineering. *EMBO Reports*, 5(11), pp.1025–1028.
- Moretti, A. et al., 2010. Patient-specific induced pluripotent stem-cell models for long-QT syndrome. *The New England journal of medicine*, 363(15), pp.1397–1409.
- Möller, L. et al., 2011. Preparation and evaluation of hydrogel-composites from methacrylated hyaluronic acid, alginate, and gelatin for tissue engineering. *The International journal of artificial organs*, 34(2), pp.93–102.
- Murry, C.E. et al., 2004. Haematopoietic stem cells do not transdifferentiate into cardiac myocytes in myocardial infarcts. *Nature Cell Biology*, 428(6983), pp.664–668.
- Murry, C.E., Reinecke, H. & Pabon, L.M., 2006. Regeneration gaps: observations on stem cells and cardiac repair. *Journal of the American College of Cardiology*, 47(9), pp.1777–1785.
- Na, J. et al., 2010. Molecular mechanisms of pluripotency and reprogramming. *Stem cell research & therapy*, 1(4), p.33.
- Nagata, M. et al., 2003. Efficient gene transfer of a simian immuno-deficiency viral vector into cardiomyocytes derived from primate embryonic stem cells. *The*

- journal of gene medicine*, 5(11), pp.921–928.
- Naito, H., 2006. Optimizing Engineered Heart Tissue for Therapeutic Applications as Surrogate Heart Muscle. *Circulation*, 114(1_suppl), pp.I–72–I–78.
- Nottle, M.B. et al., 2007. Production of homozygous alpha-1,3-galactosyltransferase knockout pigs by breeding and somatic cell nuclear transfer. *Xenotransplantation*, 14(4), pp.339–344.
- Nussbaum, J. et al., 2007. Transplantation of undifferentiated murine embryonic stem cells in the heart: teratoma formation and immune response. *The FASEB Journal*, 21(7), pp.1345–1357.
- Nygren, J.M. et al., 2004. Bone marrow-derived hematopoietic cells generate cardiomyocytes at a low frequency through cell fusion, but not transdifferentiation. *Nature Medicine*, 10(5), pp.494–501.
- Oberpriller, J., 1974. Response of the adult newt ventricle to injury. *Journal of Experimental ...*
- Okano, T. et al., 1993. A novel recovery system for cultured cells using plasma-treated polystyrene dishes grafted with poly(N-isopropylacrylamide). *Journal of Biomedical Materials Research Part A*, 27(10), pp.1243–1251.
- Okita, K., Nakagawa, M., Hyenjong, H., Ichisaka, T. & Yamanaka, S., 2008a. Generation of mouse induced pluripotent stem cells without viral vectors. *Science*, 322(5903), pp.949–953.
- Okita, K., Nakagawa, M., Hyenjong, H., Ichisaka, T. & Yamanaka, S., 2008b. Generation of Mouse Induced Pluripotent Stem Cells Without Viral Vectors. *Science*, 322(5903), pp.949–953.
- Olivetti, G., Melissari, M. & Capasso, J., 1991. Cardiomyopathy of the aging human heart. Myocyte loss and reactive cellular hypertrophy. *Circulation research*.
- Orlic, D. et al., 2001. Bone marrow cells regenerate infarcted myocardium. *Nature*, 410(6829), pp.701–705.
- Ott, H.C. et al., 2008. Perfusion-decellularized matrix: using nature's platform to engineer a bioartificial heart. *Nature Medicine*, 14(2), pp.213–221.
- Peterkofsky, B., 1991. Ascorbate requirement for hydroxylation and secretion of procollagen: relationship to inhibition of collagen synthesis in scurvy. *The American journal of clinical nutrition*, 54(6), p.1135S.
- Poirier, P. et al., 2006. Obesity and cardiovascular disease: pathophysiology, evaluation, and effect of weight loss: an update of the 1997 American Heart Association Scientific Statement on Obesity and Heart Disease from the Obesity

- Committee of the Council on Nutrition, Physical Activity, and Metabolism. In *Circulation*. *Circulation*. pp. 898–918.
- Porrello, E.R. et al., 2011. Transient Regenerative Potential of the Neonatal Mouse Heart. *Science*, 331(6020), pp.1078–1080.
- Poss, K.D., 2002. Heart Regeneration in Zebrafish. *Science*, 298(5601), pp.2188–2190.
- Qiao, H. et al., 2009. Death and Proliferation Time Course of Stem Cells Transplanted in the Myocardium. *Molecular Imaging and Biology*, 11(6), pp.408–414.
- Radisic, M. et al., 2006. Biomimetic approach to cardiac tissue engineering: oxygen carriers and channeled scaffolds. *Tissue Engineering*, 12(8), pp.2077–2091.
- Radisic, M. et al., 2007. Biomimetic approach to cardiac tissue engineering. *Philosophical Transactions of the Royal Society B: Biological Sciences*, 362(1484), pp.1357–1368.
- Radisic, M. et al., 2004. Functional assembly of engineered myocardium by electrical stimulation of cardiac myocytes cultured on scaffolds. *Proceedings of the National Academy of Sciences of the United States of America*, 101(52), pp.18129–18134.
- Rihal, C.S. et al., 2003. Indications for coronary artery bypass surgery and percutaneous coronary intervention in chronic stable angina: review of the evidence and methodological considerations. *Circulation*, 108(20), pp.2439–2445.
- Ringeisen, B.R. et al., 2004. Laser printing of pluripotent embryonal carcinoma cells. *Tissue Engineering*, 10(3-4), pp.483–491.
- Robertson, E. & Evans, M., 1983. X-chromosome instability in pluripotential stem cell lines derived from parthenogenetic embryos. *Journal of embryology and*
- Roeder, B.A. et al., 2002. Tensile mechanical properties of three-dimensional type I collagen extracellular matrices with varied microstructure. *Journal of biomechanical engineering*, 124(2), pp.214–222.
- Rose, R.A., Jiang, H., et al., 2008a. Bone marrow-derived mesenchymal stromal cells express cardiac-specific markers, retain the stromal phenotype, and do not become functional cardiomyocytes in vitro. *Stem Cells*, 26(11), pp.2884–2892.
- Rose, R.A., Keating, A. & Backx, P.H., 2008b. Do Mesenchymal Stromal Cells Transdifferentiate Into Functional Cardiomyocytes? *Circulation research*, 103(9), pp.e120–e120.

- Roura, S. et al., 2010. Exposure to cardiomyogenic stimuli fails to transdifferentiate human umbilical cord blood-derived mesenchymal stem cells. *Basic research in cardiology*, 105(3), pp.419–430.
- Roussel, J.C. et al., 2008. Outcome of Heart Transplants 15 to 20 Years Ago: Graft Survival, Post-transplant Morbidity, and Risk Factors for Mortality. *The Journal of Heart and Lung Transplantation*, 27(5), pp.486–493.
- Rumyantsev, P.P., 1991. *Growth and Hyperplasia of Cardiac Muscle Cells*, Harwood Academic.
- Rust, W., Balakrishnan, T. & Zweigerdt, R., 2009. Cardiomyocyte enrichment from human embryonic stem cell cultures by selection of ALCAM surface expression. *Regenerative Medicine*, 4(2), pp.225–237.
- Salameh, A., Karl, S., et al., 2010a. Opposing and synergistic effects of cyclic mechanical stretch and α - or β -adrenergic stimulation on the cardiac gap junction protein Cx43. *Pharmacological Research*, 62(6), pp.506–513.
- Salameh, A., Wustmann, A., et al., 2010b. Cyclic mechanical stretch induces cardiomyocyte orientation and polarization of the gap junction protein connexin43. *Circulation research*, 106(10), pp.1592–1602.
- Schaaf, S. et al., 2011. Human engineered heart tissue as a versatile tool in basic research and preclinical toxicology. *PLoS ONE*, 6(10), p.e26397.
- Scholer, H.R. et al., 1990. Oct-4: a germline-specific transcription factor mapping to the mouse t-complex. *The EMBO journal*, 9(7), pp.2185–2195.
- Schwanke, K. et al., 2006. Generation and Characterization of Functional Cardiomyocytes from Rhesus Monkey Embryonic Stem Cells. *Stem Cells*, 24(6), pp.1423–1432.
- Schwartz, A.R. et al., 2003. Toward a causal model of cardiovascular responses to stress and the development of cardiovascular disease. *Psychosomatic medicine*, 65(1), pp.22–35.
- Sekine, H. et al., 2011. Cardiac Cell Sheet Transplantation Improves Damaged Heart Function via Superior Cell Survival in Comparison with Dissociated Cell Injection. *Tissue Engineering Part A*, 17(23-24), pp.2973–2980.
- Serruys, P. & Kutryk, M., 2006. Coronary-Artery Stents — NEJM. *New England Journal of*
- Serruys, P., Unger, F. & Sousa, J., 2001. Comparison of Coronary-Artery Bypass Surgery and Stenting for the Treatment of Multivessel Disease — NEJM. ... *England Journal of*

- Sharma, A. et al., 2003. Pig cells that lack the gene for [alpha]1-3 galactosyltransferase express low levels of the gal antigen. *Transplantation*, 75(4), p.430.
- Shevchenko, R.V., James, S.L. & James, S.E., 2010. A review of tissue-engineered skin bioconstructs available for skin reconstruction. *Journal of the Royal Society, Interface / the Royal Society*, 7(43), pp.229–258.
- Shimizu, T. et al., 2003. Cell sheet engineering for myocardial tissue reconstruction. *Biomaterials*, 24(13), pp.2309–2316.
- Shimizu, T. et al., 2002. Fabrication of Pulsatile Cardiac Tissue Grafts Using a Novel 3-Dimensional Cell Sheet Manipulation Technique and Temperature-Responsive Cell Culture Surfaces. *Circulation*.
- Shimko, V.F. & Claycomb, W.C., 2008. Effect of Mechanical Loading on Three-Dimensional Cultures of Embryonic Stem Cell-Derived Cardiomyocytes. *Tissue Engineering Part A*, 14(1), pp.49–58.
- Silva, J. et al., 2009. Nanog is the gateway to the pluripotent ground state. *Cell*, 138(4), pp.722–737.
- Smits, P.C. et al., 2003. Catheter-based intramyocardial injection of autologous skeletal myoblasts as a primary treatment of ischemic heart failure: clinical experience with six-month follow-up. *JAC*, 42(12), pp.2063–2069.
- Soonpaa, M.H. & Field, L.J., 1998. Survey of studies examining mammalian cardiomyocyte DNA synthesis. *Circulation research*, 83(1), pp.15–26.
- Spradling, A., Drummond-Barbosa, D. & Kai, T., 2001. Stem cells find their niche. *Nature*, 414(6859), pp.98–104.
- Sprangers, B., Waer, M. & Billiau, A.D., 2008. Xenotransplantation: where are we in 2008? *Kidney international*, 74(1), pp.14–21.
- Statistisches-Bundesamt-Deutschland, 2010: Herz-/Kreislaufferkrankungen verursachten rund 41 % aller Todesfälle. pp.1–2. Available at: [Accessed October 13, 2011].
- Steg, P.G., 2006. WEST: new data on the integration of early thrombolysis and mechanical intervention in the early management of STEMI. *European Heart Journal*, 27(13), pp.1511–1512.
- Stevens, K.R. et al., 2009. Physiological function and transplantation of scaffold-free and vascularized human cardiac muscle tissue. *Proceedings of the National Academy of Sciences*, 106(39), pp.16568–16573.
- Strüber, M. et al., 2009. The current status of heart transplantation and the

- development of "artificial heart systems". *Deutsches Ärzteblatt international*, 106(28-29), pp.471–477.
- Suemori, H. et al., 2001. Establishment of embryonic stem cell lines from cynomolgus monkey blastocysts produced by IVF or ICSI. *Developmental Dynamics*, 222(2), pp.273–279.
- Suzuki, K. et al., 2004. Role of interleukin-1beta in acute inflammation and graft death after cell transplantation to the heart. *Circulation*, 110(11 Suppl 1), pp.II219–24.
- Szmitko, P.E., 2003. Endothelial Progenitor Cells: New Hope for a Broken Heart. *Circulation*, 107(24), pp.3093–3100.
- Takahashi, K. & Yamanaka, S., 2006. Induction of Pluripotent Stem Cells from Mouse Embryonic and Adult Fibroblast Cultures by Defined Factors. *Cell*, 126(4), pp.663–676.
- Takahashi, K. et al., 2007. Induction of Pluripotent Stem Cells from Adult Human Fibroblasts by Defined Factors. *Cell*, 131(5), pp.861–872.
- Tallini, Y.N. et al., 2009. c-kit expression identifies cardiovascular precursors in the neonatal heart. *Proceedings of the National Academy of Sciences*, 106(6), pp.1808–1813.
- Tanabe, T. et al., 2005. Multiphoton excitation–evoked chromophore-assisted laser inactivation using green fluorescent protein. *Nature Methods*, 2(7), pp.503–505.
- Tendera, M., 2006. How much does Europe invest in the treatment of cardiovascular diseases? *European Heart Journal*, 27(13), pp.1521–1522.
- Thomson, J. & Kalishman, J., 1995. Isolation of a primate embryonic stem cell line. In *Proceedings of the ...* Proceedings of the
- Thomson, J., Itskovitz-Eldor, J. & Shapiro, S., 1998. Embryonic stem cell lines derived from human blastocysts. *Science*.
- Tiburcy, M. et al., 2011. Terminal Differentiation, Advanced Organotypic Maturation, and Modeling of Hypertrophic Growth in Engineered Heart Tissue. *Circulation research*, 109(10), pp.1105–1114.
- Toma, C. et al., 2002. Human mesenchymal stem cells differentiate to a cardiomyocyte phenotype in the adult murine heart. *Circulation*, 105(1), pp.93–98.
- Trounson, A., Thakar, R. & Lomax, G., 2011. Clinical trials for stem cell therapies. *BMC medicine*.
- Tulloch, N.L. et al., 2011. Growth of Engineered Human Myocardium With Mechanical

- Loading and Vascular Coculture. *Circulation research*, 109(1), pp.47–59.
- Uosaki, H. et al., 2011. Efficient and Scalable Purification of Cardiomyocytes from Human Embryonic and Induced Pluripotent Stem Cells by VCAM1 Surface Expression F. Prosper, ed. *PLoS ONE*, 6(8), p.e23657.
- van Kempen, M.J. et al., 1991. Spatial distribution of connexin43, the major cardiac gap junction protein, in the developing and adult rat heart. *Circulation research*, 68(6), pp.1638–1651.
- Velde, I., De Jonge, B. & Verheijck, E., 1995. Spatial Distribution of Connexin43, the Major Cardiac Gap Junction Protein, Visualizes the Cellular Network for Impulse Propagation From Sinoatrial Node to Atrium. *Circulation*.
- Vogel, A. et al., 2005. Mechanisms of femtosecond laser nanosurgery of cells and tissues. *Applied Physics B*, 81(8), pp.1015–1047.
- WHO, 2011. Fact sheet, No. 317. Cardiovascular diseases. 2011. pp.1–4. Available at: [Accessed August 10, 2011].
- Wollensak, G. et al., 2004. Keratocyte apoptosis after corneal collagen cross-linking using riboflavin/UVA treatment. *Cornea*, 23(1), pp.43–49.
- Wollensak, G., Spoerl, E. & Seiler, T., 2003a. Riboflavin/ultraviolet-a-induced collagen crosslinking for the treatment of keratoconus. *American journal of ophthalmology*, 135(5), pp.620–627.
- Wollensak, G., Spoerl, E. & Seiler, T., 2003b. Stress-strain measurements of human and porcine corneas after riboflavin-ultraviolet-A-induced cross-linking. *Journal of cataract and refractive surgery*, 29(9), pp.1780–1785.
- Wollert, K. et al., 1996. Cardiotrophin-1 Activates a Distinct Form of Cardiac Muscle Cell Hypertrophy. *Journal of Biological ...*
- Xu, T. et al., 2005. Inkjet printing of viable mammalian cells. *Biomaterials*, 26(1), pp.93–99.
- Xu, X.Q. et al., 2008. Chemically defined medium supporting cardiomyocyte differentiation of human embryonic stem cells. *Differentiation*, 0(0), pp.080613083032327–???
- Yang, L. et al., 2008. Human cardiovascular progenitor cells develop from a KDR+ embryonic-stem-cell-derived population. *Nature*, 453(7194), pp.524–528.
- Yildirim, Y. et al., 2007. Development of a Biological Ventricular Assist Device: Preliminary Data From a Small Animal Model. *Circulation*, 116(11_suppl), pp.I–16–I–23.

- Yoon, J. et al., 2005. Transdifferentiation of mesenchymal stem cells into cardiomyocytes by direct cell-to-cell contact with neonatal cardiomyocyte but not adult cardiomyocytes. *Annals of hematology*, 84(11), pp.715–721.
- Yu, J. et al., 2007. Induced Pluripotent Stem Cell Lines Derived from Human Somatic Cells. *Science*, 318(5858), pp.1917–1920.
- Zhao, T. et al., 2011. Immunogenicity of induced pluripotent stem cells. *Nature*, 474(7350), pp.212–215.
- Zimmermann, W.-H. et al., 2006. Engineered heart tissue grafts improve systolic and diastolic function in infarcted rat hearts. *Nature Medicine*, 12(4), pp.452–458.
- Zimmermann, W.-H., Melnychenko, I. & Eschenhagen, T., 2004. Engineered heart tissue for regeneration of diseased hearts. *Biomaterials*, 25(9), pp.1639–1647.
- Zimmermann, W.H., 2001. Tissue Engineering of a Differentiated Cardiac Muscle Construct. *Circulation research*, 90(2), pp.223–230.
- Zimmermann, W.H. et al., 2000. Three-dimensional engineered heart tissue from neonatal rat cardiac myocytes. *Biotechnology and Bioengineering*, 68(1), pp.106–114.
- Zimmermann, W.H. et al., 2002. Tissue engineering of a differentiated cardiac muscle construct. *Circulation research*, 90(2), pp.223–230.
- Zvibel, I., Smets, F. & Soriano, H., 2002. Anoikis: roadblock to cell transplantation? *Cell transplantation*, 11(7), pp.621–630.

6 Appendix

Table of figures

Figure 1: Heart waiting list of patients at year's end	11
Figure 2: Mechanical assist device for myocardial defects.....	13
Figure 3: Cardiovascular lineages during mammalian embryonic development and ESC differentiation.....	19
Figure 4: The three pillars of tissue engineering.....	27
Figure 5: Cardiac tissue engineering strategies known to improve heart function, or electrically interconnect to the host myocardium <i>in vivo</i>	34

List of abbreviations

2D	two-dimensional
3D	three-dimensional
AA	ascorbic acid
ANF	atrial natriuretic factor
BCT	bioartificial cardiac tissue
BMBF	Bundesministerium für Bildung und Forschung
BMC	bone marrow derived cell
BMP	bone morphogenetic protein
CABG	coronary artery bypass graft
CaCl ₂	calcium chloride
CAD	coronary artery disease
CB	cardiac body
CM	cardiomyocyte
CNTN2	contactin-2
CO ₂	carbon dioxide
CPC	cardiac progenitor cell
cTnT	cardiac troponin T
CVD	cardiovascular disease
Cx	connexin
DAPI	4',6-diamidino-2- phenylindole
DKK1	dickkopf homolog 1
DMEM	Dulbecco's modified Eagle's medium
DNA	desoxyribonucleic acid
EB	embryoid body
ECM	extracellular matrix
EHT	engineered heart tissue

EPC	endothelial progenitor cell
ESC	embryonic stem cell
FACS	fluorescence activated cell sorting
FGF	fibroblast growth factor
Flk1	fetal liver kinase 1
FOXA2	forkhead box protein A2
fs	femtosecond
HCN4 gated channel 4	potassium/sodium hyperpolarization activated cyclic nucleotide-
HEPES	2-(4-(2-hydroxyethyl)- 1-piperazinyl)-ethansulfonic acid
HF	heart failure
HSC	hematopoietic stem cell
iPSC	induced pluripotent stem cell
J	Joule
KCl	potassium chloride
KDR1	kinase insert domain receptor
Klf4	Krüppel-like factor 4
LIF	leukemia inhibitory factor
LO	lysyl oxidase
LVAD	left ventricular assist device
MACS	Magnet-assisted cell separation
MEF	murine embryonic fibroblast
Mef2c	myocyte-specific enhancer factor 2C
MESP	mesoderm posterior protein
MHC	myosin heavy chain
MI	myocardial infarction
MLC2a/v	myosin light chain 2a and/or 2v
MSC	mesenchymal stem cell

MTE	myocardial tissue engineering
MYH	myosin heavy chain
N	Newton
NIR	near infrared
NPPA	natriuretic peptide precursor A
NRCM	neonatal rat cardiomyocyte
NRG1	neuregulin 1
Oct3/4	Octamer binding transcription factor 3/4
OSKM	Oct4, Sox2, Klf4, c-Myc
Pa	Pascal
PCR	polymerase chain reaction
PDGF	platelet-derived growth factor
PDGF-R	PDGF receptor
PERV	porcine endogenous retrovirus
PIPAAm	poly(N-isopropylacrylamide)
PSC	pluripotent stem cell
PTCA	percutaneous transluminal coronary angioplasty
qPCR	quantitative PCR
RF	riboflavin
SCN5A	sodium channel protein type 5 subunit α
SCNT	somatic cell nuclear transfer
SEM	standard error of mean
SKMB	skeletal myoblast
SLOT	scanning laser optical tomography
SOX	SRY-related high-mobility-group box
SSC	spermatogonial stem cells
TBX	T-box transcription factor

TE	tissue engineering
TEM	transmission electron microscopy
TF	transcription factor
TMRM	tetramethylrhodamin-methylester
UV-A	ultraviolet A
VEGF	vascular endothelial growth factor
VEGFR-2	VEGF-receptor 2
WHO	World Health Organization

Curriculum vitae

Personal

Family name: Kensah
Given name: George
Address: Dieterichsstr. 38
30159 Hannover, Germany
Date and place of birth: July 7, 1976, Düsseldorf, Germany

PhD (11.2005 – 03.2012)

Institution: Medical School Hannover
Department: Leibniz Research Laboratories for Biotechnology and Artificial Organs (LEBAO)
Supervisor: Prof. Dr. Ulrich Martin
Adress: Carl-Neuberg-Str. 1
30625 Hannover, Germany
Telephone: +49 511 532 8947
Telefax: +49 511 532 8819
E-mail: Kensah.George@mh-hannover.de

Education

05.2001 – 04.2005: Studies in biology, Humboldt-University, Berlin;
Diploma

- 09.1998 – 04.2001: Studies in biology; Heinrich-Heine-University, Düsseldorf; Intermediate diploma
- 08.1986 – 04.1995: Grammar school, Monheim am Rhein; A-levels

Internships and related work

- 06.2005 – 10.2005: Internship in the group of Prof. Dr. Elke Dittmann at the Institute of Genetics, Humboldt-University, Berlin.
- Aim: Characterizing an ORF of the cyanobakterium *Microcystis aeruginosa* PCC7806, which probably is involved in a non-ribosomal peptide synthesis pathway.
- Methods: PCR, RT-PCR, Cloning, insertional Knockout mutagenesis, heterologous gene expression, purification of tagged proteins, detection of target proteins (Western Blot), HPLC-Analysis.
- 06.2003 – 02.2004: Internship in the group of Dr. Metin Artuc in the Department of Experimental Dermatology, Charité, Berlin.
- Topic: Functional Analysis of the c-Kit Receptor in human mast cells.
- Methods: Mast cell isolation and purification (MACS), PCR, RT-PCR, cloning, development of siRNAs, stable and transient transfection of mast cells (lipofection), FACS analysis.
- 08.2001 – 05.2003: Student assistant in the group of Dr. Metin Artuc in the Department of Experimental Dermatology, Charité, Berlin.
- Topic: Impacts on the regulation of the epidermal growth factor receptor (EGF-R) by Angiotensin II.
- Methods: Fibroblast and keratinocyte isolation and cultivation, immunoprecipitation of target proteins, analysis of the phosphorylation status of membrane bound proteins (Western Blot).

Work experience abroad

06.2004 – 04.2005: Research for the diploma thesis in the group of Prof. Dr. Brett A. Neilan at the University of New South Wales, Sydney, in cooperation with Prof. Dr. Elke Dittmann, Humboldt-University, Berlin.

Topic: Characterization of an ORF on contig578 of *Microcystis aeruginosa* PCC7806 putatively involved in an NRPS mechanism and of *mcyJ*, a putative O-methyltransferase of the microcystin-LR gene cluster.

Methods: PCR, sequencing, molecular cloning, heterologous gene expression, detection of target protein (Western Blot) and its purification (Ni^{2+} -affinity), protein activity measurement (PP 2A inhibition assay), site directed mutagenesis (Megaprimer PCR), *in silico* analysis of the primary, secondary and tertiary structures of polypeptides.

List of publications

Abstracts

Angelica Roa Lara, George Kensah, Anke Gawol, David Skvorc, Kristin Schwanke, Robert Zweigerdt, Ulrich Martin, Ina Gruh; "Generation of Human Bioartificial Cardiac Tissue based on Pluripotent Stem Cell-derived Cardiomyocytes"; Keystone Symposium "Cardiovascular Development and Regeneration", January 2012, Taos, USA

Julia Dahlmann, Andreas Krause, George Kensah, Lena Möller, Gerald Dräger, Ulrich Martin, and Ina Gruh; "Adjustable mechanical properties of Bioartificial Cardiac Tissue based on defined extracellular matrix blends"; 6th Annual Congress of the German Society for Stem Cell Research (DGZ), November 2011, Düsseldorf

Julia Dahlmann, George Kensah, David Skvorc, Anke Gawol, Ulrich Martin, and Ina Gruh; "Rapid soft lithography for large scale embryoid body formation of iPS cells on agarose microwells"; 6th Annual Congress of the German Society for Stem Cell Research (DGZ), November 2011, Düsseldorf

Michael Pflaum, George Kensah, Julia Dahlmann, Jennifer Bonse, Mathias Wilhelmi, Axel Haverich; "Tissue Constructs for the Functioning Test of Smooth Muscle like Cells differentiated from Adipose Tissue Stromal Cells"; 38th congress of the European Society of Artificial Organs (ESAO), September 2011, Porto, Portugal

Julia Dahlmann, George Kensah, Andreas Krause, Lena Möller, David Skvorc, Gerald Dräger, Ulrich Martin, and Ina Gruh; "Towards transplantable bioartificial cardiac tissue: Animal-free extracellular matrix for myocardial tissue engineering using large amounts of induced pluripotent stem cell-derived cardiomyocytes"; 7th Hydra Summer School for Stem cell and Regenerative Medicine, September 2011, Hydra, Greece

Kamilla Babicz, Julia Dahlmann, Anna e. Müller, George Kensah, Ina Gruh, Wolfgang A. Linke, Martina Krüger; "Insulin mediates rapid titin phosphorylation via NO-dependent activation of PKG"; 90th Annual Meeting of the German Physiological Society, March 2011, Regensburg

George Kensah, Angelica Roa Lara, David Skvorc, Anke Gawol, Christina Mauritz, Monica Jara-Avaca, Robert Zweigerdt, Hans Schoeler, Ina Gruh, Ulrich Martin; "Murine Induced Pluripotent Stem Cells for Cardiac Tissue Engineering"; Keystone Symposium "Mechanisms of Cardiac Growth, Death and Regeneration", February 2011, Keystone, USA

George Kensah, Julia Dahlmann, David Skvorc, Anke Gawol, Ingrid Schmidt-Richter, Ulrich Martin, Ina_Gruh; "Modulation of Bioartificial Cardiac Tissue mechanical properties induced by stretch and ascorbic acid involves ECM remodeling"; Keystone Symposium on "Extracellular Matrix and Cardiovascular Remodeling", January 2011, Tahoe, USA

Julia Dahlmann, George Kensah, Ulrich Martin, Ina Gruh; "Engineering of three-dimensional Bioartificial Cardiac Tissues using a defined hyaluronic acid-based matrix"; Combined Meeting of the ESGCT, GSZ, DG-GT and ISCT, November 2009, Hannover

Julia Dahlmann, George Kensah, Ulrich Martin, Ina Gruh; "Engineering of three-dimensional Bioartificial Cardiac Tissues using a defined hyaluronic acid-based matrix"; Combined Meeting of the ESGCT, GSZ, DG-GT and ISCT, November 2009, Hannover

George Kensah, Ina Gruh, David Skvorc, Henning Schumann, Wolfram-Hubertus Zimmermann, Axel Haverich, Ulrich Martin; "A novel miniaturized bioreactor for the Generation, Stimulation and Observation of Stem Cell Derived 3D Bioartificial Cardiac Tissue"; World Conference on Regenerative Medicine, Oktober, 2009, Leipzig

George Kensah, Ina Gruh, Christina Mauritz, Kristin Schwanke, Stephanie Wunderlich, David Skvorc, Henning Schumann, Wolfram-Hubertus Zimmermann, Rudolf Jaenisch, Hans Schoeler, Axel Haverich, Ulrich Martin; "A novel miniaturized Bioreactor for the generation, stimulation, and observation of stem cell derived 3D Bioartificial Cardiac Tissue"; 7th Dutch-German Joint Meeting of Molecular Cardiology Groups, February 2009, Hamburg

George Kensah, Ina Gruh, Christina Mauritz, Stephanie Wunderlich, David Skvorc, Jörg Viering, Michael Breyvogel, Wolfram-Hubertus Zimmermann, Holm Zaehres, Hans Schoeler, Axel Haverich, U. Martin; "Application of pluripotent stem cell-derived cardiac cells for 3D tissue engineering"; 3rd Congress on Regenerative Biology and Medicine / 3rd Congress of the German Society for Stem Cell Research, October 2008, Stuttgart

George Kensah, Ina Gruh, Marten Bierbaum, Christian Krause, Jörg Viering, Michael Breyvogel, Axel Haverich, Ulrich Martin; "A novel bioreactor for miniaturized bioartificial cardiac tissue engineering"; 28th Annual Meeting & Scientific Sessions International Society for Heart and Lung Transplantation, April 2008, Boston, USA

George Kensah, Ina Gruh, Stephanie Wunderlich, Kristin Schwanke, Payam Akhyari, Jörg Viering, Michael Breyvogel, Wolfram-Hubertus Zimmermann, Axel Haverich, Ulrich Martin; "Bioartificial Cardiac Tissue engineered from Rhesus monkey Embryonic Stem Cell derived Cardiomyocytes"; 6th Dutch-German Joint Meeting of Molecular Cardiology Groups, February 2008, Amsterdam, Netherlands

George Kensah, Ina Gruh, Stephanie Wunderlich, Kristin Schwanke, Payam Akhyari, Marten Bierbaum, Christian Krause, Jörg Viering, Michael Breyvogel, Axel Haverich, Ulrich Martin; “Bioartificial Cardiac Tissue engineered from Rhesus monkey Embryonic Stem Cell derived Cardiomyocytes”; Keystone Symposium „Pathological and Physiological Regulation of Cardiac Hypertrophy“, January 2008, Copper Mountain, USA

George Kensah, Ina Gruh, Marten Bierbaum, Christian Krause, Jörg Viering, Michael Breyvogel, Axel Haverich, Ulrich Martin; “A novel bioreactor for miniaturized bioartificial cardiac tissue engineering“; Conference of Regenerative Medicine, Micro- and Nanotechnologies in Regenerative Medicine, Oktober 2007, Hannover

Metin Artuc, George Kensah, B.M. Henz, T. Unger, U.M. Steckelings; “Angiotensin II as a modulator of fibrosis in human skin“; 28th Scientific Congress of the German Hypertension League, November 2004, Düsseldorf

Journal Publications

George Kensah, Julia Dahlmann, Angelica Roa Lara, Azadeh Azizian, Jan Hegemann, David Skvorc, Anke Gawol, Robert Zweigerdt, Stefan Wagner, Matthias Ochs, Axel Haverich, Ina Gruh*, & Ulrich Martin*; “Fibroblast-dependent Fusion of iPSC-derived Cardiac Bodies results in structurally and functionally homogenous Bioartificial Cardiac Tissue and is supported by Mechanical Load and Ascorbic Acid“; in preparation

Kai Küttemeyer*, George Kensah*, Marko Heidrich, Heiko Meyer, Ulrich Martin, Ina Gruh, and Alexander Heisterkamp; “Two-photon induced collagen cross-linking in bioartificial cardiac tissue“; Optics Express, Volume 19, Issue 17, August 15, pp 15996 - 16007

George Kensah*, Ina Gruh*, Jörg Viering, Henning Schumann, Julia Dahlmann, Heiko Meyer, David Skvorc, Antonia Bär, Payam Akhyari, Alexander Heisterkamp, Axel Haverich, and Ulrich Martin; “A Novel Miniaturized Multimodal Bioreactor for Continuous *In Situ* Assessment of Bioartificial Cardiac Tissue During Stimulation and Maturation“; Tissue Engineering Part C: Methods, Volume 17, Issue 4, April 1, 2011, pp 463 - 473

*these authors contributed equally

Danksagung

Mein äußerster Dank gilt Ulrich Martin für die Überlassung des Themas und die Betreuung meiner Dissertation. Auch wenn jetzt alles ein "bisschen" länger gedauert hat als geplant, konnte ich mich während der ganzen Zeit auf Deine Unterstützung verlassen. Das hat mir auch in Zeiten verstärkter Frustration, die in den vergangenen Jahren recht häufig waren, Mut gemacht. Auch Deine Betreuung war so, wie ich sie jedem Doktoranden wünschen würde. Ideen mit Dir zu besprechen führten immer zu einem Erkenntnisgewinn, auch wenn sich dieser manchmal erst nach einiger Zeit einstellte. Oft nach dem schmerzhaften Eingeständnis, dass man da auch schon eher hätte drauf kommen können. Auch Deine Herangehensweise ("Mach doch einfach mal!") hat mir schon häufig das vielzitierte Brett vor'm Kopp entfernt. Ich danke Dir dafür.

In gleicher Weise möchte ich Ina Gruh danken, die sich aufopferungsvoll für den Erfolg unserer Publikationen und meiner Promotion eingesetzt hat. Dein konsequentes und zielgerichtetes Arbeiten an unseren Manuskripten und Deine kritischen Anmerkungen haben mich sehr motiviert. Auch wenn ich dachte, dass es jetzt mal an der Zeit wäre nach Hause zu gehen hast Du weitergemacht. Ich kann mich noch dran erinnern, als ich mal wieder frustriert spät Feierabend gemacht habe und Du zur gleichen Zeit *zur* Arbeit gefahren bist weil Du Zellen füttern musstest. Ich weiß nicht mehr wie spät es war, aber es war schon seit langem dunkel. So etwas motiviert. Auch hast Du dafür gesorgt, dass für alle Ideen immer die nötigen Mittel vorhanden waren, was wahrscheinlich auch auf Deine (im positivsten Sinne) preußische Einstellung zurückzuführen ist. Danke!

Professor Thomas Scheper möchte ich herzlichst für Übernahme des Korreferats meiner Dissertation danken. Speziell für den lockeren Umgang mit der Verschiebung der Abgabe der Dissertation bin ich Ihnen sehr dankbar. Es ist mir heute noch sehr unangenehm. In diesem Zusammenhang möchte ich mich auch bei dem vorgeschlagenen Drittprüfer Professor Anaclet Ngezahayo bedanken, der ähnlich verständnisvoll („Akuna Matata, George“) reagiert hat.

Ohne die exzellente Unterstützung, die ich in den vergangenen Jahren von allen Mitgliedern der AG Gruh erfahren habe wäre ich nicht im Stande gewesen die Arbeit in der vorliegenden Form anzufertigen. Man kann es nur aufopferungsvoll nennen, wenn kurzfristige Anfragen (fast immer) kommentarlos bearbeitet werden, auch wenn das ungeplante Überstunden bedeutet, oder die Routine anderweitig beeinträchtigt wird. Ich hoffe, dass diese Hingabe nicht ausschließlich nach dem Motto „der arme Junge muss auch mal fertig werden“ erfolgte. Ich bin mir aber fast sicher, dass dem nicht so ist, da ich meine, diese Unterstützung schon in der „Regelpromotionsdauer“ erfahren zu haben. Neben dem oben genannten Dank unserer Chefin gegenüber möchte ich mich daher ausdrücklich bei allen Mitgliedern der AG Gruh, namentlich Mine Bakar, Julia Dahlmann, Anke Gawol, Angelica Roa Lara, Ingrid Schmidt-Richter und David Skvorc bedanken. Ihr seid eine unschlagbare Mannschaft und ich denke dass es schwer sein wird, eine solche Konstellation an tollen Kollegen wiederzufinden, was mir jetzt schon Kopfzerbrechen bereitet. Im Speziellen muss ich mich jedoch bei Julia bedanken. Dafür, dass sie mich in den vergangenen fast drei Jahren liebevoll unterstützt hat. Ich hoffe, ich kann das alles irgendwann wieder gut machen. Vielleicht in den „heißen“ Phasen der Promotion, die Du ja auch erleben wirst und von denen es bei meiner nicht gemangelt hat (gefühlte war es eine einzige heiße Phase). Oder vielleicht mit einem Schubser auf eine coole Welle?

Für die Einführung in die Methoden der Stammzellkultivierung möchte ich mich bei Kristin Schwanke und Sandra Menke bedanken. Frische Luft schnappen war auch immer lustig mit Dir Sandra.

Für die hilfreichen Diskussionen im Gang oder auf dem „heißen Stuhl“ bei Progress Reports im LEBAO möchte ich mich bei Dir, Robert Zweigerdt, herzlich bedanken. Auch dafür, dass Du Dir die Zeit genommen hast, mir bei meinem ersten Keystone Kongress mit den „Großen“ in allen Belangen unter die Arme zu greifen, also kongress-, und wintersportmäßig meine ich.

Dem Hilfiger Kardiomyozyten-Team, bestehend aus Tibor, Marco, Zlata, Eric und Birgit danke ich auch für die tolle Zusammenarbeit. Deren Chef, Res und seiner Frau

Denise möchte ich ebenfalls für hilfreiche Tipps bezüglich Tissue Engineering und allgemeiner Zellkultur danken.

Dem Team aus der Forschungswerkstatt, bestehend aus Henning Schumann, Michael Breyvogel, Jörg Viering, Jürgen Fiedler, Jörg Klaus und Eric Mahnke, gilt besonderer Dank, da diese erfolgreiche Kooperation die Grundlage für alle Arbeiten in dieser Dissertation geschaffen hat.

Für die wiederholte erfolgreiche Kooperation möchte ich mich auch bei Marko Heidrich, Heiko Meyer, Kai Küttemeyer und Alexander Heisterkamp vom Laser Zentrum bedanken. Ich hoffe, dass wir diese fortführen können, und wünsche Dir, Kai eine tolle Zeit bei Olympus (vielleicht gibt's ja mal ein Objektiv zum EK, so auf die alten Zeiten).

Neben Alexandru Calistru, Michael Pflaum, Mirela Wilkening, Ivonne Reimann, Ines Böttcher, Bernd Paruschke, Alexandra Haase, Ruth Olmer, Karin Kallweit, Monica Jara-Avaca, Sylvia Merkert, Stefanie Wunderlich und Monica Winkler möchte ich mich bei allen weiteren Mitgliedern aus dem LEBAO für eine gute Zusammenarbeit und eine tolle Zeit bedanken. Alle, die ich nicht namentlich erwähnt habe, bitte ich dies mir zu verzeihen.

Bei folgenden Mitgliedern der HTTG möchte ich mich im speziellen bedanken:

Bei Professor Axel Haverich, dessen Enthusiasmus für den Bereich Tissue Engineering meine eigene Begeisterung für diesen Ansatz auch in schwierigen Zeiten aufrecht erhalten hat und im gleichen Zusammenhang bei Hassina Baraki und Ingo Kutschka, deren chirurgischen Fähigkeiten bewiesen haben, dass eine Transplantation der Konstrukte im Kleintiermodell zu vielversprechenden Ergebnissen führen kann. Payam Akhyari, einem ehemaligen Mitglied dieser Abteilung möchte ich ebenfalls danken. Schade, dass Du nicht mehr da bist.

Des Weiteren möchte ich mich bei Professor Wolfram-Hubertus Zimmermann für seine Unterstützung in Fragen des kardialen Tissue Engineering bedanken.

Erklärung zur Dissertation

gemäß §6(1) der Promotionsordnung der Naturwissenschaftlichen Fakultät der
Gottfried

Wilhelm Leibniz Universität Hannover

für die Promotion zum Dr. rer. nat.

Hierdurch erkläre ich, dass ich meine Dissertation mit dem Titel

**Pluripotent Stem Cell-based
Myocardial Tissue Engineering Using
Advanced Bioreactor Technology**

selbstständig verfasst und die benutzten Hilfsmittel und Quellen sowie
gegebenenfalls die zu Hilfeleistungen herangezogenen Institutionen vollständig
angegeben habe.

Die Dissertation wurde nicht schon als Masterarbeit, Diplomarbeit oder andere
Prüfungsarbeit verwendet.

George Kensah

Hannover, den 20.12.2011